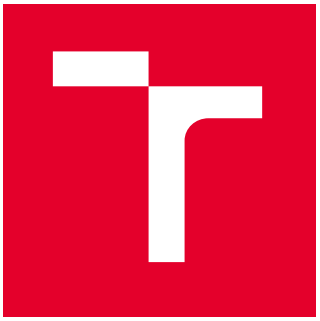

BRNO UNIVERSITY OF TECHNOLOGY

VYSOKÉ UČENÍ TECHNICKÉ V BRNĚ

FACULTY OF CHEMISTRY

FAKULTA CHEMICKÁ

INSTITUTE OF FOOD SCIENCE AND BIOTECHNOLOGY

ÚSTAV CHEMIE POTRAVIN A BIOTECHNOLOGIÍ

ENCAPSULATION OF MICROORGANISMS FOR APPLICATION IN AGRICULTURE

ENKAPSULACE MIKROORGANISMŮ PRO ZEMĚDĚLSKÉ APLIKACE

DOCTORAL THESIS

DIZERTAČNÍ PRÁCE

AUTHOR — **Ing. Diana Černayová**

AUTOR PRÁCE

SUPERVISOR — **prof. Ing. Stanislav Obruča, Ph.D.**

ŠKOLITEL

BRNO 2025

BRNO UNIVERSITY OF TECHNOLOGY
FACULTY OF CHEMISTRY

Doctoral Thesis Assignment

Number of thesis:	FCH-DIZ0269/2025	Academic year: 2025/26
Institute:	Institute of Food Science and Biotechnology	
Student:	**Ing. Diana Černayová**	
Study programme:	Biophysical Chemistry	
Study field:	no specialisation	
Head of thesis:	**prof. Ing. Stanislav Obruča, Ph.D.**	

Title of Doctoral Thesis:

Encapsulation of microorganisms for application in agriculture

Doctoral Thesis assignment:

1. Conduct a comprehensive literature review focused on plant growth-promoting bacteria (PGPB) and their application in agriculture, with particular emphasis on the current state of knowledge in the preparation and utilization of bioinoculants.
2. Select a suitable bacterial candidate for the preparation of hydrogel-based bioinoculants, in which the gelling agent will consist of extracellular polysaccharides produced by the bacterium itself.
3. Optimize cultivation conditions and strategies, including the transfer of cultures to a laboratory bioreactor, with the aim of maximizing the yield of polysaccharides and other biopolymers relevant to the agricultural application of the prepared hydrogel formulation.
4. Investigate the gelation mechanisms and characterize selected biophysical and biological properties of the prepared gel formulations.
5. Experimentally verify the efficacy of the prepared bioinoculants using selected model plants in appropriate laboratory systems.

Deadline for Doctoral Thesis delivery: 31. 10. 2025

Doctoral Thesis is necessary to deliver to a secretary of institute in the number of copies defined by the dean. This assignment is part of Doctoral Thesis.

Ing. Diana Černayová	prof. Ing. Stanislav Obruča, Ph.D.	prof. RNDr. Ivana Márová, CSc.
Student	Head of thesis	Head of institute

In Brno, 1. 9. 2024

prof. Ing. Michal Veselý, CSc.
Dean

ABSTRACT

Plant Growth-Promoting Rhizobacteria (PGPR) serve as effective bioinoculants that stimulate plant growth and enhance soil fertility. Encapsulating PGPR within hydrogel matrices provides a protective environment that improves their survival, stability and overall bioactivity in agricultural applications. This dissertation presents a novel self-encapsulation method employing *Azotobacter vinelandii*, a bacterium capable of synthesizing its own alginate, a natural exopolysaccharide that forms a stable gel upon Ca^{2+} crosslinking. Six *A. vinelandii* strains from German and Czech microbial collections were investigated for their growth performance, alginate yield and plant growth-promoting traits. Among them, strains DSM 87, DSM 720 and CCM 289 produced the alginate concentrations (4.9 ± 0.6 g/L, 3.5 ± 0.5 g/L and 2.2 ± 0.3 g/L, respectively) with easy ability to form strong gels. These strains also demonstrated strong PGPR activities, including indole-3-acetic acid production (up to 10.5 μg/mL), siderophore synthesis and phosphate solubilization. Further experiments focused on different gelation possibilities including multivalent ions, organic acids and gelation in the whole volume by dissolving insoluble $CaCO_3$ presented in the cultivation media. Focusing on application and industrial potential of this process for biofertilizer production, the entire procedure was up-scaled to bioreactors, where the effects of agitation speed and filling volume were tested for strain DSM 87. To evaluate the plant growth-stimulation properties of the obtained bacterial gels, lettuce plants were cultivated under different treatment conditions. The results demonstrated that bacterial gelled cultures positively influenced plant growth and improved plant survival under drought stress.

This work demonstrates a cost-effective and environmentally sustainable approach to bioinoculant production by using *A. vinelandii*'s alginate-forming capacity, providing a promising alternative to conventional biofertilization methods.

KEY WORDS

Plant growth-promoting rhizobacteria, PGPR, alginate, polyhydroxyalkanoates, biopolymers, bioinoculants, agriculture, cultivation experiments

ABSTRAKT

Baktérie podporujúce rast rastlín (PGPR) slúžia ako účinné bioinokulanty, ktoré stimulujú rast rastlín a zvyšujú úrodnosť pôdy. Obalenie PGPR v hydrogelových nosičoch poskytuje ochranné prostredie, ktoré zvyšuje ich prežitie, zlepšuje stabilitu a celkovú bioaktivitu v poľnohospodárskych aplikáciách.

Táto dizertačná práca predstavuje nový spôsob prípravy bioinokulantov pomocou baktérie *Azotobacter vinelandii*, schopnej produkovať vlastný alginát, exopolysacharid tvoriaci stabilný gél pri väzbe s iónmi Ca^{2+}. V práci bolo testovaných šesť kmeňov *A. vinelandii* pochádzajúcich z nemeckých a českých mikrobiálnych zbierok. Kmene boli skúmané na základe ich rastu, produkcie alginátu a podporujúcich vlastností pre rast rastlín. Medzi nimi kmene DSM 87, DSM 720 a CCM 289 produkovali koncentrácie alginátu (4,9 ± 0,6 g/L, 3,5 ± 0,5 g/L a 2,2 ± 0,3 g/L), pričom vykazovali dobrú schopnosť vytvárať pevné gély. Tieto kmene zároveň preukázali výrazné PGPR aktivity, vrátane produkcie indol-3-octovej kyseliny (až do 10,5 μg/mL), syntézy sideroforov a solubilizácie fosfátov. Ďalšie experimenty sa zamerali na rôzne možnosti gélovania, vrátane využitia multivalentných iónov, organických kyselín a rovnomerného gélovania v celom objeme prostredníctvom rozpúšťania nerozpustného $CaCO_3$ prítomného v kultivačnom médiu. Pri zameraní sa na samotný aplikačný a priemyselný potenciál tohto procesu pri výrobe biohnojív bol celý postup vyskúšaný aj v bioreaktoroch, kde boli pre kmeň DSM 87 testované vplyvy rýchlosti miešania a objemu naplnenia. Pri vyhodnotení stimulačných účinkov bakteriálnych gélov na rast rastlín boli pestované rastliny šalátu za rôznych podmienok ošetrenia. Výsledky ukázali, že bakteriálne gélové kultúry pozitívne ovplyvnili rast rastlín a zlepšili ich prežitie pri strese spôsobenom suchom.

Táto práca predstavuje efektívny, lacný a environmentálne udržateľný postup na výrobu bioinokulantov využitím schopnosti *A. vinelandii* produkovať alginát, čím ponúka ekologickú alternatívu ku konvenčným metódam hnojenia.

KĽÚČOVÉ SLOVÁ

Baktérie stimulujúce rast rastlín, PGPR, alginát, polyhydroxyalkanoáty, biopolyméry, bioinokulanty, poľnohospodárstvo, kultivačné experienty

ČERNAYOVÁ, Diana. *Encapsulation of microorganisms for application in agriculture*. Online, doctoral Thesis. Stanislav OBRUČA (supervisor). Brno: Brno University of Technology, Faculty of Chemistry, 2025. Available at: https://www.vut.cz/en/students/final-thesis/detail/174083. [accessed 2025-10-22].

Declaration

Acknowledgements (Poďakovanie)

Od začiatku doktorského štúdia ma veľmi podporovali moji školitelia, profesor Stanislav Obruča a docent Petr Sedláček, ktorým patrí obrovská vďaka za ich cenné prínosy, nápady, motiváciu a podporu. Rovnako tak by som sa veľmi chcela poďakovať ďalším akademickým pracovníkom z UCHPBT a UFSCH, s ktorými som počas štúdia prišla do styku pri experimentálnych meraniach, vyhodnocovaniach, alebo pomoci pri učení sa nových laboratórnych techník.

Veľké ďakujem si zaslúžia aj kolegyne a kolegovia z PHAntastic group, špeciálne z „Centrálneho kancu", pretože psychická podpora, dobrá nálada a veľa smiechu mnoho krát spríjemňuje aj náročné dni.

In this part I would also like to thank prof. Johannes Rousk and dr. Albert Brangarí, who helped me and motivated me during my stay in Lund University and showed me the perks of Microbial Ecology.

Samozrejme by som sa veľmi chcela poďakovať mojej rodine za podporu aj napriek tomu, že stále nerozumejú čo toľko študujem. Ďakujem aj mojim kamarátkam a kamarátom a hlavne môjmu priatelovi, ktorý mi niekedy verí viac ako si verím ja.

V neposlednom rade by som sa chcela poďakovať aj svojím študentom, niekedy tomu bolo naopak a naučili ma viac ako som ja naučila ich.

CONTENT

1 INTRODUCTION

Encapsulation of microorganisms has emerged as a versatile and promising technology with broad applications across food industry, agriculture and medicine. This technique involves the entrapment of microbial cells within protective matrices (e.g. polysaccharides, lipids or proteins) that can cover the cells from environmental stresses, control their release and enhance their functional stability. Encapsulation not only improves microbial survival during storage and application but also facilitates targeted delivery, enabling microorganisms to exert their beneficial effects more effectively (Dusso & Salomon, 2023; Gunzburg et al., 2020).

Besides the advantageous roles in medicine and the food industry, this thesis focuses on agriculture and explores new possibilities for ecological soil fertilization. There are high demands on crop production. Excessive use of chemical fertilizers can infiltrate into groundwater and cause long-term negative effects, such as biodiversity loss and soil degradation (Ferreira et al., 2019). Combined with the challenges posed by climate change, the agricultural sector faces multiple urgent issues that must be addressed. Progress in solving these challenges is ongoing but gradual. Key priorities in agriculture include maintaining and improving soil quality, enriching soil nutrient levels and preventing erosion, all of which are essential for achieving high crop yields and sustainable plant growth. Maintaining high soil quality through the use of environmentally friendly alternatives to chemical fertilizers often faces challenges, primarily due to higher initial costs. However, a progress in a bioinoculant development and their application has been made in recent years (dos Reis et al., 2024; Monica et al., 2025). Bioinoculants, also known as bacterial inoculants, are microorganisms that positively influence plant growth and contribute to soil bioremediation by participating in the biological activities of the soil ecosystem. Their beneficial effects include the production of plant growth regulators, nitrogen fixation, binding of toxic metals and other functions that support plant health and soil quality (Chandra et al., 2018; Haruta & Kanno, 2015; Song et al., 2015).

Plant growth-promoting rhizobacteria (PGPR) are a key group of bioinoculants known for their diverse abilities to enhance the soil microbiome, maintain a healthy rhizosphere and ultimately support plant growth. These beneficial bacteria improve soil fertility by increasing the availability of vital nutrients such as nitrogen and phosphorus, suppressing soil-borne pathogens that compete for plant resources and producing siderophores (compounds that chelate iron and make it more accessible to plants) (Song et al., 2015). Nevertheless, in this

case, the primary limiting factor appears to be the survivability rate of PGPR following their introduction into the soil environment (Beshah et al., 2024; Shah et al., 2021). When bacterial strains are transferred from nutrient-rich cultivation media to natural soils, they are suddenly exposed to fluctuating pH, variable temperature regimes, desiccation stress and competition with indigenous microbial communities (Chandra et al., 2018; Haruta & Kanno, 2015). These factors can significantly impair cell viability and, consequently, reduce the intended functional benefits, such as nutrient solubilization, phytohormone production, or pathogen suppression (Beshah et al., 2024). To enhance survival, PGPR are frequently delivered in the form of liquid inoculants, which can be applied for a seed treatment. This method ensures close proximity between the bacteria and the emerging roots, increasing the probability of successful colonization (L. Chen et al., 2021). However, seed coating is often time-consuming, requires specialized equipment and is associated with higher costs, making it less feasible for large-scale agricultural deployment (Ahemad & Kibret, 2014). An alternative approach involves applying the liquid inoculant directly into the soil, either alone or integrated with liquid fertilizers (L. Chen et al., 2021; Kelbessa et al., 2023). While this strategy can facilitate rapid bacterial distribution, the survival of PGPR under such conditions is typically short-lived, necessitating repeated applications to maintain effective population levels (Calvo et al., 2014).

Another potential solution involves incorporating beneficial bacteria into a gel matrix composed of polysaccharides, lipids, or proteins, forming a protective barrier through the process of encapsulation. PGPR encapsulated in matrices such as alginate, chitosan, or xanthan gum are shielded from adverse environmental factors, while the gel structure retains moisture, creating a microenvironment that supports bacterial viability (Barrera et al., 2020; Bashan et al., 2014). These encapsulated microorganisms are gradually released from the gel into the surrounding soil, where they can colonize the rhizosphere and interact with native microbial communities. Because the release is controlled and continuous, the beneficial effects are sustained over a longer period, reducing or eliminating the need for frequent reapplications (John et al., 2011; Malusá et al., 2012). Furthermore, gel formulations can be freeze-dried for extended shelf life and later rehydrated upon application, which facilitates easier storage, transportation and handling without significant loss of viability (Barrera et al., 2020; Malusá et al., 2012). This approach offers a practical means of delivering bioinoculants while maintaining long-term efficacy under field conditions.

In this dissertation, we proposed and investigate a novel approach; self-entrapping bacteria within a hydrogel matrix that they produce themselves. This strategy could be both feasible and

cost-effective, as it eliminates the need for additional gelation agents. The key requirement was to select bacterial strains that not only belong to the PGPR group but also possess the ability to synthesize extracellular polysaccharides of sufficient quality to form a protective hydrogel barrier, enabling self-encapsulation.

From the available candidates, *Azotobacter vinelandii* was chosen due to its GRAS (Generally Recognized As Safe) status, non-toxicity and well-established capacity for nitrogen fixation via its nitrogenase enzyme. In addition, *A. vinelandii* exhibits diverse potential bioactivities, making it a promising candidate for multifunctional agricultural applications.

By developing and evaluating this self-encapsulation concept, this work aims to contribute both to the advancement of bioinoculant formulation technology and to the broader goal of sustainable, resource-efficient agriculture.

2 THEORETICAL PART

2.1 BIOINOCULANTS AND THEIR APPLICATION IN THE AGRICULTURAL SECTOR

Microbial inoculants, also referred to as bioinoculants, are substances containing living microorganisms, which are expected to benefit plant growth after their application (Koutsougera et al., 2023). Microorganisms include living bacteria, fungi and microalgae isolated from soil, plants and/or water (Makhaye et al., 2021). Applied to seeds, aerial parts of the plants, or the soil, they positively affect plant growth and work as fertilizers of biological origin (Vessey, 2003). Generally, the delivery system formulation should have all desired properties such as high solubility, stability, effectiveness, non-toxicity and enhanced targeted activity with effective concentration (Vejan et al., 2019).

The composition of microbial inoculants depends on their intended effect on a crop/plant and the form of the application. Bioinoculants can be directly applied to the soil, coated on the seeds or sprayed on the plant's surfaces (Ajilogba et al., 2017). Liquid inoculants allow alternative application methods, such as in-furrow and can be sprayed on soil or applied through "foliar" application These modern methods may be advantageous in some cases, for example, in-furrow inoculation to alleviate the impact of pesticides used for seed treatments in contact with the bacteria (Fukami et al., 2016). However, there are limiting factors that restrict the use of liquid inoculants in some areas. Biotic and abiotic stresses may affect the effectiveness of the bioinoculant application, making it inefficient in cases such as nutrient-poor or unbalanced soils, increasing temperatures, salinity, water stress, pests and diseases, among others (Matte et al., 2018). Therefore, besides the liquid form of application, efforts have also been made to improve the efficiency of inoculants supporting them with a carrier matrix (Yousefi et al., 2017). A great variety of materials have been used as carriers, for instance clay minerals (e.g. bentonite, vermiculite, attapulgite), high organic matter materials (e.g. sugarcane bagasse, sewage sludge, sawdust), or polysaccharides (alginate, carrageenan, xanthan) (Koutsougera et al., 2023; Vassilev et al., 2020). Microbes are mixed with clay minerals or organic materials and then applied to the soil along the roots. Another technique for the formulation is to encapsulate the microbes into polymeric beads to maintain their viability and also to provide easy handling by the end user (Koutsougera et al., 2023) .

The current definition and regulation of bioinoculants was provided by the European Union in 2019/1009 includes, regulates and defines plant biostimulants products (including

bioinoculants such as *Azospririllum* spp., *Azotobacter* spp. and mycorrhizal fungi) (*https://Eur-Lex.Europa.Eu/*, 2019; Koutsougera et al., 2023), although they have been used much earlier. The first inoculant to be commercially produced, was "Nitragin", in 1890s, in the USA and gelatine was used as a carrier for bacterial cells, while the used microorganisms were dependent on host legume species (*Bradyrhizobium japonicum*, *Rhizobium leguminosarum*, *Sinorhizobium meliloti*, *Bradyrhizobium* sp.). Due to the low viability rate, these carriers were soon replaced by peat, which remained as the "gold" carrier until the end of the 1990s, when the scenario began to change and peat were replaced by liquid inoculants (Santos et al., 2019b). Since the beginning of the manufacturing of inoculants, the industry has been concerned about generating increasingly efficient products, at a low cost, with easy manipulation and the good quality required by farmers. An important aspect is the choice of the carrier for the microorganisms, providing long cellular viability and easy application (Parveen et al., 2023).

Mechanisms of the improvement of plants and crops growth will be described in detail later (Chapter 2.2). However, it is important to note, that N_2 fixation, phytohormone production, enhancing plant resistance to diseases and pests are only few mechanisms involved in organisms considered beneficial bacteria (PGPR) (Majkowska-Gadomska et al., 2021). New technologies are at the centre of research to increase application relying on the use of mixed inoculants, aiming to promote plant growth by combining distinct mechanisms of different microorganisms. The synergic effect of two or more types of inoculants can provide excellent results and show the great potential of being increasingly used by farmers (Ferri et al., 2017). This thesis will be focused on bacterial inoculants, therefore primary PGPR will be described further in the following parts.

The great majority of the first manufactured inoculants contained only single species of microorganism and in general one strain, which had the best inoculation results for a particular crop. Exceptions included a maximum of two microorganisms "of the same type", for example, two *Bradyrhizobium* strains or species for soybean. Particularly in the last decade, the use of inoculants containing microorganisms of "different types" has expanded. The combination of strains or species acting in different microbial processes results in higher benefits and, ultimately, yields. For example, microorganisms affecting plant growth (*Bradyrhizobium* spp., *Rhizobium* spp.), phytohormone production (e.g., *Azospirillum* spp., *Pseudomonas* spp.), solubilization of phosphate (*Bacillus* spp.), or biological control (*Pseudomonas* spp., *Bacillus* spp.). The application of mixed inoculants is usually called co-

inoculation or mixed inoculation and it is currently possible to find co-inoculants for several crops in the market (Santos et al., 2019b).

The efficiency of co-inoculation is a result of many factors, such as the selection of appropriate strains, the cellular concentration of each one, the method of inoculation (applied to the seeds, foliar spray, in-furrow) and the plant genotype. Therefore, research is needed to generate knowledge aimed at the production of new formulations for commercial inoculants with mixed bacteria and on alternative methods of application of inoculants and microbial molecules (Fukami et al., 2016).

These ongoing research efforts are part of a broader global trend toward more sustainable agricultural practices, in which microbial inoculants play a key role. For instance, the first studies in Brazil focused on clover (*Trifolium* spp.) and alfalfa (*Medicago sativa*) crops intended for livestock production. In the 1960s, the application of rhizobia has also increased in soybean (*Glycine max*) and since then the application has spread to over 110 authorized strains of rhizobia (Bomfim et al., 2021). In 2018 the use of inoculants in Brazil covered approximately 78 % of the crop area (36.5 million hectares) (Santos et al., 2019b).

Another top country using bioinoculants is India (Samago et al., 2018), where the usage of biofertilizers has dramatically increased in the last 15 years. In the years 2020 and 2021, India over 134 thousand tonnes of solid carrier based biofertilizers and about 26,000 kilolitres of liquid biofertilizers (Garcha, 2023). Indian companies dominating the market in bioinoculant production include International Panaacea Limited, SOM Phytopharma Limited, Kan Biosys, Multiplex Biotech Private Limited Karnataka, Krishak Bharati Cooperative Limited (KRIBHCO) among others (Garcha, 2023).

Worldwide, another leading biofertilizer-producing company include Novonesis (Denmark), Symborg (Spain), Kiwa Biotech (China), Mapleton Agribiotech (Australia), Lallemand Inc. (Canada), or RizobacterArgentina S.A (Argentina) (Garcha, 2023).

2.2 PLANT GROWTH-PROMOTING RHIZOBACTERIA

In the soil, specifically in the rhizosphere, important and intensive interactions take place between the plant, soil, microorganisms, fungi and soil microfauna (Meena et al., 2017). Plant growth-promoting rhizobacteria (PGPR) are free-living bacteria colonizing the root surface and are involved in many beneficial activities contributing to plant growth. PGPR affect the soil by improving soil organic matter (SOM) and its mineralization by enriching the soil with nitrogen

and phosphorus nutrients, phytohormone synthesis, production of siderophores for binding toxic metals (cadmium, cobalt, etc.) and pathogen elimination, all of which help in soil fertility improvement and enhance the productivity of the soil environment (Ahemad & Kibret, 2014).

PGPR invade plant tissues and survive in intracellular spaces of the host plant while causing unapparent and asymptomatic infections. Generally, PGPR can be classified as extracellular plant growth-promoting rhizobacteria and intracellular plant growth-promoting rhizobacteria. Extracellular PGPR are found in the rhizosphere or in the root cortex, while according to their proximity to the plant root, they live near the roots but without contact, colonizing the root surface and sometimes living in intracellular spaces of the root cortex. Meanwhile, intracellular PGPR can enter plant cells and can produce specialized structures, called nodules (Meena et al., 2017).

Rhizobacteria associated with roots synthesize a large number of various biomolecules (hormone regulators, siderophores, hydrolytic enzymes etc.), which aside from the direct effect on plant physiology also improves soil health and quality. Following death, plant residues filled with organic compounds undergo decomposition and mineralization and lead to higher nutrient levels. Apart from soil mineralization, PGPR synthesize many growth-responsible agents (indole acetic acid, 1-aminocyclopropane-1-carboxylic acid deaminase), which ultimately affect plant root morphology. An important factor for the colonization of PGPR in the rhizosphere is soil moisture. Water content in soil affects the physiological state of microorganisms and plants, impacts respiration and is essential for maintaining the catalytically active state of soil enzymes. The positive effect of PGPR on root growth contributes to moisture retention. The production of small catechol molecules by PGPR leads to the enrichment of the iron in a form accessible for plant utilization. Some rhizobacteria have the ability to bind heavy metals (Cd, Pb) and remove phytotoxic substances and pathogens, which are all part of bioremediation and help to restore the soil quality for agricultural purposes (González Henao & Ghneim-Herrera, 2021; W. Schmidt et al., 2020). An overview of the mentioned PGPR properties are shown in Figure 1.

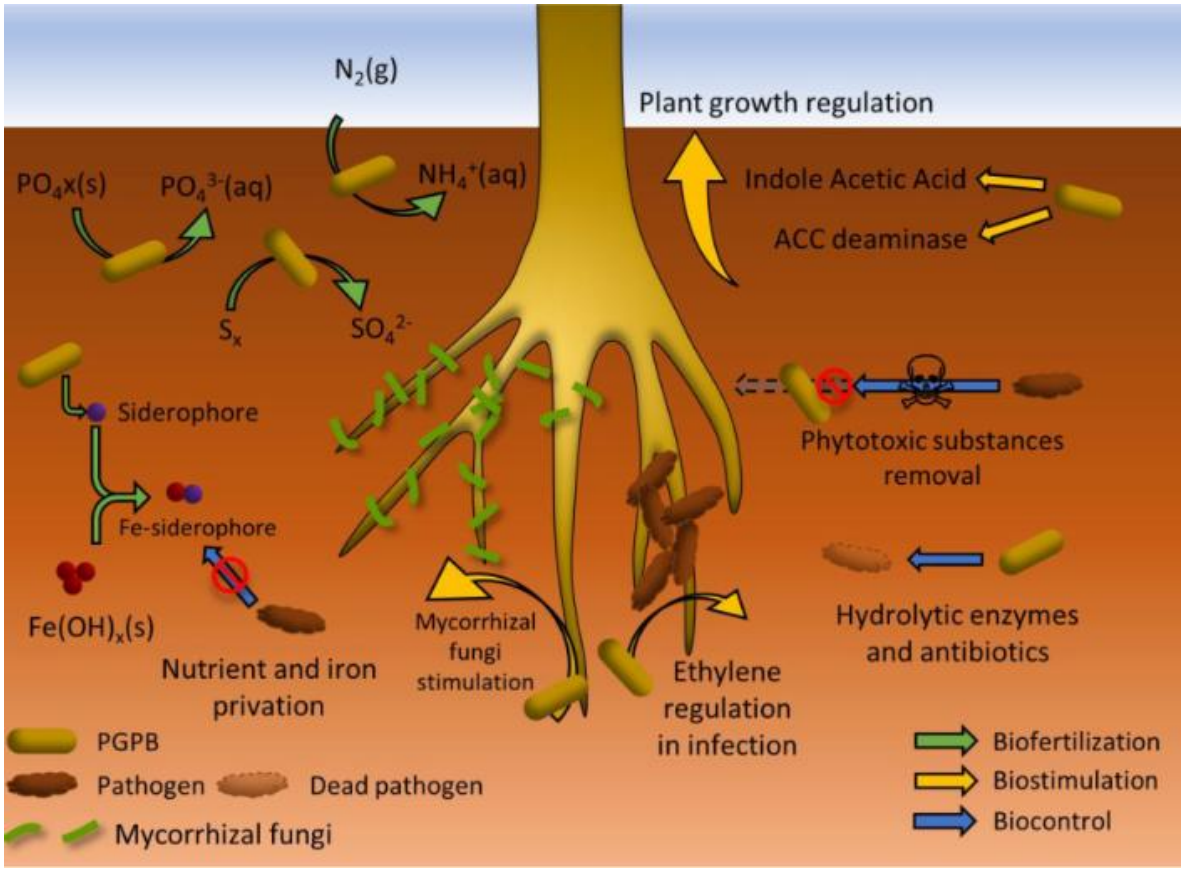

Figure 1 Mechanisms of plant growth-promoting effects in rhizosphere; Biofertilization mechanisms (*green arrows*)*, biostimulator mechanisms* (*yellow arrows*) *and biocontrol mechanisms* (*blue arrows*) *(Ferreira et al., 2019).*

2.2.1 Production of phytohormones

One of the direct mechanisms of how PGPR influences plant growth and development is the ability to produce precursors for plant hormones (phytohormones) such as indole acetic acid (IAA) and ACC deaminase, a precursor of ethylene. The first-mentioned hormone, IAA is synthesized by up to 80 % of rhizobacteria colonizing the seeds and root surfaces and it is the most common natural auxin with a positive effect on root growth (Shailendra Singh, 2015). In plants, IAA stimulates cell proliferation and enhances the plant's uptake of minerals and nutrients from the soil. Auxins affect plant cell division and differentiation, stimulate seed and tuber germination and increase the rate of xylem and root development (Etesami et al., 2009; Spaepen & Vanderleyden, 2011). Moreover, IAA as the most well-known auxin controlling processes of vegetative growth, initiates root formation and mediates the response to light, gravity and fluorescence. Pigment formation and biosynthetic pathways influenced by IAA have an impact on plant photosynthesis. The main precursor necessary of the biosynthesis of

IAA is the amino acid tryptophan, commonly found in root exudates (Etesami et al., 2009; Vessey, 2003).

Cytokinins and gibberellins are phytohormones influencing the elongation of stems and leaf growth and are produced by bacteria such as *Azotobacter* sp., *Bacillus subtilis*, *Pseudomonas fluorescens* or *Rhizobium* sp. (Hamzi & Skoog, 2015). However, according to Glick (2012) it appears that plant-growth-promoting rhizobacteria produce lower cytokinin levels compared to phytopathogens, making the stimulatory effect of the PGPR on plant growth less than the inhibitive effect of cytokinins produced by the pathogens (Glick, 2012; Zafar-ul-Hye et al., 2013).

The phytohormone ethylene is the only gaseous hormone, promoting root initiation, fruit ripening, stimulation of seed germination and other processes. Ethylene affects cell proliferation in the root architecture by inducing overproduction of lateral roots and root hairs with a subsequent increase in nutrient and water uptake. As it was already mentioned, the enzyme 1-aminocyclopropane-1 carboxylic acid (ACC) is a precursor for ethylene production, catalysed by ACC oxidase. Bacterial strains exhibiting ACC deaminase activity have been identified in a wide range of genera such as *Azospirillum*, *Bacillus*, *Burkholderia*, *Enterobacter*, *Pseudomonas* and *Rhizobium* (Ahemad & Kibret, 2014).

Microbially produced phytohormones are synthesized and released continuously, which contributes to greater effectiveness in plant growth (Shailendra Singh, 2015).

2.2.2 Nitrogen fixation

The role of nitrogen and its presence in the soil is very important, considering it belongs to one of the most vital nutrients for living organisms, including in our case plant growth and productivity. Although the amount of nitrogen in the atmosphere is about 78%, this form is inaccessible to growing plants, so the atmospheric nitrogen has to be converted into plant-utilizable form ammonia (NH_3) by biological nitrogen fixation (Gaby & Buckley, 2012). Some nitrogen-fixing microorganisms are capable of the biological conversion of atmospheric nitrogen into ammonia by using a complex enzyme system known as nitrogenase. Approximately two-thirds of globally fixed nitrogen is from microbial fixation, while the rest is synthesized industrially by the Haber-Bosch process. In addition, the biological nitrogen fixation by microorganisms represents an economically beneficial and environmentally friendly alternative to chemical fertilizers (Bhattacharyya & Jha, 2012; Galloway et al., 2008).

Generally, nitrogen-fixing microorganisms are categorized as symbiotic and non-symbiotic. Symbiotic bacteria form a symbiosis with leguminous plants and non-leguminous trees (such as members of groups *Frankia*, *Rhizobia*), whereas non-symbiotic bacteria are free-living bacteria in the soil and water (e.g. members of the genera *Azospirillum*, *Azotobacter*). However, non-symbiotic nitrogen-fixing bacteria provide only a small amount of the fixed nitrogen that the bacterially associated host plant requires. Symbiotic nitrogen-fixing rhizobacteria infect and establish symbiotic relationships with the roots of host plants, which requires and involves a complex interplay between host and symbiont resulting in the nodule formation, where the rhizobacteria colonize as intracellular symbionts. Nitrogen-fixing PGPR in non-leguminous plants are also called diazotrophs capable of forming a non-obligate interaction with the host plant (Ahemad & Kibret, 2014).

As it was mentioned above, the process of nitrogen fixation is carried out by an enzyme called nitrogenase complex. The complex consists of two-component metalloenzymes, from which one is the nitrogenase reductase with iron protein and nitrogenase with a metal cofactor. Nitrogen reductase provides electrons with high reducing power, while nitrogenase uses these electrons to reduce molecular nitrogen (dinitrogen N_2) to amonnia (NH_3) (F. V. Schmidt et al., 2024). Based on the metal cofactor three different nitrogen-fixing systems have been identified: molybdenum-, vanadium- and iron- nitrogenases. Among different bacterial genera, there are various nitrogen-fixing systems, nevertheless, most biological nitrogen fixation is carried out by the activity of the molybdenum nitrogenases (Rubio & Ludden, 2008).

Furthermore, it was discovered recently that all three nitrogenases can also reduce carbon monoxide (CO) to hydrocarbons (F. V. Schmidt et al., 2024).

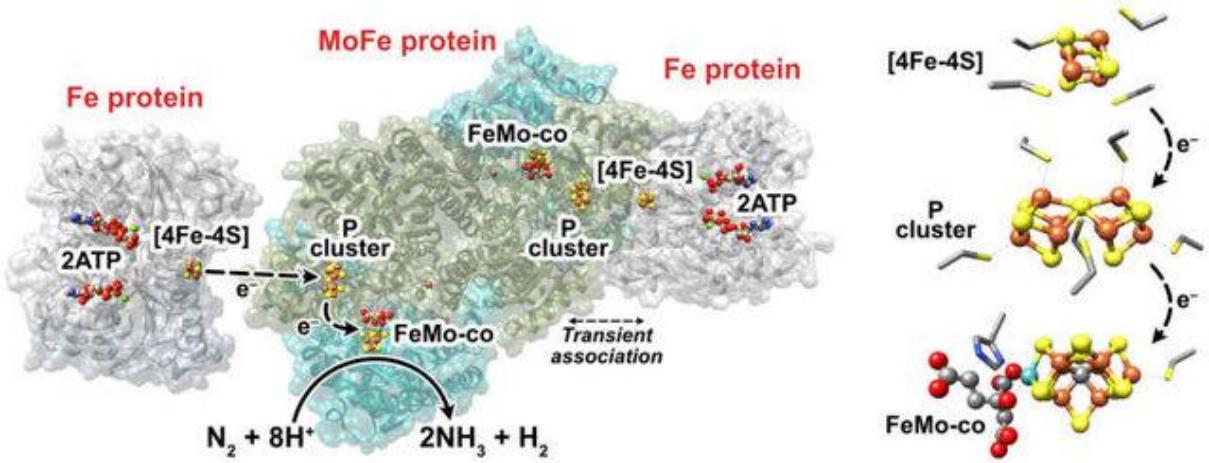

Figure 2 Representation of Mo-nitrogenase in Azotobacter vinelandii. The Fe proteins at both sides are shown in grey, while MoFe protein is shown in the middle (*in two subunits: yellowish-NifD, α-subunit; in light blue- NifK, ß-subunit*) *(Gu & Milton, 2020)*.

Nitrogenases have demanding biochemical requirements including oxygen sensitivity, a need for reductants (ferredoxin, flavodoxin), ATP and access to metals used in the assembly of the metalloclusters (Johnston et al., 2023). The genes for nitrogen fixation are found in both symbiotic and free-living systems. Nitrogenase genes include structural genes, genes involved in the activation of the Fe protein, iron-molybdenum cofactor biosynthesis, donation of electrons and necessary regulatory genes required for the synthesis and function of the whole enzyme. In diazotrophs, genes for nitrogen fixation are typically found in a cluster of around 20–24 kb with seven operons encoding 20 different proteins. The symbiotic activation of these genes in *Rhizobium* is dependent on low oxygen concentration, which is regulated by another set of genes known as fix genes, common for both symbiotic and free-living bacteria. The process of nitrogen fixation is highly energy-demanding, requiring at least 16 moles of ATP for every mole of nitrogen reduced. To meet energy demands, it is more effective if bacterial carbon resources are directed toward oxidative phosphorylation, which results in the synthesis of ATP, rather than the accumulation of storage compounds (Galloway et al., 2008; Goyal et al., 2021).

2.2.3 Phosphate solubilization

Phosphorus (P) is a macronutrient that plays the essential role in many metabolic processes. Phosphorus as a vital element can be found in biological molecules, including nucleic acids, co–enzymes, phosphoproteins and phospholipids. Therefore, it is one of the main limiting elements for biomass production, as a plant-available P represents only a small fraction of total

soil P (approximately 0.05 %). Phosphorus is one of the main limiting elements for biomass production in terrestrial ecosystems, therefore the addition of P-fertilizers is common and extensive, causing the ongoing eutrophication of continental and coastal waters (Tian et al., 2021). Therefore, the use of phosphate solubilizing microorganisms (PSMs) helps address the challenge by improving soil fertility and reducing the need for chemical fertilizers. PSMs can break down insoluble forms of phosphorus, such as phosphates, in the soil and convert them into easily absorbed, soluble forms available to plants (C. Wang et al., 2023).

Plant cells can absorb several forms of P, but the greatest part is absorbed mainly as anions, such as HPO_4^{2-} or $H_2PO_4^{2-}$ depending on soil pH. The concentration of soluble P in the soil solution is usually at levels varying from ppb in very poor soils to 1 mg/L in heavily fertilized soils, whereas insoluble phosphates generally account for 95 up to 99 % of total phosphorus in the soil (Kalayu, 2019). Among the whole microbial population in soil, P-solubilizing bacteria comprise 1 – 50 % of the total respective population. Apart from those species, symbiotic nitrogen-fixing rhizobia have also shown phosphate phosphate-solubilizing activity (KB et al., 2017).

In the soil, PSMs apply various approaches such as lowering soil pH, chelation and mineralization, to make phosphorus accessible to plants. The mechanism behind lowering pH is microbial production of organic acids or the release of protons. The production of organic acids together with the decrease of the pH by the action of microorganisms result in P solubilization. The most common organic acid produced by PSMs are gluconic and 2-ketogluconic, however, citric, lactic, oxalic, acetic, malic and more may also be synthetized by different bacterial species (Kalayu, 2019).

The hydroxyl and carboxyl groups of acids produced by PSMs chelate the cations bound to phosphates, leading to their conversion into soluble forms in the soils. These acids may compete for fixation sites of Fe and Al insoluble oxides, react with them and stabilize them, making them so-called “chelates” (Pradhan & Sukla, 2005).

The other mechanism of phosphorus solubilization is mineralization. Organic phosphate is transformed into utilizable form by PSMs through the process of mineralization, in the soils with an extensive amount of plant and animal residues, containing high levels of organic phosphorus. PSMs mineralize soil organic P by the production of enzymes such as phytase, hydrolysing organic phosphate compounds, while releasing inorganic phosphorus that can be absorbed by plants. Alkaline and acid phosphatases use organic phosphate as a substrate to

convert it into inorganic form. Mixed cultures of PSMs (e.g. *Bacillus* spp.) have shown enhanced efficiency in phosphorus solubilization due to synergistic interactions between different strains (Aseri, 2009; KB et al., 2017).

2.2.4 Additional benefits of plant growth-promoting bacteria

Production of Siderophores

Siderophores are low-weight molecules (range between 500 and 1500 Da) that exhibit high affinity and selectivity for binding ferric iron (Fe^{3+}). These compounds are produced by various microorganisms, including bacteria and fungi, as well as by certain gramineous plants, to facilitate the uptake of the iron and other metals from the soil (Hider & Kong, 2010). Under physiological conditions, Fe^{3+} ions are extremely insoluble (approximately 10^{-17} mol/L), making iron poorly bioavailable at circumneutral pH and thus insufficient for plant uptake (Ilbert & Bonnefoy, 2013; Meena et al., 2017).

Siderophores typically contain negatively charged oxygen atoms with a high electron density, which strongly attract for instance and for our focus– Fe^{3+} ions. The geometry of these molecules depends on the type of donor groups and the number of ligands they contain. Factors such as the nature of donor atoms, side chains and complexation energies all influence the stability of the siderophore. Moreover, the denticity (the number of donor atoms within a single ligand that can bind to the central iron ion) is a critical parameter for the stability of the chelated complex (Miethke & Marahiel, 2007).

In nature, the most common siderophores are hexadentate containing six containing six ligand donor atoms arranged in linear or cyclic structures. Soil pH also affects siderophore types: hydroxamate-type siderophores are more prevalent in neutral to acidic environments, while catecholate-type siderophores tend to dominate in neutral to alkaline conditions (Schalk et al., 2012). Several bacterial genera were described to produce siderophores, such as *Azotobacter*, *Azospirillum*, *Bacillus*, *Nocardia, Pantoea, Streptomyces,* etc (Ma, 2005). Under iron-limiting conditions, such as in the rhizosphere, bacteria like *Azotobacter vinelandii* excrete siderophores that chelate iron into stable complexes. These complexes are then transported into the bacterial cell via highly specific transport systems. *A. vinelandii* produces a range of siderophores, including monocatechols (e.g., 2,3-dihydroxybenzoic acid and aminochelin), bis(catechol) compounds (e.g., azotochelin), tris(catechol) structures (e.g., protochelin) and the yellow-green fluorescent pyoverdine-type siderophore known as azotobactin (Díaz-Barrera & Soto, 2010).

Pathogen and toxic metals antagonism

The PGPR mechanisms employ several mechanisms to deter phytopathogens, which can be classified as chemical, environmental, or metabolic strategies (Glick, 2012). Chemically, PGPR secrete a variety of microbial metabolites such as antibiotics and hydrolytic enzymes that directly inhibit the growth of plant pathogens and reduce the severity of infections (Table 1). These bioactive compounds are effective against both bacterial and fungal pathogens preventing root penetration and contributing to overall plant health. Environmentally, PGPR can outcompete pathogenic microbes through niche exclusion and resource competition, effectively displacing them from the rhizosphere. Metabolically, PGPR can trigger induced systemic resistance (ISR) or systemic acquired resistance (SAR) in plants, priming the plant's immune system and modifying hormonal pathways that influence plant defence responses (Iqbal et al., 2024). The role of PGPR in both natural and induced soil suppressiveness has been widely investigated, particularly for their capacity to enhance antibiotic production in the rhizosphere. Effective and sustained colonization by PGPR genera such as *Azospirillum*, *Bacillus*, *Burkholderia*, *Coniothyrium*, *Pseudomonas* and *Staphylococcus* has been shown to significantly improve plant growth and resilience over time (Bhat et al., 2023; González Henao & Ghneim-Herrera, 2021; Hakim et al., 2021; Meena et al., 2017).

Table 1 Mechanisms employed by plant growth-promoting rhizobacteria against pathogens (Bashan et al., 2014; Clauss & Koch, 2006; Haas & Défago, 2005; Pieterse et al., 2014; Ryu et al., 2003).

Mechanisms	Effect on plant growth
Competition for Fe^{3+} ions through siderophore production	Reduced disease incidence and severity and increase biomass of plants
Antibiotic production	
Production of small toxic molecules	
Production of hydrolytic enzymes	
Competition for nutrients, colonization sites and displacement of pathogens	
Induced and acquired systemic resistance	Make plant more resistant to infection by pathogens and increase biomass of plants
Change ethylene levels in plants	Reduce noxious effect of excess ethylene production in plants
Suppression of deleterious rhizobacteria	Increase biomass of plants

Furthermore, PGPR enhance soil quality and play a critical role in bioremediation by binding and detoxifying toxic metals such as arsenic (As), lead (Pb) and cadmium (Cd). The accumulation of these heavy metals in the soil is of significant concern, as even low concentrations can be highly toxic to living organisms and are considered one of the major threats to terrestrial and aquatic ecosystems (Atobatele & Olutona, 2015a).

To combat metal toxicity, microorganisms have evolved various adaptive strategies. These microbial detoxification mechanisms offer promising tools for the development of eco-friendly remediation technologies (Atobatele & Olutona, 2015).

PGPR contribute to metal detoxification through the release of intracellular and extracellular compounds such as organic acids, protons, metal-binding proteins, enzymes and siderophores, many of which are also present in root exudates. As illustrated in Figure 3 these molecules alter metal bioavailability by transforming toxic metal ions into less bioavailable or inactive forms. For instance, organic acids and protons produced by microorganisms help solubilize heavy

metals and convert them into forms less harmful to plants. In addition, phytochelatins, synthesized by plants and associated microbes, chelate heavy metals and facilitate their sequestration. PGPR also produce metal-detoxifying enzymes, such as methyltransferases, which can modify heavy metal compounds, thereby alleviating stress and enhancing plant tolerance (Devi et al., 2022).

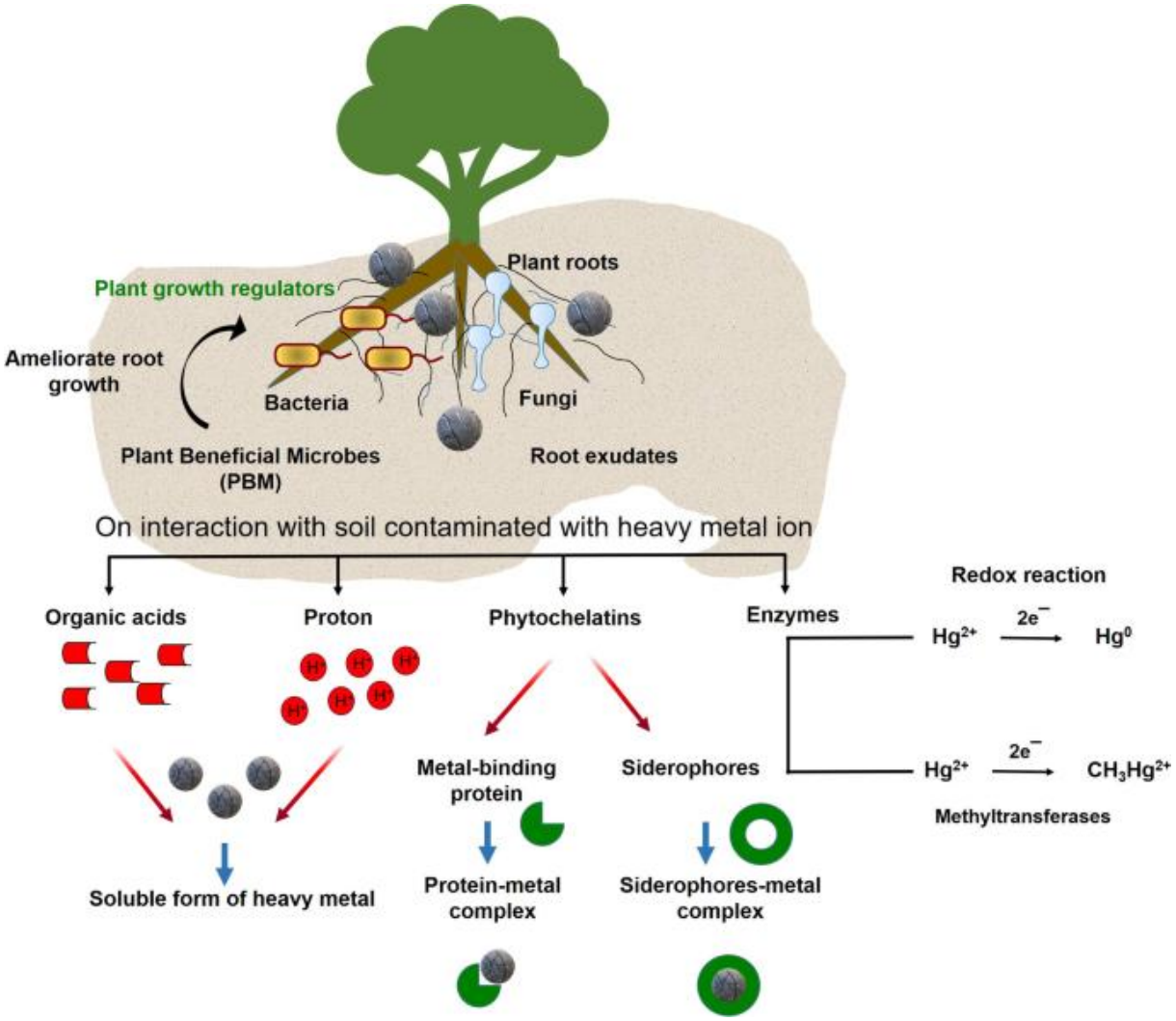

Figure 3 Overview of PGPR impacts on heavy metals in the soil by release of intracellular binding molecules– organic acids, protons, enzymes and phytochalins. Phytochelatins are able to form complexes with heavy metals and help in their detoxification leading to bioremediations of the soil. Siderophores may be used by PGPR to bind e.g. iron (Devi et al., 2022)

Moreover, numerous microbial species have developed cytosolic sequestration systems to evade heavy metal toxicity. In this mechanism, metal ions are absorbed into the microbial cell and subsequently transformed into less toxic or inert forms, minimizing their harmful effects (Ahemad, 2012). In addition to detoxification, microbes also enhance nutrient availability by

facilitating ion exchange and producing organic acids in both soil and soilless environments. These organic compounds contribute to the mobilization of chemically bound nutrients, making them more accessible for plant uptake and thereby improving overall soil fertility (Haferburg & Kothe, 2007).

2.3 THE USE OF EXTRACELLULAR POLYMERS AS BIOINOCULANT MATRICES

Extracellular polymers (EPs), also referred to as extracellular polymeric substances (EPS), are high-molecular-weight mixtures complexes of polymers secreted by a wide range of bacterial species. These species belong to both gram-negative (*Alphaproteobacteria*, *Betaproteobacteria* and the *Gammaproteobacteria* class) and gram-positive bacteria classes (*Bacilli*, *Clostridia*, *Actinomycetia*) (Netrusov et al., 2023). The production of EPS is important for bacteria for several reasons since they enhance their survival and adaptability in the environment. Also, EPS play a fundamental role in a formation of biofilm, cell aggregation and assist in adhesion mechanisms to biotic and abiotic surfaces through cell recognition and their cooperation (Prete et al., 2021). EPS provide diverse protective functions: they shield bacterial cells from extreme temperatures, high salinity, aridity, UV radiation, unfavourable pH, osmotic stress, phagocytosis and chemical stressors such as antibiotics, heavy metals and oxidants (Netrusov et al., 2023). In particular, EPS have shown cryoprotective effects for arctic bacteria (J. Wang et al., 2019). The specific mechanisms and protective roles of EPS will be further discussed in the following sections.

Bacteria produce various compounds marked as extracellular polymers, such as polysaccharides (alginate, chitosan, agar) and polyamids (poly-γ-glutamic acid) (Ghosh et al., 2021). The chemical structure is diverse, whereas the most dominant components of EPS are proteins and carbohydrates (75 – 90 %). The composition of EPS may be influenced by the function of the EPS, substrate and the type of microorganism producing it, with lipids, nucleic acids and humic substances affecting the EPS composition (More et al., 2014).

Extracellular polymers in the protection against abiotic and biotic stresses

The protective role of EPS is extensive and crucial for microbial survival under various environmental stresses. One of the key functions is drought protection, which is particularly important in the context of increasing climate variability. EPS possess a high water-holding capacity, enabling them to retain moisture effectively. Under drought conditions, EPS act like a protective sponge, shielding bacterial cells from desiccation. This moist layer not only

preserves water but also provides a reservoir of nutrients, helping bacteria to survive during dry periods and allowing time for metabolic adjustments to environmental stress (Costa et al., 2018).

EPS also play a significant role in tolerance to salt stress, benefiting not only microorganisms but also their associated host plants. EPS produced by NaCl-tolerant microbial isolates can reduce sodium (Na^+) uptake by binding and immobilizing Na^+ ions, thereby lowering their availability to plant roots. This action helps prevent nutrient imbalance and mitigates osmotic stress, both of which are critical for the survival of microorganisms under saline conditions. As a result, plants benefit from improved ion homeostasis and enhanced stress tolerance (Upadhyay et al., 2011).

Temperature extremes, both high and low, represent significant challenges for microbial survival and EPS contribute substantially to microbial resilience under such conditions. As previously noted, EPS serve as cryoprotectants, especially for sea-ice microorganisms, helping to prevent cellular damage caused by freezing. In fact, high concentrations of EPS have been observed in Antarctic bacterial communities, where they not only shield microbes from physical damage and desiccation, but also act as barriers against harmful contaminants such as heavy metals. This multifunctional protection enhances microbial survivability in cold and chemically extreme environments (Lo Giudice et al., 2020). On the other hand, only few studies have been conducted on the relationship between EPS and heat resistance. Research of *Metallosphaera sedula*, extremely thermoacidophile archae, proving that secretion of EPS improves heat resistance of microorganism (Yu et al., 2019).

In a biofilm immobilized by EPS, cells are held in proximity, facilitating intense interactions and formation of synergistic micro-consortia. This close association also provides a continuous source of carbon-, nitrogen- and phosphorus-containing compounds to support the biofilm community (Flemming & Wingender, 2010). In this complex system, EPS help retain extracellular enzymes that break down compounds outside the cell, capturing molecules from the surrounding water and making them available as nutrient and energy sources (Costa et al., 2018).

Moreover, EPS can adsorb not only nutrients but also bind or entrap metal ions, clay minerals, colloids and oxides, playing an important role in environmental bioremediation. The factors influencing metal adsorption by EPS include the nature of binding sites and their chemical structure, pH, metal concentration in the environment, ionic strength, molecular weight and

degree of branching of EPS (Costa et al., 2018). The amphiphilic properties of EPS are key to heavy metal adsorption, as polyvalent metal ions can bind to both proteins and carbohydrates within the EPS matrix. The ratio of protein to carbohydrate in EPS is often used as an indicator of adsorption capacity. For example, the adsorption of divalent ions such as Cu^{2+}, Cd^{2+} and Pb^{2+} is generally higher in EPS with a greater protein-to-carbohydrate ratio, whereas Zn^{2+} tends to preferentially bind with carbohydrates (Wei et al., 2017).

Structurally, extracellular polymers can be classified as homo-polymers or hetero-polymers based on their subunit composition. Homo-polymers consist of identical monomers, such as the homopolysaccharide cellulose, while hetero-polymers are composed of two or more different monomers (monosaccharides in the case of carbohydrates), such as alginate or xanthan (Z. Wang et al., 2023).

Alginate as a representant of extracellular polysaccharides

This work will primarily focus on polysaccharides, specifically alginate, although other common and widely used polymers such as cellulose and xanthan will also be mentioned. Alginate is a well-known biopolymer predominantly produced by brown algae. It is composed of two monomeric subunits: β(1,4)-D-mannuronic acid (M) and α(1,4)-L-guluronic acid (G). as illustrated in Figure 4. The structural composition of alginate is influenced by environmental factors such as oxygen availability, pH and temperature (Silva et al., 2017). Different species of brown seaweed produce alginates with varying proportions and sequences of M and G residues, which determine the molecular weight, physical properties and functional characteristics of the polymer and its derivatives. Interestingly, certain bacteria like *Azotobacter* and *Pseudomonas* are also capable of producing alginate. Bacterial production offers the advantage of tailoring the polysaccharide's quality and properties - such as the M/G ratio and molecular weight- which is often difficult to achieve through seaweed extraction (Kivilcimdan Moral & Yildiz, 2016).

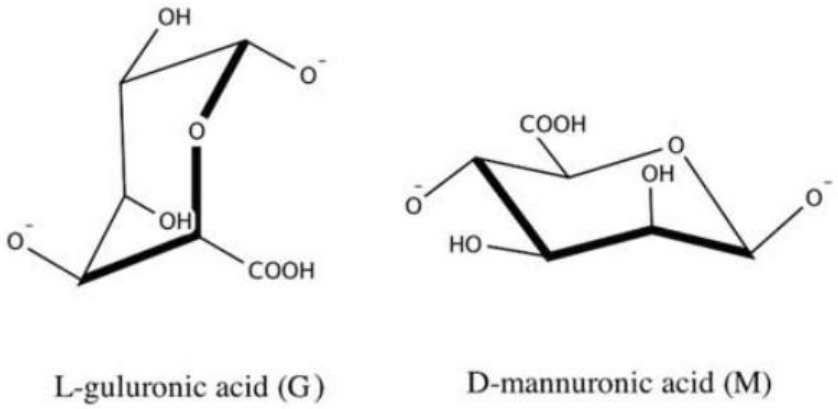

Figure 4 Structure of two alginate subunits, which form polymer chains in alginate: L-Guluronic acid (*left*) *and D-mannuronic acid* (*right*) *(Ching et al., 2017).*

These monomers (M, G) of alginate link together to form polymers with varying qualities and gelation capacities. The basic structure of alginate consists of linear, unbranched chains of these monomers arranged in distinct blocks: regions of consecutive M residues (M-blocks), consecutive G residues (G-blocks) and alternating sequences of M and G residues (MG-blocks) (Donati & Paoletti, 2009). The polymer may contain segments exclusively composed of one monomer type or a combination of alternating residues. Commercially available alginates, typically derived from seaweed, are found in the form of their sodium, potassium, or ammonium salts. The molecular weight of alginate usually ranges from 60 to 700 kDa but can exceed this range depending on the specific biosynthetic conditions (Ching et al., 2017b).

However, when comparing the costs, alginate derived from seaweed dominates industrial production, while bacterial alginate remains less competitive in the market. A key factor influencing the price of bacterial alginate is the carbon source used for production. For years, research on bacterial alginate synthesis has primarily focused on using simple and readily assimilable carbon sources such as glucose and sucrose, which bacteria efficiently convert into the polysaccharide product (Ching et al., 2017).

Gel forming properties of extracellular polymers

Various representatives of polysaccharides (alginate, cellulose, chitosan) and proteins (collagen) have gelation properties and are used in hydrogel production. Hydrogels are polymers forming three-dimensional network porous structure. The porous structure of hydrogels, their high permeability, softness, mechanical strength allows their utilization as a material for cell adhesion and tissue engineering (S. Wang et al., 2023). Moreover, water is an important part of hydrogels, typically ranging from 70 to 90 % by weight, whereas in some

cases it may reach up to 99 % by weight (Hoare & Kohane, 2008). In hydrogels, water exists in three forms: bound, intermediate and free water. Bound water forms hydrogen bonds with hydrophilic groups in the polymer chains, while free water does not interact with the polymers. Intermediate water interacts weakly with the polymer. The relative amounts of these three types of water depend on factors such as the overall water content, the polymer type, its side chains and the method of cross-linking during gelation. During dehydration, the shrinkage of the polymer network is largely influenced by the hydrogen-bonding structure among these types of water (Naohara et al., 2022).

Gelation of hydrogels, the process of a network formation of polymer chains, may vary according to the hydrogel type and the targeted properties of the material. The formation of polymer network occurs though chemical process (condensation, addition polymerization, or by chemical reaction with linear polymer precursor), or physical process (change of pH, temperature or ionic gelation). During a condensation reaction, where molecules with three or more reactive groups, such as –OH groups, react with a networking agent. In the case of addition polymerization, free radical reacts with a double bond, causing the creation of another bond between monomers. When there are multiple double bonds in the molecule, branching is possible. The third type of reaction forms structures with side chains and involves a chemical reaction starting with a linear polymer precursor, which becomes networked or vulcanized by forming chemical bonds (Larson R.G, 1999).

Physical gelation forms intermolecular interactions, different from chemical bonds, causing the formation of a network structure by van der Waals bonds, electrostatic interactions and hydrogen bonds. For instance, the gelation mechanism of thermo-responsive hydrogels is based on the dissolution of the gelling material at elevated temperatures. During cooling, double helices are formed, followed by aggregation of these helices. Stabilization of the double helix is achieved through hydrogen bonding interactions between the polymer chains (Karoyo & Wilson, 2017). Nevertheless, ionic gelation, a specific type of physical gelation, due to its importance and the focus of this thesis, will be mentioned further (Larson R.G, 1999).

The ability to form an ionic gel in the presence of multivalent cations (Ca^{2+}, Mg^{2+}, Ni^{2+}, Mn^{2+}) is widely utilized in the encapsulation of bioactive substances in the food industry, drugs in the pharmaceutical industry and cell immobilization in the biotechnology industry. For the alginate, for which ionic gelation is typical, the affinity towards cations is directly dependent on the number of G-blocks present in the alginate structure. For the medical and environmental

applications, the use of highly concentrated solution with cations such as Pb, Cu and Cd is limited. Therefore, the most commonly used reagent for ionic gelation is calcium chloride because of its availability and non-toxicity. However, a major limitation of the calcium alginate gel is its instability in the presence of Ca-chelators such as citrates, phosphates, lactates and carbonates. Cooperative binding of divalent cations and the G-block regions of the polymer produces gels. The mechanism of gelation is induced by the addition of bivalent/multivalent ions, such as Ca^{2+} into the alginate polymer causing the binding of two G chains on opposite sides and forming a diamond-shaped hole. This shape consists of a hydrophilic cavity that binds the Ca^{2+} ions by multiple coordination using the oxygen atoms from the carboxyl groups. This tightly bound polymer configuration results in the formation of a junction zone known as 'egg box' (demonstrated in Figure 5). Each cation binds to four G residues in the egg-box formation to form a network of these interconnected regions. It has been shown that in the case of Ca^{2+}, the formation of a stable junction requires eight to twenty adjacent G residues (Sosnik, 2014; Yang et al., 2013).

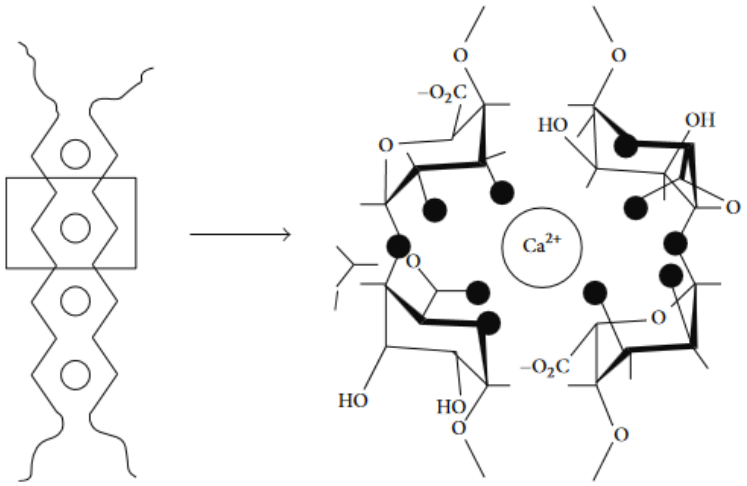

Figure 5 Polymeric chains of alginate, consisting specifically of guluronic subunits react with divalent ions of calcium and create 'egg-box' structure. Reproduced from (Sosnik, 2014).

As mentioned earlier, cations can also bind to block sequences other than G-blocks in alginate. For example, binding studies have revealed that Ca^{2+} is capable of binding to both G and MG blocks, Ba^{2+} to G and M blocks and Sr^{2+} to G-blocks only (Donati & Paoletti, 2009). Alginate is also able to form gels in the presence of trivalent cations such as $Al^{3+}$and Fe^{3+} and the binding of trivalent cations to alginate is generally enhanced compared to that of divalent cations.

Trivalent cations interact simultaneously with three carboxyl groups of different alginate biopolymer at the same time and form a bonding structure, which results in a more compact gel network (Yang et al. 2013).

The formation of gel particles can occur by either external or internal gelation depending on the different methods by which cross-linking ions are introduced to the alginate polymer. The internal gelation method includes the controlled exposure of alginate to cations to achieve a homogeneous distribution of alginate in the hydrogel. Gelation occurs simultaneously at multiple locations (both internal and external of hydrogel particles) resulting in a homogeneous hydrogel structure (Phillips & Williams, 2009). Inactive forms of Ca^{2+} (such as $CaCO_3$ or $CaSO_4$) are mixed with sodium alginate solution and extruded into oil followed by acidifying the mixture in order to release Ca^{2+} from insoluble compounds. Acidification can be achieved immediately by the direct addition of mineral acid (glacial acetic acid) or in a controlled fashion using a slowly hydrolyzing lactone (D-glucono-d-lactone (GDL) (Ching et al., 2017; Donati & Paoletti, 2009). The external method (diffusion-controlled) of gelation is rapid and gel formation is instantaneous. Cations diffuse from a higher concentration region into the interior of the alginate particle. Rapid and instantaneous gelation allows alginate to be used in cell or bioactive immobilization, where the cells or bioactive substances are entrapped in a single alginate gel bead. Moreover, rapid gel formation is also important in applications where a certain size and shape of the hydrogel is required (medicine) (Ching et al., 2017).

The usage of acids in the gelation affects the pH of the solution, bringing it down below the dissociation constant (pKa) of the polymer. In the case of alginate, M and G residues have pKa of 3.38 and 3.65, respectively. Hence, alginate is negatively charged across a wide range of pH values (Phillips & Williams, 2009). A decrease in the pH of the alginate solution can occur in two ways. A rapid pH decreases result in the precipitation of alginic molecules as aggregates while a slow and steady drop in pH results in the formation of a continuous alginic acid bulk gel. In contrast to ionic gels, acid gels of alginate are stabilized by hydrogen bonding and M-blocks residues have been shown to play a part in the gelation process. Nevertheless, acid gels are very similar to ionic gels and gel strength is correlated to the G-block content in the polymer chain. However, alginic acid gels are less studied compared to ionic gels due to their limited applicability (Draget et al., 2006).

Industrial applications of extracellular polymers

Extracellular polymers, especially polysaccharides are widely used in the food industry, wastewater treatment and medicine due to their biocompatibility, hydrophilic character and thickening and gelling agent properties. For instance, polysaccharides such as alginate, agar and carrageenan have application potential in the food industry as a stabilizer, gelling agent, thickener and film-forming agent. In addition, alginate and its modified forms serve as a water-soluble dietary fibre because it does not contribute a significant nutritional value or calories as it passes through the human digestive system (Jiao et al., 2019). Moreover, polysaccharides such as alginate can be used in wastewater treatment to remove various pollutants such as heavy metals (cadmium, chromium, copper, etc.), dyes and phenolic compounds (Bashan, 2014). The application of polysaccharide may be found in the cosmetic industry, applying them to toothpastes, shampoo aids, mask shapers, etc. This cross-linking of polysaccharides and their ability to form hydrogels are used in the pharmaceutical industry as drug carriers (Pérez-Ramos et al., 2016). The usage of extracellular polymers as suitable carriers for microbial strains is also common. These carriers provide stabilization and protection of microbial strains during transport and storage and secure the continuous release of microorganisms, which may be important in the pharmacological and agricultural industry (Chaudhary et al., 2020).

2.4 *AZOTOBACTER VINELANDII* - PLANT GROWTH-PROMOTING BACTERIUM

The microorganism, on which this work will be focused on, is a gram-negative bacterium *Azotobacter vinelandii* belonging to the group of plant growth-promoting bacteria. *Azotobacter* spp. live as a free-living saprophyte in soil, fresh water and marine environments. *A. vinelandii* was adopted as a model organism for different metabolic pathways, such as the study of aerobic nitrogen fixation, respiration, microorganism physiology and enzyme kinetics (Noar & Bruno-Bárcena, 2018). Multiple important discoveries were made by studying the genus *Azotobacter,* including Lineweaver-Burk kinetic model, studying how the inhibitor competes with enzyme activity and genetic code (Christiansen et al., 2000; Setubal et al., 2009). However, the most interesting characteristics, which have been studied, are *Azotobacter´*s nitrogenase activity and aerobic physiology. The bacterium is characterized by its high respiration rate compared to other prokaryotes under similar growth conditions and even when it is exposed to high oxygen concentration, it also fixes nitrogen (N_2). Under conditions of nitrogen fixation and high oxygen concentration, the main mechanism proposed to prevent nitrogenase inactivation is respiratory

protection. Due to the production of siderophores, phytohormone precursors and the ability to fix nitrogen, *Azotobacter vinelandii* belongs to the group of plant growth-promoting rhizobacteria, hence, it stimulates plant growth and enriches the soil with nutrients (Noar & Bruno-Bárcena, 2018; Urtuvia et al., 2017). All the mentioned biotechnological properties will be described further in the following subchapters.

Furthermore, the importance of choosing *A. vinelandii* as a working microbe in the presented thesis, is not only due to its plant growth-promoting properties, but also because of its ability to produce two biopolymers of special importance for the intended application: extracellular alginate, a polysaccharide described earlier and intracellularly accumulated polyhydroxyalkanoates.

Polyhydroxyalkanoates (PHA) are polyesters of hydroxyacids, accumulated in intracellular granules of various bacterial species (e.g. *Cupriavidus*, *Burkholderia*, *Hallomonas*, *Psuedomonas*, *Rhodospirillum*), cyanobacteria (e.g.*Synechococcus*, *Synechocystis*) and/or archaebacteria (e.g *Haloferax*) (Koller et al., 2017; Obulisamy & Mehariya, 2021). Bacterial cell produces PHA in an environment with a surplus of a suitable carbon source and a limitation by a nutrient such as nitrogen, or phosphorus, improving the microorganisms's stress tolerance. Metabolic pathways for PHA production will be described later, nevertheless, the key enzymes such as PHA synthase, PHA depolymerase and phasins (structural PHA granule associated proteins) play an important role in PHA synthesis (Bresan et al., 2016).

2.4.1 Respiration in *Azotobacter vinelandii*

Azotobacter sp. has been widely studied due to its ability of nitrogen fixation by nitrogenase. To protect nitrogenase from inactivation by oxygen, *Azotobacter* has developed several adaptive mechanisms, among which "respiratory protection" is one of the most critical and well-characterized (Dixon & Kahn, 2004). Respiratory protection involves an increase in the cellular respiration rate under high oxygen concentrations during diazotrophic growth, effectively reducing intracellular oxygen levels and protecting nitrogenase activity (Poole & Hill, 1997). The respiratory chain components involved include cytochrome bd oxidase and type II NADH dehydrogenase (NDH II), which play essential roles in this protection mechanism (Castillo et al., 2020).

The electron transport chain of *Azotobacter vinelandii* is branched, containing multiple terminal oxidases that allow the bacterium to adapt efficiently to fluctuating oxygen levels in its environment (Reed et al., 1994; Cotruvo & Stubbe, 2011). Electrons donated by substrates such

as NADH and L-malate initiate the respiratory chain, while NADPH indirectly contributes electrons via the transhydrogenase enzyme, which transfers reducing equivalents to NADH (Thorneley & Lowe, 1985). These electrons travel through ubiquinone (Q8) along two main pathways: one involving cytochromes b and c, terminating in a hem-copper oxidase with high oxygen affinity but lower activity, which predominates under low-oxygen conditions (Reed et al., 1995); the other, a faster quinol oxidase pathway involving cytochrome bd oxidase, characterized by lower oxygen affinity and reduced ATP yield, yet crucial under high-oxygen or oxidative stress conditions (Poole & Hill, 1997; Cotruvo & Stubbe, 2011).

Importantly, although cytochrome bd oxidase is often considered less coupled to ATP synthesis, evidence suggests it may still contribute to proton motive force generation (Giuffrè et al., 2014). *A. vinelandii* dynamically regulates the use of these two branches in response to environmental redox conditions, utilizing cytochrome bd oxidase to protect nitrogenase under oxygen-rich, potentially toxic conditions, while favouring the b/c branch when oxygen levels are low (Reed et al., 1995). This flexible respiratory strategy is a key adaptation that allows *Azotobacter* to thrive in complex redox habitats, maintaining nitrogen fixation even in fluctuating oxygen environments (Kennedy et al., 1997). The schematic representation is shown in Figure 6).

Increased production of carbon dioxide and elevated respiration rates lead to higher aldolase activity, which channels carbon through the pentose phosphate pathway. This redirection of metabolic flux affects both the biomass yield and specific growth rate, as energy and carbon are diverted toward respiratory protection rather than other metabolic functions (Noar & Bruno-Bárcena, 2018).

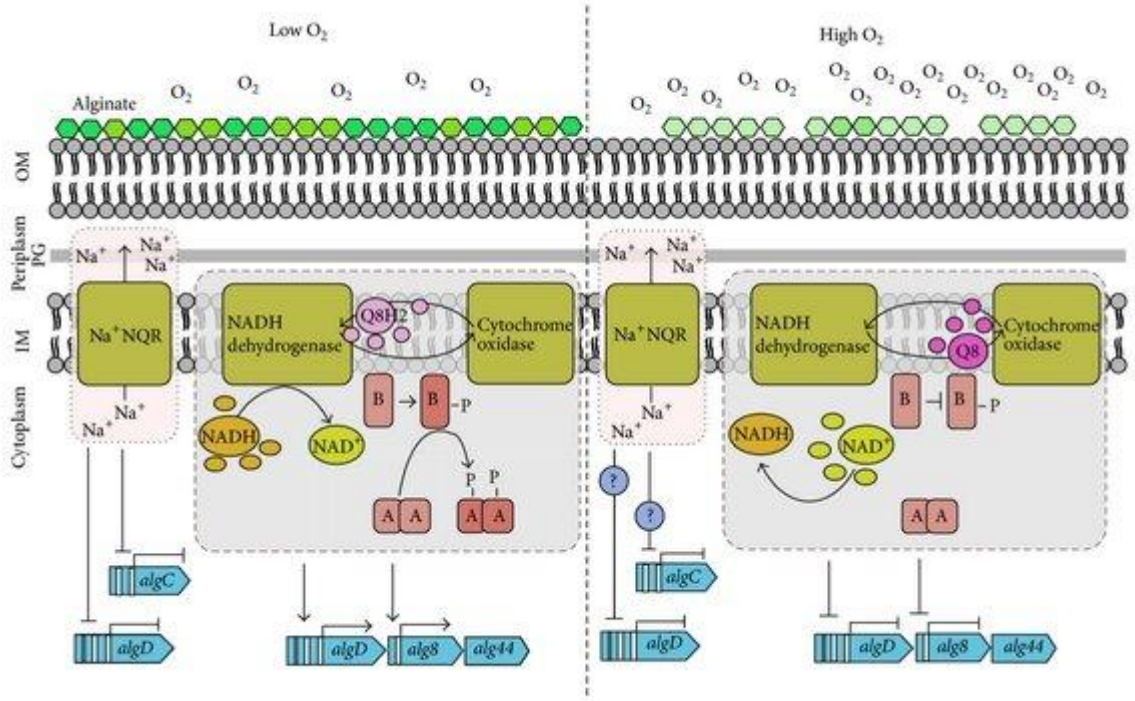

Figure 6 Schematic of Oxygen-Dependent Gene Regulation in Azotobacter vinelandii: low (*left side*) *oxygen and high* (*right side*) *oxygen levels influencing gene expression via two systems: Under low oxygen* (*left*), *reduced quinones* (*$Q8H_2$*) *activate ArcB, leading to ArcA phosphorylation* (*ArcA-P*), *which in turn activates algD, alg8 and alg44. This promotes alginate production, shown as green polysaccharides. Under high oxygen* (*right*), *oxidized quinones* (*Q8*) *inhibit ArcB, preventing ArcA activation and gene expression. Additionally, Na^+NQR may repress algC and algD, although this mechanism is not fully understood. As a result, alginate synthesis is reduced, depicted by faded polysaccharide chains (Castillo et al., 2020).*

2.4.2 Nitrogenase activity in *Azotobacter vinelandii*

In the subchapter 2.2.2, general information has already been mentioned about the nitrogenase complex. The effectiveness and complexity of the whole metabolic process depend on specific regulations influenced by the presence or absence of different metals (Mo, V and Fe). For instance, the presence of molybdenum represses the activity of V- or Fe- nitrogenases, though it activates the activity of Mo-nitrogenase and in reverse. If the bacterial culture exhausts its supply of Mo and V are not present, the bacterium *A. vinelandii* depends on the Fe-nitrogenase to grow. Regarding fixed nitrogen sources, *A. vinelandii* is capable of using both inorganic

sources (such as ammonium or nitrates) and several organic sources (aspartate, glutamate, urea, etc.) (Noar & Bruno-Bárcena, 2018).

Nitrogenase activity may be repressed by the presence of nitrogen compounds in the environment, such as ammonium salts or nitrate salts, especially when cells are pre-adapted to them, or even organic compounds (e.g aspartate, adenine). The mechanism responsible for shutting off nitrogenase activity, which is almost immediate, appears to be a decrease in proton motive force, restricting the access of nitrogenase to reducing equivalents it requires. Factors that modify the force of repression include the amount of oxygen and the potential respiratory rate (too little oxygen, or too much without an adequate increase in respiration, increases nitrogenase repression). High pH also enhances repression, providing supporting evidence for a mechanism involving the proton motivation force. *A. vinelandii* does not appear to store nitrogenase protein inactivated by fixed nitrogen-induced regulation over long periods (unlike *Rhodospirillum rubrum* stores nitrogenase by ADP-ribosylation), hence, the inactive protein is degraded in *A. vinelandii* (Ponnuraj et al., 2005).

All nitrogenase reductase (DNR) versions can be irreversibly inactivated by oxygen and its reactive species, preventing *A. vinelandii* from growing diazotrophically. As mentioned above, the bacterium uses various strategies to protect its enzymes from oxygen. Like most aerobes, *A. vinelandii* produces superoxide dismutase (SodB), while the production of SodB is proportional to oxygen exposure, the same as catechol siderophores. In strains that produce siderophores, the polysaccharide alginate may limit exposure to oxygen. There is evidence that DNR itself can directly reduce oxygen, in the effect known as 'auto-protection' (Thorneley & Ashby, 1989).

Furthermore, *A. vinelandii* employs a strategy called conformational protection, in which a small iron-sulfur protein, called FeSII or Shethna protein, binds to DNR and temporarily inactivates it in a reversible manner. Reactivation of DNR occurs once oxygen is no longer a threat to the nitrogenase complex. Thus, under sudden oxygen stress or carbon substrate depletion, *Azotobacter* ceases to proliferate (Dingler & Oelze, 1985; Franke et al., 2025).

2.4.3 Polyhydroxyalkanoates

Polyhydroxyalkanoates (PHA) are polyesters of hydroxyalkanoic acids, which are produced and accumulated by numerous prokaryotic microorganisms (bacteria, cyanobacteria and archaea) in the form of intracellular granules. The primary biological function of PHA is the storage of energy, carbon and reducing power, playing a key role in the survival of cells under

starvation conditions and nutrient limitations, such as nitrogen and phosphorus. However, the presence of PHA granules in bacterial cells also enhances their robustness against various external stress factors such as UV radiation, higher or lower temperature, oxidative stress and osmotic imbalance (Obruca et al., 2016). The presence of PHA in bacterial cells substantially enhances their ability to maintain cell integrity when suddenly exposed to stress factors (osmotic pressure, UV radiation). PHA can serve as chemical protection, shielding proteins and other biomolecules from denaturation by extreme temperature, heavy metals or oxidative stress and can act as a highly efficient cryo-protectant (Obruca et al., 2018; Sedlacek et al., 2019). For instance, in the case of the non-halophilic bacterium *Cupriavidus necator*, the presence of PHA reduced plasmolysis-induced cytoplasmic membrane damage during osmotic up-shock. In contrast, sudden induction of osmotic up-shock and subsequent down-shock resulted in massive hypotonic lysis of cells lacking PHA granules (Sedlacek et al., 2019).

Furthermore, the biocompatibility, biodegradability and renewable origin of PHA have attracted considerable attention as promising "green" alternatives to petrochemical polymers. However, commercial production of PHA is scarce, especially due to high production costs. Biotechnological processes for PHA production are focusing on reducing costs, for instance, by using cheap waste substrates (such as molasses, bran and brew's span grains) as carbon sources (Koller, 2019).

Structure and composition of polyhydroxyalkanoates

The number of carbon atoms in the polymer and the length of the polymeric chain categorize PHA into three groups: common PHA with short-chain length (scl-PHA), medium-chain length (mcl-PHA) and extremely rare long-chain length (lcl-PHA) PHA (Kunasundari & Sudesh, 2011). Scl-PHA contain 3 to 5 carbon atoms per monomer unit, while mcl-PHA consist of 6 – 14 carbon atoms per unit. Polymer chains consisting of 15 and more carbon atoms in every unit do not occur frequently (Tan et al., 2014). To date, at least 150 different monomers possessing various structures have been found (Amstutz et al., 2019).

Copolymers of PHA may include scl-PHA and mcl-PHA monomers such as 3-hydroxybutyrate, 3-hydroxyvalerate, 3-hydroxyhexanoate and 4-hydroxybutyrate (G. Q. Chen & Wu, 2005). Blends of PHA with short and long-chain lengths are superior for industrial uses because of their suitable physical properties such as crystallinity, elongation to break and more. The low substrate specificity of some PHA synthases (from various bacteria) supports the variety of biosynthetic PHA, which results in the formation of monomers having unusually branched,

unsaturated or aromatic side groups (Steinbuchel et al., 1995). With the addition of supplemental compounds or carbon sources, containing substituted side chains, functional groups (e.g hydroxyl, carboxylic, epoxy, phenoxy groups and halogens) can be introduced into the side chain (Shahid et al., 2021).

PHA is synthesized by many types of bacteria and stored as in the form of intracellular granules in bacterial cells. The surface layer of the granule, shown in Figure 7, is free of phospholipids and consists of proteins distributed across it, known as phasins. Phasins are thought to be non-catalytic proteins consisting of hydrophobic and hydrophilic domains, where the hydrophobic domain binds to the PHA surface of the granules. The amphiphilic coating of phasins stabilizes PHA granules and prevents them from aggregation (Shahid et al., 2021).

In the centre of the PHA granules are localized PHA molecules and most likely also a small amount of "intra-granullar" water. The presence of residual water inside the PHA granules was also confirmed experimentally by Barnard and Sanders already in 1989 (Obruca et al., 2020). Moreover, the question of whether the intracellular polymer exists in a crystalline or amorphous state had been a major interest. The analysis by Steinbuchel (1998) demonstrated that the polymer within the cell behaves like an elastomer. The authors supported this conclusion with X-ray diffraction analysis of PHA-producing bacteria, which showed an absence of a significant amount of crystalline polymer in the cells (Amor et al., 1991; Steinbüchel & Füchtenbusch, 1998).

In conclusion, within bacterial intracellular granules, native PHA is found in a thermodynamically unstable amorphous state, although this state can be altered by certain physical or chemical treatments (e.g. freezing, centrifugation, extraction) (Sedlacek et al., 2019).

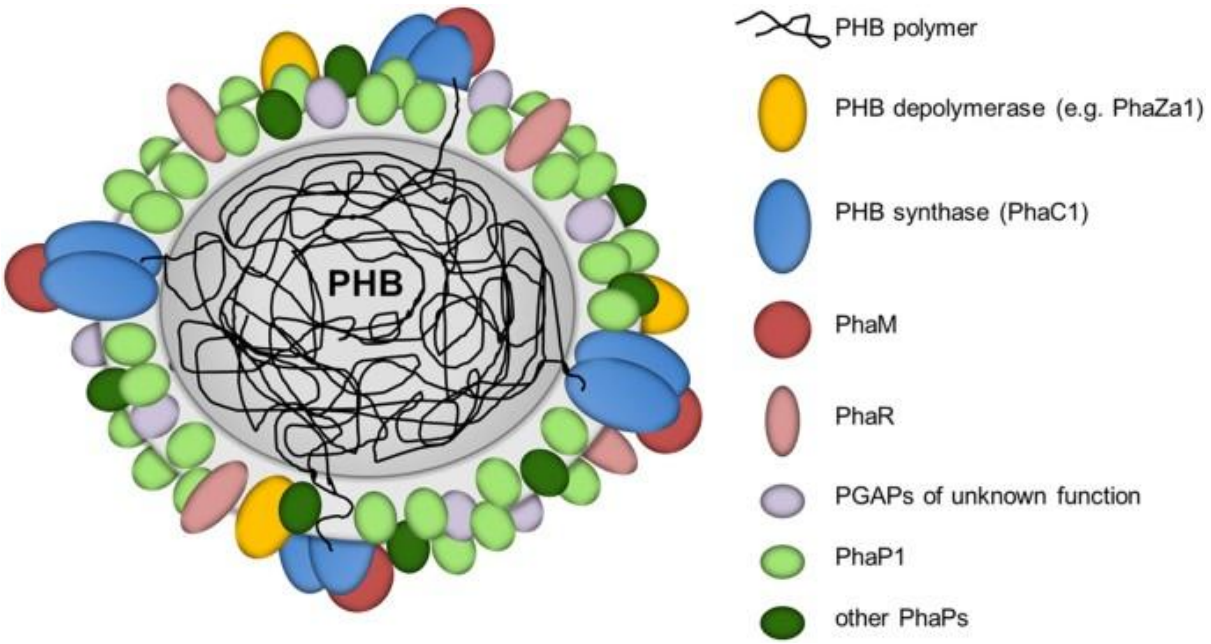

Figure 7 Polyhydroxyalkanoate granule; The presently known PHB granule associated proteins (*PGAPs*) *are symbolized by differentially coloured globules. The polymer chains of PHB are inside the granule, whereas on the surface are phasins* (*proteins stabilizing the structure and enzymes*) *PHB synthase and PHB depolymerase. The dimension of the surface layer is enlarged relative to the polymer core for better visibility (Bresan et al., 2016).*

Role of polyhydroxyalkanoates in bacterial cell stress survival

The results of the study by Sedlacek and colleagues confirmed the fundamental importance of PHA granules, which also have practical biotechnological significance. This is due to PHA-rich bacterial cells are resistant to osmotic imbalances, so they could be utilized in-situ bioremediation technologies or during enrichment of mixed microbial consortiums in PHA producers under conditions of fluctuating salinity (Sedlacek et al., 2019).

Research by Novackova *et al.* studied the adaptation of PHA-producing bacteria *Cupriavidus necator* to high osmolarity and copper ions and confirmed an important role of PHA granules in the survival of the bacteria. Most importantly, accelerated turnover of the PHA cycle provides increased levels of PHA monomers with chaperoning and osmo-protective functions (Novackova et al., 2022).

Non-optimal temperature is another stress factor for bacterial cells. Obruca et al. (2016) investigated the cryoprotective role of polyhydroxybutyrate (PHB) in *Cupriavidus necator* H16 and its PHB-deficient mutant PHB^{-4}. They found that intracellular PHB granules enhance

bacterial survival during freeze-thaw cycles. Additionally, the exogenous addition of 100 mM 3-hydroxybutyrate (3HB) increased cell viability in both strains, demonstrating that both intracellular PHB and its monomer contribute to protection against freezing stress (Obruca et al., 2016).

Furthermore, bacteria isolated from Antarctic freshwater, confirmed PHA accumulation as an efficient adaptation strategy to avoid damage produced by intracellular ice crystals, oxygen-reactive species and severe dehydration (Ciesielski et al., 2014). When exposed to low temperatures, PHA were observed to be essential for maintaining the redox state in the Antarctic bacterium *Pseudomonas* sp. (Ayub et al., 2009).

From the reports summarized above, it can be concluded that the protective role of PHA represents a general phenomenon regardless of the individual microorganism or the specific stressor. Nevertheless, the particular protective mechanisms of PHA are not yet fully understood; thus, not just one single mechanism is responsible for the protective effects of PHA. However, it seems that the presence of PHA granules has numerous biological and biophysical consequences, which synergistically enhance the overall stress resistance of PHA-containing cells (Obruca et al., 2018).

2.4.4 Biosynthetic pathways of PHA and alginate produced by genus *Azotobacter*

Azotobacter sp. primarily produces PHA in the late exponential phase (as do most of the strains in standard batch culture) and consumes it in the stationary phase. PHA production is connected with the encystment of bacteria, where PHA may serve as a storage polymer for this process in strains that produce cysts. In controlled conditions related to nitrogen limitation, *Azotobacter* species induce the production of PHA and when oxygen limitation is lifted, the bacteria reassimilate the PHA. Moreover, oxygen limitation can cause the accumulation of excess reductant, which PHA formation can alleviate by acting as an electron sink. A similar effect as that of PHA formation can be caused by the impairment of NADH oxidation (Pyla et al., 2009). The increased production of PHA may be affected by iron limitation (through genetically increasing *phbBAC* transcription according to Muriel-Millán and/or the selection of carbon sources (monosaccharides, disaccharides, acetate, butanol, *etc*.) (Muriel-Millán et al., 2014).

The biosynthesis of PHA, in particular the most common member of PHA family – poly(3-hydroxybutyrate) (PHB) begins with the condensation of two molecules of acetyl-CoA to give acetoacetyl-CoA by an enzyme, known as β-ketothiolase. Acetoacetyl-CoA is reduced by

NADPH-dependent acetoacetyl-CoA reductase to β-hydroxybutyryl-CoA. This activated monomer is then polymerized by the stereospecific enzyme PHA synthase to form PHB (Pyla et al., 2009).

The production and degradation of PHA in *A. vinelandii* can be affected by both culture medium conditions and directly through the genetic regulations of *Azotobacter*. PhbR protein up-regulates the PHA-producing operon (*phbBAC*) along with the adjoining gene (*phbR*). The sigma factor (RpoS) and the global two-component response regulator system, GacS/GacA, is also involved in this up-regulation (Hernandez-Eligio et al., 2011). Other regulatory factors, such as the *arrF* gene, are enconded in a regulatory small RNA, *ArrF*, which is expressed under iron limitation and regulates the expression of iron-containing proteins such as superoxide dismutase and FeSII/ Shethna protein. Knocking out the *arrF* gene increases the production of PHA even under well-aeration conditions. The *ptsP* gene, involved in the regulation of nitrogen fixation and respiratory protection under carbon-limited conditions, enhances the production of PHA. Regulation of metabolic pathways in *A. vinelandii,* as in other microorganisms is a complex process, so it is likely that this summary is not an exhaustive list of all relevant factors. However, it is clear that polymer production is important to different aspects of *A. vinelandii* metabolism (Jung & Kwon, 2008).

The production and regulation of PHA in *A. vinelandii* are also related to alginate production. Both metabolic pathways are connected, especially at the carbon source, which serves as the starting point for polymer synthesis. Extracellularly produced alginate is a polysaccharide of varying composition that many strains of *A. vinelandii* produce, while others, known as 'non-gummy' strains do not. Under various conditions, such as low aeration, overproducing PHA strains also produce more alginate than wild-type strains. Alginate, like PHB, is involved in the cyst structure and encystment and germination processes of *A. vinelandii*. However, PHB and alginate may compete for the carbon source, so the production of one or the other can be affected by removing the gene responsible for the production of PHB or alginate from *A. vinelandii* (Page et al., 2001). Synthetic pathways of both, PHB and alginate in *A. vinelandii*, are demonstrated in Figure 8.

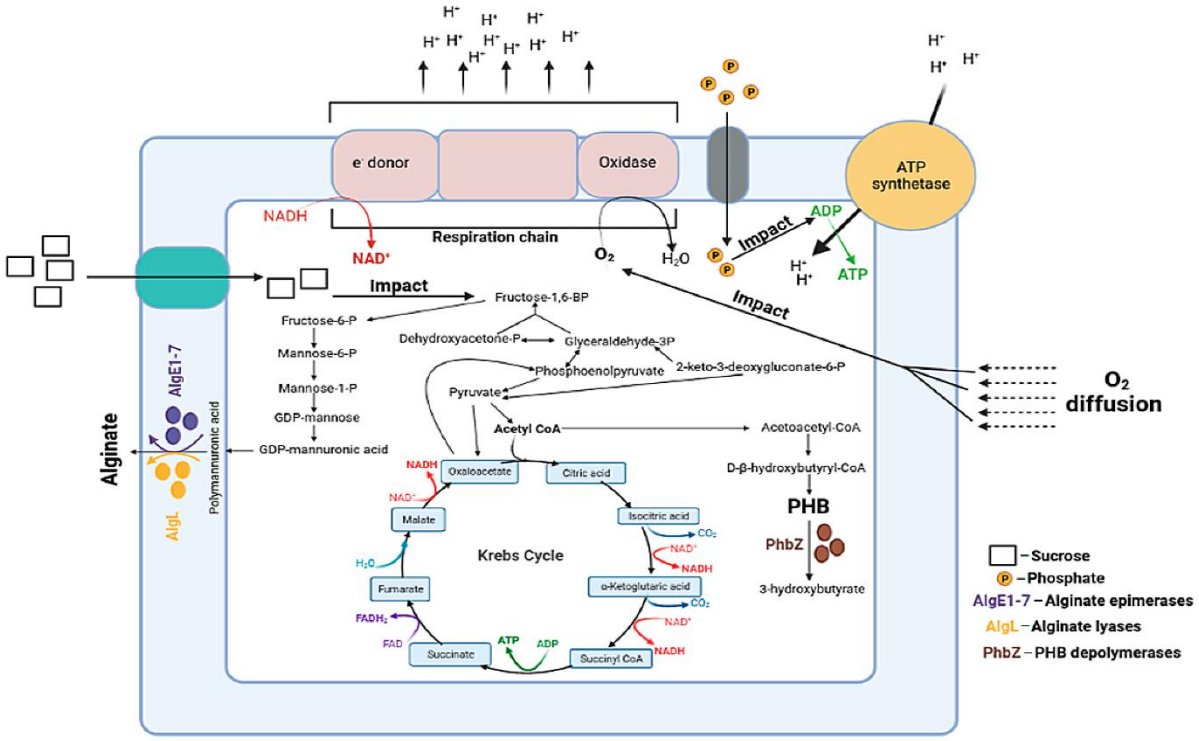

Figure 8 Metabolic pathways linking alginate synthesis, central carbon metabolism (including Krebs cycle and glycolysis) and polyhydroxybutyrate (PHB) synthesis in A. vinelandii. Scheme shows how oxygen diffusion and the electron transport chain influence energy penetration though ATP synthase activity (Dudun et al., 2021).

The non-gummy phenotype can be determined by the insertion of a transposon into the *algU* gene (an activator of alginate production), in which alginate forms a protective part of the cyst coat, helping it resist desiccation. Also, blocking or cutting other genes can lead to partial or complete loss of alginate production (e.g. in the synthesis of GDP-mannuronic acid, or during polymerization) (Dudun et al., 2021). The rate of production and molecular properties of alginate (molecular weight, ratio of mannuronic to guluronic acid, degree of acetylation) depend on the level of oxygen in the cellular environment (C. Peña et al., 2006).

The main structural difference between algal and bacterial alginates is the presence of O-acetyl groups in the latter, where the acetyl groups are invariably linked to the M residues in the C-2 and C-3 positions. Since acetylated M-residues are not epimerized, acetyl substitution also controls C-5 epimerization (Aarstad et al., 2019).

The alginate biosynthetic pathway is similar in both *Azotobacter* and *Pseudomonas* species, which are unique among bacterial sources of alginate. The synthesis of the alginate precursor, GDP-mannuronic acid, starts in the cytoplasm of the cell. Fructose-6-phophate as a primary

compound is converted by four enzymatically catalysed reactions to GDP-mannuronic acid. First, fructose-6-P is isomerized into mannose-6-phosphate by the bifunctional enzyme phosphomannose isomerase/guanosine diphosphomannose pyrophosphorylase (AlgA). Mannose-6-phosphate is then converted by phosphomannomutase (AlgC) to mannose-1-phosphate, after which AlgA catalyses the conversion of mannose-1- phosphate to GDP-mannose. Finally, GDP-mannose is oxidized to GDP-mannuronic acid by GDP-mannose dehydrogenase (AlgD) (Remminghorst & Rehm, 2006).

GDP-mannuronic acid, as a precursor for alginate synthesis, is transported into periplasmic space. Polymerization of GDP-mannuronic acid begins in the periplasmatic space and it is enzymatically catalysed by a polymerase located on the cytoplasmatic membrane. The subunit Alg8 is responsible for the catalytic activity of the polymerase and the transport through the outer membrane is coordinated by a multi-protein complex. In the periplasmatic space, also most alginate modifications occur, such as acetylation and epimerization. Transacetylation occurs on hydroxylic groups on C2 and C3 of mannuronic acid residues, preventing epimerization at C5 and the formation of α-L-guluronic acid by alginate lyases. Moreover, *Azotobacter* is capable of additional epimerization by extracellular epimerases, which differ from intracellular epimerases in their primary structure (Figure 9) (Pacheco-Leyva et al., 2016).

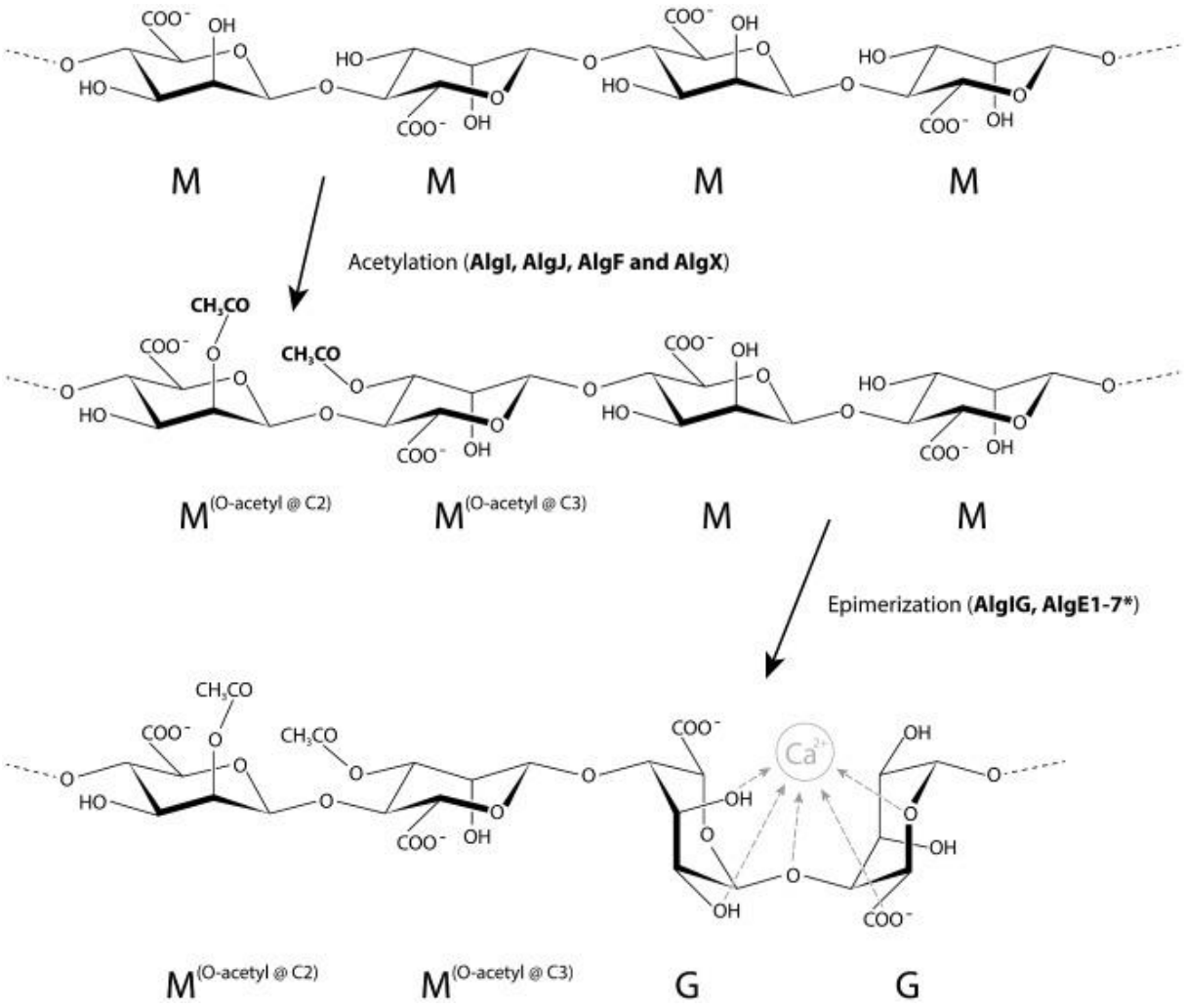

Figure 9 Modular structure of alginate homopolymer M-subunits, their acetylation by alginate enzymes (AlgI, AlgJ, AlgF and AlgX) and subsequent epimerization by AlgG and AlgE to produce G-subunits, which form an egg-box structure with multivalent ions (Aarstad et al., 2019).

Alginate lyases, or alginases, serve to modify the length and molecular weight of the polymer. Each lyase acts specifically on a different substrate; some prefer glycosidic linkages between mannuronate residues, while others prefer polyguluronate as a substrate. Alginate transport is mediated by the AlgE alginate transport porin (or by AlgJ protein in *A. vinelandii*) (Aarstad et al., 2019).

The proteins involved in polymerization, modification (acetylation and epimerization) and transport of the nascent polymer chain function within the periplasmic space and facilitate excretion to the extracellular environment (Ertesvåg, 2015).

This remarkable ability of *Azotobacter* to produce both PHA and alginate simultaneously can be utilized for biotechnological production on an industrial scale. However, the synthesis of alginate represents a competing pathway, consuming substrate during the optimization of PHA production and vice versa. One of the strategies used to enhance PHB or alginate production involves blocking one of the genes responsible for the production of either alginate or PHB through genetic engineering approaches. However, the targeted mutations in PHB production in the *Azotobacter* strain to increase yields, as studied by Pena et al. and Mejía et al. led to different results (Mejía et al., 2010; R. J. Peña et al., 2002). By comparing two strains, one being a mutant with decreased PHA accumulation (marked as AT268) and the other was the wild-type, Pena et al. showed that in batch cultures conducted in a bioreactor (at 3 % dissolved oxygen tension, or DOT), the alginate production generated by the mutants was lower (2.6 g/L) than in the wild type (3.5 g/L) (R. J. Peña et al., 2002). From these results, the authors suggested that the regulation of carbon flux is a very complex process and that the consumed carbon source is not necessarily directed toward alginate biosynthesis (Mejía et al., 2010; R. J. Peña et al., 2002).

The production of PHB and alginate is under a highly complex genetic control, nevertheless, it is possible to influence their synthesis by implementing different cultivation strategy. Many factors affecting cell culture growth and the production of biopolymers with varying properties have been studied. Among the most important are the carbon and nitrogen source and dissolved oxygen tension (Castillo et al., 2020). The acetylation rate is also an important factor in determining alginate properties and it can be influenced by the addition of 3-(N-morpholino)propane sulfonic acid into the culture medium (C. Peña et al., 2006).

2.4.5 Further research and scale-up process of biopolymer production by *Azotobacter vinelandii*

Studies of the scaling-up of the biotechnological process are necessary to ensure that the optimal production (on a small scale) can be maintained at a larger scale. Although there is extensive literature on process scale-up, there is no common or universally applicable scale-up strategy. Furthermore, scale-up is complicated due to the high oxygen demand or the need for high aeration speeds, especially when the rheological properties of the broth show high resistance to mass transfer, as in alginate production. Studies regarding fermentation strategies (at the bioreactor scale), with the aim of increasing PHA production in the bacterium *A. vinelandii*, are

rare. In contrast, there is an abundance of literature regarding PHA production using other microorganisms (J. Lee et al., 2021).

One of the main challenges in cultivating *A. vinelandii* at larger scales is the inability to reach high biomass amounts due to their characteristically high respiration rates. The respiration rates of *A. vinelandii* are determined by the strain, the specific growth rate, nitrogen source and oxygen availability. The nitrogen source (nitrates, ammonia, urea etc.) affects the respiration rates of *A. vinelandii* due to the high energetic costs associated with the cellular maintenance in cultures grown under diazotroph conditions and at high oxygen concentrations because of respiratory protection (Castillo et al., 2020; Díaz-Barrera & Soto, 2010). During scale-up production, when the bioprocess is translated from Erlenmeyer flasks to a laboratory bioreactor, production of both biopolymers is accompanied by a considerable decrease in alginate molecular weight and the viscosity of the broth. However, the same collective of authors demonstrated that, by simulating the evolution of the dissolved oxygen tension (occurring in shake flasks) in a stirred bioreactor, it was possible to produce alginates with a very similar molecular weight (1,800 kDa) and concentration (4.0 g/L) in a 14-liter bioreactor (C. Peña et al., 2008).

Mejía et al., described a two-stage fermentation processes (no oxygen-limited and oxygen-limited conditions) for *A. vinelandii* cultures. Although this fermentation strategy was designed to improve alginate production, the cultures using the wild-type strain showed an increase in the PHB yield from 0.03 to 0.44 g/g (Mejía et al., 2010).

From an industrial perspective, one potential problem with the cultivation of *A. vinelandii* cultures is that optimal alginate production can be obtained when the DOT is accurately controlled within a microaerophilic range. *A. vinelandii* cultures cultivated at low DOT (0 – 1 %) showed a decrease in alginate production, which was linked to an increase in intracellular storage of PHB whereas at high DOT (approximately 10 %), *A. vinelandii* cells use the carbon source mainly for biomass production (Mejía et al., 2010). However, it is known that *A. vinelandii* exhibits a high level of respiration, which is important to consider for its use in industrial bioprocess. Due to this fact, it is possible that biomass of *A. vinelandii* may not reach sufficiently high densities in a typical fermentation strategy at the bioreactor scale, which could be a challenge when the purpose is to implement the production of alginate or PHB at an industrial scale (Jiao et al., 2019; Mejía et al., 2010).

2.5 STATE OF THE ART IN BIOINOCULANTS

Over the past decades, agriculture has remained a cornerstone of national economic development, particularly in regions where food production is closely tied to livelihood and export revenue. In many developing countries, however, the availability and equitable distribution of water resources are severely limited due to both scarcity and inefficient water-use practices. To offset the decline in soil fertility resulting from continuous cropping and to meet the growing demand for food, synthetic nitrogen fertilizers (e.g. urea) are widely used in modern agriculture. However, their long-term application has raised serious concerns, including soil acidification, eutrophication of water bodies, greenhouse gas emissions and the depletion of beneficial soil microorganisms (Ahmad et al., 2022; Leif Marvin R. Gonzales et al., 2015). Chemical fertilizers typically have low nutrient-use efficiency. Urea is utilized by plants at a rate of only 30 – 40 %, with the remainder lost through leaching, volatilization and runoff, especially in arid and semi-arid regions (Leif Marvin R. Gonzales et al., 2015). These inefficiencies not only waste resources but also pollute surface and groundwater and contribute to atmospheric emissions of nitrous oxide, a potent greenhouse gas.

Consequently, there is an urgent need for sustainable and eco-friendly agricultural solutions. In the face of rapid global population growth, climate instability and declining soil fertility, agriculture is under immense pressure to increase food production while minimizing environmental degradation. One such promising solution is the application of bacterial bioinoculants, also referred to as microbial inoculants or biofertilizers. These are formulations containing beneficial bacteria, typically PGPR, that are introduced into the soil or onto plant surfaces to stimulate growth, enhance nutrient availability and improve plant resistance to stress. Unlike synthetic inputs, these microbial formulations improve the natural soil microbiome, contribute to nutrient cycling and do not harm the environment (Bashan et al., 2014). Bacterial inoculants provide a biological alternative that enhances nutrient uptake and plant growth without polluting the environment. PGPR such as *Azospirillum*, *Rhizobium*, *Pseudomonas* and *Bacillus* fix atmospheric nitrogen, solubilize phosphorus, produce growth-promoting hormones and help plants withstand drought, salinity and pathogen stress (Ahmad et al., 2022; Valetti et al., 2016).

2.5.1 Current situation worldwide with bacterial inoculants

The adoption of bioinoculants varies globally. In Latin America, particularly Brazil and Argentina, bioinoculants have been successfully integrated into large-scale farming. Brazil, for

instance, uses *Bradyrhizobium* spp. inoculants on more than 85 % of its soybean cultivation area, supplying nearly all nitrogen requirements biologically and saving approximately USD 4.5 billion annually (Hungria et al., 2006). In contrast, North America and Europe have advanced regulatory frameworks and infrastructure but lower field adoption rates, often due to economic inertia and reliance on inexpensive chemical inputs. Nevertheless, the global market for bacterial inoculants has grown significantly over the past decade. It is projected to rise from approximately USD 457.6 billion in 2024 to USD 681.3 billion by 2032, with a compound annual growth rate (CAGR) of 5.1 % (*Data Bridge Market Research*, 2025). This growth reflects increasing demand for sustainable agricultural products and regulatory pressure to reduce chemical fertilizer usage. Key market drivers include the rise in organic farming, advancements in microbial formulation technologies and growing awareness of the environmental consequences of chemical inputs.

2.5.2 The application of liquid bacterial inoculants

In agricultural systems, PGPR such as *Bacillus subtilis*, *Pseudomonas fluorescens* and *Azospirillum spp.* are frequently applied as inoculants due to their ability to enhance plant growth through multiple mechanisms. These bacteria secrete phytohormones (e.g., auxins, cytokinins), siderophores, antifungal compounds and stress-alleviating enzymes, which collectively contribute to improved nutrient acquisition, disease suppression and stress resilience in crops (S.-K. Lee et al., 2016). Among the various formulations, liquid inoculants have become increasingly dominant in the global market owing to their relatively low production costs. However, despite their convenience, liquid formulations present significant limitations. The microbial cells within these preparations are susceptible to abiotic stresses, particularly nutrient depletion, desiccation and thermal shocks. These factors lead to a rapid decline in viable microbial populations during storage and after application, reducing field efficacy (Allouzi et al., 2022; Lobo et al., 2019). To maintain biological effectiveness, a minimum viable cell concentration of 10^7 colony-forming units (CFU) per mL is required during storage and application (Kumar et al., 2022; Valetti et al., 2016). Sustaining such populations under fluctuating environmental conditions remains a challenge and highlights the need for enhanced formulation strategies.

Importantly, microbial communities do not operate in isolation; their interactions within the rhizosphere significantly influence soil structure, microbial diversity and the system's resilience to abiotic stresses. A long-term study by Wu et al. (2020) demonstrated that the application of

organic fertilizers in combination with reduced chemical fertilizer input led to improved soil organic matter content, higher levels of available nitrogen and phosphorus and a moderate decline in pH (Wu et al., 2020). These effects were most pronounced after two years of consistent treatment, underscoring the cumulative benefits of bio-based amendments (Ehinmitan et al., 2024; Molina-Romero et al., 2017).

A comprehensive review of experimental trials across multiple crops (including tomato, maize, wheat, cotton and peanut), which has further confirmed the efficacy of PGPR under abiotic stress conditions. Strains such as *Achromobacter piechaudii*, *Pseudomonas fluorescens*, *Klebsiella oxytoca* and *Bacillus spp.* have been shown to improve key plant growth parameters (e.g., height, biomass, root length), chlorophyll content, water-use efficiency and reduce sodium uptake under salinity stress. Certain strains, particularly those producing ACC deaminase, can mitigate ethylene accumulation in plant roots, thus enhancing tolerance to drought and salt stress (Nayak et al., 2015; Parveen et al., 2023). Some PGPR also increase the activity of antioxidant enzymes such as superoxide dismutase and catalase, providing additional protection against oxidative damage. Moreover, inoculated plants often exhibit enhanced uptake of essential nutrients like nitrogen, phosphorus, potassium and calcium (Parveen et al., 2023).

In summary, while liquid bacterial inoculants offer a cost-effective and efficient method for delivering PGPR to agricultural soils, their sensitivity to abiotic stressors limits their performance. Addressing these limitations through improved formulation techniques is critical to fully realizing the potential of bioinoculants in sustainable and climate-resilient agriculture.

2.5.3 Application of bacterial inoculants encapsulated in polymer matrices

To improve nutrient use efficiency and minimize environmental degradation, slow-release fertilizers (SRFs) have emerged as a promising alternative to conventional chemical fertilizers. Unlike traditional formulations, SRFs offer significant advantages, including delayed nutrient release, reduced leaching and runoff and enhanced crop quality (Junaid et al., 2024a). A key advance in this field is the encapsulation of live bacterial cultures within biodegradable polymer matrices such as alginate, or chitosan. This microbial encapsulation process involves mixing liquid inoculants containing beneficial bacteria with gel-forming polymers, often crosslinked by di- or trivalent ions (e.g., Ca^{2+}, Al^{3+}) or multi-carboxylic acids, resulting in solid hydrogel beads that harbour high concentrations of viable cells. Encapsulation offers multiple benefits beyond controlled release compared to liquid bioinoculants: it simplifies handling, storage and

transportation and provides protection to microbial inoculants from adverse environmental factors such as high temperatures, desiccation and UV radiation (Nayak et al., 2015). Furthermore, the biodegradable and non-toxic nature of these polymer carriers aligns well with sustainable agricultural practices

These encapsulated beads with PGPR can be applied directly to seeds or soil, where they gradually degrade and release the bacteria into the rhizosphere, ensuring sustained colonization and activity.

There are several types of encapsulation matrices. The first of these carriers relied mainly on solid substrates, such as peat, lignite, or vermiculite, which provided relatively inexpensive and accessible materials. Historically, solid carriers have formed the backbone of commercial microbial inoculant formulations, with peat in particular serving as the conventional standard due to its high organic matter content, water-holding capacity and ability to buffer cells during storage and application (Santos et al., 2019). Nevertheless, peat extraction raises sustainability concerns and its physical and chemical properties can vary between sources. Due to these concerns recent work highlights biochar as a promising peat substitute because of its porosity, high surface area and ability to adsorb and shelter microbial cells, enhancing survival under stress and improving compatibility with soil systems (Bolan et al., 2023). Solid formulations, available as wet or dry types, containing microbial cultures embedded in granules or powders with organic or inorganic carriers (Khan et al., 2023). Wet formulations retain high moisture levels during storage and application and utilize carriers such as alginate, peat, clay, biogas sludge, or biochar (Schoebitz et al., 2014; Vassilev et al., 2020). Carrier selection depends on cost, toxicity, chemical stability and ease of use for farmers (Malusá et al., 2012). Across all solid carrier types, key formulation challenges persist. Notably maintaining viability during drying and storage, avoiding contamination from organic matrices and ensuring consistent, scalable processing, which helps explain the ongoing shift in the literature toward encapsulation and gel-based approaches that better control microbial protection and release (Fadiji et al., 2024).

Hydrogel-based encapsulation addresses many of these challenges effectively. Hydrogels' three-dimensional polymeric networks retain moisture, provide mechanical protection and enable the gradual release of encapsulated bacteria. Their tissue-like structure makes them ideal for delivering bioactive agents in agricultural settings (Junaid et al., 2024b). Natural polysaccharides such as alginate, chitosan, cellulose, starch and pectin are favoured over

synthetic polymers for their biodegradability, biocompatibility and low toxicity. These polymers, composed of monosaccharide units linked by glycosidic bonds, exhibit high flexibility, water absorption and encapsulation efficiency. Importantly, their physicochemical properties (including mechanical strength and porosity) can be tailored by adjusting cross-linking density and polymer composition, improving stability and controlled-release behaviour of the microbial inoculants (Gao et al., 2025; Kowalska et al., 2022).

The compatibility of polysaccharide-based hydrogels with soil environments enhances bacterial colonization and persistence under stress conditions like drought and salinity. However, economic feasibility remains a key hurdle for large-scale adoption of encapsulated inoculants. Nevertheless, ongoing research and development by agro-biotech companies focus on creating cost-effective, scalable and field-ready products. Future progress depends on increased investment in biopolymer science, formulation engineering and innovation to meet the growing demand for sustainable biofertilizers that can replace chemical inputs (Bashan et al., 2002; Date, 2001) (Bashan et al., 2002).

Natural polymers such as alginate, chitosan, starch and pectin are widely used for bacterial encapsulation, often forming hydrogel beads or coatings that protect microbial viability during storage and ensure gradual, controlled release into the rhizosphere (Hert et al., 2009; van Gijtenbeek & Kok, 2017). Additives like glycerol act as osmoprotectants, reducing desiccation stress on encapsulated cells, while polysaccharide blends such as xanthan-gellan improve mechanical strength and acid resistance of the matrices. Compared to free-cell suspensions, hydrogel formulations sustain higher viable counts (up to 10^9 CFU/g) and demonstrate superior plant growth promotion and disease resistance. For example, encapsulated *Bacillus subtilis* strains improved root rot control in cucumber by over 50% relative to liquid inoculants and similar benefits in biomass and nutrient uptake have been observed in oats and rapeseed. Hydrogel technology also supports multi-strain inoculation, facilitating synergistic interactions among beneficial microbes like *Azospirillum*, *Herbaspirillum* and *Pseudomonas*, which enhance drought resilience, soil nutrient cycling and crop yield (Cortés-Patiño et al., 2021). Despite the clear potential of hydrogel bioinoculants, challenges remain in scaling production, cost reduction and thorough field validation (Buitrago-Arias et al., 2025).

Overall, dry formulations either of solid or hydrogel carriers, with low moisture content, extend shelf life and include powders made by freeze drying, air drying, spray drying, or desiccation. Freeze drying, a gentler method, preserves bacterial viability with the help of protectants,

though drying techniques vary widely in cost and energy consumption (Berninger et al., 2018). Talc is a commonly used natural carrier for dry inoculants due to its hydrophobicity and low moisture absorption, which aids long-term storage (Follett et al., 2016). Dry immobilization often employs alginate or zeolite encapsulation combined with protective additives like gelatin, carboxymethyl cellulose, arabic gum, disaccharides, maltodextrin, or milk-derived compounds, all of which improve bacterial survival (Berninger et al., 2018; Schoebitz et al., 2013). The efficacy of these protectants varies with microbial species and requires careful optimization (Lahlali et al., 2006). Compounds such as sodium glutamate enhance membrane fluidity and drying resistance, while milk proteins stabilize formulation structure, further improving viability (Follett et al., 2016; Khan et al., 2023). Low-cost additives like glycerol, maize bran residue and whey also serve as both nutrients and protectants (Vassilev & de Oliveira Mendes, 2018).

2.5.4 The focus on next-generations bioinoculants as the subject of this thesis

Methods for carrying beneficial microorganisms in agriculture, such as freeze-dried bacterial cultures or liquid formulations, continue to evolve, with encapsulation into hydrogel carriers being a key research area to develop more efficient and stable products. According to Bashan et al. (2014), industrial residues and agricultural by-products like sugarcane bagasse, sawdust, or brewery waste can serve as inexpensive carriers for microbial inoculants. However, these raw materials often have inconsistent compositions and pose sterilization challenges, limiting their widespread application. One major challenge in inoculant production is maintaining long-term cell viability. Techniques like freeze-drying reduce intracellular water content, thereby lowering metabolic activity and extending microbial lifetime (Bashan, 2014). While freeze-dried inoculants offer improved shelf life, their commercial production requires specialized equipment and skilled labour, which contribute to high costs. Thus, research efforts aim to reduce production costs while maintaining bioinoculant quality. Moreover, factors such as dosing frequency and the recovery time of cells from liquid or gel formulations remain significant barriers to adoption, especially over large-scale agricultural areas like soybean farms in South America (Santos et al., 2019).

Hydrogel bioinoculants present additional benefits including improved water retention and enhanced drought resistance, which are critical for sustainable agriculture under changing climatic conditions (Ali et al., 2024). The concept of this dissertation focuses on PGPR of the genus *Azotobacter vinelandii* (described in subchapter 2.4). *A. vinelandii* is a gram-negative,

non-pathogenic bacterium known for its dual capability to promote plant growth and produce biotechnologically valuable compounds such as extracellular alginate and intracellular PHA. Despite its high alginate yields and beneficial plant interactions, the potential of *A. vinelandii* as a bioinoculant combining both traits have not been fully explored, to our knowledge This thesis proposes a novel "self-encapsulation" strategy, where the bacteria produce alginate in situ, which upon crosslinking forms hydrogel entrapping the cells. This approach promises to simplify the inoculant preparation process and reduce costs significantly, making it an innovative advancement in PGPR applications.

The agricultural application of *A. vinelandii* has been already studied and commercialized to some extent, especially due to its ability to fix atmospheric nitrogen. *Azotobacter* species are ubiquitous in soils worldwide, with their abundance depending on specific soil conditions. As a plant growth-promoting rhizobacterium, *A. vinelandii* enhances crop yields by providing biologically fixed nitrogen that plants can utilize. Additionally, *A. vinelandii* contributes to improving crop nutritional quality by increasing vitamin content and protein levels (Aasfar et al., 2021; Das, 2019; Gross-Urrego et al., 2025).

Integrating bacterial inoculants like *Azotobacter* into nutrient management systems offers a sustainable approach improving soil health and productivity while reducing chemical inputs. Biofertilizer inoculation is a promising strategy to boost crop productivity while minimizing chemical fertilizer use, supporting environmentally friendly agriculture (Ammar et al., 2023; Bhardwaj et al., 2014; Vergel-Castro & Boom-Cárcamo, 2025). However, inconsistencies in field performance of PGPR inoculants remain a challenge due to differences between controlled lab or greenhouse conditions and complex field environments. To overcome these limitations, biofertilizer formulations are increasingly amended with organic materials, cell protectants and nanoparticles to enhance microbial survival and efficacy. Furthermore, advances in next-generation sequencing, gene editing, synthetic biology and computational modelling offer powerful tools to optimize microbial strains and plant-microbe interactions for sustainable crop production (Bakker et al., 2013; Díaz-Rodríguez et al., 2025).

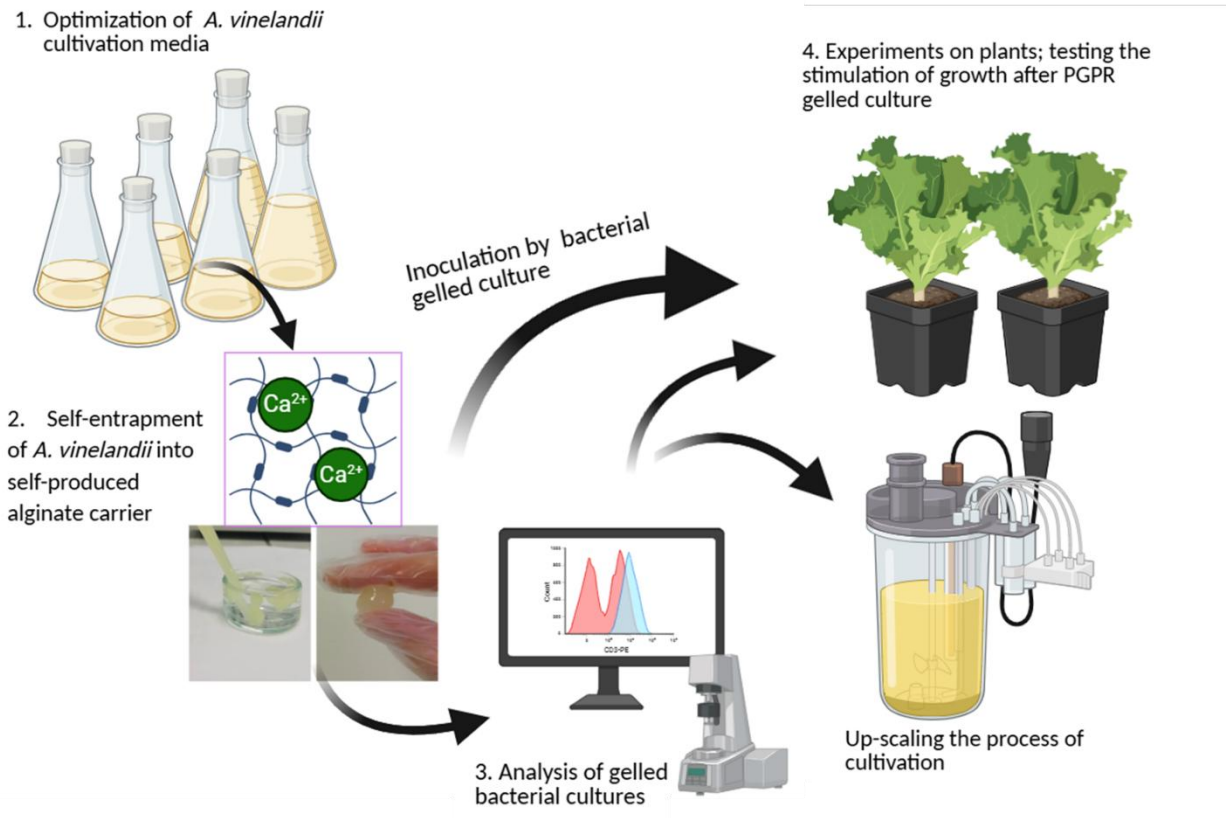

Figure 10 The scheme of the experimental part of our research strategy; 1. Optimization of growth media for A. vinelandii with a focus on production of alginate for gel formation, 2. Gelation of the bacterial culture and characterization of the physical and chemical properties of bacterial gelled culture, 3. Application and evaluation of plant growth stimulation.

3 RESEARCH AIM AND OBJECTIVES

The topic *"Encapsulation of Microorganisms for Their Application in Food Industry, Agriculture and Medicine."* is broad, combining elements of biotechnology and physical chemistry; however, the primary focus of this research is the encapsulation of bacterial cells and their application in agriculture. To achieve the objectives of the study, the research has been divided into several tasks.

The thesis involves selecting of suitable bacterial strains capable of producing two biopolymers: polyhydroxyalkanoates and alginate of the required quality. Various strains of the plant growth-promoting rhizobacterium (*Azotobacter vinelandii*) are selected from a microbial collection based on previous literature screening. The main object is to gel bacteria directly by its own produced alginate. The second task involves analyzing the properties of gels containing encapsulated bacteria, including rheology, stability and bacterial release, using various physicochemical methods. Finally, the encapsulated bacteria will be applied to soil to evaluate their effects on plant growth and yield.

1. Phase

- Screening and characterization of *A. vinelandii* strains deposited in various public collections of microorganisms
- Characterization of microbial strains:
  - PHB content
  - Alginate content and quality (monomer composition, molecular weight)
  - Gelation properties of the culture

2. Phase

- Analyzation of prepared gelled bacterial culture
  - Time of gelation, gelation agents, quality of the gel
- Bacterial viability
- Release of the bacterial culture from the gel

3. Phase

- Application of PGPR in encapsulated form into the soil with plant seeds
- Release of PGPR into the soil

4 MATERIAL AND METHODS

4.1 CHEMICALS USED IN DISSERTATION THESIS

^{14}C-acetate, radioactive, provided by Lund University

CASEIN AM (Thermo Fisher Scientific, USA)
Potassium dihydrogen phosphate (Lachner, Czech Republic)
Disodium hydrogen phosphate dodecahydrate (Lachner, Czech Republic)
Dipotassium hydrogen phosphate (Lachner, Czech Republic)
Sodium hydrogen phosphate dihydrate (Lachner, Czech Republic)
Sodium chloride (Lachner, Czech Republic)
Potassium chloride (Lachner, Czech Republic)
Calcium chloride dihydrate (Lachner, Czech Republic)
Calcium carbonate (Penta, Czech Republic / Chemapol, Czechoslovakia)

DNS- 3,5-dinitrosalicylic acid (Sigma-Aldrich, Czech)
Ammonium sulfate (Lachner / Lachema, Czech Republic)
Magnesium sulfate heptahydrate (Lachner, Czech Republic)
Manganese(II) sulfate tetrahydrate (Lachner, Czech Republic)
Zinc sulfate heptahydrate (Lachner, Czech Republic)
Copper(II) sulfate pentahydrate (Lachema, Czech Republic)
Ferrous sulfate heptahydrate (Lachner, Czech Republic)
Ferric chloride heptahydrate (Lachner, Czech Republic)
Sodium molybdate dihydrate (Lachema, Czech Republic)
Sodium azide (Lachner, Czech Republic)
Sodium hydroxide (Lachner, Czech Republic)
Hydrochloric acid (37%) (Lachner, Czech Republic)
Sulfuric acid, concentrated (Penta / Lachner, Czech Republic)
Perchloric acid (Penta, Czech Republic)
Acetic acid (Lachner, Czech Republic)
Benzoic acid (Lachner / Penta, Czech Republic)
Citric acid monohydrate (Lachner, Czech Republic)
Sodium citrate (Penta, Czech Republic)
Sodium acetate trihydrate (Sigma-Aldrich, Germany)
Ethanol (including 97%) (Lachner, Czech Republic)

Formalin (Sigma-Aldrich, USA)

Indole Acetic Acid (Sigma-Aldrich)
Isopropyl alcohol (Penta, Czech Republic)
Methanol (VWR, USA)
Acetone (Penta, Czech Republic)
EDTA, disodium salt (Lachner, Czech Republic)
D-glucose monohydrate / Glucose monohydrate (Lachner / Lachema, Czech Republic)
Gluconic acid (Sigma-Aldrich, Germany)
L-tryptophan (Sigma-Aldrich, Germany)
L-DOPA (L-3,4-dihydroxyphenylalanine) (Sigma-Aldrich, Germany)
Indole-3-acetic acid (IAA) (Sigma-Aldrich, Germany)
Chrom azurol S (CAS) (Sigma-Aldrich, Germany)
Cetrimonium bromide (CTAB) (Sigma-Aldrich, Germany)
Piperazine (Sigma-Aldrich, Germany)
MOPS (3-(N-morpholinyl) propanesulfonic acid), sodium salt (Sigma, Germany)
Agar powder (HiMedia, India)
Peptone (HiMedia, India)
Nutrient broth with 1% peptone (HiMedia, India)
Yeast extract / Yeast extract powder (HiMedia, India)
SYTOX™ Green (Thermo Fisher Scientific, USA)
DAPI (4′,6-diamidino-2-phenylindole) (Thermo Fisher Scientific, USA)
Propidium iodide (PI) (Thermo Fisher Scientific, USA)

Perlite (Agro, Czech Republic)

Potassium hydroxide (Lachner, Czech Republic)

Radioactive and non-radioactive ^{3}H-leucine (Leu), provided by Lund University

Scintillation cocktail (Ultima gold, USA)

Soil substrate (Agro, Czech Republic)

Thymidine, provided by Lund University

Tricalcium phosphate (Lachner)

Trichloroacetic acid (Sigma-Aldrich, USA)

4.2 INSTRUMENTS USED IN DISSERTATION THESIS

Autoclave VX-150, Systec, USA

Bioreactor Biosan RTS-1, SIA Biosan, Latvia

Bioreactor Biostat B plus, Sartorius

Bioreactor RALF, Bioengineering AG

ELISA, Multimode reader, Synergy HTX, BioTek

Centrifuge EBA 200, Hettich

Centrifuge EBA 20, Hettich

Thermoblock SBH 130, Stuart

Vortex shaker BV 1000-E, Biosan / Benchmark Scientific

Magnetic stirrer without heating MMS-3000, Biosan

Magnetic stirrer without heating MMS-300

Magnetic stirrer with heating H2760-HS-E, Benchmark Scientific

Magnetic stirrer KARTELL TKO

Analytical balance PA224C, Ohaus

Laboratory balance EW 620, Kern

Precision balance Scout Pro, Ohaus

Laminar flow hood Aura Mini, Bio Air Instruments

Safety Bunsen burner schuett phoenix II eco, Schuett-biotec

Nanophotometer PEARL, Implen

Rheometer HR-2, TA Instruments

GC system: Finnigan TRACE GC Ultra with FID detector, Thermo Scientific

GC column: J&W DB-WAX, 30 m × 0.25 mm, Agilent

MALS Dawn Heleos II and dRI Optilab T-rEX, Agilent Technologies, 1260 Infinity, column – PL aquagel-OH MIXED-M 8 µm, 300 × 7.5 mm

Digital orbital shaker SHO-2D, ZWYR-D2401, Labwit

Automatic micro viscometer, Anton Paar

Centrifuge EBA, Hettich

DLS – ZetaSizer Nano ZS, Malvern Instruments

Encapsulator BUCHI B-395

Densitometer DMA 4500, Anton Paar

FTIR spectrophotometer Nicolet iS50, Thermo Scientific

pH meter pH 50+ DHS, XS Instruments

Plant growth lighting 300 W LED Grow Light, Viparspectra

Plant growth lighting 1200 W LED Grow Light, Viparspectra

High-pressure freezing platform. EM ICE, EM AFS2, Leica Microsystems

HPLC, Agilent Technologies

Liquid Scintillator Counter, Perkin Elmer

Scanning electron microscope, Magellan 400/L, FEI

Spectrophotometer U-3900H, Hitachi

Synergy HTX multi-mode microplate reader, ELx808, BioTek

Flow cytometer NL-2000, Cytek Biosciences, Fremont

Universal centrifuge Z 36 HK, HermLe

Ultra-low temperature freezer ULUF 490, Arctiko

Laboratory fume hood N 1500/900 M2, Merci

Mini incubator 10L-Analog, Domel

Temperature-controlled shaker ES20, Biosan

Universal water bath BL4/150, 12 L, WSL

Biological incubator IP60-M, LTE Scientific

Biological incubator IP100-U, LTE Scientific / Biotech

Shaker Unimax 1010 + Incubator 1000, Heidolph

Microcentrifuge 1-14, Sigma

Transmission electron microscope (Morgagni, FEI)

4.3 MICROBIAL CULTURES AND CULTIVATION

Freeze–dried bacterial cultures of *Azotobacter vinelandii* (DSMZ 85; DSMZ 87; DSMZ 576; DSMZ 720; DSMZ 13529) were obtained from the German Collection of Microorganisms and Cell Cultures; Braunschweig, Germany. Freeze-dried bacterial culture *Azotobacter vinelandii* CCM 289 and *Pantonea ananatis* CCM 2407 and *Azospirullum brasilense* CCM 3862 were obtained from the Czech Collection of Microorganisms; Brno, Czech Republic. The bacterial cultures were maintained as frozen stock cultures at –80°C in the presence of glycerol (10 % *w/w*).

Cultivations for the inoculum preparation were performed in 100 mL Erlenmeyer flasks containing 35 mL of modified Ashby's medium glucose (20.0 g/L, yeast extract 6.0 g/L, Na2HPO4 2.0 g/L, $MgSO_4.7H_2O$ 0.3 g/L, $(NH4)_2SO_4$ 0.6 g/L and $CaCO_3$ 1 g/L) for 24 h at 30°C with constant shaking at 180 rpm.

After 24 hours, the inoculum was transferred (5 % *v/v*) into mineral medium of the composition dependent on the experiment. Generally, the composition described above was used, with a fructose or sucrose were used as carbon source (20 g/L), with the amount of $CaCO_3$, varying according to experiment (1.0, 2.0 or 5.0 g/L). The media were sterilized at 120°C for 15 min. The volume in flask (250 mL) similarly varied according to experiment while maintaining the same inoculum-to-medium ratio (5 % *v/v*). The media volume of 100 mL was used as a control, the volume of 50 and 150 mL were used in chapter 5.2.3 to study how the medium filling effects polymer and biomass production. The bacterial cultivations were performed at 30 °C, typically at 220 rpm from 3 – 7 days.

The cultivations of *A. brasilense* and *P. ananatis* were performed in Nutrient Broth medium of a volume of 50 mL in Erlenmayer flask (100 mL) for 24 hours. The grown cultures were either stored at –80 °C in the presence of 10 % (*w/w*) glycerol or inoculated onto specific media to assess PGPR properties (see Chapter 4.4)

4.4 TEST FOR PLANT GROWTH-PROMOTING PROPERTIES

4.4.1 Production of Indole Acetic Acid

Cultivation for indole acetic acid production assay was performed in King B media containing glycerol 15 g/L, peptone 20 g/L, K2HPO4 1.15 g/L and MgSO4.7H2O 1.50 g/L. Stock bacterial cultures of *A.vinelandii* and positive controls (*A. brasilense* and *P. ananatis*) of the volume of 0.75 mL were pipetted into 3 mL autoclaved tubes containing King B medium

supplemented with 2.5 mM tryptophan. The cultivation was performed at 30°C with constant shaking at 180 rpm for 3 days.

The standard method VIS spectroscopic analysis was employed (Gordon & Weber, 1951): 0.5 mL supernatant from the centrifuged (5,400 × g and 10 mins) bacterial culture (cultivated in King B media) was used and mixed with 0.5 mL Salkowski reagent ($FeCl_3.6H_2O$ 12 g/L, 96%H_2SO_4 421 mL/l) (Ambrosini & Passaglia, 2017). The samples were incubated for 30 min in the dark, then 150 µl of the mixture was applied into 96-wells microplates. Absorbance (530 nm) was measured with a microplate reader ELx808 by BioTek. Pure IAA (Sigma-Aldrich) was used as a calibration standard, *A. brasilense* and *P. ananatis* were used as a positive control.

4.4.2 Production of siderophores

The method used to detect siderophore is based on identifying isolates capable of producing siderophores through the utilization of Chromazurol S (CAS), a blue dye (Neilands, 1987). When bacteria produce siderophores, the absorption of Fe^{3+} turns the blue colour of Chromazurol S into red, which creates reddish halo zones around bacterial colonies.

Iron CAS agar plates were prepared by mixing CAS reagent with sterile King B (described above). Agar plates were inoculated with bacterial cultures and a positive control (*Pantonea ananatis*) and an uninoculated plate was taken as a negative control. After inoculation, plates were incubated at 30 °C for 3 – 5 days in the dark and observed for the formation of orange zone around the bacterial colonies (Arora & Verma, 2017).

Siderophore production was quantified using the Chrome Azurol S (CAS) assay. Briefly, the supernatant from the grown bacterial cultures was collected and mixed in a 1:1 (*v/v*) ratio with CAS reagent. The mixtures were incubated at room temperature for 30 minutes and absorbance was measured at 630 nm against a CAS reagent blank.

Siderophore production was expressed as percent siderophore units (PSU) using the formula

$$\text{PSU}\ (\%) = \frac{A_{\text{blank}} - A_{\text{sample}}}{A_{\text{blank}}} \times 100.$$

Pantoea ananatis supernatant was included as a positive control.

4.4.3 Phosphate solubilization

Pikovskaya's medium for phosphate solubilization contained: glucose 10 g/L, tri calcium phosphate 5 g/L, yeast extract 0.5 g/L, calcium chloride 0.1 g/L, magnesium sulphate

heptahydrate 0.25 g/L, agar 15 g/L. The medium was autoclaved at 121°C for 15 minutes. *Azotobacter* strains were inoculated into the sterilized agar medium by gently applying microbial loop with grown culture. Plates were incubated at 30°C for 3–5 days and observed for the formation of clear halo zones around the colonies.

4.5 ANALYSIS PERFORMED DURING AND AFTER THE BACTERIAL CULTIVATION

Analyses were performed to monitor optical density (OD at 630 nm), biomass, alginate production and gelation potential. During the initial cultivations of *A. vinelandii* strains, every 24 h were taken subsamples from bacterial cultures. Bacterial growth was monitored indirectly by measuring optical density at 630 nm using water as a blank.

In the later phases of the experiments, after the initial growth monitoring, analyses were performed following the termination of the cultivation (after 4–6 days, depending on the bacterial strain).

For monitoring the biomass, 10 mL of bacterial cultures were collected daily and centrifuged at 6,000 rpm for 5 min. Supernatant containing alginate was separated from sediment and precipitated with ethanol for further analysis described in 4.6. The sediment containing the biomass was washed with 10 mL of distilled water and dried at 70°C to constant weight.

The gel forming properties were also tested. Few drops of bacterial culture from the sample were pipetted into calcium chloride solution (2 % *w/w*) and it was monitored gel formation.

4.6 DETERMINATION OF BIOPOLYMERS AND MOLECULAR WEIGHT ANALYSIS OF ALGINTE

The content of poly(3–hydroxybutyrate) (PHB) in dry biomass was determined using gas chromatography (Trace 1300, Thermo Scientific, column: ZB–WAXplus 30 m by 0.50 mm) with flame–ionization detector (GC–FID) (Brandl et al., 1989). Commercially available PHB was used as a standard; benzoic acid was utilized as an internal standard. Each sample was measured in triplicate.

The alginate was precipitated from supernatant by using cold ethanol (96 %) (Clementi et al., 1999) and determined gravimetrically. Generally, 3 mL of supernatant was mixed with 6 mL of cold ethanol (4 °C) and the sample was centrifuged at 4,500 rpm for 15 mins at 4°C. The supernatant was poured out and the precipitated alginate was washed with distilled water and a

double volume of ethanol. Afterwards, the centrifugation was repeated. The supernatant was poured out again and the final precipitated alginate was dried in a thermostat at 70 °C for 24 – 48 hours and weighed. The analysis was performed in duplicates for each bacterial culture.

Molecular weights of precipitated alginate were analysed using size exclusion chromatography coupled with multi-angle light scattering (Dawn Heleos II, Wyatt Technology, Santa Barbara, CA, USA) and differential refractometry (Optilab T-rEX, Wyatt Technology, Santa Barbara, CA, USA). 2.0 mg of the dried alginate was dissolved in 1.5 mL of 50 mmol/L sodium citrate solution and subsequently passed through syringe filters with nylon membrane (0.45 µm). A total of 100 µL of each sample was injected into the size exclusion chromatography system (Infinity 1260 system with PL aquagel-OH MIXED-H column, Agilent Technologies, Santa Clara, CA, USA). As a mobile phase, 50 mmol/l of sodium citrate (filtered through 0.1 µm membrane filters) at a flow rate of 0.6 mL/min was used. To determine the weight-average molecular weight (M_w), ASTRA software (version 7.3.2, Wyatt Technology, Santa Barbara, CA, USA) was used.

Determination of the M/G subunit ratio using Fourier transform infrared spectroscopy

Dried alginate samples obtained by precipitation were examined using a Fourier transform infrared (FTIR) spectrometer iS50 (Thermo Scientific, Waltham, MA, USA). Analyses were conducted at room temperature in a controlled air-conditioned environment, employing a built-in single-reflection diamond attenuated total reflectance (ATR) crystal. Each absorption spectrum represented the average of 16 scans, recorded at a resolution of 4 cm^{-1} and a data interval of 0.5 cm^{-1}. For every *A. vinelandii* strain, five separate alginate samples were measured to obtain independent spectra. Absorbance values at 780; 810; 1600 and 1,720 cm^{-1} were extracted from each spectrum to determine structural parameters, including the M/G ratio and acetylation level, according to the procedure outlined by (Bonartseva et al., 2017).

4.7 SELF-ENTRAPMENT OF THE BACTERIAL CULTURE INTO THE HYDROGEL MATRIX

Gelation agents for bioinoculants were prepared using calcium chloride in the concentration of 2 % *w/w*, or 5 % *w/w*, respectively.

For the basic tests of gelation ability, the as-cultivated bacterial cultures were added dropwise into a double volume of gelation agent via slow pipetting to form macrogels of unidentified shape. The process of gelation was done at room temperature without stirring the mixture to

avoid disintegration and to preserve the gel's shape. The time of the gelation was set up for 30 min and followed by the filtration of prepared gels carefully through filter paper (category KA 1) or nylon layer to remove the redundant gelation agent solution.

4.7.1 Gelation by using multi-ions, acids and glucono- δ -lactone

Ionic gelation

For the gelation ionic gelation $FeCl_3$, $CuCl_2$ in the concentration of 2 % *w/w*. The preparation of gels was similar as with $CaCl_2$. Cultivated *A. vinelandii* cultures (10 – 20 mL) were added dropwise into a double volume of the ion solution using slow pipetting. Gelation was allowed to proceed for 30 minutes. After gelation, the gels were carefully filtered to remove excess ion solution.

Acidic gelation

For low-pH gelation, organic acids were used at a concentration of 0.5 M. The chosen acids were citric, maleic and oxalic acid.

Gelation with GDL (Glucono-δ-Lactone)

For GDL-induced gelation, the ratio of $CaCO_3$ to GDL was set at either 1:2 or 1:4 (*w/w*). Calcium carbonate was present in the bacterial culture as a media component and freshly prepared GDL solution was added immediately to avoid premature hydrolysis. The mixture was left at room temperature to allow slow acidification and gel formation, after which the pH was measured. For the rheological time-sweep test (4.9.1), the mixture was quickly transferred to the measuring device immediately after mixing.

4.8 FREEZE-DRYING OF BACTERIAL GELS

Prepared gels (see section 4.7) freed from excess crosslinking agent, were freeze-dried using a freeze-dryer at –20 °C, with the condenser set to –50 °C. The pressure in the freeze-drying chamber was set to 10 Pa. The freeze-drying process lasted 2 – 3 days, depending on the water content of the sample.

4.9 CHARACTERIZATION OF THE GEL FORMULATIONS

4.9.1 Mechanical properties

The gels prepared by self–entrapping of the bacterial cultures CCM 289, DSM 87, DSM 720 and DSM 13529 were further analyzed to investigate their rheological properties. The

oscillatory rheometry analyses of bacterial gels were performed on Rheometer Discovery HR (TA Instruments). Amplitude tests were performed with the deformation strain ranging from 0.1 to 1,000.0% and with a constant frequency of oscillation at 1 Hz. The macro-gels were measured at 25 °C; 6 points per decade, while the amplitude of deformation was increasing. After the measurement, the evolution of the storage modulus (G') and loss modulus (G") was recorded to assess gelation kinetics and stiffness development.

The rheological properties of the bacterial gels formed with GDL were monitored using a time-sweep test over a period of 70 minutes. 25°C, frequency at 1 Hz, while using Peltier Concentric Cylinder (TA Instruments).

4.9.2 Morphological analysis by electron microscopy

The encapsulated bacterial cultures were prepared using cryogenic sample fixation prior to imaging in either transmission or scanning electron microscopy, following protocols developed by colleagues from Institute of Instrumentation Technology, Brno, Czech Republic.

For TEM analysis, a small portion of the sample was excised with a scalpel and placed on 3 mm Au/Cu type A carriers, then covered with the flat side of 3 mm Au/Cu type B carriers. The samples were preserved by high-pressure freezing (EM ICE, Leica Microsystems, Vienna, Austria) and subsequently subjected to freeze substitution (EM AFS2, Leica Microsystems, Vienna, Austria). The substitution medium contained 1% OsO_4 and 0.1% uranyl acetate in fresh acetone and the process was carried out at −90 °C for 60 hours. The samples were then gradually warmed to −54 °C at a rate of 2 °C per hour and maintained at this temperature for 8 hours. They were further heated to −24 °C at 5 °C per hour and held for 15 hours, followed by a final warming phase at 4 °C for 18 hours. After fixation, samples were infiltrated with epoxy resin (Epoxy Embedding Medium kit, Sigma Aldrich, Darmstadt, Germany) and polymerized for 48 hours at 62 °C. The embedded specimens were sectioned into ultrathin slices (~80 nm) using a diamond knife (Ultra 45°, DiATOME, Nidau, Switzerland) on an ultramicrotome (EM UC7, Leica Microsystems, Vienna, Austria). Sections were mounted on PELCO Cu 200 Mesh TEM grids and stained with conventional agents: 2% aqueous uranyl acetate and 3% lead citrate (Reynolds method). Imaging was performed using a TEM (Morgagni, FEI) operated at 80 kV.

For cryo–SEM analysis, hydrogel samples were trimmed to fit 6 mm aluminum carriers (side A) for high-pressure freezing. The carriers containing the sample were filled with culture medium and frozen using high-pressure freezing (EM ICE, Leica Microsystems, Vienna, Austria). Samples were then transferred into a cryogenic vacuum chamber (ACE600, Leica

Microsystems), fractured and sublimated at −95 °C for 7 minutes. Hydrogels containing PHB-producing bacteria were visualized using a scanning electron microscope (Magellan 400/L, FEI) equipped with a cryo-stage, at −120 °C with an electron beam energy of 1–2 keV.

4.10 CULTIVATION OF *AZOTOBACTER VINELANDII* IN BIOREACTORS

4.10.1 Up-scaling of cultivation process

Bacterial cultures of *Azotobacter vinelandii* DSM 87 or CCM 289 were inoculated at 5 % *v/v* into the bioreactors, with working volumes adjusted according to the treatment, either 3 L or 4 L. The inoculum, cultivated in Erlenmeyer flasks (100 mL volume in 250 mL flask) consisted of 24-hour-old cultures with an optical density at 630 nm (OD_{630}) of approximately 3 and the cultivation temperature was maintained at 30 °C.

The bioreactor conditions varied depending on the experiment. The working volume ranged from 3 L to 4.5 L, with media components calculated proportionally to the selected volume. Agitation in the RALF bioreactor was maintained at a constant speed of 350 – 450 rpm, while in the Biostat B Plus bioreactor dynamic agitation ranged from 150 – 450 rpm or 250 – 750 rpm, depending on the specific experiment. Oxygen input was set to a partial pressure of 1% *v/v*/m, supplied either through constant mixing in the RALF bioreactor or via cascade control in the Biostat B Plus, depending on the experimental setup. Glucose (20 g/L), used as the carbon source, was sterilized separately and added directly to the bioreactor. The duration of cultivation depended on the growth rate, gelation potential of the culture and the available carbon source. Subsamples were taken at selected time points, according to the culture's growth progression, to assess gelation potential and for the determination of glucose concentration, alginate production and biomass. Only *A. vinelandii* DSM 87 was used in these experiments, as the CCM 289 strain was unable to form a gel even after several attempts. For comparative purposes, bacterial cultures were also inoculated at 5 % *v/v* following the standard cultivation protocol. When foam formation was observed during the cultivation, an antifoam agent (0.5 mL) was added to the culture.

Table 2 Cultivation of Azotobacter vinelandii DSM 87 in RALF and Biostat B Plus Bioreactors Under Various Conditions to Determine the Optimal Gelation Potential of Bacterial Cultures.

Glucose was added at a concentration of 20 g/L, with variations in bioreactor type, working volume, agitation speed, glucose supplementation mode and cultivation duration.

Experiment	Bioreactor	Volume (L)	Stirring (rpm)	Glucose addition	Time of the cultivation (h)
a) Control	RALF	3	400	×	42
b) Increased mixing	RALF	3	450	×	30
c) Increased volume	RALF	4	400	×	30
d) Fed-batch	RALF	3	350	Yes, 2 g addition	48
e) Dynamic agitation	Biostat B plus	4	250 – 750	×	26
f) Mild dynamic agitation	Biostat B plus	4	150 – 450	Yes, 1 g addition	36

4.10.2 Cultivation in minibioreactors RTS-1

After 24 hours of cultivation in the inoculation medium, the culture of *Azotobacter vinelandii* DSM 87, prepared one day in advance, was transferred into Falcon tubes with aero lids at 5 % *v/v* to working volumes of 10, 20, or 30 mL, supplemented with glucose to a final concentration of 20 g/L. The cultures were then placed into Biosan RTS-1 minibioreactors under constant rotary shaking, with the optical density at 850 nm (OD_{850}) automatically monitored and later calculated. The cultivation typically lasted three days, depending on when the measured OD_{850} began to decline, indicating bacterial death.

4.10.3 Determination of residual sugars using the DNS method

During the DNS method, 3,5-dinitrosalicylic acid reacts with D-glucose to form 3-amino-5-nitrosalicylic acid. The reaction requires energy, which is typically supplied by heating the mixture. This leads to a color change from yellow to orange, making it a colorimetric reaction.

A calibration curve was prepared from a glucose stock solution with a concentration of 3 g/L, which was subsequently diluted to 0.6, 1.2, 1.8, 2.4 and 3 g/L. Then, 500 µL of the appropriately diluted glucose solution (supernatant from centrifuged biomass) was pipetted into a glass test tube. Next, 500 µL of DNS reagent was added. The test tubes containing this mixture were incubated for 10 minutes in a water bath at 70 °C. After incubation, the samples were cooled to room temperature and brought to a final volume of 10 mL with distilled water.

The absorbance of the samples was measured on a spectrophotometer at 540 nm against a blank, which consisted of the same mixture as the test samples, but with 500 µL of distilled water instead of the supernatant. All samples were prepared in triplicate.

4.11 FLOW CYTOMETRY ANALYSIS

4.11.1 Testing of fluorescent probes

Stock solutions of the fluorescent probes (Propidium Iodide, Fluorescein diacetate, Sytox, Calcein AM) were prepared at a concentration of 1 mg/mL, or according to the manufacturer's instructions. Cell cultures were first washed and diluted 10–1000× using phosphate buffer. To each diluted culture, 1–5 µl of the fluorescent probe stock solution was added, depending on the specific probe used. The samples were then incubated in the dark at room temperature for 5–20 minutes, as recommended for each probe.

After incubation, the samples were ready for analysis by flow cytometry. Data acquisition was performed by recording 10,000 events (i.e., detected cells) and the results were processed using the SpectroFlo software. The phosphate buffer composition is described in Table 3.

Table 3 The composition of phosphate buffer in 1,000 mL of distilled water

Compound	Weight (g)
NaCl	8.000
KCl	0.200
$Na_2HPO_4 . 2H_2O$	0.144
KH_2PO_4	0.240

4.11.2 Testing of viability after release of encapsulated bacteria from gelled culture

Bacterial gelled cultures were prepared by mixing 10 mL of bacterial culture with 5 mL of gelation agents. The mixture was allowed to gel and then further released into physiological saline. The gelled cultures were gently mixed in phosphate buffer for one hour. From this suspension, aliquots were pipetted and diluted 10 – 100× as needed.

Propidium iodide (PI) was used as a viability probe by adding 5 µl from a 1 mg/mL stock solution, followed by incubation for 10 minutes at laboratory temperature. Data acquisition involved recording 10,000 events (i.e., detected cells) and the results were processed using the SpectroFlo software.

4.12 PLANT CULTIVATION

The application of bioinoculants and their influence was tested on plants of *Lactuca sativa* (variety *lento*). The plants were cultivated in two different experiments. The seeds were germinated on petri dishes for 5–8 days, depending on their growth and transformed into the soil when for the first one was performed in the laboratory conditions with temperature around 24 °C and humidity regulated by irrigation system on 60 % twice a day with 12 hours day/night cycle with watering every third day. The experiments were performed in 1 L pots with organic soil (Argo) and perlite in ratio 4:1. Treatments varied according to experiment. In the first experiment, gels with encapsulated bacteria, bacteria in liquid phosphate buffer and control without any treatment were used. The inoculation of treatment was done in the first day of lettuce cultivation and in 14 days. The experiment lasted for 30 days.

The second experiment was performed in glasshouse in the cooperation with Lund University, Faculty of Biology. The temperature in the glasshouse was set on 18 °C with constant humidity on 60 %. The day/night cycle was set on 16/8 hours with the use of commercial soil. The experiment was performed in 1 L pots with watering every third day, while monitoring their water content in the soil. After the germination of the seeds, two treatments were performed and negative control. In this experiment, gels with encapsulated bacteria and hydrogel without bacteria were chosen as treatments. The same as previous experiments, one pot was inoculated with 4 germinated seeds and inoculated by gel (bacterial and with bacteria) or nothing as negative control. From each treatment, negative control respectively, 16 pots were inoculated. 4 pots from each treatment, negative control, respectively were not inoculated by plants, only treatment for monitoring behaviour of microbes without interfering plant mechanisms. The

second application of treatment was not performed. After 35 days of watering, half of grown plants, or negative control respectively were randomly selected not to be water anymore to monitoring their drought resistance.

During the experiments, samples of soil were taken to determine bacterial, fungal growth and microbial respiration.

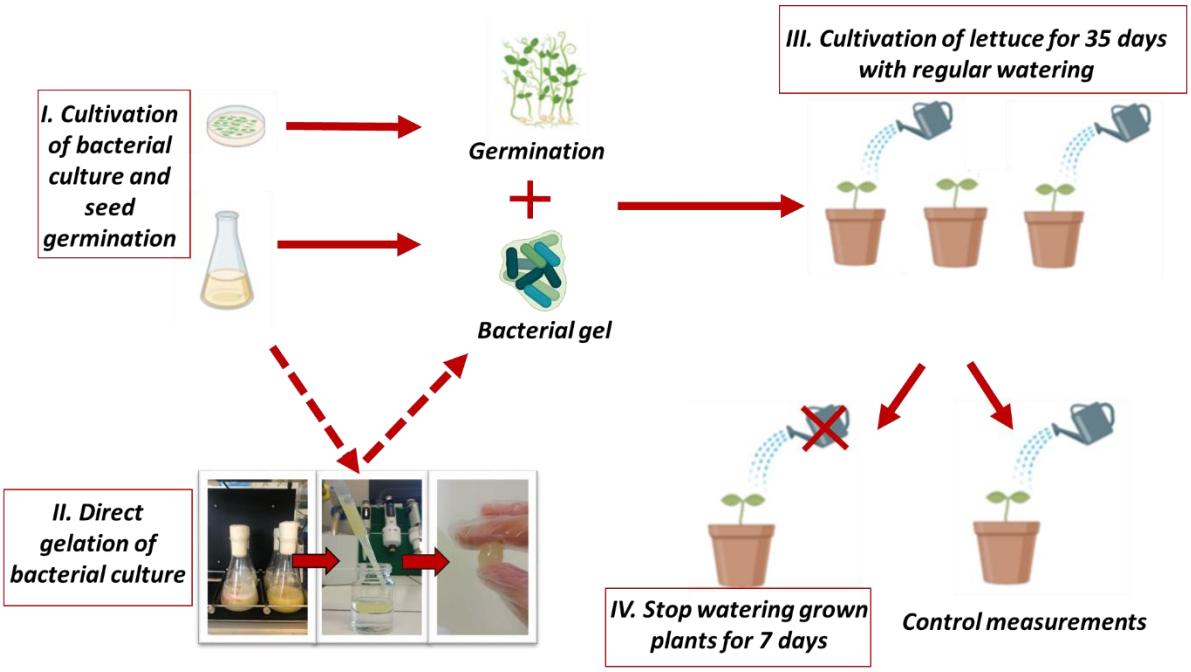

Figure 11 Schematic representation of 2nd cultivation experiment of lettuce, focusing on drought resistance of treated and untreated plants; where two treatments were used: bacterial gelled culture, bacterial gel without cells and untreated controls. Treatment was applicated only once and after 35 days of cultivation half of each treatment/untreated control was tested for drying and rest were cultivated as before.

Soil characterization

The water content (WC) was analysed gravimetrically by drying at 105 °C to constant mass Water holding capacity (WHC) was measured by saturating 5.0 g of the fresh soil with distilled water for 24 h and weighted after 6 h of draining by gravity.

4.12.1 Bacterial and fungal growth measurements

Bacterial growth was estimated by measuring the rate of incorporated ^{3}H-leucine (Leu) into bacteria. Bacteria in weighted amount of the soil were extracted by centrifugation according to (Bååth et al., 2001). 1 mL of Scintillation cocktail (Ultima Gold) was added into pellet, vortexed

and centrifuged (16,200×g for 2 min). After centrifugation, samples were measured using a liquid scintillation counter (Ultima Gold) to determine the amount of incorporated leucine in extracted bacteria (in pmol Leu g^{-1} h^{-1}).

For the estimation of fungal growth, acetate-in-egosterol method was used described by (Bååth et al., 2001). Similarly to the estimation of bacterial growth, 1 g of soil was weighted into glass tubes and mixed with 20 µl of ^{14}C-acetate solution [1–^{14}C] acetic acid, sodium salt, 2.07 GBq.mmol^{-1}, Perkin Elmer) and non-reactive sodium acetate, resulting in a final concentration of 220 µmol/L. Soil samples were incubated at 18°C for 2 h, when the formalin (500 µL) was added to terminate the growth. Ergosterol and incorporated acetate were washed according to (Rousk & Bååth, 2007) 3 mL of scintillation cocktail (Ultima Gold; PerkinElmer, USA) was added and measured on scintillation counter PerkinElmer, USA. The rate of fungal growth was determined in pmol ace-in-erg g^{-1} h^{-1}.

Data evaluation

All data that for bacterial and fungal growth was converted to C units. For the conversion from Leucine to C units, first converted the leucine to thymidine equivalents which were done in Cruz-Parades et al. (2021) by multiplying the leucine data by 0.096628 (Cruz-Paredes et al., 2017). Following this it was used a conversion factor in Soares and Rousk (2019) to convert thymidine to C units by multiplying the thymidine data by 0.0055 (Soares & Rousk, 2019). To convert from Ergosterol to C units, conversion factor of 0.0026 was used (Soares and Rousk 2019).

When the moisture data were fitted to a curve, the data was divided by the estimated asymptote in the regressed equation causing the curve to converge at the asymptote of 1 for bacterial growth (Brangarí et al., 2022). For moisture dependent samples, data was fitted to a logistic curve:

$$y = \frac{1}{1+e^{k(WC-EC50)}},$$

While y represents bacterial growth, k is the slope coefficient determined from linear regression, WC denotes water content and EC_{50} represents the concentration at which 50% of maximal growth is achieved.

The evaluation was repeated to allow a clearer comparison of EC_{50}, which represents the concentration at which sample growth is reduced by half and can thus be related to bacterial resistance to drought stress

4.12.2 Statistical analysis

To determine if there was a difference between groups a one-way ANOVA was conducted between treatments for each of the variables- plant biomass, length of roots and leaves. Data from plant experiments were evaluated by one-way ANOVA in statistical software JASP to obtain their statistical significance (p-value).

To assess differences between groups, a one-way ANOVA was performed for each variable; plant biomass, root length and leaf length. Data from the plant experiments were analyzed using the statistical software JASP to determine statistical significance (p-value). Testing was conducted at the conventional significance level of $p = 0.05$ (statistically significant, "*"), at a high significance level of $p < 0.01$ ("**") and very high significance $p < 0.001$ ("***"), or as no significance when $p > 0.05$ ("ns").

5 RESULTS AND DISCUSSION

5.1 SCREENING OF VARIOUS *AZOTOBACTER VIENLANDII* STRAINS FOR THEIR ABILITY TO PRODUCE SELF-ENCAPSUALTED BIOINOCULANTS

In the course of this dissertation, our goal was to use the plant growth-promoting bacterium *Azotobacter vinelandii*, which naturally produces the extracellular polysaccharide alginate, to form a gel matrix upon direct crosslinking of the as-cultivated culture. Currently, the encapsulation within extracellular matrices (such as xanthan or alginate) is already used for PGPR to enhance their viability over time and to enable controlled release in the environment. However, our concept does not rely on addition of external commercial alginate with bacterial cultures as we aim to produce alginate of sufficient yield and suitable quality directly in the PGPR culture. This novel preparation method introduces a novel type of bacterial inoculant, which, to the best of our knowledge, has not been previously reported.

The immediate gel formation using only the bacterial culture would significantly reduce the cost of inoculant production by eliminating the need for commercially sourced encapsulation matrices. Additionally, industrial biotechnological processes can more easily lead to contamination and typically require further equipment and sterile facilities. Our simplified method offers an alternative that is more efficient and less resource intensive.

The gelation process, in which the grown bacterial culture is directly pipetted into a crosslinking agent (a divalent ion solution, in our case 2 % *w/w* $CaCl_2$), is illustrated in Figure 12. The gel forms immediately upon contact. This concept improves the bacterial inoculant preparation process by eliminating the need for external matrices. In our approach, *A. vinelandii* produces its own encapsulating matrix (alginate), making the encapsulation process feasible, streamlined and cost-effective.

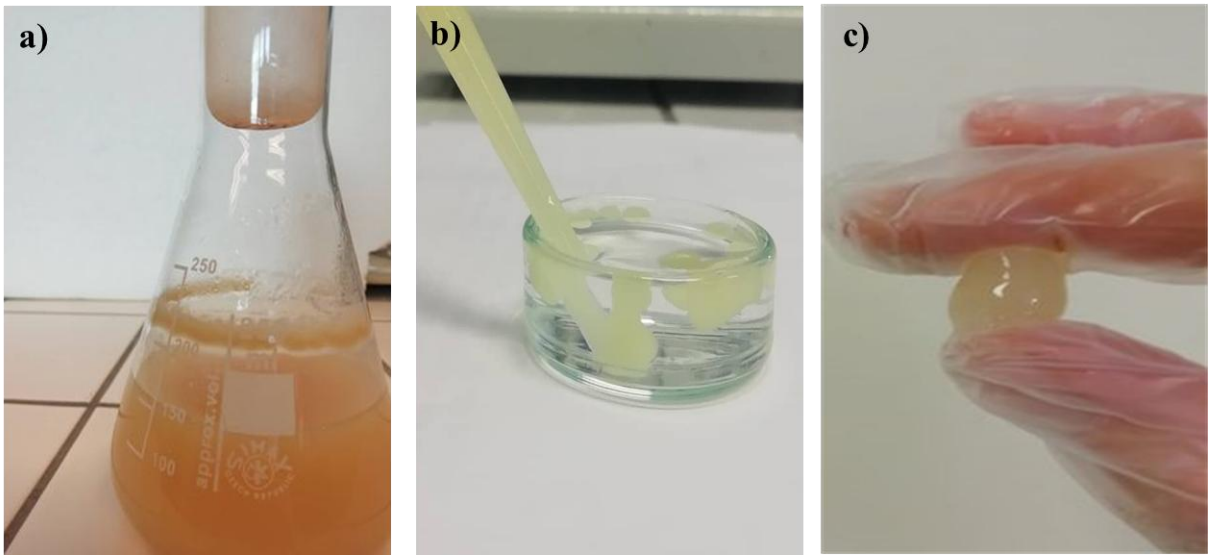

Figure 12 The process of gel formation using a novel approach directly from a 5-day-old bacterial culture of A. vinelandii DSM 87: The bacterial culture, grown to the stationary phase (a), is directly pipetted into a 2 % w/w $CaCl_2$ solution (b), which serves as a multivalent ion gelation agent. This interaction results in the formation of a strong bacterial gel with encapsulated plant growth-promoting bacteria (c), facilitated by the self-produced alginate matrix.

5.1.1 Growth of *Azotobacter vinelandii* strains and their ability to produce biopolymers

Throughout the dissertation thesis we worked with six different strains of *A. vinelandii,* five of them were obtained from German Collection of Microorganisms (labelled as "DSM") and one from Czech collection of Microorganisms (labelled as "CCM") to test our hypothesis in preparation of new version of bacterial inoculant.

The strains were cultivated on a modified Ashby's medium. The medium was partially nitrogen-limiting, with glucose as the sole carbon source and $CaCO_3$ added to support alginate synthesis and maintain desired pH. In the initial stage of experiments, the cultivation was focused on *Azotobacter*'s ability to produce the extracellular polysaccharide alginate, known for its gel-forming potential (Ciarleglio et al., 2023; Kapoor et al., 2025). From the beginning, our goal was to prepare new type of bioinoculant, which could be encapsulated into its own polysaccharides-based gels directly from growth bacterial culture without the need of an external gel forming agents. By this concept we aimed at minimizing production costs of bacterial inoculants and avoiding use of external gelation matrices such as alginate or xanthan.

Hence, our goal was to cultivate bacterial culture containing sufficient amount of alginate with high molecular weight and low M/G ratio to obtain gel formation easily. Due to this reason, we monitored the extracellular polymer content (gravimetrically) and gelation ability (via dropwise addition of the culture to crosslinking solution – 2 % (*w/w*) calcium chloride) of each tested strain during the time course of cultivations.

In the first two days of cultivation, bacterial growth was evident by increased optical density (OD), nevertheless, no gelation potential was observed during this early cultivation phase, only a turbid solution was obtained upon addition to $CaCl_2$. Starting from the third day, gelation ability of bacterial cultures became visually noticeable by biofilm formation on the flask walls for strains DSM 87 and CCM 289. The gel formations after addition of bacterial culture into $CaCl_2$ solution were detect for strains DSM 87, DSM 576, DSM 13529 and CCM 289. Notably, DSM 720 demonstrated gelation potential later, on the fifth day of cultivation, with an alginate yield of 3.5 g/L. Despite producing a comparable alginate amount (2.1 g/L), strain DSM 85 failed to form any gels and instead yielded only a turbid solution upon pipetting into 2% (*w/w*) calcium chloride, the gelation agent. A full overview of gel formation abilities is provided in Table 4.

Table 4 Summary of analysed properties of A. vinelandii strains: production yields of polyhydroxybutyrate (PHB) and alginate, structural characteristics of alginate – molecular weight, ratio of mannuronic and guluronic acids (M/G), acetylation degree – all on 4th day of cultivation. The best gelation performance with 2% w/w $CaCl_2$ characterizes the consistency of the bacterial gelled culture.

Strain	PHB production	Alginate production		Alginate structure			Gelation ability (-)
	PHB (% cdw)	Day of max. alginate production	Alginate (g/L)	Molecular weight (kDa)	M/G ratio (A_{810}/A_{780})	Acetylation degree ($A_{1,720}/A_{1,600}$)	Ability to form gel (-)
DSM 85	7.04 ± 3.57	6th	2.14 ± 0.01	319.00 ± 0.91	2.2 ± 0.1	0.06 ± 0.01	No gel formation
DSM 87	21.95 ± 10.62	5th	4.87 ± 0.57	492.85 ± 15.49	1.7 ± 0.1	0.54 ± 0.01	Compact gel
DSM 576	14.38 ± 10.2	5th	3.09 ± 1.19	181.60 ± 0.14	2.8 ± 0.3	0.17 ± 0.02	Weak, easily disintegrated gel
DSM 720	30.21 ± 2.08	6th	3.52 ± 0.54	344.85 ± 2.76	1.6 ± 0.3	0.08 ± 0.02	Compact gel
DSM 13529	24.02 ± 5.28	5th	3.78 ± 0.78	308.20 ± 6.08	2.0 ± 0.5	0.10 ± 0.03	Compact gel
CCM 289	22.3 ± 1.12	4th	2.18 ± 0.35	430.83 ± 1.69	2.4 ± 0.3	0.20 ± 0.06	Compact gel

PHB serves primarily as an internal carbon and energy reserve (M. S. Lee & Salleh, 2025) however, its presence is also associated with increased cellular robustness, enhancing survival during stress conditions and improving bacterial viability (Grzesiak et al., 2024; Jaffur et al., 2023; Tienda et al., 2024), which is particularly relevant for agricultural applications where cells are introduced into soil environments with fluctuating resources and environmental conditions. Generally, investing carbon sources into the production of two polymers is not optimally effective for the cells with respect to achieving maximal yields of a single product. Thus, it was expected, that cells with higher PHB amount will have low alginate content and vice versa. Nevertheless, our experiments showed the opposite and strains as DSM 85 and DSM

576 with low gelation ability, while reaching 2.1 and 3.1 g/L of alginate, did not produce high amounts of PHB either (7 and 14 % of cdw, respectively). Results of screening strains of *A. vinelandii* (Table 4) are particularly notable, as they contrast with literature reports indicating a decline in alginate production during the stationary phase (Ponce et al., 2021). In our case, significant yields were obtained even in later cultivation stages, when carbon availability is typically limited. Generally, late-phase productivity can be attributed to the accumulation of PHB, detected via GC analysis at levels of approximately 20 – 30 % of cdw for strains DSM 87, DSM 720, DSM 13529 and CCM 289. The strains with limited PHB production were DSM 85 (7.04 % of cdw) and DSM 576 (14.4 % of cdw).

Nevertheless, for us, obtaining a good alginate yield was necessary, as the quantity of alginate plays a key role in gel formation. However, it became evident that yield alone is not sufficient and the ability to form a stable and compact gel also depends on the quality of the alginate, particularly its structural properties.

Among all tested strains, DSM 87 exhibited the highest alginate yield (4.9 g/L) on the 5th day of cultivation and was the only strain to produce a compact, stable gel immediately upon contact with the gelation agent. This confirmed its suitability for our approach, which relies on self-produced alginate for encapsulation without the need for commercial additives. Other strains, such as DSM 720 and DSM 13529, also produced relatively high amounts of alginate (3.5 g/L and 3.8 g/L, respectively) and were able to form compact gels, though not as efficiently or consistently as DSM 87. DSM 576 produced 3.09 ± 1.19 g/L, but the resulting gel was weak and easily disintegrated, indicating that despite a moderate yield, the alginate quality was insufficient for forming a stable matrix. Interestingly, DSM 85 and CCM 289 produced similar amount of alginate (2.1 g/L and 2.2 g/L, respectively), however, the gelation potential was significantly different. While DSM 85 was unable to form any gel and easily mix with gelation agent, strain CCM 289, despite its low yield, managed to form a compact, stable gel. This was likely due to better structural properties of the alginate, which lead us to further investigate alginate structure and quality.

First of the key structural factors expected to influence property of alginate was the molecular weight (M_w). Higher M_w alginate is generally associated with easier gel formation, as it enhances the degree of cross-linking between polymer chains. In this context, the M_w of alginate produced by the strains ranged from 181 to 500 kDa (see Table 4). On the 4th day of cultivation, when EPS production was well established, DSM 87 produced alginate with an M_w approaching

500 kDa, despite an overall alginate yield of less than 2 g/L. CCM 289 followed with molecular weight reaching 430 kDa. Similar M_w values were observed in DSM 720 and DSM 13529**,** suggesting that even strains with moderate alginate production may synthesize polymers with high gel-forming potential. However, interestingly strain DSM 85 with alginate of M_w reaching 319 kDa did not show any gelation properties. Also, weakly gel-forming DSM 576 produced alginate with an M_w of 181 kDa, consistent with previously reported values after 48 hours of cultivation (Clementi & Parente, 1997).

Other studies have also documented a wide M_w range under varying cultivation conditions; for example, (Díaz-Barrera et al., 2021) reported an increase from 200 kDa to 520 kDa during cultivation in bioreactor using *A. vinelandii*. It is generally accepted that M_w values above ~240 kDa contribute to stronger gel networks, as they promote more robust calcium-mediated cross-linking (Fernández Farrés & Norton, 2014). Nevertheless, even alginates with M_w below 100 kDa have been shown to form gels under certain conditions (Ramos et al., 2018), indicating that M_w is important but not the always determinant with respect to gelation capability. Our results and previous studies confirm, that besides M_w, also the monomer composition of alginate plays a critical role in defining gel formation and its strength. The mannuronic-to-guluronic acid (M/G) ratio is particularly relevant, with a higher guluronic acid content supporting stronger gels due to the formation of stable egg-box structures through Ca^{2+} ion coordination (Donati & Christensen, 2023). This structural specificity enables tighter cross-linking. Moreover, acetylation of alginate can increase viscosity but inhibits calcium binding, thereby reducing gelation potential (Skjåk-Bræk et al., 1989).

Understanding the structural composition of alginate is essential, as its monomeric makeup significantly influences its physicochemical properties and gel-forming capabilities. For this reason, we conducted a detailed analysis of the alginates produced by different *Azotobacter* strains using FTIR spectrometry. This technique allows for the identification of specific functional groups based on characteristic absorption bands within the infrared region, thereby providing insights into the molecular structure of the polysaccharide. In our study, we focused on absorbance peaks at 780 cm^{-1}, 810 cm^{-1} and 1720 cm^{-1}, which correspond to guluronic acid (G), mannuronic acid (M) and acetyl groups, respectively. These wavenumbers were selected based on previous findings by (Bonartseva et al., 2017), who demonstrated their relevance in the analysis of *Azotobacter*-derived alginates. The structural parameters obtained from FTIR spectroscopy are summarized in Table 4.

The calculated M/G ratios of the analysed alginates ranged from 1.6 to 2.8, indicating a relative guluronate content between 26 % and 37 %. These values are consistent with the monomer composition reported for *A. vinelandii* alginates in the aforementioned study (Bonartseva et al., 2017). Among the strains tested, the highest G content was observed in the DSM 87 culture, followed closely by CCM 289. Notably, both of these strains are known to form strong and cohesive bacterial gels, suggesting a direct correlation between guluronate content and gel strength. In contrast, DSM 576 exhibited the lowest G content and was associated with weaker gel formation. Interestingly, while acetyl groups were detected in varying amounts, there was no clear relationship between the degree of acetylation and the gelation behaviour in our experimental setup. This suggests that, under the conditions tested, acetylation does not appear to play a significant role in influencing gel formation.

5.1.2 Plant growth-promoting activities of *Azotobacter vinelandii* strains

PGPR support plant development through multiple pathways, including the synthesis of phytohormones, suppression of pathogens and alteration of the surrounding soil microbiota (Olanrewaju et al., 2017). In our study, we focused on evaluating three key plant-beneficial traits in selected *A. vinelandii* strains: phosphate solubilization, iron-chelating compounds (siderophores) and the production of IAA. These parameters were selected to comparatively verify the PGP potential of the tested strains. Illustrative images of qualitative assays on agar media are provided in the Figure 13, while a summary of quantitative results of siderophore and IAA production are provided in Figure 14 and Figure 15. Another important trait associated with PGPR is nitrogen fixation, which was not directly tested in our study, as the presence and activity of nitrogenase in *A. vinelandii* has been well documented in previous studies (Natzke et al., 2018; Rivier et al., 2023).

Phosphate solubilization is an essential trait contributing to the efficiency of biofertilizers. Since much of the phosphorus in soil is bound in insoluble forms, it becomes inaccessible to plants. Certain PGPR strains can mobilize this phosphorus through the secretion of organic acids, thereby increasing its bioavailability (Aasfar et al., 2021; Hafez et al., 2016). In this investigation, phosphate solubilization was assessed using Pikovskaya's medium supplemented with tricalcium phosphate (5 g/L). After removing the colonies, halo zones became visible underneath all tested *A. vinelandii* strains, confirming their phosphate solubilization activity, shown in Figure 13a. Notably, DSM 87 and DSM 720 produced less intense halo zones, which may indicate a comparatively lower efficiency in mobilizing inorganic phosphates.

The ability to produce siderophores is a well-established characteristic of plant growth-promoting rhizobacteria (PGPR), as it aids in overcoming iron limitations in the rhizosphere. In soils, iron predominantly exists in the ferric form (Fe^{3+}), which is largely insoluble and difficult for organisms to access (Ma, 2005; Schalk, 2025). To address this, microorganisms secrete siderophores, high-affinity metal-chelating compounds, facilitating, for instance, iron uptake for both the microbial cells and the associated plants. The ability to produce siderophores was initially assessed using a qualitative method on CAS agar to determine whether the bacteria could secrete these iron-chelating compounds. The appearance of light orange halos around the colonies on the blue agar plates confirmed siderophore production. This activity was observed in all tested bacterial strains from the German and Czech collections of microorganisms. The results are presented in Figure 13b.

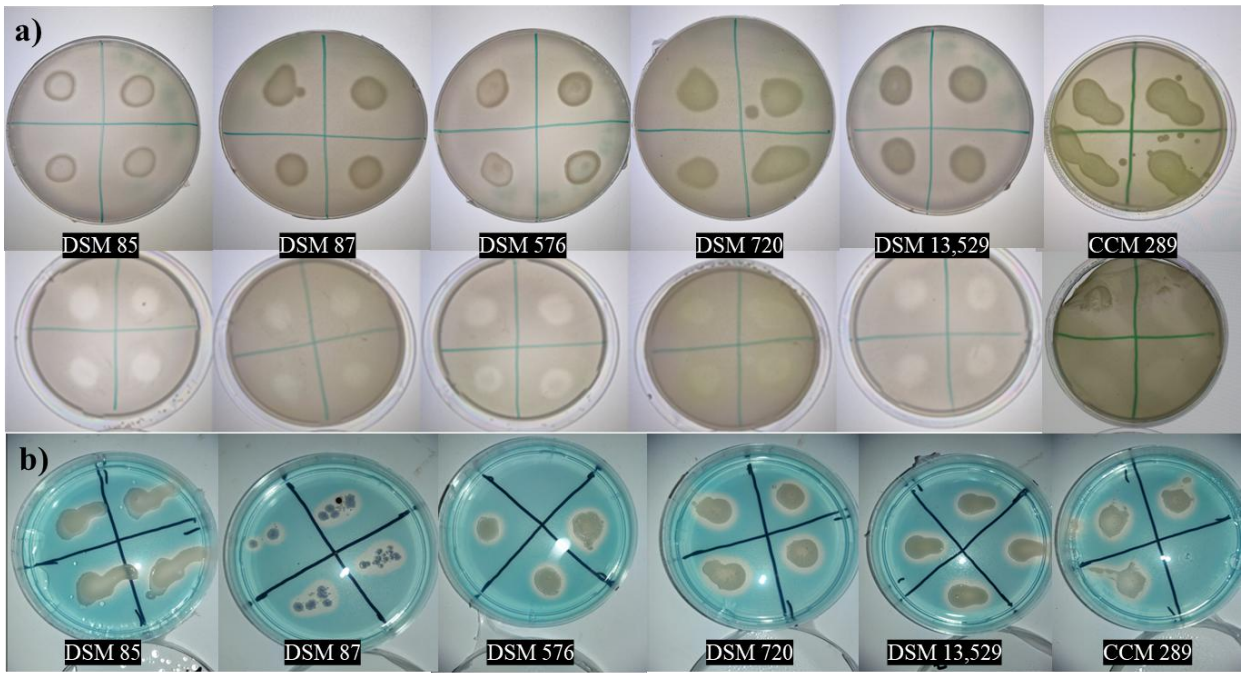

Figure 13 Qualitative plate assays for phosphate solubilization (a) and siderophore production (b) in A. vinelandii strains used in this dissertation. (a) Phosphate solubilization is indicated by the formation of clear halo zones beneath the grown colonies on Pikovskaya's medium-noticeable after wiping of bacterial colony, demonstrating the solubilization of tricalcium phosphate. (b) Siderophore production is confirmed by the appearance of orange halo zones around the colonies grown on a blue agar medium containing CAS (Chrome Azurol S) reagent.

All *A. vinelandii* strains tested positive in qualitative assays for siderophore production, indicating their potential for iron-chelation under iron-limited conditions. To further investigate

this capability, we conducted quantitative analysis using spectrophotometry, expressing the results in percent of siderophore units (PSU), represents the percentage of decolorization of CAS medium. As shown in Figure 14, strain CCM 289 exhibited the highest siderophore activity, reaching 46 PSU. This level was comparable to the positive control, *Pantonea ananatis*, suggesting that CCM 289 is particularly efficient at iron solubilization. Strains DSM 576 and DSM 720 also demonstrated relatively high activity, with values of 39 and 36 PSU, respectively, followed by DSM 87 at 26 PSU. These results suggest that siderophore production varies significantly among *A. vinelandii* strains, even though all possess the genetic potential for this trait. In contrast, DSM 13529 and DSM 85 exhibited markedly lower siderophore production, with only 19 and 5 PSU, respectively. These values represent approximately 45 % and 11 % of the activity observed in the positive control, indicating a limited ability to mobilize iron. The low production in these strains may be due to regulatory differences or reduced expression of siderophore biosynthesis genes.

Overall, the data highlight CCM 289 as a promising candidate for applications requiring efficient iron chelation, such as plant growth promotion or bioremediation. The observed variability among strains underscores the importance of strain-specific screening when selecting microorganisms for biofertilizer or biocontrol purposes.

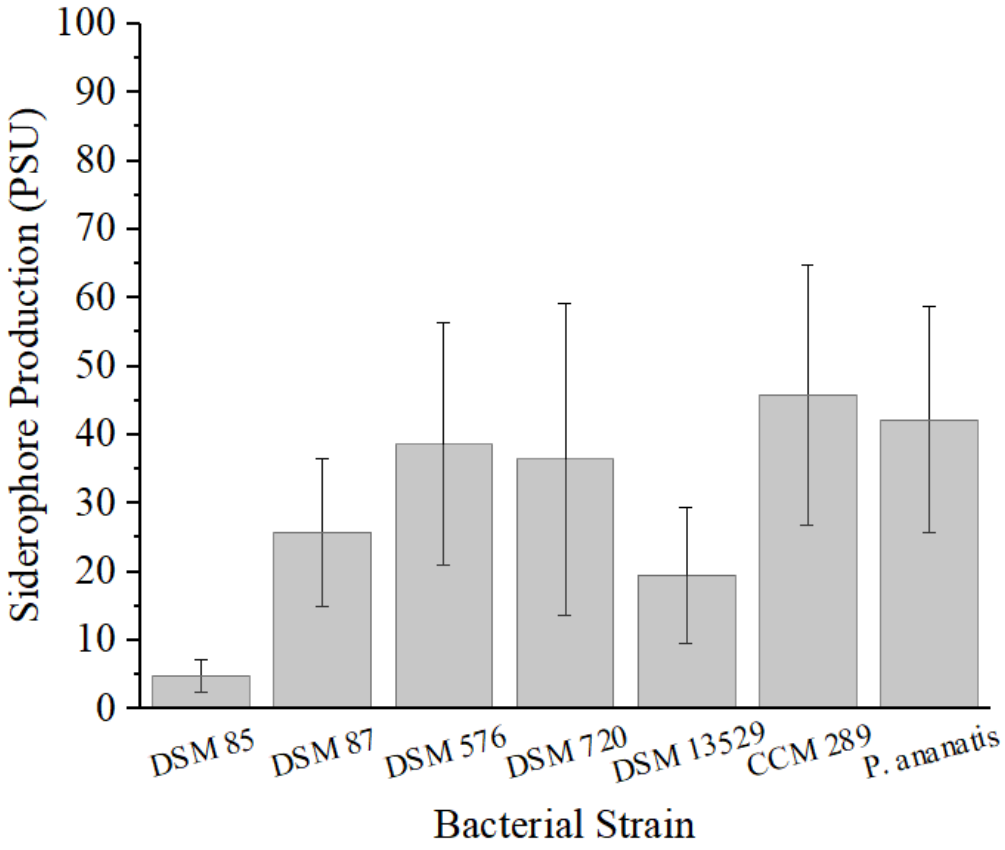

Figure 14 Quantitative estimation of siderophore production (expressed in percent siderophore units, PSU) by A. vinelandii strains and the positive control Pantonea ananatis. Siderophore production was determined spectrophotometrically at 630 nm using the chrome azurol S (CAS) assay, based on the decolorization of the blue CAS reagent to an orange-red colour indicating iron chelation.

Another bioactivity assay conducted was the quantification of IAA, a well-characterized auxin known for its critical role in promoting root elongation and branching. It is well-documented that up to 80% of soil-associated bacteria can produce IAA, which contributes to enhanced root development and improved nutrient uptake (Shailendra Singh, 2015).

In our study, all tested *A. vinelandii* strains demonstrated the ability to synthesize IAA, although the concentrations varied. The highest production was observed in strain DSM 87, reaching 10.5 µg/mL, as shown in Figure 15. Strains DSM 720 and DSM 85 also produced 9.0 and 8.7 µg/mL, while DSM 576 reached 8.5 µg/mL and both DSM 13529 and CCM 289 produced 7.6 and 7.7 µg/mL, respectively. Despite these values confirming IAA biosynthesis, they were

considerably lower than that of the positive controls, (*A. brasilense*, produced 47 µg/mL and *P. ananatis* 67 µg/mL).

Although the IAA levels in *A. vinelandii* strains were relatively low in comparison, their production still indicates auxin-related potential. However, the true bioactivity of these strains cannot be assessed solely through IAA concentration. The functional impact of IAA and other microbial metabolites on plant growth was therefore further validated in subsequent plant cultivation experiments (5.6), where the cumulative effects of bacterial bioactivities (including production of siderophores and phosphate solubilization) on root development and overall plant performance were evaluated under more realistic conditions.

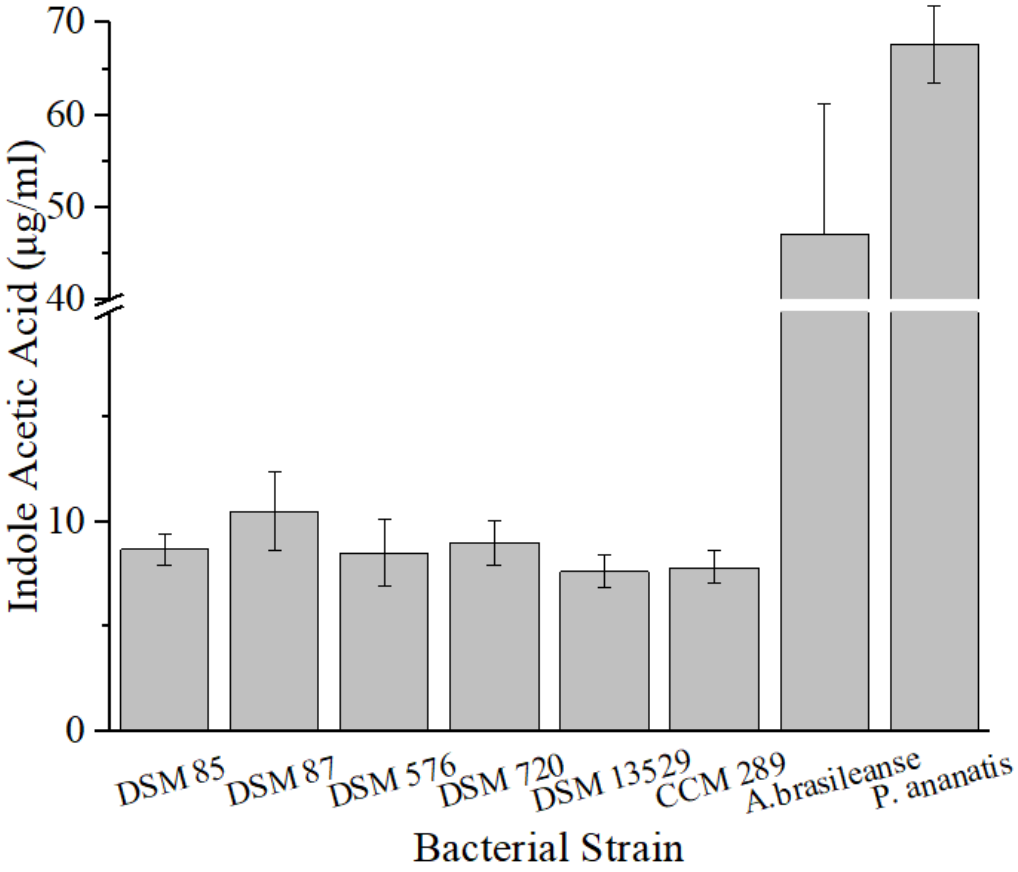

Figure 15 Quantitative estimation of indole-3-acetic acid (IAA) production (in µg/mL) by A. vinelandii strains, with Azospirillum brasilense and Pantonea ananatis were used as positive control. IAA production was induced by the addition of L-tryptophan to the growth medium and quantified spectrophotometrically at 530 nm.

Taken together, the findings reinforce the multifunctionality of *A. vinelandii* as a plant growth-promoting bacterium. Alongside the production of IAA, siderophores and phosphate-solubilizing metabolites confirmed in our assays, *A. vinelandii* is also recognized for its nitrogen-fixing ability due to the presence of nitrogenase enzymes, which contribute to soil enrichment with organic nitrogen (Natzke et al., 2018). Coupled with its capacity for PHB but chiefly also alginate synthesis, these attributes underline the biotechnological potential of *A. vinelandii* strains as promising agents in the formulation of advanced bioinoculants for sustainable agriculture (Aasfar et al., 2021).

5.1.3 Morphology of self-encapsulated bioinoculants

To investigate the ultrastructural details of *A. vinelandii* cultures and their biopolymer production, advanced imaging techniques were employed. Among these, transmission electron microscopy (TEM) was utilized due to its exceptional resolution and ability to visualize intracellular components and extracellular matrices. TEM allowed us to observe the morphology of the bacterial cells but also the organization of encapsulated materials with high precision. The concept of the preparation of hydrogel samples for TEM analysis was achieved in cooperation with colleagues from Institute of Scientific Instruments, Academy of Sciences of the Czech Republic.

As shown in Figure 16**,** TEM images of *A. vinelandii* self-encapsulated in alginate reveal an abundance of intracellular PHB granules, clearly visible as electron-dense inclusions (indicated by orange arrows). These granules are densely packed within the bacterial cytoplasm, indicating robust PHB accumulation. The strain DSM 720, that was used for TEM visualization, is capable of reaching up to 30 % of cdw of PHB as revealed by GC analysis (Table 4).

As it is also obvious from the TEM images, the gelled *A. vinelandii* cells are surrounded with a network-like structure of alginate hydrogel, resulting from direct encapsulation of the microbial culture using a 2 % calcium chloride solution. This encapsulation process facilitates the formation of Ca^{2+}crosslinked alginate chains that enclose the intact bacterial cells, evidently demonstrated in the Figure 16. The figures clearly highlight the close interaction between bacterial cells and the alginate matrix, demonstrating how effectively TEM can reveal biopolymer production and encapsulation at the microstructural level.

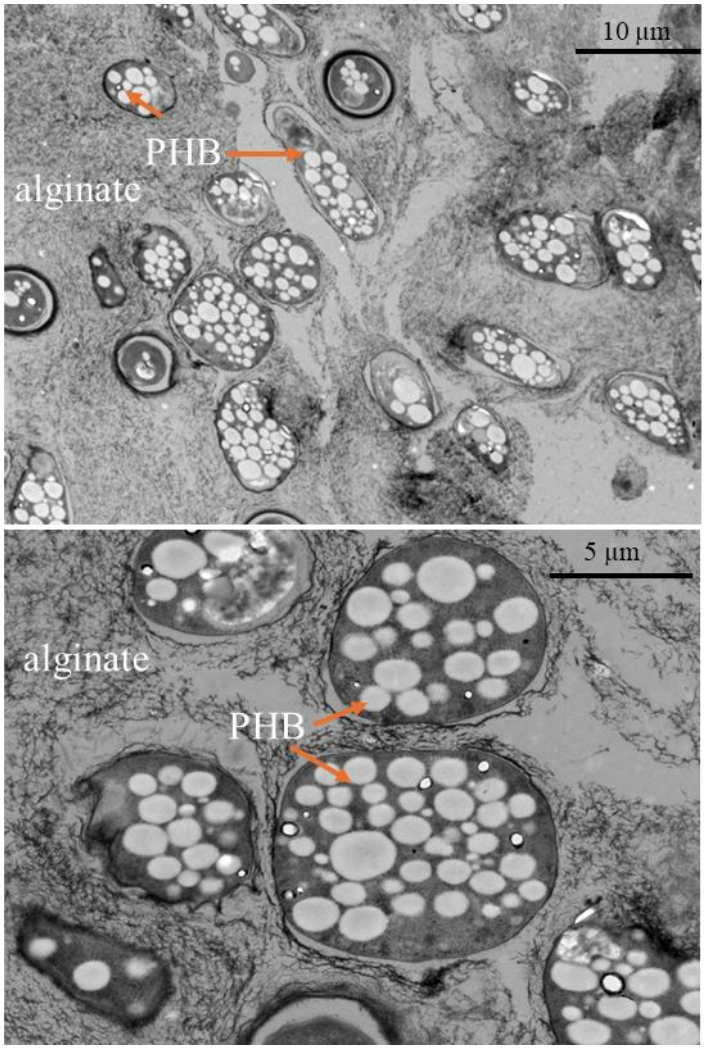

Figure 16 TEM pictures of bacterial gelled culture samples of A. vinelandii DSM 720 with $CaCl_2$ as gelation agent in two resolutions with scale 10µm (up) and 5 µm (down). Networked alginate chains are surrounding bacterial cells, while granules of PHB are inside the cells.

Moreover, the successful design, encapsulation and TEM imaging of bacteria within hydrogel matrices present significant technical challenges, primarily due to the high-water content of hydrogels. This water can interfere with conventional sample preparation techniques required for high-resolution TEM, potentially leading to structural deformation or damage to bacterial cells during dehydration and embedding processes. Encapsulating living or structurally intact bacteria in hydrogels for nanoscale characterization demands careful optimization of both the hydrogel composition and the imaging protocol. In this context, our collaborators from ISI, Brno, have made notable progress by refining fixation, dehydration and sectioning techniques specifically tailored for hydrogel-bacteria composites. These optimized methods have enabled more accurate preservation of bacterial morphology and localization within the matrix,

facilitating detailed ultrastructural analyses. The results of this methodological development, including validation experiments and imaging outcomes were recently published in Supplementary subchapter 10.3. This publication contributed valuable insights into hydrogel-bacteria interactions and the development of bioengineered systems for advanced biomedical or environmental applications.

5.1.4 Analysis of the gel stability of *Azotobacter vinelandii* strains by rheology measurements

Following the development and testing of various cultivation media, we proceeded to investigate the material properties of the encapsulated gels. The aim was to better understand the consistency, deformation and disintegration behaviour of the gel matrix of the alginate beads with encapsulated bacteria, with a view toward their future application in agriculture. Bacterial cultures were crosslinked by calcium chloride (2% *w/w*) by gentle pipetting of culture into gelation agent. Rheological analyses were performed to characterize the physical properties of the gels, specifically using amplitude sweep tests to determine the complex modulus and the limit of the linear viscoelastic region (LVR). These measurements allowed us to assess the structural strength of the gels and compare the performance of different *A. vinelandii* strains. Our goal was to identify which strains produced the most robust gels, as indicated by higher values of the complex modulus.

Strains DSM 85 and DSM 576 did not exhibit any, or exhibited weak gelation potential, only DSM 87, DSM 720, DSM 13529 and CCM 289 were included in the rheological experiment. The rheological properties of bacterial gelled cultures of *A. vinelandii* strains were evaluated through amplitude sweep tests to assess gel strength and structural integrity. The top panel in the Figure 17 illustrates the average complex modulus (G*), illustrating how each gel responds to increasing deformation, what is an approach commonly used in mechanical characterization of bacterial gels. All samples exhibited a characteristic decrease in complex modulus beyond a critical strain (10 % of amplitude sweep), indicating the end of the linear viscoelastic region (LVR) and onset of structural breakdown. Among the tested strains, CCM 289 clearly demonstrated the highest gel strength, maintaining the highest complex modulus across the LVR. This is further confirmed by the bottom panel in Figure 17, which summarizes the average complex modulus within the LVR range. CCM 289 achieved a significantly higher modulus (~16 kPa), while the remaining strains (DSM 87, DSM 720, DSM 13529) showed much lower and relatively similar values (approximately 3 – 4 kPa). These results suggest that

the strain CCM 289 produces notably stiffer and more robust gels, which may be advantageous for encapsulation-based applications where mechanical stability and controlled bacterial release are critical.

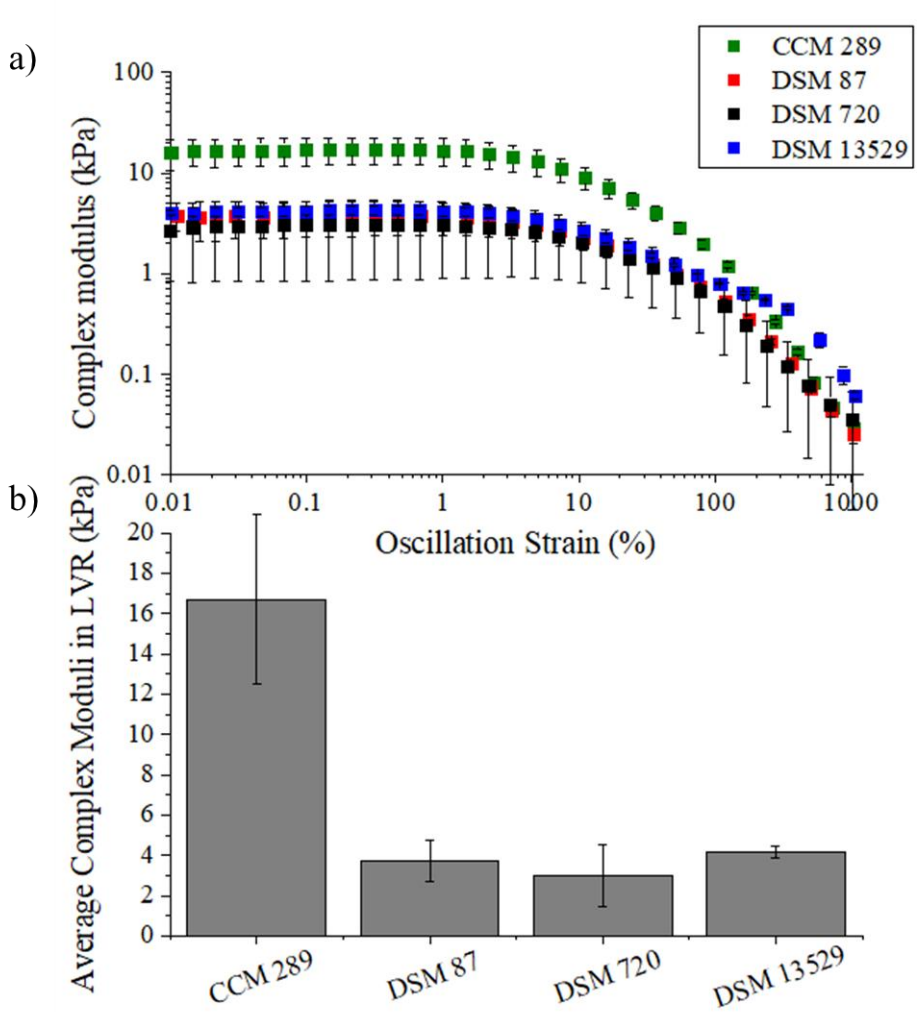

Figure 17 Rheological behaviour of gel-forming Azotobacter strains (*CCM 289, DSM 87, DSM 720 and DSM 13529*) *during amplitude sweep measurements. The top panel shows the complex modulus* (*G**) *as a function of increasing oscillatory strain, illustrating the viscoelastic response and structural integrity of bacterial gelled cultures from each strain under deformation. The bottom panel presents a comparison of the average complex modulus values for the four strains, highlighting differences in gel strength and consistency.*

In summary, all tested *A. vinelandii* strains demonstrated the ability to form bacterial gel cultures when encapsulated in calcium-alginate matrices, confirming their suitability for immobilization approaches. Rheological analysis further revealed notable differences in gel

strength among strains, with CCM 289 producing the most robust and structurally stable gels. Its significantly higher complex modulus suggests enhanced resistance to mechanical stress, which is advantageous for applications requiring long-term stability and controlled bacterial release. While the other strains (DSM 87, DSM 720 and DSM 13529) also formed structurally consistent gels with moderate strength, CCM 289 stood out as the most promising candidate for future development of encapsulated bioinoculants. These findings support the broader potential of *A. vinelandii* strains for use in gel-based formulations, paving the way for further testing in soil environments and agricultural systems.

5.2 FURTHER CHARACTERIZATION OF *AZOTOBACTER VINELANDII* WITH POTENTIAL MODIFICATION OF CULTIVATION PROCESSES TO IMPROVE THE GELATION ABILITY OF THE CULTURES

To further explore the potential of bacterial strains in gel production, we focused on optimizing key cultivation parameters to improve gel strength and reduce production costs. Specifically, we examined the effects of modifying the composition of the bacterial growth medium, adjusting the medium filling volume and supplementing the cultures with calcium carbonate. These factors were selected based on their known influence on bacterial metabolism and gel formation.

One of our main objectives was to identify cost-effective media formulations that support efficient gel bioinoculant production. We also evaluated how different filling volumes could affect oxygen availability and nutrient distribution, aiming to optimize growth conditions while minimizing media consumption. The various addition of calcium carbonate was tested for its potential to enhance gel structure and stability. Through these modifications, we aimed to find a more economical and efficient process for producing strong and stable bacterial gels.

5.2.1 Modification of cultivation media by variation of carbon source type

In the initial set of experiments, glucose was chosen as the carbon source to assess the growth and alginate production capabilities of various *Azotobacter* strains. However, recognizing the potential to broaden the range of carbon sources without compromising growth or gelation potential, we aimed to investigate additional options. This approach led us to explore a variety of alternative substrates, each capable of supporting microbial growth. By diversifying the carbon substrates available, we not only enhance the biotechnological potential of *Azotobacter* strains but also improve its ecological adaptability and possible variability of production. This

flexibility in utilizing different carbon sources underscores the bacteria's metabolic versatility, an important factor in its ability to thrive in a different environments, *Azotobacter* cultivations and its applications into soil (Sumbul et al., 2020; Tec-Campos et al., 2020).

Variety of carbon sources were chosen for this experiment, such as fructose, sucrose, maltose, arabinose, cellobiose, lactose, glycerol or starch. These carbohydrates and related compounds often originate from different industrial or agricultural waste streams, making them attractive, low-cost substrates for bacterial cultivation. For example, fructose and sucrose are commonly found in waste from fruit processing and sugar production. Maltose and cellobiose can be derived from the breakdown of starch-rich or cellulose-rich wastes such as cereal residues or potato processing by-products. Lactose is abundant in dairy industry effluents like whey. Glycerol is a major by-product of biodiesel production, while starch is widely present in agricultural residues including corn, cassava and potato waste. Using such diverse carbon sources not only provides a range of nutrients to support bacterial growth but also contributes to sustainable waste valorization by transforming low-value by-products into valuable bacterial gels. The use of waste substrates offers a dual benefit: it reduces production costs by replacing expensive raw materials and promotes environmental sustainability by recycling these by-products into new valuable materials. In this case, we produce bioinoculants to increase crop production and the waste material remaining after harvest can be reused circularly to produce new bioinoculants. This approach represents an ecological alternative that supports circular economy principles and reduces overall environmental impact.

DSM 87 and DSM 720 were cultivated on these sources for 4 days in standard 96-well microplates, while measuring optical density in selected timepoints. The noticeable growth was found only for fructose, sucrose, glucose and maltose, as it is shown in Table 5 for DSM 87 and for DSM 720 in Supplementary Table 9. Out of these screening experiment, we move to flask cultivation while selecting only sucrose and fructose as alternative carbon sources and glucose as control.

Table 5 Bacterial growth of A. vinelandii DSM 87 on various carbon substrates in concentration 20 g/L throughout 93 hours. The bacteria grew in 96-hole plate at 30°C while constant shaking 250 rpm and measured on selected times by ELISA Multi mode Reader at 630 nm.

	OD_{630}									
Hours	Fructose	Glucose	Sucrose	Xylose	Arabinose	Celobiose	Maltose	Laktose	Glycerol	Starch
0	**0.154**	**0.153**	**0.135**	0.156	0.152	0.136	**0.133**	0.141	0.127	0.139
10	**0.234**	**0.233**	**0.225**	0.226	0.246	0.269	**0.305**	0.250	0.235	0.223
25	**0.297**	**0.328**	**0.242**	0.232	0.198	0.203	**0.285**	0.238	0.275	0.203
45	**0.352**	**0.467**	**0.267**	0.323	0.227	0.244	**0.328**	0.249	0.315	0.211
69	**0.393**	**0.611**	**0.381**	0.331	0.233	0.253	**0.392**	0.248	0.328	0.205
74	**0.421**	**0.637**	**0.416**	0.339	0.241	0.258	**0.435**	0.251	0.326	0.206
93	**0.504**	**0.788**	**0.546**	0.388	0.245	0.255	**0.581**	0.293	0.393	0.215

Some previous studies have examined the impact of carbon sources on *A. vinelandii* biopolymer's production. Mainly, in order to reduce the costs various alternative resources such as molasses, maltose and starch were utilized as alternative low-cost carbon source, while the molasses reached 4.7 g/L, maltose 2.9 g/L of alginate production and no alginate was produced using starch. Sucrose and glucose reach similar alginate levels, in this case 3.5 g/L (Kivilcimdan Moral & Yildiz, 2016).

After testing *A. vinelandii* growth on various carbon substrates, we decided to focus specifically on the three most common sugars: glucose, fructose and sucrose. For instance, sucrose is traditionally used in Burk's medium as the standard carbon source for *A. vinelandii* cultivation. Glucose was used since the beginning as generally used carbon source for bacterial growth and biopolymer production and fructose was chosen based on previous 96-hole microplate test.

Our study, demonstrated in Figure 18, confirmed that cultures grown on fructose achieved the highest biomass, reaching approximately 8 g/L, along with the greatest alginate production, close to 4 g/L. In comparison, cultures supplemented with sucrose produced biomass levels exceeding 6 g/L and alginate concentrations around 3.8 g/L. Meanwhile, growth on glucose was relatively lower, with biomass around 6 g/L and alginate production approximately 2.6 g/L. These findings highlight fructose as not only the most effective substrate for biomass accumulation but also the best for maximizing alginate yield under the tested conditions.

Regarding the gelation potential, all three carbon sources supported sufficient gel formation. Each culture was able to form strong gels with the bacterial biomass without the addition of any

external gelation agents. Remarkably, fructose stood out because gelation was visually observed as early as the third day of cultivation, with the entire culture volume becoming gelled. This spontaneous gelation likely resulted from the combined effect of possible fructose's gelation-promoting properties and the presence of calcium carbonate ($CaCO_3$) in the medium, which release by decrease of pH. This media compound provides sufficient calcium ions to cross-link the alginate polymers without requiring any external carbonate source.

However, this gelation phenomenon was not sustained beyond the third day of cultivation. Over time, the constant agitation or mixing of the bacterial culture may have disrupted the gel matrix, leading to its gradual disintegration. This suggests that while fructose can promote early and strong gel formation, maintaining the gel structure in a dynamic cultivation environment remains challenging. Further investigations, for instance the measurement of pH during the time, are needed to confirm this hypothesis and to explore ways to stabilize the gel during longer cultivation periods, possibly by optimizing mixing conditions or supplementing stabilizing agents.

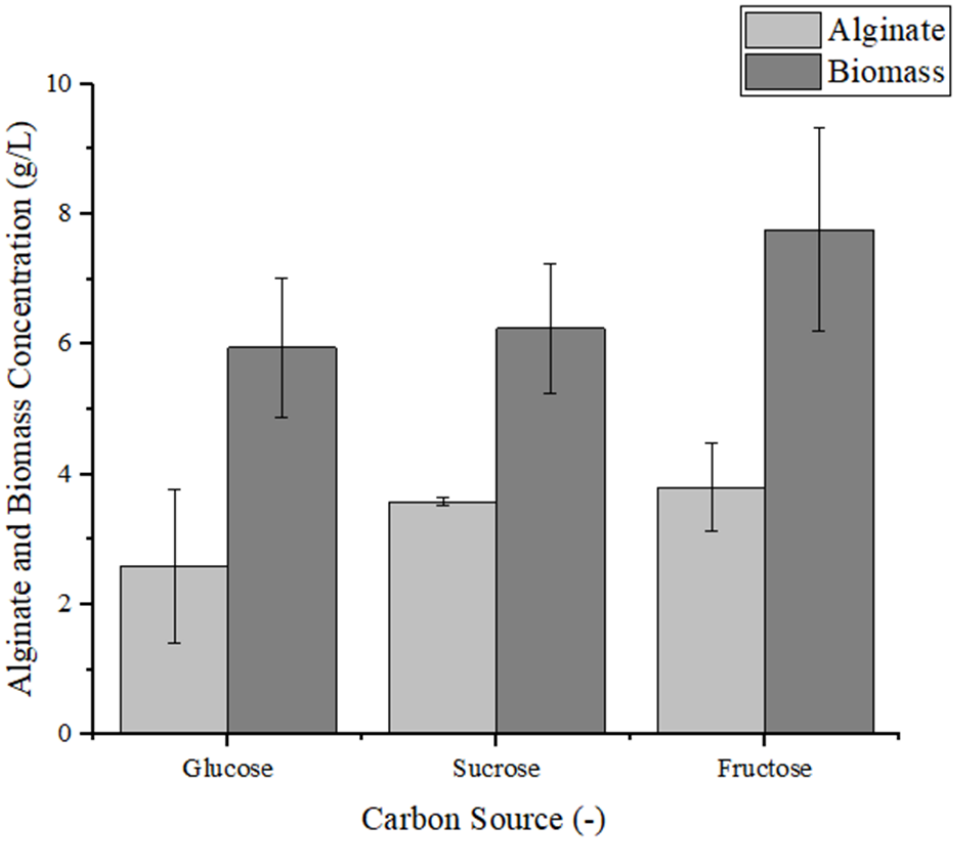

Figure 18 The production of alginate and biomass with three different carbon sources in concentration 20 g/L by A. vinelandii DSM 87 on 5th day of cultivation- glucose was used as a control, sucrose and fructose as tested alternative carbon sources.

The use of different carbon sources for *A. vinelandii* cultivation has been previously investigated, for instance by Clementi (1997), who primarily focused on the quantity of alginate produced under various conditions (Clementi & Parente, 1997). However, to our best knowledge, in previous studies, the direct gelation potential of the culture itself such as the physical ability of the culture medium to form a stable gel, has not been systematically evaluated. In our study, we observed a distinct and immediate gelation of the culture medium in the presence of fructose on the third day of cultivation, highlighting a previously underreported phenomenon. However, the interesting could be an effect of different concentrations of individual sugars, which was not considered in this study. This aspect could be explored in future research projects, such as bachelor's or master's theses, focusing specifically on how carbon source concentration affects not only bacterial growth and alginate yield but also the alginate characteristics, gelation behaviour and mechanical properties of the resulting hydrogels.

5.2.2 Effect of calcium carbonate on *Azotobacter vinelandii* media

Calcium carbonate ($CaCO_3$) is commonly used in microbial cultivation media as a buffering agent to maintain pH stability (Ashby, 1907). In the context of *A. vinelandii*, this role is particularly relevant due to the organism's metabolic activity, which can lead to acidification of the medium. However, in our study, we aimed not only at exploring its buffering capacity but also to investigate how varying levels of $CaCO_3$ could influence the strain's ability to produce alginate with enhanced gelation properties. Since $CaCO_3$ is a poorly soluble calcium source, we hypothesized that its gradual dissolution might affect both the availability of calcium ions and the structural properties of the alginate matrix. Therefore, we tested different concentrations of $CaCO_3$ in the culture medium to evaluate its impact on the gelation potential and physicochemical characteristics of the alginate produced by *A. vinelandii*.

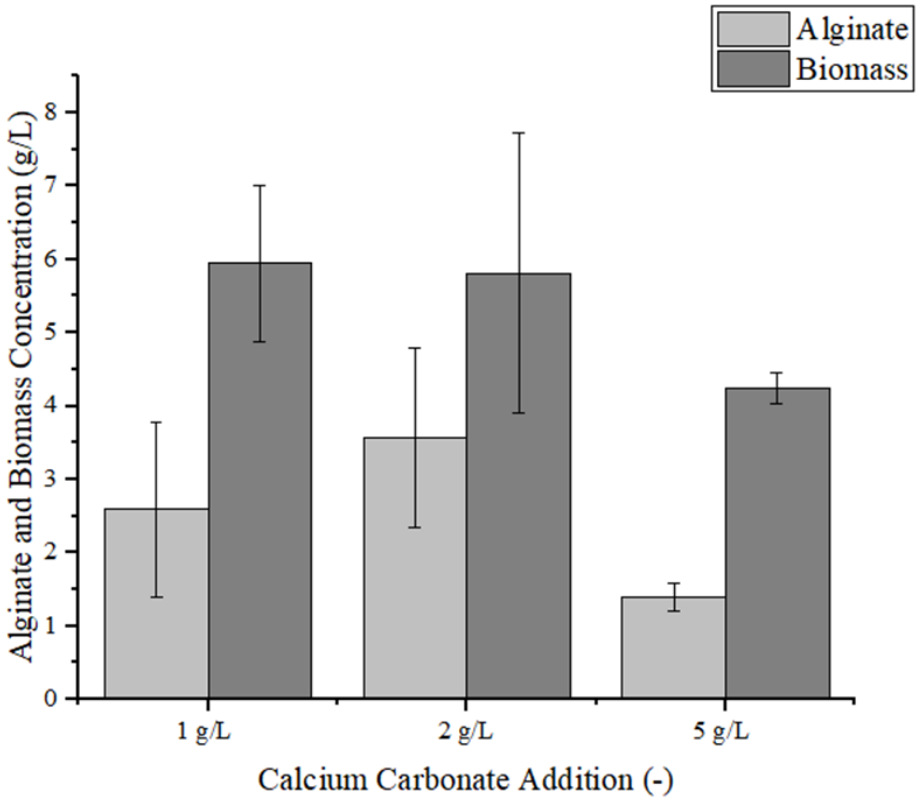

Figure 19 Alginate and biomass yield after cultivating DSM 87 for five days with varying calcium carbonate content (1, 2 and 5 g/L) and a constant glucose concentration (20 g/L). Alginate is represented by light grey columns and biomass by dark grey columns.

These findings suggest that moderate $CaCO_3$ addition (around 1 – 2 g/L) may enhance alginate production, likely due to optimal buffering of pH and improved availability of calcium ions for

alginate biosynthesis and alginate capsule formation. However, excessive $CaCO_3$ appears to inhibit alginate production, possibly by overly stabilizing the pH or altering the metabolic conditions required for alginic acid synthesis and self-encapsulation. Although several studies (Sofia Orišková, 2020) attempted to use much higher $CaCO_3$ concentrations (up to 30 g/L), they did not report increased alginate yield and observed a complete absence of gel formation. This is consistent with our observation that gel-like biofilms or self-gelation occur only under limited $CaCO_3$ availability. Interestingly, while 5 g/L $CaCO_3$ is often used in standard *A. vinelandii* cultivation protocols reported in the literature (Ashby, 1907.; Clementi & Parente, 1997; Trujillo-Roldán et al., 2001) the lack of biofilm or gelation is rarely addressed. This may indicate a key oversight and supports the novelty of our findings, which suggest that self-encapsulation and gel formation in *A. vinelandii* are strongly influenced by the balance between calcium availability and metabolic conditions, which offers a potential avenue for medium optimization in future biotechnological applications.

5.2.3 Influence of the medium volume on oxygen transfer and cell growth in cultures of *Azotobacter vinelandii*

A. vinelandii is a free-living, strictly aerobic diazotroph known for its ability to fix atmospheric nitrogen and produce the exopolysaccharide alginate (Barney, 2024; Noar & Bruno-Bárcena, 2018). This bacterium presents an interesting physiological paradox: although nitrogenase, the key enzyme responsible for nitrogen fixation, is highly sensitive to oxygen, *A. vinelandii* requires high oxygen concentrations for optimal growth and metabolic activity (Takimoto et al., 2022; Threatt & Rees, 2023). To resolve this, the organism relies on a combination of protective mechanisms, such as elevated respiratory rates to consume intracellular oxygen rapidly and the biosynthesis of extracellular polymers like alginate, which are thought to act as diffusional barriers or protective matrices around the nitrogen-fixing apparatus (Ponce et al., 2021).

Therefore, environmental conditions that affect oxygen transfer, such as agitation speed and the filling volume of cultivation vessels, are likely to influence both the growth rate and the metabolic investment into alginate biosynthesis. Previous studies have suggested that alginate production may increase under conditions of moderate oxygen limitation, potentially as a response to oxidative stress or as a means of maintaining nitrogenase activity (Sabra et al., 2000; Takimoto et al., 2022). Based on these considerations, this study aimed to investigate how varying oxygen availability, through changes in agitation speed and culture volume in

Erlenmeyer flasks, influences the production of alginate and biomass in *A. vinelandii*. By modulating these easily controllable cultivation parameters, we sought to identify cultivation conditions that optimize alginate yield, while also gaining insight into the biological role of alginate in the bacterium's response to oxygen stress.

Before assessing the effect of culture volume, we first evaluated the impact of different agitation speeds on alginate production. Under static conditions, no bacterial growth was observed. At 180 rpm, the cultures showed growth; however, during the gelation assay, the solution remained turbid and failed to form a gel. Consequently, only agitation speeds above 210 rpm were considered for further experiments. At these higher speeds, most of the tested strains consistently produced alginate capable of forming stable gels, except for DSM 85 and DSM 576, which did not yield stable gels even under increased agitation.

These preliminary results supported our initial hypothesis that agitation speed influences oxygen availability, thereby affecting alginate biosynthesis. Specifically, for strains CCM 289, DSM 87, DSM 720 and DSM 13529, increased agitation correlated with enhanced gel formation, suggesting higher alginate production under conditions of improved oxygen transfer. This aligns with the proposed biological role of alginate as a protective barrier that mitigates oxygen diffusion and helps safeguard the nitrogenase enzyme from inactivation, a phenomenon also reported by Sabra at al., 2000 (Sabra et al., 2000).

To examine further the effect of aeration, we conducted flask experiments at previously chosen agitation speed of 210 rpm using 250 mL Erlenmeyer flasks filled with 50, 100 and 150 mL of medium. Samples were collected from day 3 to day 6, measuring alginate concentration. Two strains, DSM 87 and CCM 289, were selected based on their ability to form stable alginate gels.

As shown in Figure 20, alginate production for *A. vinelandii* DSM 87 various level of flask filling was monitored over time. A small difference in alginate production was detected between filling volumes on the third day. However, a noticeable drop on day four could be attributed to poor separation of alginate from biomass, likely due to overly dense gel structures. This complicates accurate quantification of alginate via ethanol precipitation, as gravimetric analysis becomes unreliable when strong gels interfere with phase separation. From day five onward, differences between the effect of filling volumes became more apparent. The 100 mL volume resulted in the lowest alginate production, while the 150 mL volume achieved the highest yield, reaching 7 g/L on day six. However, no clear differences in bacterial-gelled-culture stability were observed among the volumes of cultivation media tested. For strain CCM 289 (in

Supplementary, Figure 39), notable differences in alginate production appeared as early as day three, again with the highest yield corresponding to the 150 mL culture. This trend continued over the following days, with the 150 mL cultures consistently outperforming the lower filling volumes.

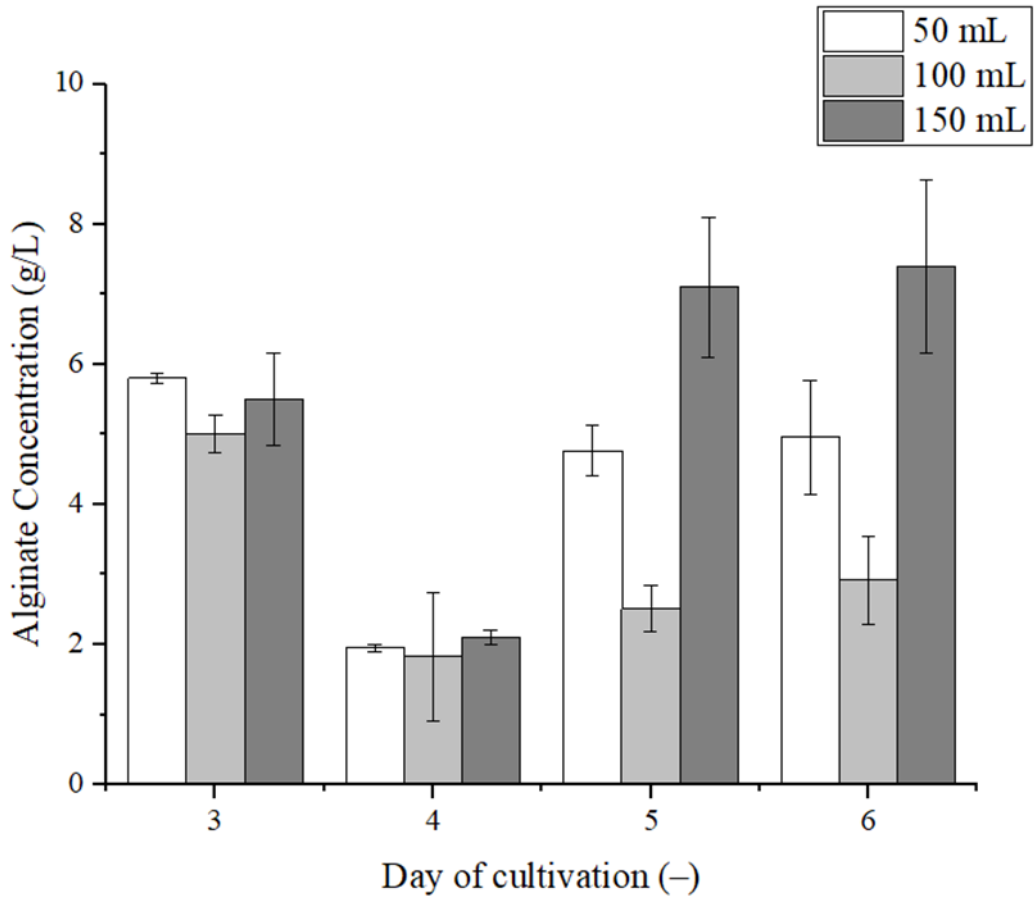

Figure 20 Determination of alginate yield throughout 3–6 days of cultivation for strain DSM 87. Different filling volumes were tested with the same agitation speed (*210 rpm*).

Generally, different levels of oxygen saturation have been tested in bioreactor cultivations to study their linear influence on both alginate content and its molecular weight influencing linearly alginate content and its molecular weight. Sabra et al. (2000), used electron microscopy to observe noticeable differences in *Azotobacter vinelandii* cells grown under 2.5 % and 20 % air saturation, demonstrating that at higher oxygen levels, cells are enveloped by a dense polysaccharide layer (Sabra et al., 2000).

Nevertheless, studies based on flask experiments have certain limitations when compared to controlled bioreactor systems. In our case, the results did not reveal as strong a correlation

between oxygen availability and alginate production as initially anticipated. While some variation in production was observed across different culture volumes, the differences remained moderate. Interestingly, cultures with higher filling volumes, typically associated with lower oxygen transfer, showed slightly better alginate yields and more consistent gel formation. Our research has suggested that oxygen transfer in shake flasks may occur differently than in stirred systems. It has been shown that under increased viscosity, shake flasks can maintain or even enhance oxygen transfer rates, in part due to the formation of a thin liquid film along the inner walls of the flask (Giese et al., 2014). This film may facilitate improved oxygen exchange, making the shake flask a more adaptive environment in terms of oxygen availability. However, the formation of biofilm on flask surfaces does not necessarily indicate oxygen limitation. Rather, this phenomenon may be influenced by multiple factors, including improved nutrient access, resistance to pH fluctuations and conditions that facilitate chemical signalling and enhanced quorum sensing (Giese et al., 2014; Malheiro & Simões, 2017).

This highlights the complexity of oxygen dynamics in small-scale systems and suggests that flask-based cultivation may involve additional mechanisms that support alginate biosynthesis under conditions not typically favourable in larger-scale bioreactors.

5.3 EVALUATION OF STRUCTURAL AND PHYSICO-CHEMICAL PARAMETRS OF GELLED BACTERIAL CULTURES

During the preparation of gelled bacterial cultures, calcium chloride (2 % *w/w*) was employed as the primary crosslinking agent due to its well-established biocompatibility, wide availability and low cost. Calcium ions, being divalent, facilitate gelation by forming an "egg-box" structure with alginate chains, resulting in a stable hydrogel network (described above in 2.4.4). Given the advantages of calcium chloride, it served as a reliable standard for initial experiments. However, in pursuit of optimizing gel strength and exploring alternative gelation pathways, we extended our investigation to other gelling agents. This included testing multi-ion crosslinking systems, gelation induced by pH reduction and specific networking of anions of various organic acids and gradual gelation through the release of insoluble $CaCO_3$ using glucono-δ-lactone (GDL). These approaches were explored not only to understand their impact on the mechanical properties and stability of the hydrogel matrices but also to identify potential alternatives that could offer improved characteristics for specific applications. The methodology and comparative results of these gelation strategies will be discussed in detail in the subsequent sections.

5.3.1 Preparation of gelled bacterial cultures using alternative cross-linking methods–multivalent ions

To develop effective hydrogel systems for encapsulating bacterial cultures, we aimed to investigate various crosslinking strategies involving multivalent ions, extending beyond the commonly used calcium chloride. While calcium chloride is widely recognized for its efficiency, biocompatibility and affordability, our goal was to evaluate the potential of alternative ionic crosslinkers and assess their influence on gelation efficiency, structural integrity and mechanical strength of the resulting hydrogels. This comparative approach was intended to identify versatile gelation agents suitable for different bacterial strains and application scenarios.

Calcium chloride (2 % *w/w*) served as the reference crosslinking agent against which the performance of alternative multivalent ions was evaluated. Our aim was to gain insights into how other di- and tri-valent ions affect formation of gels from bacterial cultures. Specifically, we tested Cu^{2+} and Fe^{3+} as interesting multivalent metal ions. These ions are capable of inducing gelation at lower concentrations and offer distinct functional properties, Cu^{2+} has known antimicrobial and biomedical utility, while Fe^{3+} is a physiologically essential trivalent ion. The alginate gelation mechanism with multivalent ions is typically attributed to the formation of an "egg-box" structure, wherein ionic interactions between divalent or trivalent cations and carboxyl groups on the polymer chains facilitate the creation of a three-dimensional gel network. Interestingly, recent molecular dynamics simulations and experimental data reveal that alginate chains contain many non-equivalent binding sites, some of which remain unbounded after gelation. Transition metal ions such as Cu^{2+} can form rapid and robust crosslink junctions, moreover, it has also led to the formation of secondary complexes that persist after standard washing, indicating stronger physical adsorption (Makarova et al., 2023). This study specifically aimed to compare the performance of di- and trivalent ions in terms of gel strength and mechanical stability.

For this study, a representative bacterial strain, *A. vinelandii* DSM 87, was selected as a model organism to standardize testing conditions across all crosslinking scenarios. To evaluate the performance of various gelation agents, rheological measurements were conducted using an amplitude sweep test. This method was used to determine the average complex modulus within the linear viscoelastic region (LVR) and the limiting oscillation strain (LOS), defined as the strain at which the structural integrity of the gel is disrupted and the material undergoes collapse

of its internal structure and irreversible deformation. These parameters provide insight into the mechanical stability and robustness of the bacterial gel network under stress. The results of these rheological analyses are presented in Figure 21. Among the tested gelation agents, Fe^{3+} achieved the highest complex modulus of all the tested cross-linking agents, reaching up to 25 kPa, at 1 % limiting strain, which is interesting when compared to the reference $CaCl_2$ (2 % *w/w*), damaging at 2.5 %. Furthermore, Ca^{2+} at 5% *w/w* resulted in a higher complex modulus than 2 % $CaCl_2$, while its LOS, marking the end of the LVR, was approximately 0.5 %. The unique properties of Fe^{3+} bacterial gelled culture arise from the specific binding behaviour of Fe^{3+} ions with alginate chains.

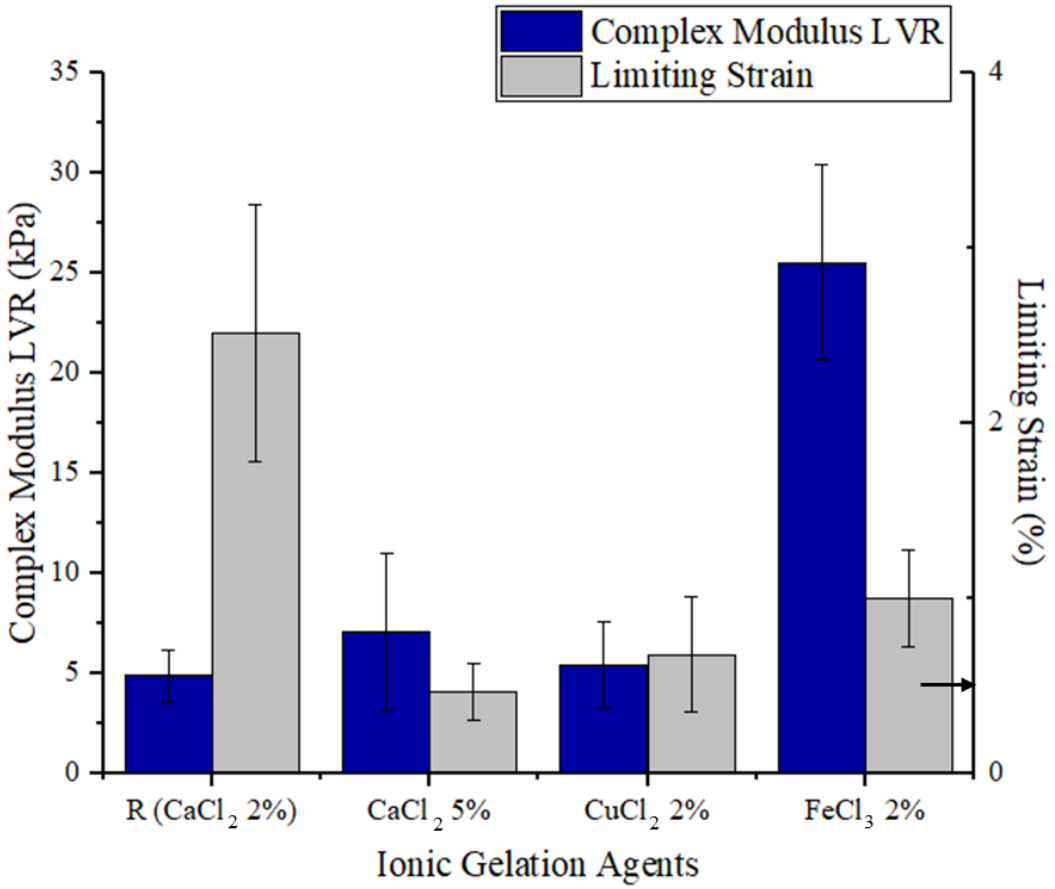

Figure 21 The comparison of multivalent gelation agents used for direct gelation of bacterial cultures of A. vinelandii DSM 87. As reference, $CaCl_2$ (2 % v/v) was used.

Among the various multivalent ions tested, Fe^{3+} ions demonstrated the highest potential for enhancing gel elasticity due to their strong crosslinking capability with carboxyl-rich polymers such as bacterial alginate. However, this increased elasticity is accompanied by decreased long-term stability as indicated by a lower LOS. Recent studies have shown that the incorporation of

additives, such as Ca^{2+}, into Fe^{3+}–alginate gels can significantly improve their mechanical stability and overall robustness (Massana Roquero et al., 2022; Y. Wang et al., 2024). It is worth noting that a reverse approach by adding small amounts of Fe^{3+} to primarily calcium-based gels, could potentially modify and enhance certain mechanical or structural characteristics of the resulting gel matrix. For instance, the addition of Fe^{3+} may be beneficial when the alginate yield or its quality (M/G) is not sufficient to form gels using Ca^{2+} alone. However, such optimization strategies, while scientifically promising, represent a distinct research direction that goes beyond the primary scope of this dissertation. The aim here was not to develop hybrid gel systems, but rather to systematically study various aspects of bacterial encapsulation relevant to the formulation and preparation of bioinoculants.

To further explore the microstructural characteristics of alginate-based hydrogels crosslinked with different ionic agents, scanning electron microscopy (SEM) was employed. Our objective was to examine how the type of crosslinking ions, or their concentration, influence the morphology of the resulting gel networks as compared to $CaCl_2$. Since it is well known that the freezing technique used prior to freeze-drying can significantly affect the observed microstructure of hydrogels (particularly in terms of pore formation and matrix architecture) we tested two different freezing approaches (freezing at −80°C and instantaneous freezing by liquid nitrogen). By combining these variables, we aimed to better understand the interplay between ionic crosslinking and sample preparation on the final morphology of the gels.

Figure 22 represents SEM micrographs of samples crosslinked with $CaCl_2$ (2 % and 5 % *w/w*) and $FeCl_3$ (2 % *w/w*), prepared using two different freezing methods: freezing at −80 °C (left: panels a, c, e) and liquid nitrogen immersion (right: panels b, d, f).

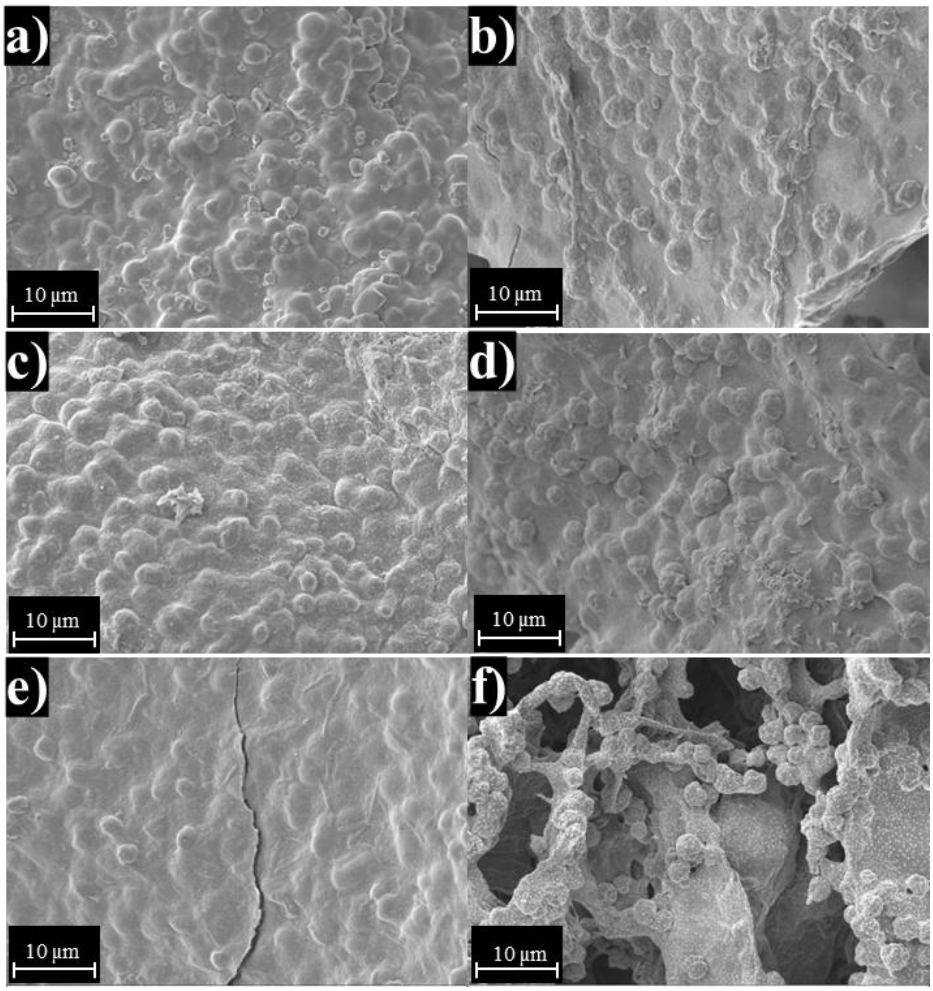

Figure 22 Scanning electron microscopy of different gelation ions, where two methods of preparation were used- frozen in -80°C (left part- a, c, e) and by liquid nitrogen (right part-b, d). f) for $CaCl_2$ 2 % (a,b), $CaCl_2$ 5 % (c, d), $FeCl_3$ 2% (e, f)

The morphology of all $CaCl_2$ (2 and 5 % *w/w*) in the Figure 22, shows noticeable differences depending on the freezing method. The −80 °C frozen sample (a, c,) reveals a moderately rough, porous texture, with rounded surface features indicative of localized shrinkage during dehydration. In contrast, the liquid nitrogen-frozen counterpart (b, d) displays a smoother, more compact structure with less pronounced surface porosity, likely due to the more rapid freezing and reduced ice crystal growth. In contrast, $FeCl_3$ (2 %)–crosslinked hydrogels show a distinctly different morphology. The −80 °C sample (e) appears smoother, yet displays cracking, possibly due to brittleness and internal stress during drying. The liquid nitrogen-frozen Fe^{3+} gel (f) exhibits a highly porous and interconnected network, characteristic of a sponge-like structure. This pronounced porosity may be attributed to the formation of secondary

structures and strong crosslinking density, which influence the hydrogel's freeze-drying behaviour.

As expected, multivalent ions demonstrated noticeable differences in the quality, strength and even the microporous structure of bacterial hydrogels. Of particular interest to our study is the observation, supported by the findings of revealed in the bachelor thesis of Svobodová, that while high concentrations of Cu^{2+} and Ba^{2+} (above 2 % *w/w*) negatively affected bacterial viability, lower concentrations (0.2 % *w/w* and below) did not have a significant impact on cell survival (Lucie Svobodova, 2024). These results suggest that the addition of multivalent gelation agents such as Cu^{2+}, Ba^{2+}, or Fe^{3+} can enhance the mechanical strength and increase the average complex modulus of bacterial hydrogels, without compromising bacterial viability at low concentrations. This opens the possibility of optimizing gel properties without ecological or biological drawbacks. However, further studies are necessary to systematically evaluate the effects of varying concentrations and combinations of multivalent ions on gel performance and bacterial encapsulation efficiency.

5.3.1 Ionotropic gelation in the whole volume using glucono-δ-lactone

In addition to exploring alternative cations and organic acids for alginate-based gel formation, we investigated the incorporation of GDL as an alternative additive to enhance the gelation process and improve the properties of the resulting gels. One of the key advantages of using GDL, compared to gelation initiated solely by calcium ions, lies in its delayed gelation mechanism. While calcium ions from $CaCl_2$ trigger rapid gelation upon contact with the polymer matrix, GDL gradually spontaneously hydrolyzes into gluconic acid, leading to a slow and controlled pH reduction. The resulting acidification dissolves $CaCO_3$ (presented in *A. vinelandii* medium), leading to the gradual release of Ca^{2+} ions into the medium. This controlled liberation of calcium ions enables slow and homogeneous gelation, allowing precise regulation of gel structure and mechanical properties. Unlike encapsulation methods that rely on multivalent ions or direct acid addition, GDL-mediated gelation offers the potential to process large volumes of bacterial cultures more efficiently, simplifying the workflow and reducing both waste and processing time.

Importantly, our decision to use this method was also logically driven by the fact that $CaCO_3$ is already an integral component of the cultivation medium. By adopting this approach, we are able to utilize $CaCO_3$ efficiently in two stages of the process. Firstly, during microbial cultivation and subsequently as a calcium source during gelation. Beyond its impact on

mechanical performance, this internal gelation strategy also provides significant processing advantages. The delayed response is particularly beneficial in applications such as bacterial encapsulation, where premature gel network formation could compromise the even distribution of cells. Moreover, the homogeneous internal release of crosslinking ions ensures consistent gelation throughout the entire matrix, in contrast to the surface-dominated and often uneven gelation observed with fast-acting ionic crosslinkers. Such volumetric uniformity is essential for applications that demand reliable mechanical and structural integrity across the entire gel body.

The mechanical properties of bacterial gelled culture crosslinked via internal gelation using GDL and $CaCO_3$ were evaluated through oscillatory rheology (Figure 23). Two molar ratios of GDL:$CaCO_3$, 1:2 (top) and 1:4 (bottom), were compared to assess their impact on gel stiffness and structure. Gels formed at the 1:4 ratio exhibited significantly higher complex moduli (G*), indicating stronger crosslinking and enhanced mechanical stability. These samples maintained elasticity over a broader strain range, while the phase angle (δ) increased more gradually, suggesting greater structural resilience. In contrast, the 1:2 ratio resulted in weaker gels with a lower G* and earlier onset of network breakdown, as seen in the sharp increase in δ beyond 100 % strain. This behaviour highlights the critical role of Ca^{2+} availability in determining gel robustness. Notably, higher molecular weight alginate (DSM 13529) produced consistently stiffer gels than lower molecular weight variants (CCM 289 and DSM 87), attributable to greater chain entanglement and network integrity.

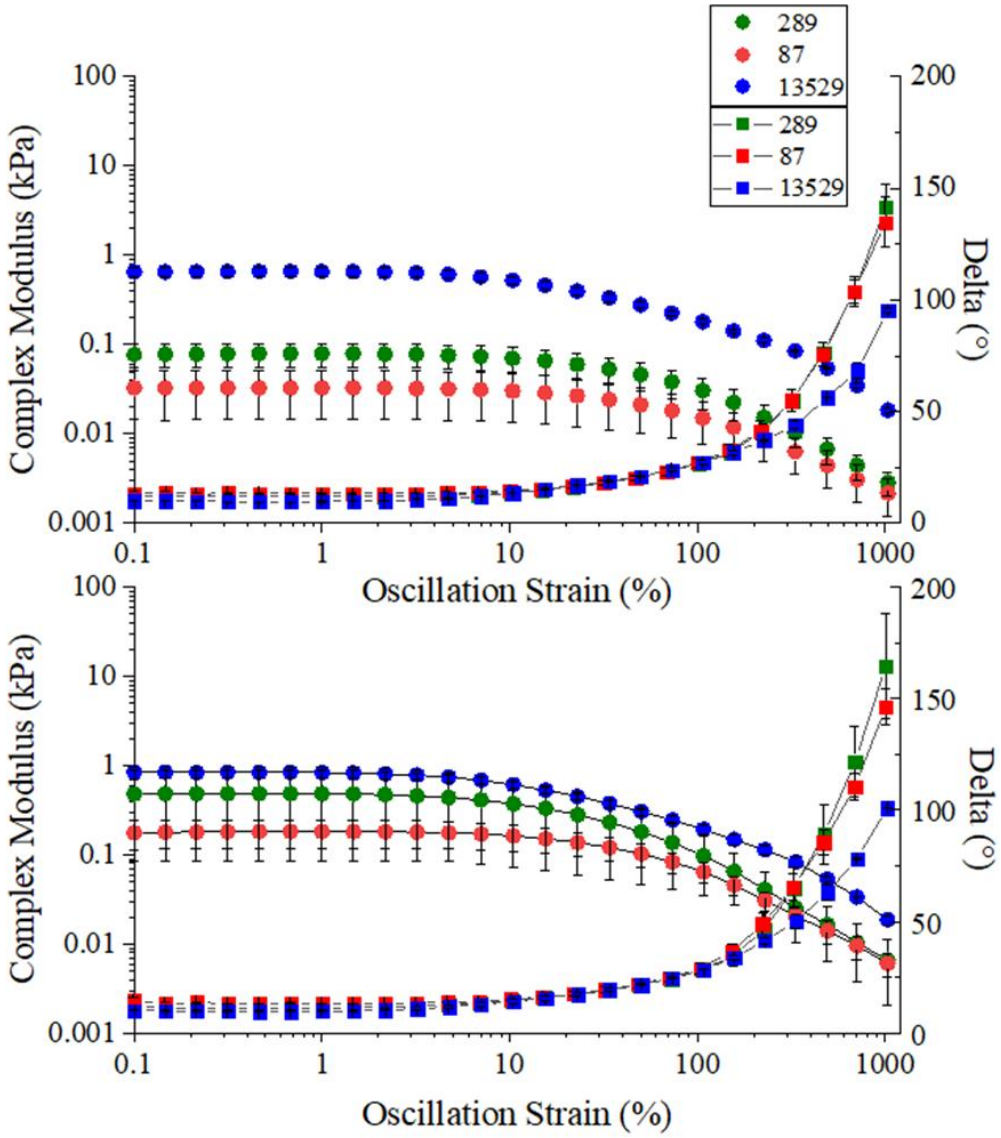

Figure 23 Complex moduli (right) of Azotobacter gels (CCM 289- green, DSM 87- red and DSM 13529- blue) and phase angle (right), formed by delayed gelation technique using GDL in ratio 1:2 ($CaCO_3$: GDL) up and ratio 1:4 (down). Circles represent complex moduli, while squares represent phase angle.

Since the advantage of GDL lies in its delayed gelation behaviour, we focused our experimental approach on investigating the kinetics of this gelation process. To characterize gel formation in detail, the gelation was monitored over time using a time sweep test, while the pH was simultaneously measured. The results are presented in Figure 24. The pH (top) gradually decreases from approximately 6.8 to 5.2 within 80 minutes, indicating progressive acidification of the medium. The viscoelastic properties of the sample (Figure 24 bottom) show a significant

increase in both the storage modulus (G′) and loss modulus (G″), with G′ rising more sharply. The early crossover point, where G′ surpasses G″, suggests that the material transitions from a predominantly viscous to a predominantly elastic behaviour within the first 10 minutes, which characterizes gel formation. As the time progresses, G′ remains significantly higher than G″, indicating the development of a strong gel network. The data demonstrate that the gelation process is strongly influenced by acidification, which enhances intermolecular interactions, resulting in increased structural rigidity of the material.

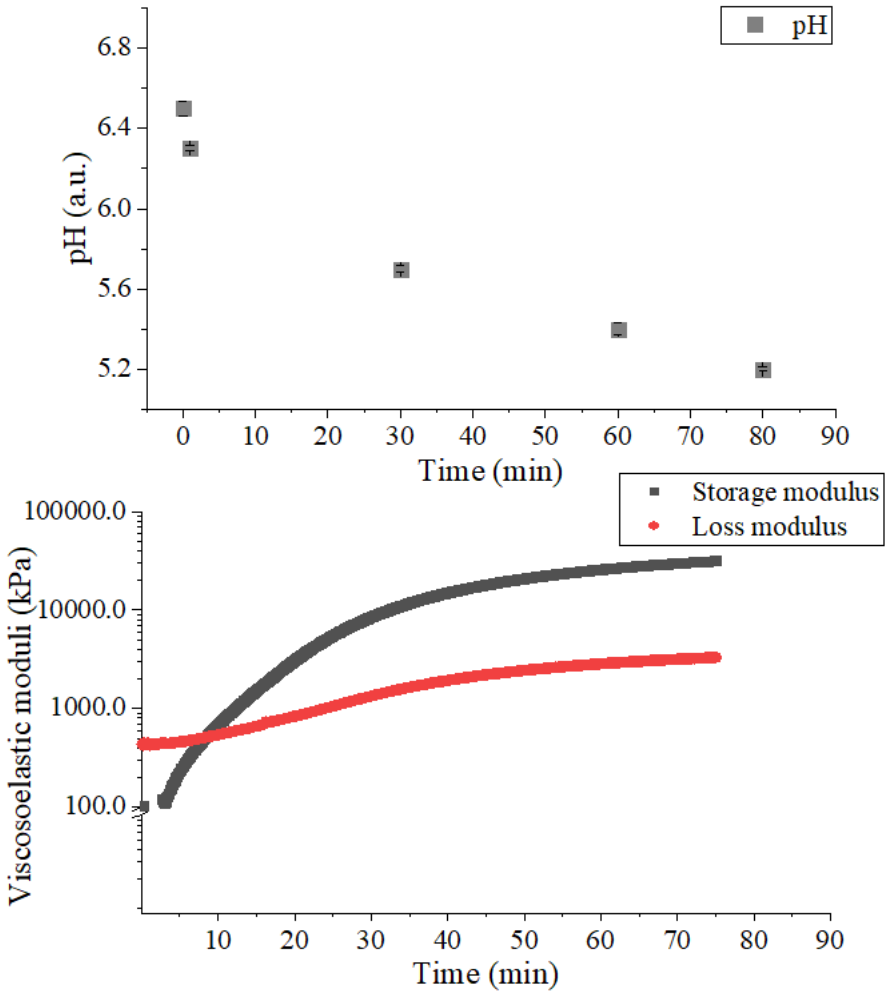

Figure 24 The continuous gelation by GDL of Azotobacter strain CCM 289 in the ratio $CaCO_3$; GDL (1:4), where in the top is measured pH of bacterial culture over time after GDL addition and in the bottom is measured rheological behaviour of formed gel

Our experiment with continuous gelation demonstrates that gel formation using GDL is possible within a relatively short time frame. Although the average complex moduli of the

resulting gels are lower compared to those formed with $CaCl_2$ or other gelling agents previously tested in Chapter 5.3.1 and 5.3.2, the potential of gradual, controlled gelation is noteworthy. This slower gelation process may offer practical advantages in biotechnological applications, where it could help simplify production workflows and reduce the need for rapid mixing or precise timing, ultimately enhancing process efficiency. Moreover, gelation in whole volume allows the formation of well-defined gel shapes that mirror the container.

5.3.2 Preparation of bacterial gels using alternative cross-linking methods with organic acids

In addition to traditional ionic crosslinking with multivalent metal ions, alternative gelation strategies based on organic acids have attracted growing interest due to their biocompatibility, tunability and potential for gentler encapsulation conditions. Among these, citric acid has emerged as a particularly promising candidate for pH-induced gelation of alginate-based hydrogels. The mechanism of acidic gelation differs fundamentally from ion-mediated gelation. Instead of forming ionic bridges between carboxylate groups using multivalent cations, acidic gelation relies on specific networking of organic acids ions. The addition of an organic acid protonates the carboxylate groups ($–COO^-$) on the alginate chains, converting them into their neutral –COOH for, leading to the neutralization of charge reduces electrostatic repulsion between polymer chains, allowing them to move closer together and form three-dimensional gel network (Massana Roquero et al., 2022).

In the context of this work, the primary aim was not to fully optimize acid-crosslinked hydrogels for advanced applications, but rather to explore their feasibility as alternative encapsulation systems for bacterial cultures of *A. vinelandii*.

Initial experiments were conducted using citric, maleic and oxalic acids, all in concentration of 0.5 M. The acids were chosen to evaluate gel formation, mechanical integrity and bacterial viability. Citric acid is commonly used in the biotechnological industry, while maleic and oxalic acids were selected as relatively strong organic acids to explore their potential as alternative gelation agents (Pérez-Madrigal et al., 2017). The results of these trials are presented in the following section, with particular attention to their relevance for practical bioinoculant preparation and demonstrated in Figure 25.

The Figure 25 demonstrate the effect of different acidic gelation agents on the complex modulus within the linear viscoelastic region (LVR) and the limiting strain (%) of hydrogels. Among the tested agents, 0.5 M oxalic acid produced the stiffest gel, with the highest complex modulus

(9 kPa), although it exhibited the lowest limiting strain (~1%), indicating a brittle structure. In contrast, the reference sample using 2% $CaCl_2$ (R) showed a moderate complex modulus (5 kPa) but the highest limiting strain (~3.5%), suggesting a more flexible and resilient gel. Citric acid (0.5 M) resulted in a gel with intermediate stiffness (6.5 kPa) and moderate limiting strain (2.5 %), while maleic acid (0.5 M) produced the softest gel (2 kPa) with a relatively low but slightly higher strain limit (1.8 %) compared to oxalic acid. These findings highlight that oxalic acid yields a rigid but fragile network, while $CaCl_2$ promotes a more elastic and deformable gel. The variability observed in the data, particularly in the oxalic acid and $CaCl_2$ groups, is reflected in the larger error bars, indicating potential inconsistency in gel formation. Overall, the choice of gelation agent significantly influences the mechanical behaviours of the resulting hydrogel, with trade-offs between stiffness and flexibility.

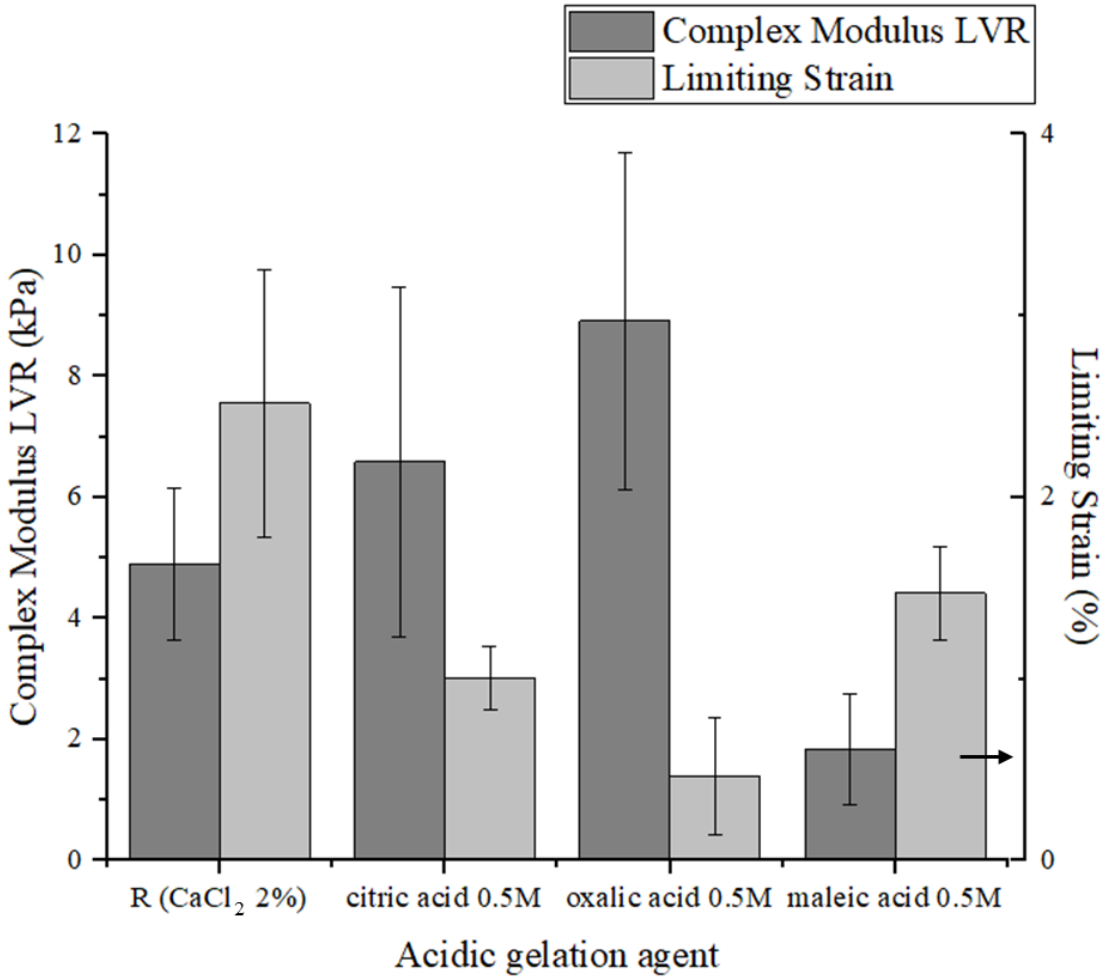

Figure 25 The comparison of acidic gelation agents used for direct gelation of bacterial cultures of A. vinelandii DSM 87. As reference, $CaCl_2$ (2 % v/v) was used.

In the context of acidic gelation, citric acid has emerged as a particularly promising alternative to reference, calcium chloride (2 % *w/w*). It is biocompatible, widely used in food and pharmaceutical products. Moreover, citric acid–based gels exhibit stimuli-responsive behavior, making them suitable for controlled drug release, wound healing and tissue engineering applications (Sütekin, 2024). However, increasing citric acid concentrations, while enhancing gelation, have been associated with reduced tensile strength and modulus in alginate films, as observed in several studies, highlighting a trade-off between gelation efficiency and mechanical robustness (Hilbig et al., 2020).

Carboxylic acid-induced gelation SEM analysis was conducted on alginate hydrogels crosslinked with 0.5 M citric acid and 0.5 M oxalic acid, chosen as representative samples. As for the ionic crosslinking, samples were prepared via two different freezing methods, frozen at –80°C and liquid nitrogen. For citric acid–gelled samples, the −80 °C preparation (Figure 26a) exhibits a densely packed and granular surface morphology, with uniformly distributed spherical or semi-spherical domains. This suggests consistent ionic- or hydrogen-bond crosslinking driven by citric acid's multiple carboxyl groups. The liquid nitrogen-frozen sample (Figure 26b) displays a slightly more open and fibrous surface, though the spherical micro-domains are still present, indicating retained structural integrity with slightly increased porosity due to the faster freezing process.

In the case of oxalic acid–crosslinked samples, a distinct difference in morphology is observed. The −80 °C sample (Figure 26c) presents a more heterogeneous and layered texture, with noticeable tearing or folding of the structure, possibly reflecting weaker crosslinking or brittle behaviour. The liquid nitrogen-prepared sample (Figure 26d) appears highly porous and fragmented, with an open, sponge-like network. This suggests that oxalic acid induces a looser gel network and its lower molecular weight and fewer functional groups compared to citric acid may contribute to reduced gel stability and mechanical strength.

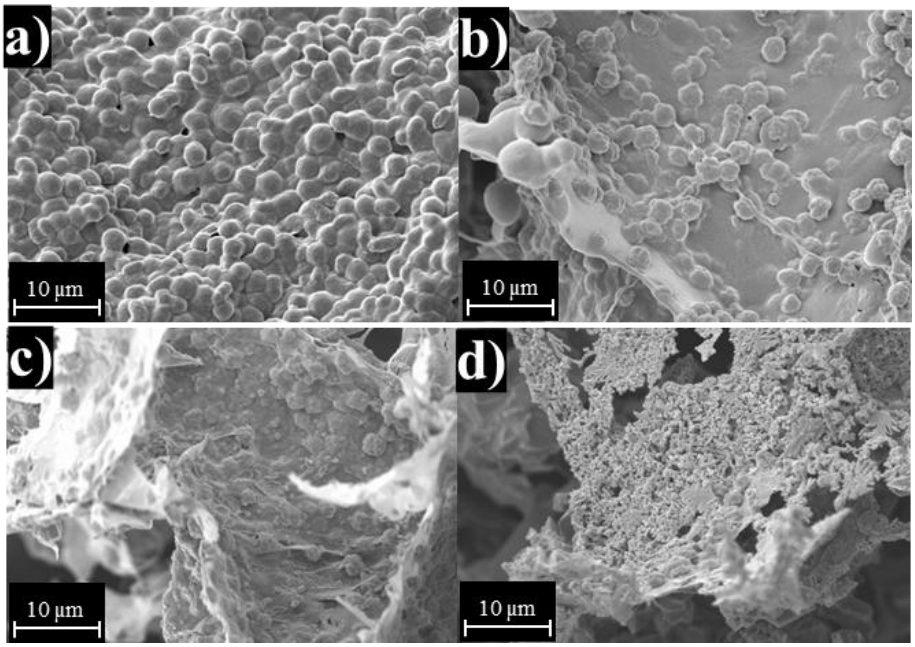

Figure 26 SEM of different carboxylic acids used in gelation- 0.5 M citric acid (a, b), 0.5 M oxalic acid (c, d) by two different methods of sample preparation; frozen at −80°C (left- a, c) and by liquid nitrogen (*right- b,d*).

These observations confirm that both the type of gelation ion and the freezing method significantly influence the final microstructure of hydrogels, which in turn affects their mechanical and functional properties. This is particularly important in applications such as biomedical engineering and encapsulation, where both strength and flexibility are critical. Among the tested gelation agents, citric acid emerges as the most promising alternative to ionic crosslinking, offering a favourable balance between stiffness and elasticity. Similar to previous findings involving multivalent ion solutions, a combination of $CaCl_2$ and an organic acid (such as citric acid) may enhance gelation behaviour and material performance. However, further investigation is needed to fully evaluate the potential interactions, optimize the formulation and assess the resulting gelled bacterial culture's properties in more detail.

5.4 INVESTIGATION OF BACTERIAL CELLS RELEASE FROM GEL MATRICES AND THEIR VIABILITY MONITORING BY FLOW CYTOMETRY

In the following chapter, we focused on studying the continuous release of bacteria from gelled bacterial cultures. Our aim was to analyse not only how the bacterial gels disintegrate over time, but also whether the bacteria remain viable at the end of the cultivation process and after encapsulation. Any changes in the medium, environmental conditions, or temperature can affect bacterial viability, particularly after gel formation, even while still keeping bacterial media.

Therefore, we wanted to determine how quickly bacteria are released from the gel, whether the gels are mechanically stable enough to resist disintegration in phosphate buffer or aqueous conditions and finally, whether the released bacteria remain viable.

5.4.1 Bacterial cells release from the gel into isotonic and hypotonic environments

In addition to rheological measurements and as a part of gel characterization, we also studied the release of the bacteria from the gel matrix to assess the differences in gel strength. The most importantly, two representative strains were studied out of this category- strain DSM 720 and CCM 289. The release studies were performed into the distilled water. As a second release environment, the phosphate buffer was studied, since it had been proven by several studies, that presence of phosphates in the buffer, dissolve the connecting alginate network (Chan et al., 2008; Urbanova et al., 2019).

Figure 27 presents the optical density measurements (at A_{630}) of the surrounding liquid media - either distilled water or phosphate buffer- used to monitor bacterial release over 6 hours under gentle agitation. Results are shown for two bacterial strains. Strain DSM 720 exhibited a rapid and continuous release in phosphate buffer, with optical density reaching A_{630}= 2 by the third hour, suggesting that phosphate ions may enhance or accelerate the release process in this strain and degradation of alginate network. In contrast, strain CCM 289 showed a slower and more gradual release, reaching a maximum A_{630} of 0.35, indicating a more stable encapsulation behaviour. Nevertheless, disintegration in distilled water was much smoother and more continuous for both gelled bacterial cultures, suggesting that release dynamics are not only strain-dependent but also strongly influenced by the composition of the release medium as well as by the stability and porosity of the alginate network. Phosphates are known for their strong chelating affinity toward Ca^{2+}, as confirmed in this experiment. Due to its capacity to react with phosphates, alginate has been extensively employed for phosphate removal from aqueous

systems. This function is not limited to calcium alginate but also extends to other metal–alginate complexes, such as those containing Fe^{3+} (Eltaweil et al., 2022).

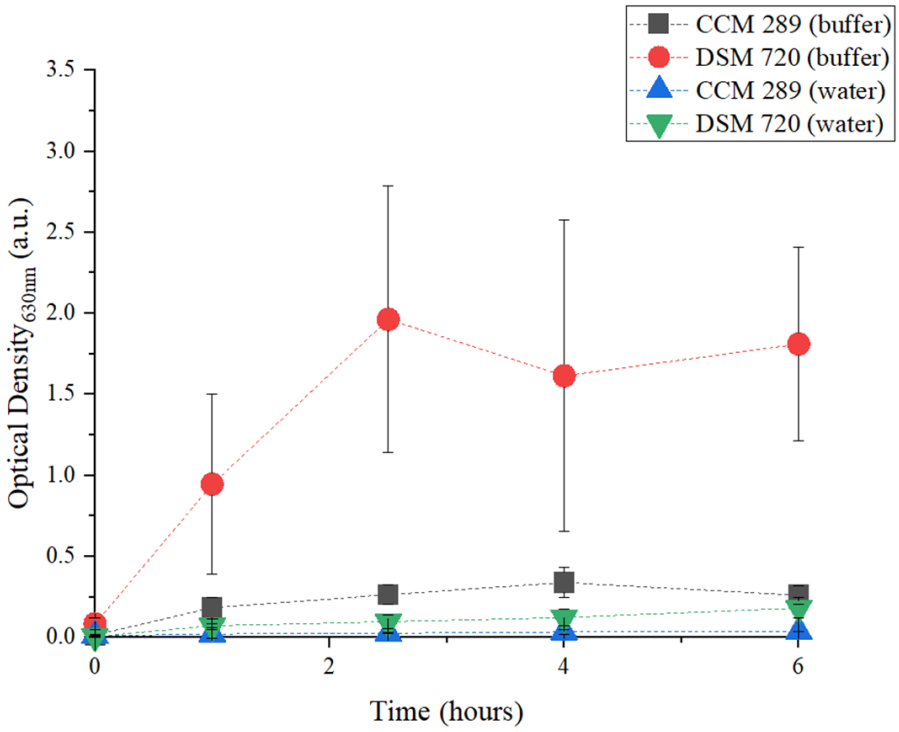

Figure 27 The release of bacterial cells from gelled bacterial cultures was monitored over a 6-hour period in two different media: phosphate buffer and water. Two Azotobacter vinelandii strains, CCM 289 and DSM 720, were evaluated to compare their release profiles in both environments.

To explore the impact of different gelation agents on bacterial release, we conducted another experiment using DSM 87, as a representative bacterial strain with sufficient gelation properties. Gels were prepared with either $CaCl_2$ (at 2 % and 5 %) or 0.5 M citric acid and the release of bacterial cells was monitored over five days. This process was evaluated in both phosphate buffer and distilled water.

The release was studied by measuring the optical density (λ= 630 nm) over 120 hours, what reveal distinct differences in microbial or a particulate growth under previously mentioned treatment conditions (see Figure 28). Notably, citric acid in buffer showed the most pronounced increase in OD_{630} reaching values above 3.0, suggesting a significantly enhanced release or turbidity compared to all other treatments. This may be explained by increased gel disintegration facilitated by phosphate ions presence in the buffer, which can influence the pH of the solution.

In contrast, both 2 % and 5 % (*w/w*) $CaCl_2$ in buffer showed moderate increases in optical density, indicating reduced level of gel disintegration. Water-based treatments generally resulted in lower OD values, with 2 % $CaCl_2$ in water showing minimal bacterial release, suggesting distilled water did not significantly influence hydrogel structure and does not lead to increase disintegration. However, bacterial viability was not assessed during the study, as the primary focus was on its release from the alginate network. This process was accelerated solely by gel disintegration under controlled and optimal liquid conditions. Among the tested formulations, 2 % $CaCl_2$ exhibited the slowest rate of cell release in distilled water, while 5 % $CaCl_2$ showed comparatively slower release in the phosphate buffer.

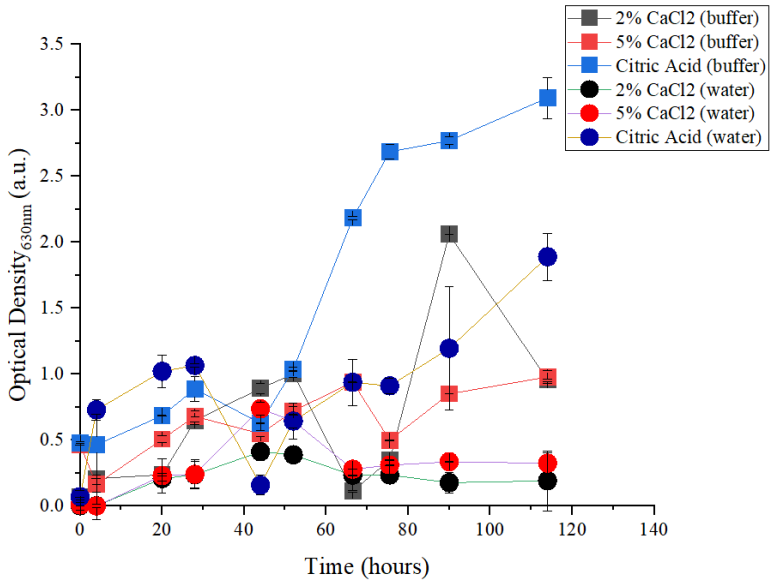

Figure 28 Release of bacteria of strain DSM 87 into phosphate buffer and water, respectively, from gels prepared with calcium chloride and citric acid as the crosslinkers.

These results confirmed that the release of bacterial cells from the gel occurs over the course of several hours to tens of hours, which is well aligned with the intended application. Furthermore, not only the type of gelation agent but also the specific bacterial strain, the quality of the formed gel and all previously mentioned parameters, including cultivation conditions, media composition and encapsulation process, significantly influence both the rate of gel disintegration and the dynamics of bacterial release. This highlights the importance of optimizing the entire preparation process in order to achieve a tailored release profile and ensure the functional stability of gelled bacterial cultures for targeted applications.

5.4.2 Verification of cell viability at different stages of inoculant preparation and application.

Moving forward, in the context of evaluating gel performance in the context of intended application, bacterial viability emerged as a key consideration. It was crucial for us to determine whether bacterial cells could survive the gelation process and whether their continuous release would compromise their viability. Especially, taking into account the rapid change in environmental conditions, such as osmotic stress during the gel-formation. We hypothesized that the robustness of these cells is supported by their ability to accumulate PHB, as suggested in several studies (Obruca et al., 2017; Sedlacek et al., 2019). Consistent with this, our data show that PHB accumulation can reach up to 30 % of cdw in various strains, indicating a possible protective role in helping bacteria withstand stress associated with gel formation and release. Similarly, also extracellular alginate can enhance the stress resistance of bacterial cells (Pezzoni et al., 2022; Svenningsen et al., 2018).

To assess cell viability, we first needed to select a suitable fluorescent probe. Four different dyes were tested: propidium iodide (PI), fluorescein diacetate (FDA), Calcein AM and DAPI. Figure 30 illustrates the fluorescence patterns observed by analysing live, dead (blanching in hot water) and mixed (50:50) bacterial populations from growth bacterial cultures. As shown in Figure 29a, PI successfully distinguishes between live and dead cells. As PI binds to nucleic acids in membrane-compromised (dead) cells, it resulted in significantly higher fluorescence intensity in dead cells compared to live ones. The mixed population also showed an intermediate signal, confirming PI's effectiveness in differentiating cell viability.

In contrast, FDA (Figure 29b) showed relatively similar fluorescence intensities for live and dead cells, although live cells did exhibit slightly stronger signals. FDA is hydrolysed by intracellular esterases in live cells to produce a fluorescent compound, making it theoretically suitable for viability assessment. However, in our case, no clear distinction was observed between the two populations. The slight differences in internal fluorescence structure, particularly in the 50:50 mix, may reflect physiological variability or differences in esterase activity between subpopulations.

Calcein AM and DAPI were evaluated in Figure 29c and Figure 29d, respectively. However, neither dye provided distinguishable fluorescence differentiation between live and dead cells. Calcein AM, which requires intracellular esterase activity and intact membranes to generate fluorescence, failed to differentiate viable cells under our conditions. Similarly, DAPI, which

stains DNA in both live and dead cells, did not yield any meaningful contrast and is not a candidate for determination of viability, only as a marking dye.

A major limitation in accurately determining cell viability may stem from the alginate matrix surrounding the cells. This layer can act as a physical barrier, not only limiting oxygen diffusion but also preventing the penetration of large molecules of the fluorescent probe. Consequently, inadequate dye uptake may have obscured reliable fluorescence signals. To improve probe effectiveness, thorough washing and optimization steps are essential before conducting viability assays on encapsulated cells.

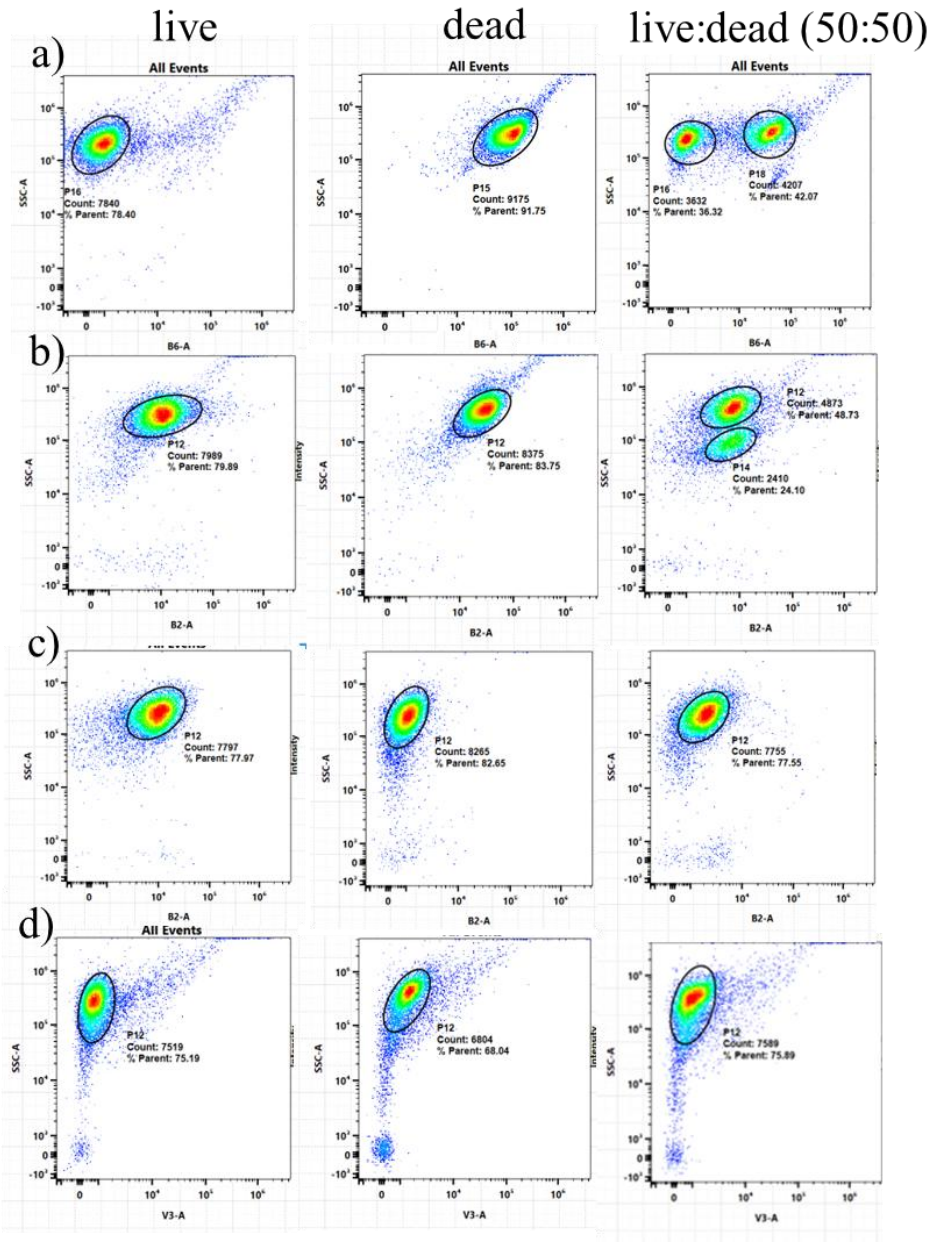

Figure 29 Flow cytometry determination of viability bacteria A. vinelandii, where different fluorescent probes were used (*a- Propidium Iodide, b- Florescein Diacetate, c- Calcein AM, d- DAPI*) *to detect viable, nonviable cells and their mix in ratio 50:50.*

After selection of suitable fluorescent probe and defining/determining its optimal concentration, PI at a concentration of 1 mg/mL was used in following experiments. PI was tested on gel-forming bacterial strains used in this study (DSM 87, DSM 720 and CCM 289) and its applicability was confirmed across all strains (Supplementary Figure 40).

Following this, cultures were subjected to gelation using a standardized procedure in which 10 mL of bacterial suspension was pipetted into 2% $CaCl_2$ as the gelation agent. After that, we

evaluated the survival of the cells after gelation and their one-hour long release. As shown in Table 6, although all strains were gelled under identical conditions, the number of released cells varied significantly. DSM 87 exhibited the highest release, with 262 × 10^5/mL cells recovered, whereas the remaining strains released no more than 32.6 × 10^5/mL cells. In contrast, DSM 720 released a much smaller number of cells (10.13 × 10^5/mL), yet exhibited the highest viability at 86 %, from all tested strains. This indicates that although the gel restricted release, it was highly protective, preserving cell integrity and viability. A similar trend was observed for CCM 289, which showed moderate release (7.54 × 10^5 cells per mL of release medium) and a relatively high viability (77 %). These findings suggest that gel conditions for these strains may have been close to optimal, balancing both controlled release and cell protection.

Table 6 Cells of A. vinelandii in 1 ml of released medium from self-produced gels for selected strains after 1 hour in phosphate buffer. Bacterial cells were analysed by flow cytometry dyed with Propidium Iodine (1 mg/ml) staining to analyse their viability

Gelated bacterial strain	**Number of bacteria (×10^5) per mL of released medium**	**Viable cells (%) after 1 hour release**
CCM 289	7.54 ± 1.48	77.01 ± 2.45
DSM 87	262.76 ± 21.87	26.43 ± 12.39
DSM 576	32.62 ± 0.66	19.72 ± 0.31
DSM 720	10.13 ± 1.35	85.89 ± 0.22

The results from our experiments highlight the strain-dependent nature of bacterial behaviour during encapsulation and release. It also suggests that both the physical characteristics of the gel matrix and the physiological properties of the bacteria play a crucial role in determining release efficiency and post-release viability. Consequently, these experiments confirm that the tested bacteria survive both gelation with calcium chloride (2 % *w/w*) demonstrating application potential in the agricultural industry for the development of bioinoculants (Oberoi et al., 2021; Yuan et al., 2022). Recent reviews and experimental studies report that typical effective inoculum concentrations used in pot and field trials range from 10^6 to 10^8 CFU/mL for liquid suspensions and approximately 10^7 to 10^8 CFU/g for carrier (solid) formulations (dos Reis et al., 2024). Because introduced strains frequently colonize only transiently, liquid applications

often have short-lived effects in the rhizosphere and therefore may need to be applied more frequently formulations (Tsegaye et al., 2022). Therefore, liquid inoculants are typically and the most effectively applied via seed coating, which ensures close contact between bacteria and emerging roots (Rocha et al., 2019).

In our system, bacteria released from gelled cultures at concentrations on the order of 10^5 to 10^7 CFU/mL within one hour of exposure to release medium, which is within the range reported to be biologically active for many PGPR and thus sufficient to stimulate or otherwise influence plant growth. Interestingly, even substantially reduced inoculant doses (below < 10^4 CFU per seed) can alter indigenous rhizosphere communities and affect plant–microbiome interactions, although the magnitude and direction of plant responses depend on inoculant strain, host plant and soil context (Chai et al., 2022).

These findings provide a sound basis for further evaluation of strain robustness and for testing the potential protective roles of intracellular polyhydroxybutyrate (PHB) and alginate encapsulation in improving survival, shelf life and field performance of bioinoculants; these questions will be addressed in Chapter 5.6.

5.5 TRANSFER OF THE CULTIVATION PROCESS OF *AZOTOBACTER VINELANDII* INTO LABORATORY BIOREACTOR

Since bacterial cultivation in Erlenmeyer flasks consistently resulted in gel formation, we decided to transfer the cultivation process to laboratory scale bioreactors. This step was important not only for increasing production volumes, but also because of the potential biotechnological applications of bacterial gels and alginate is manageable to do in bioreactors for the industrial production.

Recent studies highlight the biotechnological potential of *Azotobacter vinelandii* for producing alginate and PHB, though scaling up production remains a significant challenge. While shake flask cultures can achieve alginate yields comparable to those in small bioreactors (4.0 g/L), increasing the production scale does not necessarily enhance output, likely due to dissimilar oxygen transfer dynamics, namely, oxygen transfer rate (OTR) and dissolved oxygen tension (DOT). OTR has been identified as a critical factor in scaling up; studies conducted at 3- and 30 L scales showed that higher OTRs improved alginate yields and modified the guluronic/mannuronic (G/M) ratio. However, achieving consistent molecular characteristics across scales proved difficult (Díaz-Barrera et al., 2021). Interestingly, the specific oxygen uptake rate (qO_2) demonstrated better reliability, allowing for reproducibility in alginate

molecular weight across different bioreactor sizes. To reduce production costs, alternative carbon sources such as sugar cane juice have been explored (Chuacharoen et al., 2022). Under optimized conditions, (60 mM sucrose-equivalent, controlled nitrogen levels and pH) alginate production reached 7.29 ± 0.07 g/L with molecular weights up to 4.735 kDa. In the case of PHB, few bioreactor-scale studies exist, but notable results were obtained with the UWD mutant strain, achieving up to 3.6 g/L of PHB and 85 % of dry cell weight under a two-stage aerobic/oxygen-limited strategy. These findings underscore the importance of oxygen control and fermentation design in optimizing biopolymer yields from *A. vinelandii* (Dhanasekar et al., 2003).

Therefore, moving into these experiments was challenging from the beginning. Our first attempts using the strain CCM 289 were not successful. Although the culture grew well and produced alginate, bacterial culture did not reveal the capability of gel formation. Based on studies of molecular weight of CCM 289, we noticed that composition of G/M residues changes significantly in later phases of cultivation and M residues dominate. This means that we can assume that within a relatively short and narrow time frame, we were unable to capture the stage when the bacterial culture gelled on its own. It is possible that we missed this stage and therefore it is necessary to conduct further experiments where the gelation potential of the culture is regularly monitored at shorter intervals (e.g., every 2 hours). However, since we were also interested in testing other cultures, we decided to try strain DSM 87 as it shown consistent gel formation capacity in flasks. In this case, bioreactor cultivation was successful and we were able to obtain stable gel production.

Figure 30 shows six experiments we conducted in the bioreactor under various conditions, mainly varying agitation speed (rpm) and working volume. These factors were tested based on the assumption that the bacteria might respond differently to physical conditions in the bioreactor, even though flask-scale experiments had not shown such sensitivity. For us, it was important to study biomass, alginate production, gelation potential of the bacterial culture and glucose consumption during the process. Monitoring PHB was not necessary, although it is known that PHB production under bioreactor conditions for DSM 87 ranges from 20 to 30% of the cdw.

In the control condition (Figure 30a- 400 rpm, 3 L), glucose was depleted within 30 h, supporting robust biomass accumulation (6.2 g/L) and subsequent alginate production (1.8 g/L). Aeration was kept constant at 1 v/v/m.

Increasing the agitation speed to 450 rpm (Figure 30b) slightly reduced both biomass and alginate yields, likely due to shear stress caused by higher impeller speed. Biomass peaked at 5.4 g/L by 26 h and remained constant thereafter, while alginate reached 1.6 g/L before gradually declining.

Increasing the working volume to 4 L at 400 rpm (Figure 30c) had minimal impact on final biomass but slightly delayed both glucose consumption and alginate synthesis. Biomass reached 6.6 g/L by 30 h, while alginate production was limited to 1.1 g /L at the same time point. The change in medium volume likely altered oxygen availability, leading to a faster initial growth rate but reduced alginate production compared to the control.

Introducing a fed-batch strategy via glucose addition (Figure 30d) significantly improved performance. At 30 h, residual glucose was nearly depleted, prompting the addition of 50 mL of glucose solution (at a concentration 20 g/L) to 3 L of culture medium. This increased the glucose concentration, which remained at 6.7 g/L by 34 h. Biomass reached 7.9 g/L at this point, with alginate maintained at 1.0 g/L. By 48 h, biomass had increased to 8.7 g/L and alginate to 1.5 g/L, confirming that sustained substrate availability supports prolonged productivity.

Applying a dynamic agitation regime between 250 – 750 rpm (Figure 30e) negatively impacted both biomass and alginate formation. Biomass reached only 3.0 g/L and alginate 1.1g/L, despite complete glucose depletion. The large fluctuations in mechanical conditions likely imposed physiological stress and the culture formed dense bacterial gelled structures, potentially affecting alginate quality.

Finally, combining mild variable agitation (150 – 450 rpm) with the same fed-batch glucose addition strategy (Figure 30f) yielded both high biomass (8.0 g/L) and the highest alginate concentration (2.1 g/L) among the tested conditions. This combination of stable physical conditions and continuous nutrient availability appears to provide a favourable balance for growth and alginate synthesis, while also supporting gel stability and quality.

While shake flask experiments often overlook sensitivity to physical parameters, successful bioreactor cultivation demands precise control of agitation, aeration and feeding strategies to maintain consistent polymer quality. Overall, both our findings and those in the literature indicate that the industrial-scale application of *A. vinelandii* remains constrained by metabolic complexity, oxygen sensitivity and similarly on strain variability.

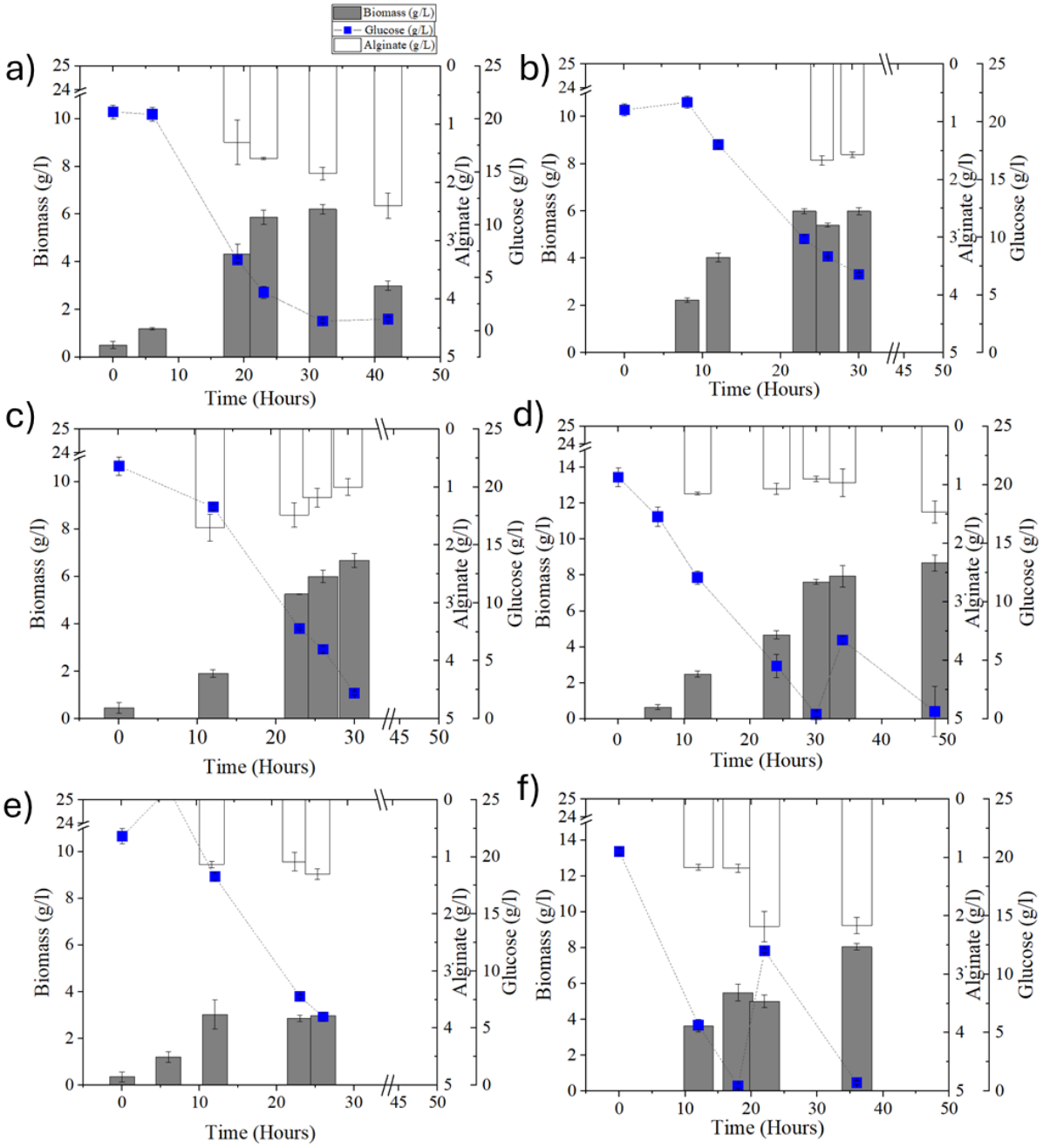

Figure 30 Bioreactor experiments with strains DSM 87 and analysis of biomass (dark grey slopes), alginate (up- white slopes) and glucose (blue points) throughout hours, where a) is control at 400 rpm in 3L volume, b) is 450 rpm and 3L, c) is 400 rpm and 4 L volume, d) 3 L, 400 rpm and addition of 50ml of glucose one time (20 g/L), e) regulation 250 – 750 rpm in 4 L volume and f) regulation 150–450 rpm in 4 L volume

Notably, our study advances the field, as there are currently no published reports evaluating the gelation potential of *A. vinelandii*. On the other hand, gel-forming capacity is the key characteristic in our concept. Overall alginate or biomass titers and yields are less critical than

the gel-forming capacity of the resulting cultures. Among all tested conditions, only intensive regulation 250 – 750 rpm in 3 L volume, did not provide any gel formation ability. Other bioreactor experiment enabled bacterial gel formation and were subsequently analysed by mechanical characterization of the gels through rheological analysis. These selected samples were subjected to oscillatory strain sweeps to evaluate their viscoelastic behaviour (Figure 31). The complex modulus (G*) across oscillation strain (%) showed that gels produced under control conditions (400 rpm, 4 L) had the highest mechanical strength, with G* values above 1 kPa over a wide strain range. Gels obtained at 450 rpm also exhibited good mechanical integrity, though slightly lower than the control. In contrast, gels formed at 350 rpm showed substantially lower moduli, suggesting weaker structural properties. Similarly, samples produced under variable agitation (150 – 450 rpm) and at 400 rpm in 4 L volume showed moderate gel stiffness, with reduced G* values and earlier onset of modulus decline with increasing strain.

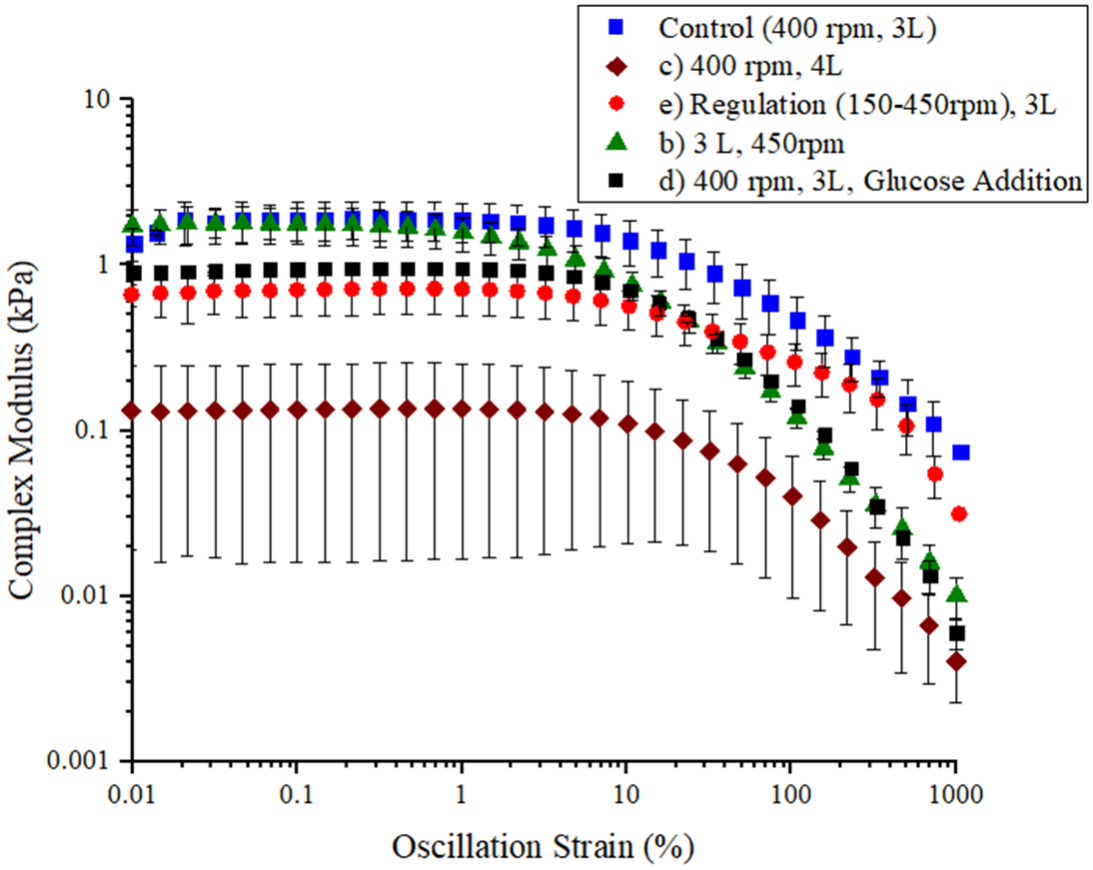

Figure 31 Amplitude sweep test and complex moduli analysis of gel formed from bacterial cultures cultivated in bioreactors crosslinking with $CaCl_2$: Cultivations of DSM 87 under various conditions are as follows: a) control at 400 rpm with 3 L volume (blue square), b) 450

rpm with 3 L volume (*green triangle*)*, c) 400 rpm with 4 L volume* (*brown square*)*, d) addition of 50 mL glucose solution* (*20 g/L*) (*black square*) *and e) agitation regulation between 150 and 450 rpm* (*red circle*).

In our scale-up process, we were successful in preparing bacterial gelled cultures directly from the media for the strain *Azotobacter vinelandii* DSM 87. However, strain CCM 289 still requires further study to enable scaling from flask cultures to large bioreactors. Our results suggest that intensive mechanical stirring may negatively affect the gelation potential of the culture, possibly due to damage to the alginate capsule surrounding the bacterial cells. For example, conditions with constant stirring at 400 rpm appeared to produce stable and good-quality gels, even with a slight increase in culture volume (up to 4 L) and agitation speeds ranging from 150 to 450 rpm. Despite the culture's high oxygen demand, it seems that maintaining relatively low stirring speeds might be necessary, as excessive mechanical stress and shear forces generated by the agitator could potentially damage the alginate capsule, which may lead to decreased alginate yield and reduced gelation ability of the culture.

5.5.1 Testing aeration at different volumes of *Azotobacter vinelandii* cultures in minibioreactors

Following the bioreactor experiments, where we observed significant variation in alginate and gel production depending on agitation and volume, we aimed to further investigate how oxygen availability and mixing influence these processes. This led us to perform a series of tests in Biosan minibioreactors RTS-1C, which differ from conventional systems in both design and mixing mechanism. In these reactors, mixing is achieved through rotation of the entire vessel rather than using a turbine stirrer. As a result, the maximum recommended working volume is limited to 30 mL out of a total 50 mL capacity, to ensure effective oxygen transfer and fluid motion. In addition, the Biosan RTS-1C bioreactors enable continuous monitoring of cell growth through automated analysis of the cultures' optical density.

Interestingly, the cultivation of *A. vinelandii* CCM 289 was successful in obtaining a gel-forming bacterial culture in a 30 mL volume, likely due to mixing by rotation rather than stirring. The obtained alginate yield was 5.6 g/L, with biomass reaching 4.7 g/L. Regarding agitation speed, we also attempted to cultivate the bacteria in tubes without stirring; however, the bacteria did not grow under these conditions.

However, to explore the impact of filling volume on growth and alginate production, three media volumes were tested: 10, 20 and 30 mL of *A. vinelandii* DSM 87. As shown in Figure 32, cultures grown at lower volumes (10 mL) reached higher optical densities more quickly and exhibited a more pronounced peak in cell density, suggesting improved oxygen availability. In contrast, the culture with the maximum volume (30 mL) showed slower growth and a lower peak in optical density, likely due to reduced oxygen availability. Interestingly, while the 10 mL culture showed the highest alginate production (8 g/L), its biomass concentration remained relatively low (4.3 g/L). At 20 mL, the alginate yield and biomass concentration were similar, with 5.8 g/L each. Conversely, the 30 mL culture had the highest biomass (7 g/L) but a lower alginate yield (5.4 g/L).

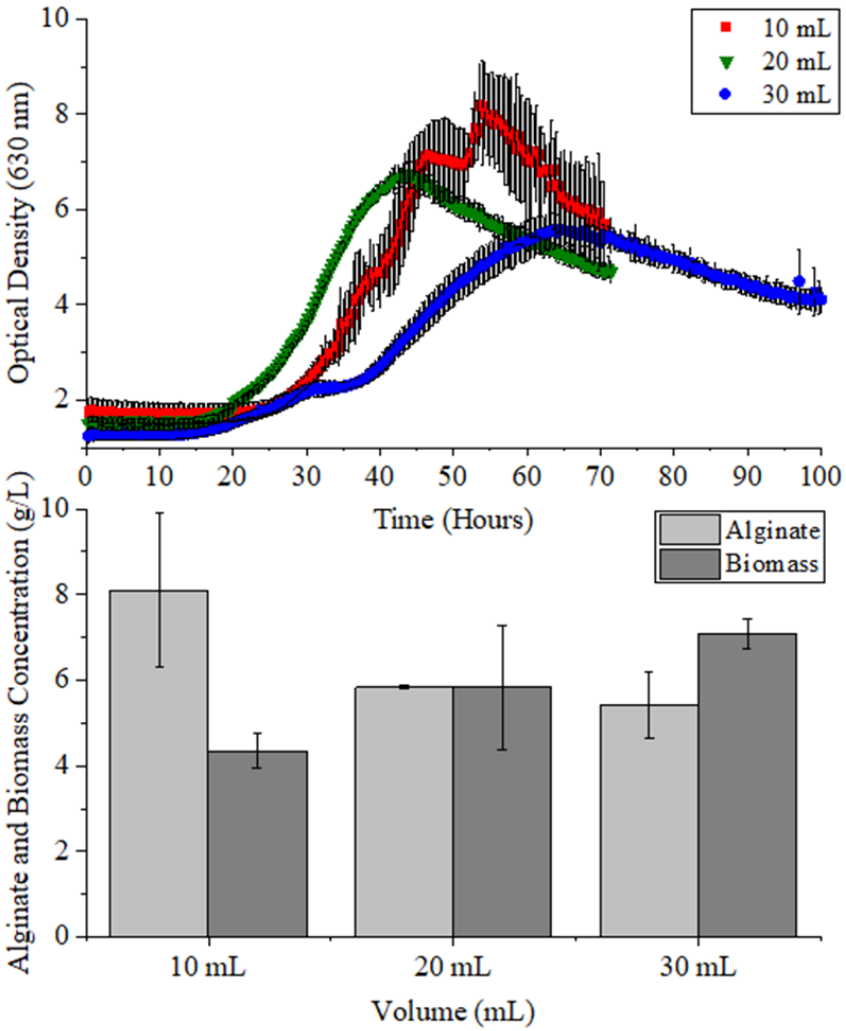

Figure 32 Cultivations of DSM 87 in Biosan RTS-1C minibioreactors with different cultivation filling volumes- 10, 20 and 30 mL.

The bacterial gelation potential was also evaluated visually by dropping the bacterial cultures into a gelation agent (2 % *w/w* $CaCl_2$) after the end of the cultivations- for 10 and 20 mL at 70 hours and for 30 mL at 100 hours. Nevertheless, in all tested volumes, the resulting gels maintained a well-defined shape without any visible disintegration, demonstrating strong structural integrity. Photographs of the gels in Figure 33 clearly show their uniform, stable form, indicating effective gelation and promising mechanical stability across different culture volumes.

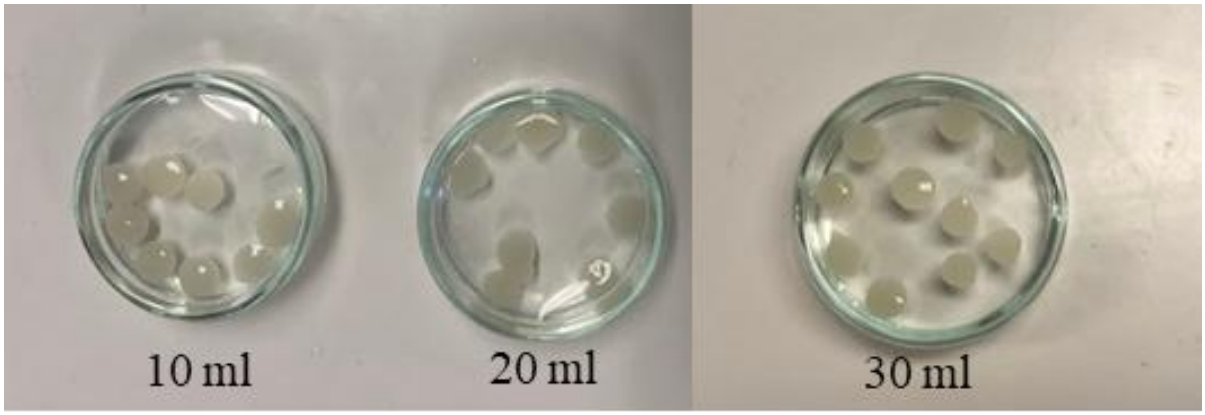

Figure 33 Tested self-bacterial gel formation for strains A. vinelandii DSM 87, for different cultivation volumes (*10, 20 and 30 ml*). *Noticeable gel drops of consistent shape are shown for all three volumes, for 10 and 20 ml at 70 hours and 30 ml at 100 hours.*

The results obtained in the Biosan RTS-1C minireactors confirm our observations from previous experiment in laboratory stirred bioreactors (5.5) that oxygen availability plays a crucial role in the growth and alginate production of *A. vinelandii* DSM 87. However, equally important is that the mixing method does not generate excessive shear forces, likely to prevent damage to the alginate capsule surrounding the bacterial cells. In the Biosan RTS-1C system, good aeration was achieved alongside a mixing mechanism that produces very low shear stress. This balance between sufficient oxygen supply and gentle mixing should be carefully considered in further optimization of cultivation conditions in bioreactors.

To the best of our knowledge, this type of reactor system has not yet been tested with *Azotobacter* strains, particularly in the context of alginate production and gelation applications. Therefore, these findings provide novel insights into how small-scale, rotational mixing systems may influence both growth kinetics and polymer biosynthesis in this genus, opening new avenues for scalable production of bacterial alginate gels.

5.6 PILOT ASSESSMENT OF GROWTH-PROMOTING ACTIVITY OF BIOINOCULATS ON THE MODEL PLANTS

5.6.1 Pivotal cultivation of lettuce plants bioinoculated with *Azotobacter vinelandii*

By gathering comprehensive data on bacterial cultivation, bioactivity assays and rheological characterization, we aimed to investigate the effects of the developed bioinoculants on plant growth. To maintain simplicity and reproducibility, we employed a basic experimental setup: *A. vinelandii* cultures were grown in Erlenmeyer flasks and gelation was induced by dropwise addition into a calcium chloride solution (2 % *w/w*). Consistent gel formation was observed across all tested strains, with *A. vinelandii* CCM 289 demonstrating particularly strong gelation ability and promising PGPR potential. The strain was chosen based on several criteria, including laboratory-tested bioactivities such as siderophore and IAA production, phosphate solubilization and stable gel-forming capacity. PHB content in CCM 289 reached up to 30% of cell dry weight (4.6). Further evaluation of this strain was conducted to assess plant cultivation and growth.

Lettuce (*Lactuca sativa*) was selected as the model plant due to its fast growth and well-documented sensitivity to environmental and microbial treatments (Abou Jaoudé et al., 2025; Burgess et al., 2024). This sensitivity makes lettuce an effective indicator for detecting significant growth responses to PGPR inoculation. To assess plant growth effects, we conducted a preliminary greenhouse experiment in laboratory conditions (Supplementary Figure 41) under controlled conditions. Plants were cultivated for one month with regular watering and stable humidity (60 %), as is further described in chapter 4.12. The experimental design included two treatments and one untreated control. The first treatment involved inoculation with bacterial gel prepared using CCM 289 cultured in flasks, while the second treatment used only bacterial cells suspended in phosphate buffer, without alginate. The experiment was maintained over a one-month period to evaluate plant responses with respect to crucial parameters such as dry plant biomass weight, length of roots and leaves, pigment concentrations.

The results of the experiment confirmed the positive effect of bacterial biofertilizer treatments on lettuce growth, as shown in Table 7. Both the liquid bacterial culture and the bacterial gel significantly improved plant development compared to the untreated control. Notably, the dry plant biomass increased from 41 ± 28 mg in the control to 194 ± 68 mg and 193 ± 74 mg in the liquid culture and gel treatments, respectively ($p < 0.001$). Leaf length also showed a

statistically significant improvement, doubling from 2.1 ± 0.7 cm in the control to 4.3 ± 1.2 cm and 4.3 ± 1.0 cm in the treated groups ($p < 0.001$). While the root length increased as well (from 13.9 ± 4.2 cm in the control to 17.4 ± 6.0 cm and 18.3 ± 5.2 cm in treated groups), this difference was not statistically significant ($p = 0.058$). Conductivity of soils especially in the liquid bacterial culture group reached 27.1 $\mu S \cdot cm^{-1}$, compared to the control 12.0 $\mu S \cdot cm^{-1}$ ($p = 0.003$), signifies higher presence of ions possibly affecting nutrient availability in the soil. As part of the experimental protocol, the treatments were repeated after two weeks, which may have further enhanced the biofertilizer effect. These findings suggest that both bacterial formulations- liquid and gel, effectively promote plant growth, with particular benefit to biomass accumulation and leaf development.

Table 7 The results of pivotal pot experiments such as soil conductometry, roots and leaves lengths and dry biomass weights of treated and untreated plants and statistical analysis from 16 replicates in each treatment. Very high statistical significance (***)*, high statistical significance* (**) *and no statistical significance* (*ns*) *evaluated by one way Anova.*

Treatment	Soil conductometry ($\mu S \cdot cm^{-1}$)	Length of roots (cm)	Length of leaves (cm)	Dry plant biomass (mg)
Liquid bacterial culture	27.1 ± 3.0	17.4 ± 6.0	4.3 ± 1.2	194 ± 68
Bacterial gel	15.6 ± 3.4	18.3 ± 5.2	4.3 ± 1.0	193 ± 74
Negative control	12.0 ± 3.6	13.9 ± 4.2	2.1 ± 0.7	41 ± 28
Statistical significance	** $p = 0.003$	ns $p = 0.058$	*** $p < 0.001$	*** $p < 0.001$

Photo documentation of treated and untreated plants in the end of the cultivation is demonstrated in Figure 34 Photo documentation of the plant cultivation experiment, where red (a, left) labels treated plants with liquid bacterial culture, blue (b, middle) labels gelled bacterial culture and green (c, right) stands for untreated control. Significant differences were observed between treated (a, b) and untreated (c) plants in terms of root length and leaf richness in lettuce.Figure 34, where untreated control is noticeably smaller for plants and shorter for roots as compared to treated plants.

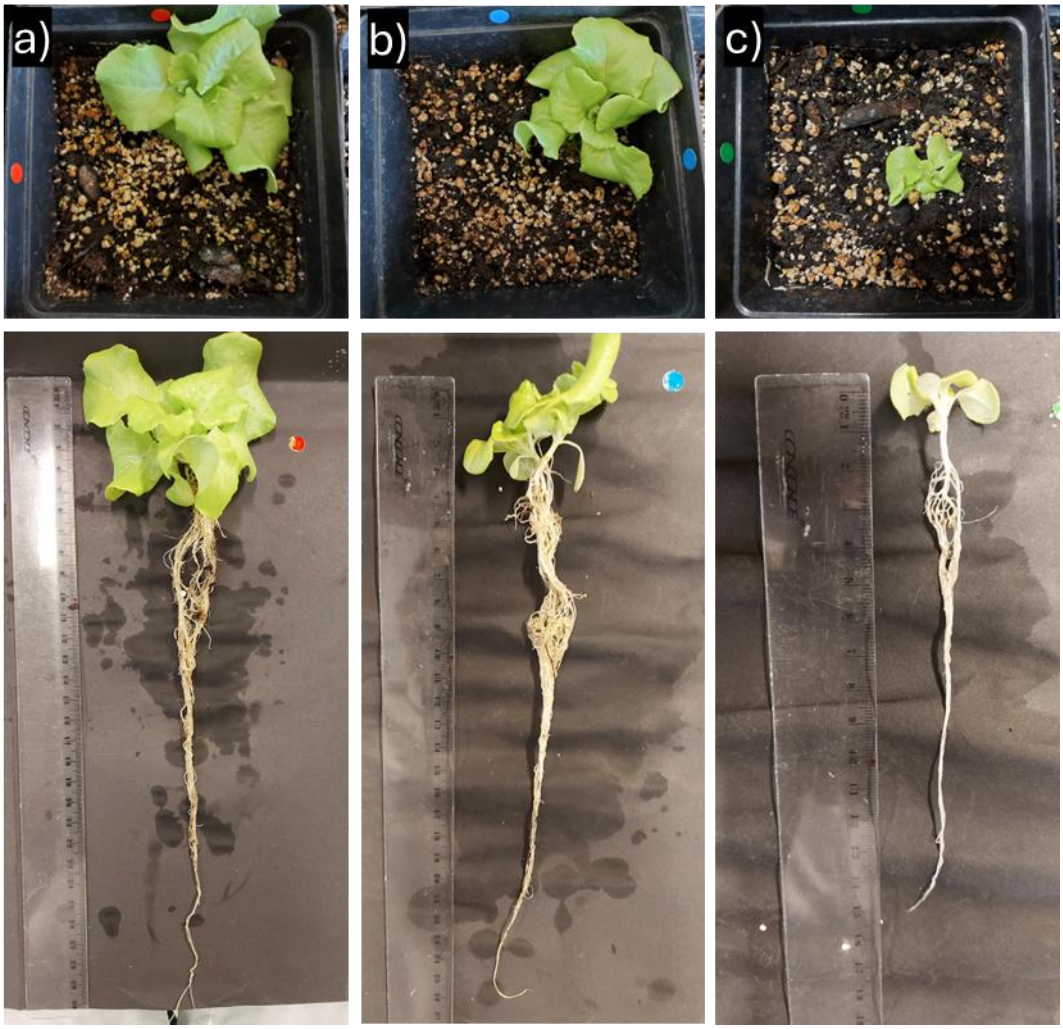

Figure 34 Photo documentation of the plant cultivation experiment, where red (a, left) labels treated plants with liquid bacterial culture, blue (b, middle) labels gelled bacterial culture and green (c, right) stands for untreated control. Significant differences were observed between treated (a, b) and untreated (c) plants in terms of root length and leaf richness in lettuce.

The analysis of pigment concentrations in plant leaves was an essential step in characterizing plant condition, as the amount of pigments directly influences photosynthetic efficiency and nutrient acquisition. From the measured absorbance values at specific wavelengths were calculated concentrations of photosynthetic pigments, which are shown in Figure 35. The highest pigment levels were found in leaves from plants treated by bacteria in buffer (chlorophyll a: 6 ± 1 µg/mL, chlorophyll b: 7 ± 2 µg/mL, carotenoids: 3.6 ± 0.5 µg/mL). Moderate levels were observed in plants treated by bacterial gels and the lowest concentrations were recorded in untreated control. These differences align with overall plant development, particularly leaf length and biomass (see Table 7).

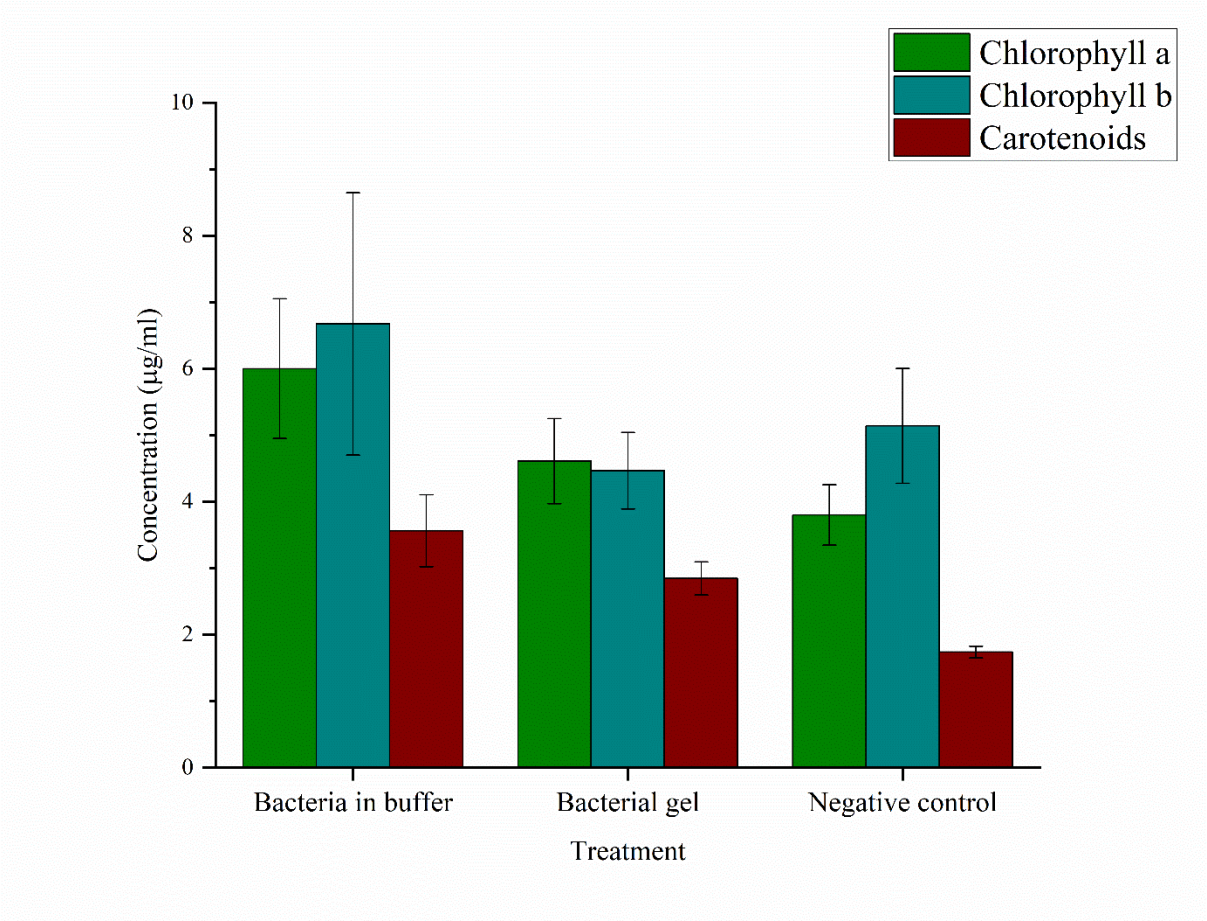

Figure 35 Concentration of pigments obtained from leaves of treated (bacterial gelled culture/bacterial gel and liquid bacteria in phosphate buffer) and untreated plants (control) in the end of the cultivation- chlorophyl a (green), chlorophyll b (cyanoblue) and carotenoids (red) measured spectrophotometrically.

Even under laboratory conditions and using a two-step inoculation process, we observed significant differences between plants treated with PGPR and untreated controls. It was essential to test whether bacterial gelled cultures could stimulate plant growth by releasing bacteria effectively. Our results showed that bacterial cultures released from the gel did improve plant growth, although a slightly less compared to liquid bacterial inoculation. This difference may be due to the immediate availability of nutrients, especially nitrogen, in liquid inoculation, which is critical for early plant growth. In contrast, bacteria released slowly from the gelled cultures likely provided a more gradual nutrient supply, leading to slower initial plant growth. Nevertheless, *A. vinelandii* CCM 289 in both treatments positively influenced plant growth. This was also supported by spectrometric analysis of plant pigments, such as chlorophyll and

carotenoids, confirming that CCM 289 actively stimulates plant growth even after self-entrapment in bacterial gels.

5.6.2 Followed up plant cultivation experiment in greenhouse observing microorganisms responding to different treatments

Following the laboratory experiments, the study was extended to a larger-scale trial under greenhouse conditions with 60% relative humidity and controlled day–night cycles (described in 4.12.1) during the internship in Lund university, Sweden with supervising of prof. Rousk. This phase aimed to evaluate the plant growth-promoting properties of *A. vinelandii* CCM 289 under semi-controlled, environmentally relevant conditions. As described in detail in 4.12.1, three treatments were applied: plants inoculated with bacterial gelled cultures, plants treated with alginate hydrogel without bacteria and an untreated control. Given that some bacteria are reported to exhibit antifungal activity through the production of antimicrobial compounds that inhibit or outcompete other microorganisms, (Gurikar et al., 2022), this experiment also monitored bacterial and fungal populations over a 47-day lettuce cultivation period. The primary objective was to determine whether bacterial gels could reduce fungal growth while supporting plant development.

Figure 36 illustrates the progression of bacterial (top panel) and fungal (bottom panel) growth over time. Regarding bacterial growth, the highest values were observed in the treatments with bacterial gels and gels without bacteria, particularly on Day 1. This is expected for the bacterial gel treatment due to the deliberate introduction of bacteria. The unexpectedly high bacterial counts in the gel without bacteria may suggest incomplete removal of bacterial residues during gel preparation, as some bacterial cells may have remained despite washing. In contrast, the untreated control exhibited significantly lower bacterial growth, likely reflecting the natural microbial environment of the soil.

Bacterial growth (Figure 36, top) generally declined over time, although a notable resurgence occurred around Day 17, especially in the treated samples. This increase may be attributed to the gradual disintegration of the gel matrix, which could have released previously trapped bacteria, thus stimulating microbial activity. After Day 30, a sharp decline in bacterial growth was observed across all treatments.

Fungal growth analysis over the 47-day period (Figure 36, bottom) revealed no significant differences among the three treatment groups. Fungal biomass levels were comparable at all sampling points, including in plants treated with the bacterial gel. These results indicate that,

under the conditions tested, the bacterial gel did not exhibit measurable antifungal effects. Consequently, this experiment did not provide evidence to support antifungal activity of the applied bacterial gels.

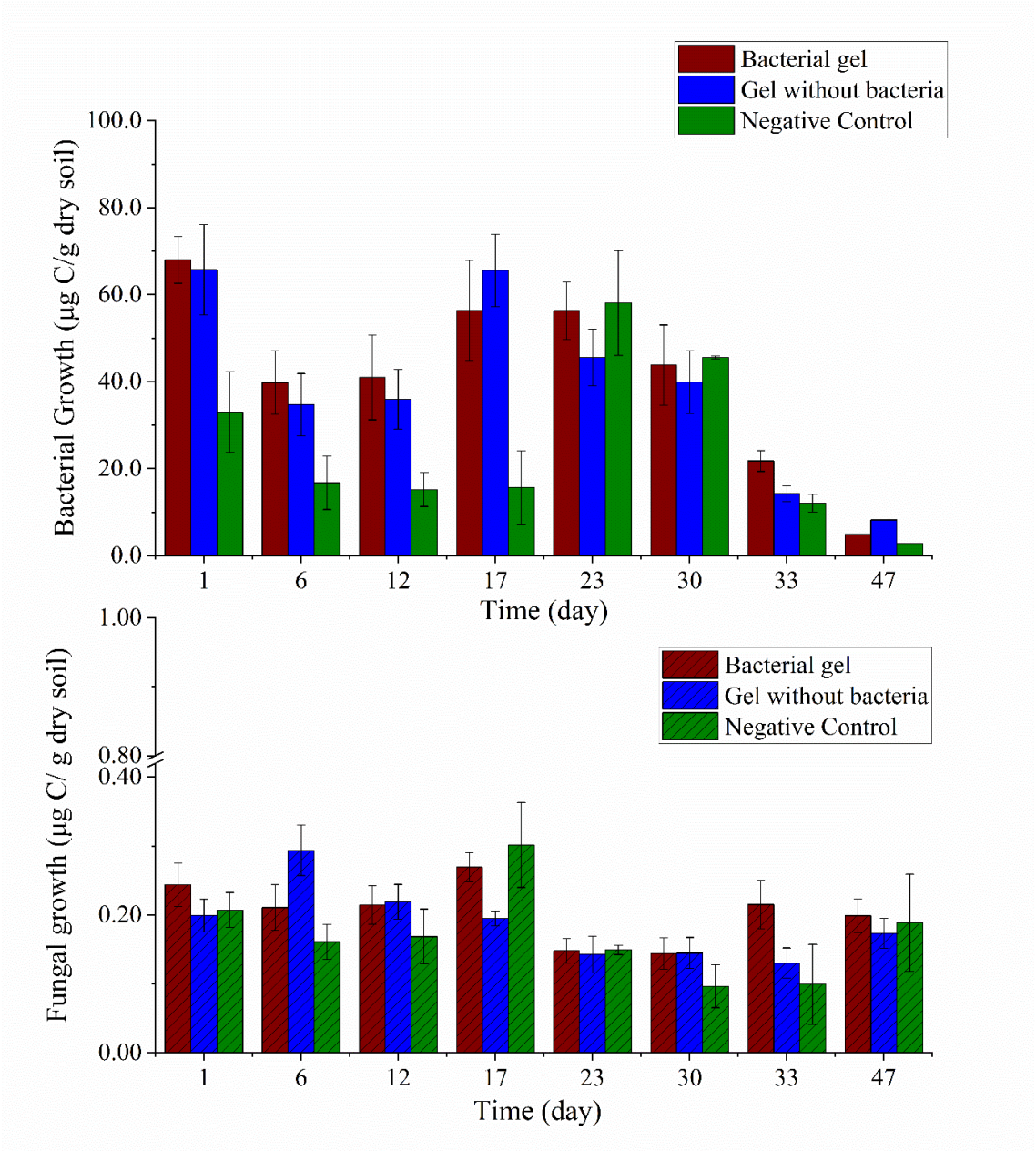

Figure 36 Bacterial (top) and fungal down) growths throughout cultivation days of lettuce plants: while three treatments were implied bacterial gel/gelled bacterial culture of A. vinelandii CCM 289 (red column), alginate gel produced by A. vinelandii CCM 289 without bacteria (blue) and untreated control (green). Fungal and bacterial growth were analysed by radioisotope determination of H^3 and C^{13} from soil samples.

During a cultivation period exceeding two months, lettuce plants were subjected to three treatments to test both antibacterial and antifungal activities. Differences in bacterial abundance between treated and untreated plants were apparent only during the initial 17 days of cultivation, thereafter, bacterial counts in the untreated control approached those in the treated groups. This convergence may be attributable to factors such as repeated sampling of the pots, which could have disturbed the rhizosphere and facilitated bacterial redistribution, or the gradual establishment of a natural bacterial microbiome within the soil. Regarding antifungal activity, our cultivation tests with lettuce plants showed no detectable differences in fungal growth between the treatments. Therefore, under the tested conditions, *A. vinelandii* CCM 289 did not have a significant impact on the soil microbiome and appeared to maintain stable microbiome conditions.

5.6.3 Drought resistance of treated and untreated plants

The final experiment discussed in this thesis tested our hypothesis that a bacterial gelled culture, embedded in a hydrogel matrix, could enhance both plant and bacterial resistance under climate change. Due to their high water-holding capacity, containing typically >80% water (Savić Gajić et al., 2023), providing a slow release of moisture and reducing the need for frequent irrigation. We conducted this pilot study in Sweden at Lund University, in collaboration with the Rousk research team, using their facilities and expertise.

The experiment run in the end of the plant cultivation for 7 days. The plants were not freshly treated, however despite the temporal gap of two months following inoculation, the persistence of treatment effects remains biologically meaningful due to multiple converging mechanisms. Firstly, alginate-based delivery systems act as controlled-release matrices, meaning that the gel gradually disintegrated and released viable bacterial inoculants over extended periods (Colin et al., 2024; Tanmoy & LeFevre, 2024). Secondly, drought-tolerant bacteria can survive in dormant or stress-resistant forms and sustain their ecological functions long after the initial inoculation, contributing to improved soil enzyme activity, water retention and plant biomass under water limitation (Li et al., 2023). Moreover, the concept of a microbial “legacy effect” underscores that prior inoculations can reshape soil microbial community composition and functionality, influencing plant performance and drought resilience even after the inoculant’s active phase ends (Meisner et al., 2018).

To evaluate drought resistance, both bacterial and plant responses to reduced soil moisture were assessed across three treatments: gelled bacterial culture, gel without bacteria and an

untreated control. Drought resistance was defined as the ability to retain water in the soil-microbial-plant system, expressed as grams of water per gram of dry soil. Bacterial resistance was measured through microbial biomass under drought stress, while plant wilting was monitored visually throughout the experiment.

As shown in Figure 37, bacterial resistance was highest in the treatment with gel without bacteria, followed by the negative control and bacterial gel. Conversely, plant wilting, labelled as "plant resistance" in the figure, was highest in the negative control, followed by bacterial gel and was lowest in the gel without bacteria treatment. This divergence between microbial and plant responses highlights an important aspect of soil-plant-microbe interactions under water-limited conditions. In particular, the bacterial gel treatment demonstrated a moderate level of drought resistance for both microbes and plants, suggesting a more balanced microenvironment under stress.

The data indicate a complex relationship between soil microbial activity and plant performance under drought conditions. Hydrogels, by retaining moisture, are generally expected to support both microbial survival and plant water availability (Montesano et al., 2015). However, the results reveal contrasting outcomes depending on the treatment. Interestingly, the gel without bacteria treatment showed the highest bacterial resistance, possibly due to the gel's physical properties alone enhancing microbial hydration. However, this treatment was associated with the latest plant wilting, suggesting that microbial persistence in this condition may not benefit the plant, or may even compete for available water. This reflects a potential trade-off in hydrogel-based treatments when microbial and plant needs are not aligned.

In contrast, bacterial gel treatments yielded moderate resistance for both bacteria and plants. This may point to a synergistic effect where introduced bacteria, although not maximally drought-resistant, contributed to a more stable and cooperative soil environment, indirectly benefiting plant water retention. These bacteria may produce exopolysaccharides or other compounds that enhance soil structure and water holding capacity, indirectly supporting plant performance.

The negative control, with no gel or bacterial input, surprisingly showed high plant drought resistance, due to better root adaptation or lack of microbial competition under stress. Yet, bacterial resistance was lower than in gel treatments, indicating reduced microbial resilience in the absence of moisture-retaining amendments. Together, these results emphasize that drought resistance is not a singular outcome but a product of interactions among soil properties,

microbial dynamics and plant physiology. While hydrogels, especially those incorporating beneficial bacteria, can offer balanced support for both microbes and plants, their design and application must be carefully optimized to avoid unintended trade-offs.

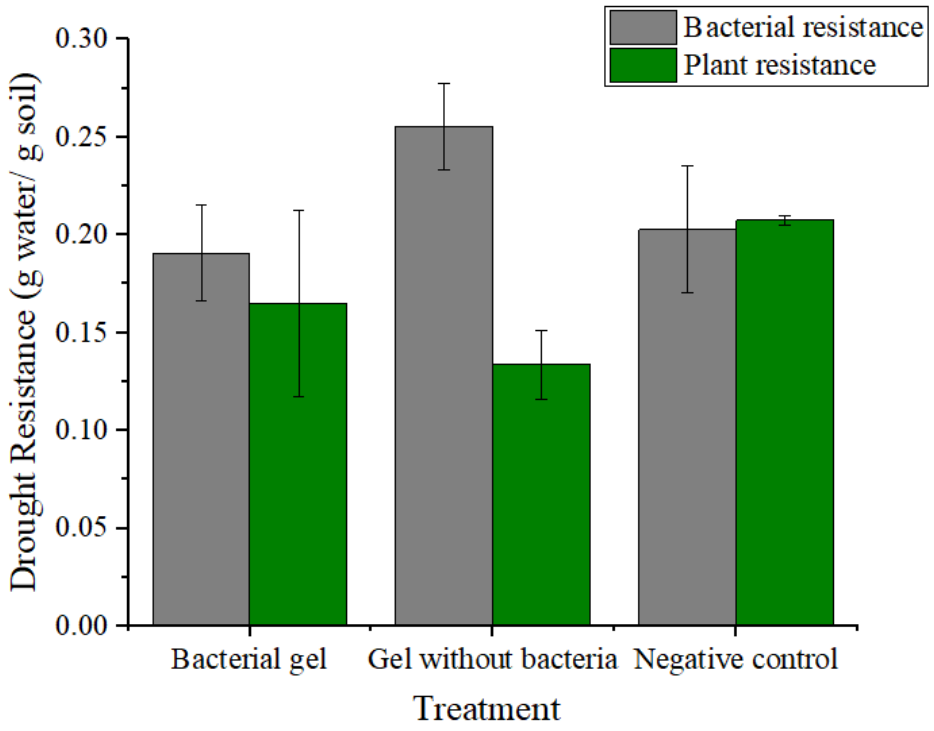

Figure 37 Drought bacterial resistance of gelled bacterial culture, gel without bacteria and negative control (*bacterial resistance in grey slopes, plant resistance or plant wilting in green slopes*). *Drought resistance, expressed in g water per g soil, represents the soil moisture level at which bacterial growth reached the* EC_{50} *value.*

The Table 8 presents root length and dry plant biomass measurements under two conditions: drying (drought) and regular watering. Under drying conditions, the bacterial gel treatment resulted in the longest roots (20.1 ± 7.9 cm) and a relatively high dry biomass (1.7 ± 0.3 g), suggesting an enhanced root system that could access deeper moisture. Interestingly, although the negative control produced shorter roots (13.3 ± 0.3 cm), its biomass was equal to the bacterial gel, indicating that root elongation may have been more strongly influenced by bacterial presence than by biomass accumulation alone. The gel without bacteria showed moderate root length (16.2 ± 2.1 cm) but the lowest biomass (1.2 ± 1.0 g), suggesting that while hydrogels support some drought resilience, the absence of bacteria limits plant productivity.

Under regular watering, all treatments supported root growth, with the negative control surprisingly having the longest roots (21 ± 1.0 cm). However, this did not translate to higher biomass. Plants treated with bacterial gel achieved the highest dry biomass (2.8 ± 0.7 g), more than double that of the other groups, indicating enhanced nutrient uptake and plant resistance likely due to microbial interactions. The gel without bacteria and negative control both showed lower biomass (1.3 ± 0.6 g and 1.1 ± 0.4 g, respectively), reaffirming that bacterial presence is key to maximizing plant growth, especially when moisture is not a limiting factor. However, no statistically significant differences were found between treatments, except for bacterial resistance ($p < 0.05$). This suggests that changes between treatments were not evident, which may be due to the small number of plant replicates used in the experiment.

Table 8 Overview of final parameters from lettuce drought experiment: Drying and regular watering as a control, length of the roots were examined, dry plant biomass and bacterial resistance for drought for all three treatments with inoculation of bacterial gelled culture, only alginate gel produced by bacteria and untreated control. Statistical significance was also performed by one-way ANOVA: no statistical significance "ns", low statistical significance ""*

Treatment	**Drying**			**Regular watering**	
	Length of roots (cm)	Dry plant biomass (g)	Bacterial Resistance	Length of roots (cm)	Dry plant biomass (g)
Bacterial gel	20.1 ± 7.9	1.7 ± 0.3	0.19 ± 0.02	19.0 ± 1.3	2.8 ± 0.7
Gel without bacteria	16.2 ± 2.1	1.2 ± 1.0	0.25 ± 0.02	16.5 ± 3.1	1.3 ± 0.6
Negative control	13.3 ± 0.3	1.7 ± 0.9	0.20 ± 0.03	21 ± 1.0	1.1 ± 0.4
Statistical significance	ns p=0.607	ns p=0.607	* p=0.027	ns p=0.681	ns p=0.526

Similarly, in this experiment, pigments were measured from fresh leaves to determine the effect of bacterial gel application on photosynthetic pigment retention under two watering regimes: drying and regular watering.

Figure 38 represents the bar graph illustrates the concentrations of major photosynthetic pigments, specifically carotenoids, chlorophyll *a* and chlorophyll *b*, in leaves under drying and

regular watering conditions, across three treatments: bacterial gel, gel without bacteria and negative control.

Under drying conditions, plants treated with the bacterial gel maintained notably higher levels of chlorophyll *a* (~8.5 µg/mL) compared to those treated with gel without bacteria (~6 µg/mL), while the negative control showed the highest value (~9.5 µg/mL). Carotenoids and chlorophyll *b* followed similar trends but with smaller differences. This indicates that the bacterial gel may contribute to better pigment preservation during water stress, possibly by mitigating oxidative damage or supporting photosynthetic function. After regular watering, the pigment content was generally highest in the negative control, with chlorophyll *a* peaking around 12 µg/mL. Both gel treatments (with and without bacteria) showed lower pigment concentrations, suggesting that the presence of the gel matrix might slightly limit pigment accumulation, or that no additional benefit is conferred under optimal watering.

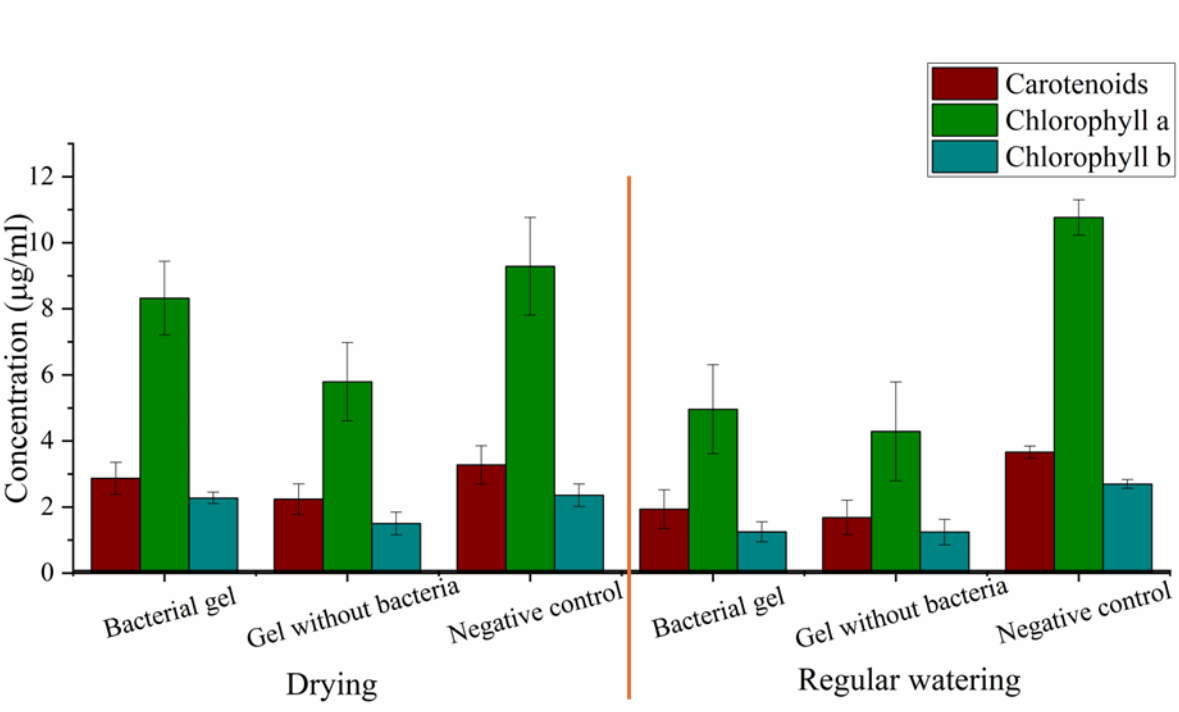

Figure 38 The pigment concentration in leaves of treated and untreated plants after the drying experiment and compared to regularly watered controls was analysed spectrophotometrically at specific wavelengths. Carotenoids are shown in red, chlorophyll a in green and chlorophyll b in cyan.

Based on this experiment we studied drought effect on lettuce plants and bacterial growth. Results indicates that the application of bacterial gel can enhance drought resilience in lettuce

plants by promoting root elongation and maintaining biomass under water-limited conditions. While hydrogels alone provided some support, the presence of bacteria was crucial for maximizing plant growth and nutrient uptake, especially under regular watering. Although statistical significance was limited likely due to a small sample size. The observed trends suggest that bacterial inoculation supports both plant and microbial drought tolerance. Additionally, bacterial gel treatments helped preserve photosynthetic pigments during drought, further underscoring their protective role. Overall, these findings highlight the potential of bacterial gel formulations as a promising strategy to improve plant performance under climate-related water stress.

6 CONCLUSION

The aim of this PhD thesis was to study bacterial inoculants and their novel way of preparation and usage in agricultural industry. In our experiment, we successfully screened six strains of *Azotobacter vinelandii* and, for the first time to our knowledge, developed bacterial inoculants through self-entrapment of bacterial cultures in alginate gels produced endogenously, without external polysaccharide addition.

Comprehensive characterization of biopolymer production, including alginate and PHB concentrations, alongside detailed analysis of alginate properties such as acetylation degree, M/G ratio and molecular weight, enabled the identification of the most promising *A. vinelandii* strains for gel formation. Advanced TEM imaging techniques were successfully developed to visualize bacterial morphology within hydrogels without compromising cell integrity, providing critical insights into bacterial encapsulation. Rheological assessments revealed distinct strain-dependent variations in gel strength and bacterial release profiles, which are crucial for tailoring effective bioinoculant formulations. Among the strains tested, CCM 289 demonstrated superior gelation capacity, producing gels with the highest average complex moduli, indicative of enhanced mechanical stability and durability. These findings establish CCM 289 as a prime candidate for the development of robust bacterial gel inoculants, advancing the potential for sustainable agricultural applications through improved microbial delivery and plant growth promotion under stress conditions. Furthermore, besides CCM 289, also DSM 87 consistently produced high-quality, structurally stable gels. This multifunctionality of bacterium *A. vinelandii*, including nitrogen fixation, production of plant growth-promoting substances (IAA, siderophores, phosphate solubilization) and robust alginate synthesis, underlines its strong biotechnological potential as a bioinoculant in sustainable agriculture.

During the course of this dissertation, modifications of the cultivation medium were also investigated with the aim of reducing production costs of bacterial inoculants and improving gel quality. Three carbon substrates (glucose, fructose and sucrose) were evaluated for their effects on bacterial growth and gelation. Among these, fructose proved particularly interesting, as it enabled full gelation of the entire medium after just one day of cultivation. However, after prolonged cultivation, the gel began to disintegrate, although a high amount of alginate was still maintained. This finding is significant because fructose, which can be sourced from waste materials, presents a cost-effective carbon source for large-scale production, potentially

lowering overall inoculant manufacturing expenses. The effect of calcium carbonate addition was also studied, revealing that concentrations above 5 g/L did not promote gelation as initially expected. Instead, higher levels appeared to inhibit the process, likely due to pH stabilization, which reduced the production of alginic acid necessary for effective self-entrapment of bacterial cultures within the gel matrix. Lastly, the influence of cultivation volume on gelation potential was assessed, considering that *A. vinelandii* produces alginate partly as an oxygen diffusion barrier linked to its nitrogenase activity. Within the flask-scale volumes tested, no significant differences in gelation ability were observed, suggesting that oxygen availability at this scale does not critically impact alginate-mediated gel formation.

Moreover, calcium chloride ($CaCl_2$) at 2 % concentration is the standard gelation agent for alginate hydrogels due to its effective crosslinking. However, our study expanded this approach by investigating a variety of ionic and acidic gelation agents, as well as gelation by dissolving insoluble Ca^{2+} salts using glucono-δ-lactone (GDL), aiming to develop scalable and controllable bioinoculant production methods. Among the ionic agents tested, Fe^{3+} and Cu^{2+} ions showed strong potential to enhance gel strength and mechanical stability by forming more robust crosslinking networks. Their toxicity at higher concentrations, however, limits their direct use; blending these ions with $CaCl_2$ may offer an optimal compromise, improving gel properties while preserving bacterial viability. Organic acids, particularly citric acid, were also explored due to their non-toxic nature and use in the food industry. Citric acid demonstrated favourable effects on gel elasticity and porosity without harming bacterial cells, making it a promising alternative for sustainable agricultural applications. Slow gelation with GDL proved especially interesting, as it hydrolyzes gradually, enabling controlled gel formation within the first 10 minutes. This gradual process promotes uniform gelation throughout the culture volume, reducing inconsistencies and mechanical stress during encapsulation and possibility to produced gels of defined shapes and sizes. These can be advantages particularly valuable for large-scale bioreactor production.

Nevertheless, in our first attempts of scaling up, it was essential to determine whether cultivation of *Azotobacter vinelandii* is feasible in bioreactors, as factors like different mixing regimes, increased bacterial growth and oxygen availability can all affect the gelation potential of the culture. Initially, cultivation of strain CCM 289 in bioreactor conditions was unsuccessful, likely because the timing of gelation was missed, or the bacterial culture was too fragile to withstand the stirring forces. However, after switching to *A. vinelandii* DSM 87, gelation potential was maintained even over extended cultivation periods (approximately 5–6

hours). We identified the optimal time for obtaining high-quality alginate suitable for bacterial self-entrapment at around 26–30 hours, confirmed through rheological measurements. Using 3 L culture volume and stirring at 400 rpm as a control, gelation occurred successfully. In contrast, more intensive stirring speeds (150–750 rpm) prevented gel formation, probably due to mechanical disruption of the alginate polymer chains by the stirrer. Slower stirring speeds (150–450 rpm), however, proved effective, enabling successful gelation of the bacterial culture.

Together, these findings emphasize the importance of optimizing gelation agents and conditions to balance mechanical stability, bacterial survival and scalability. They open promising avenues for developing tailored bacterial gels that enhance bioinoculant effectiveness and meet the demands of sustainable agriculture and industrial biotechnology. For the future research it may be interesting to study also the addition of GDL directly into bioreactor, which may lead to gelation of the whole volume and following freeze-drying of the bacterial gelled culture.

Nevertheless, based on the bacterial characterization experiments evaluating bioactivities (IAA production, siderophore synthesis and phosphate solubilization) and close monitoring of bacterial survival after release from the gels, we proceeded to test the bacterial gelled cultures on model plants, specifically lettuce, to assess the effects of the bioinoculants on plant growth, soil microbiome and drought tolerance. In planta experiments showed that bacterial gels, particularly those containing CCM 289, significantly enhanced plant growth parameters and preserved photosynthetic pigments under drought stress, confirming their protective and growth-promoting roles. While hydrogels alone offered some drought resilience, the presence of bacteria was essential for maximizing biomass accumulation and nutrient uptake. Although statistical significance was limited, most likely due to small number of replicates, the observed trends clearly indicate benefits of bacterial gel inoculation for both plants and microbial drought tolerance. Furthermore, no adverse effects on fungal soil communities were observed, suggesting stable microbiome interactions.

Overall, our results demonstrated that, although the thesis initially focused on testing *A. vinelandii* strains for their potential to produce alginate and in the same time be a PGPR. However, we were able to achieve much more: these strains not only produced high-quality alginate but were also capable of being directly gelled within it, giving *A. vinelandii* an exceptional potential with strong gelation properties to produce encapsulated bioinoculants. Not only had this method not been reported before, but we were also able to establish a functional concept, producing gels directly through bacterial culture gelation with remarkable consistency.

Among the six strains tested, CCM 289 and DSM 87 stood out due to their bioassay activities in plant stimulation, which was confirmed in plant experiments by significantly increased root and plant biomass. Most importantly, the scalability of these bacterial cultures is feasible and essential for future applications. Each chapter of this work opens further avenues for research and investigation, offering enormous potential for innovation. This approach turned out to be both highly effective and truly innovative, offering a flexible platform that could be used in agriculture and related fields, with great potential for future research and practical applications.

7 REFERENCES

Aarstad, O. A., Stanisci, A., Sætrom, G. I., Tøndervik, A., Sletta, H., Aachmann, F. L., & Skjåk-Bræk, G. (2019). Biosynthesis and Function of Long Guluronic Acid-Blocks in Alginate Produced by Azotobacter vinelandii. *Biomacromolecules*, *20*(4), 1613–1622. https://doi.org/10.1021/acs.biomac.8b01796

Aasfar, A., Bargaz, A., Yaakoubi, K., Hilali, A., Bennis, I., Zeroual, Y., & Meftah Kadmiri, I. (2021). Nitrogen fixing Azotobacter species as potential soil biological enhancers for crop nutrition and yield stability. *Frontiers in Microbiology*, *12*, 1–19. https://doi.org/10.3389/fmicb.2021.628379

Abou Jaoudé, R., Luziatelli, F., Ficca, A. G., & Ruzzi, M. (2025). Effect of Plant Growth-Promoting Rhizobacteria Synthetic Consortium on Growth, Yield, and Metabolic Profile of Lettuce (Lactuca sativa L.) Grown Under Suboptimal Nutrient Regime. *Horticulturae*, *11*(1), 64. https://doi.org/10.3390/horticulturae11010064

Ahemad, M. (2012). Implications of bacterial resistance against heavy metals in bioremediation: A review. *IIOAB Journal*, *3*(3), 39–46.

Ahemad, M., & Kibret, M. (2014). Mechanisms and applications of plant growth promoting rhizobacteria: Current perspective. *Journal of King Saud University - Science*, *26*(1), 1–20. https://doi.org/10.1016/j.jksus.2013.05.001

Ahmad, A., Aslam, Z., Javed, T., Hussain, S., Raza, A., Shabbir, R., Mora-Poblete, F., Saeed, T., Zulfiqar, F., Ali, M. M., Nawaz, M., Rafiq, M., Osman, H. S., Albaqami, M., Ahmed, M. A. A., & Tauseef, M. (2022). Screening of Wheat (Triticum aestivum L.) Genotypes for Drought Tolerance through Agronomic and Physiological Response. *Agronomy*, *12*(2), 287. https://doi.org/10.3390/agronomy12020287

Ajilogba, C. F., Olanrewaju, O. S., & Babalola, O. O. (2017). *Application of Bioinoculants for Seed Quality Improvement* (pp. 265–280). https://doi.org/10.1007/978-981-10-6241-4_14

Ali, K., Asad, Z., Agbna, G. H. D., Saud, A., Khan, A., & Zaidi, S. J. (2024). Progress and Innovations in Hydrogels for Sustainable Agriculture. *Agronomy*, *14*(12), 2815. https://doi.org/10.3390/agronomy14122815

Allouzi, M. M. A., Allouzi, S. M. A., Keng, Z. X., Supramaniam, C. V., Singh, A., & Chong, S. (2022). Liquid biofertilizers as a sustainable solution for agriculture. *Heliyon*, *8*(12), e12609. https://doi.org/10.1016/j.heliyon.2022.e12609

Ambrosini, A., & Passaglia, L. M. P. (2017). Plant Growth–Promoting Bacteria (PGPB): Isolation and Screening of PGP Activities. *Current Protocols in Plant Biology*, *2*, 190–209. https://doi.org/10.1002/pb.20054

Ammar, E. E., Rady, H. A., Khattab, A. M., Amer, M. H., Mohamed, S. A., Elodamy, N. I., AL-Farga, A., & Aioub, A. A. A. (2023). A comprehensive overview of eco-friendly bio-fertilizers extracted from living organisms. *Environmental Science and Pollution Research*, *30*(53), 113119–113137. https://doi.org/10.1007/s11356-023-30260-x

Amor, S. R., Rayment, T., & Sanders, J. K. M. (1991). *NMR X-ray*. *2*, 4583–4588.

Amstutz, V., Hanik, N., Pott, J., Utsunomia, C., & Zinn, M. (2019). Tailored biosynthesis of polyhydroxyalkanoates in chemostat cultures. *Methods in Enzymology*, *627*, 99–123. https://doi.org/10.1016/bs.mie.2019.08.018

Arora, N. K., & Verma, M. (2017). Modified microplate method for rapid and efficient estimation of siderophore produced by bacteria. *3 Biotech*, *7*, 1–9. https://doi.org/10.1007/s13205-017-1008-y

Aseri, G. (2009). *Hydrolysis of Organic Phosphate Forms by Phosphatases and Phytase Producing Fungi of Arid and Semi Arid Soils of India*. https://www.researchgate.net/publication/237544658

Ashby, S. F. (1907). *Some Observations on te Assimilation of atmospheric nitrogen by a free lving soil organism.- Azotobacter chroococcum of Bei-Jerinck*.

Atobatele, O. E., & Olutona, G. O. (2015a). Distribution of three non-essential trace metals (Cadmium, Mercury and Lead) in the organs of fish from Aiba Reservoir, Iwo, Nigeria. *Toxicology Reports*, *2*, 896–903. https://doi.org/10.1016/j.toxrep.2015.06.003

Atobatele, O. E., & Olutona, G. O. (2015b). Distribution of three non-essential trace metals (Cadmium, Mercury and Lead) in the organs of fish from Aiba Reservoir, Iwo, Nigeria. *Toxicology Reports*, *2*, 896–903. https://doi.org/10.1016/j.toxrep.2015.06.003

Ayub, N. D., Tribelli, P. M., & López, N. I. (2009). Polyhydroxyalkanoates are essential for maintenance of redox state in the Antarctic bacterium Pseudomonas sp. 14-3 during low

temperature adaptation. *Extremophiles*, *13*(1), 59–66. https://doi.org/10.1007/s00792-008-0197-z

Bååth, E., Pettersson, M., & Söderberg, K. H. (2001). Adaptation of a rapid and economical microcentrifugation method to measure thymidine and leucine incorporation by soil bacteria. *Soil Biology and Biochemistry*, *33*(11), 1571–1574. https://doi.org/10.1016/S0038-0717(01)00073-6

Bakker, P. A. H. M., Berendsen, R. L., Doornbos, R. F., Wintermans, P. C. A., & Pieterse, C. M. J. (2013). The rhizosphere revisited: root microbiomics. *Frontiers in Plant Science*, *4*. https://doi.org/10.3389/fpls.2013.00165

Barney, B. M. (2024). Azotobacter vinelandii. *Trends in Microbiology*, *32*(10), 1034–1035. https://doi.org/10.1016/j.tim.2024.07.006

Barrera, E. L., Spanjers, H., Romero, O., Rosa, E., & Dewulf, J. (2020). A successful strategy for start-upof a laboratory-scale UASB reactor treating sulfate-rich sugar cane vinasse. *Journal of Chemical Technology & Biotechnology*, *95*(1), 205–212. https://doi.org/10.1002/jctb.6222

Bashan, Y. (2014). *Bacteria / Plant growth-promotion*. *January 2005*.

Bashan, Y., de-Bashan, L. E., Prabhu, S. R., & Hernandez, J. P. (2014). Advances in plant growth-promoting bacterial inoculant technology: Formulations and practical perspectives (1998-2013). *Plant and Soil*, *378*, 1–33. https://doi.org/10.1007/s11104-013-1956-x

Bashan, Y., Hernandez, J. P., Leyva, L. A., & Bacilio, M. (2002). Alginate microbeads as inoculant carriers for plant growth-promoting bacteria. *Biology and Fertility of Soils*, *35*(5), 359–368. https://doi.org/10.1007/s00374-002-0481-5

Berninger, T., González López, Ó., Bejarano, A., Preininger, C., & Sessitsch, A. (2018). Maintenance and assessment of cell viability in formulation of non-sporulating bacterial inoculants. *Microbial Biotechnology*, *11*(2), 277–301. https://doi.org/10.1111/1751-7915.12880

Beshah, A., Muleta, D., Legese, G., & Assefa, F. (2024). Exploring stress-tolerant plant growth-promoting rhizobacteria from groundnut rhizosphere soil in semi-arid regions of Ethiopia. *Plant Signaling & Behavior*, *19*(1). https://doi.org/10.1080/15592324.2024.2365574

Bhardwaj, D., Ansari, M. W., Sahoo, R. K., & Tuteja, N. (2014). Biofertilizers function as key player in sustainable agriculture by improving soil fertility, plant tolerance and crop productivity. *Microbial Cell Factories*, *13*(1), 66. https://doi.org/10.1186/1475-2859-13-66

Bhat, M. A., Mishra, A. K., Jan, S., Bhat, M. A., Kamal, M. A., Rahman, S., Shah, A. A., & Jan, A. T. (2023). Plant Growth Promoting Rhizobacteria in Plant Health: A Perspective Study of the Underground Interaction. *Plants*, *12*(3), 629. https://doi.org/10.3390/plants12030629

Bhattacharyya, P. N., & Jha, D. K. (2012). Plant growth-promoting rhizobacteria (PGPR): Emergence in agriculture. *World Journal of Microbiology and Biotechnology*, *28*(4), 1327–1350. https://doi.org/10.1007/s11274-011-0979-9

Bolan, S., Hou, D., Wang, L., Hale, L., Egamberdieva, D., Tammeorg, P., Li, R., Wang, B., Xu, J., Wang, T., Sun, H., Padhye, L. P., Wang, H., Siddique, K. H. M., Rinklebe, J., Kirkham, M. B., & Bolan, N. (2023). The potential of biochar as a microbial carrier for agricultural and environmental applications. *Science of The Total Environment*, *886*, 163968. https://doi.org/10.1016/j.scitotenv.2023.163968

Bomfim, C. A., Coelho, L. G. F., do Vale, H. M. M., de Carvalho Mendes, I., Megías, M., Ollero, F. J., & dos Reis Junior, F. B. (2021). Brief history of biofertilizers in Brazil: from conventional approaches to new biotechnological solutions. *Brazilian Journal of Microbiology*, *52*(4), 2215–2232. https://doi.org/10.1007/s42770-021-00618-9

Bonartseva, G. A., Akulina, E. A., Myshkina, V. L., Voinova, V. V., Makhina, T. K., & Bonartsev, A. P. (2017). Alginate biosynthesis by Azotobacter bacteria. *Applied Biochemistry and Microbiology*, *53*, 52–59. https://doi.org/10.1134/S0003683817010070

Brandl, H., Knee, E. J., Fuller, R. C., Gross, R. A., & Lenz, R. W. (1989). Ability of the phototrophic bacterium Rhodospirillum rubrum to produce various poly (β-hydroxyalkanoates): Potential sources for biodegradable polyesters. *International Journal of Biological Macromolecules*, *11*(1), 49–55. https://doi.org/10.1016/0141-8130(89)90040-8

Brangarí, A. C., Lyonnard, B., & Rousk, J. (2022). Soil depth and tillage can characterize the soil microbial responses to drying-rewetting. *Soil Biology and Biochemistry*, *173*(August), 108806. https://doi.org/10.1016/j.soilbio.2022.108806

Bresan, S., Sznajder, A., Hauf, W., Forchhammer, K., Pfeiffer, D., & Jendrossek, D. (2016). Polyhydroxyalkanoate (PHA) granules have no phospholipids. *Scientific Reports*, *6*(March), 1–13. https://doi.org/10.1038/srep26612

Buitrago-Arias, C., Gañán-Rojo, P., Torres-Taborda, M., Perdomo-Villar, L., Álvarez-López, C., Jaramillo-Quiceno, N., & Hincapié-Llanos, G. A. (2025). Analysis of the Growth of Hydrogel Applications in Agriculture: A Review. *Gels*, *11*(9), 731. https://doi.org/10.3390/gels11090731

Burgess, A. J., Pranggono, R., Escribà-Gelonch, M., & Hessel, V. (2024). Biofortification for space farming: Maximising nutrients using lettuce as a model plant. *Future Foods*, *9*, 100317. https://doi.org/10.1016/j.fufo.2024.100317

Calvo, P., Nelson, L., & Kloepper, J. W. (2014). Agricultural uses of plant biostimulants. *Plant and Soil*, *383*(1–2), 3–41. https://doi.org/10.1007/s11104-014-2131-8

Castillo, T., García, A., Padilla-Córdova, C., Díaz-Barrera, A., & Peña, C. (2020). Respiration in Azotobacter vinelandii and its relationship with the synthesis of biopolymers. *Electronic Journal of Biotechnology*, *48*, 36–45. https://doi.org/10.1016/j.ejbt.2020.08.001

Chai, Y. N., Futrell, S., & Schachtman, D. P. (2022). Assessment of Bacterial Inoculant Delivery Methods for Cereal Crops. *Frontiers in Microbiology*, *13*. https://doi.org/10.3389/fmicb.2022.791110

Chan, A. W., Whitney, R. A., & Neufeld, R. J. (2008). Kinetic Controlled Synthesis of pH-Responsive Network Alginate. *Biomacromolecules*, *9*(9), 2536–2545. https://doi.org/10.1021/bm800594f

Chandra, D., Pallavi, Barh, A., & Sharma, I. P. (2018). *Plant Growth Promoting Bacteria* (pp. 318–338). https://doi.org/10.4018/978-1-5225-3126-5.ch020

Chaudhary, T., Dixit, M., Gera, R., Shukla, A. K., Prakash, A., Gupta, G., & Shukla, P. (2020). Techniques for improving formulations of bioinoculants. *3 Biotech*, *10*(5), 199. https://doi.org/10.1007/s13205-020-02182-9

Chen, G. Q., & Wu, Q. (2005). The application of polyhydroxyalkanoates as tissue engineering materials. *Biomaterials*, *26*(33), 6565–6578. https://doi.org/10.1016/j.biomaterials.2005.04.036

Chen, L., Hao, Z., Li, K., Sha, Y., Wang, E., Sui, X., Mi, G., Tian, C., & Chen, W. (2021). Effects of growth-promoting rhizobacteria on maize growth and rhizosphere microbial community under conservation tillage in Northeast China. *Microbial Biotechnology*, *14*(2), 535–550. https://doi.org/10.1111/1751-7915.13693

Ching, S. H., Bansal, N., & Bhandari, B. (2017). Alginate gel particles–A review of production techniques and physical properties. *Critical Reviews in Food Science and Nutrition*, *57*(6), 1133–1152. https://doi.org/10.1080/10408398.2014.965773

Christiansen, J., Seefeldt, L. C., & Dean, D. R. (2000). Competitive Substrate and Inhibitor Interactions at the Physiologically Relevant Active Site of Nitrogenase. *Journal of Biological Chemistry*, *275*(46), 36104–36107. https://doi.org/10.1074/jbc.M004889200

Chuacharoen, T., Aroonsong, S., & Chysirichote, T. (2022). Alginate Production of *Azotobacter vinelandii* Using Sugar Cane Juice as the Main Carbon Source in an Airlift Bioreactor. *Industrial & Engineering Chemistry Research*, *61*(34), 12329–12337. https://doi.org/10.1021/acs.iecr.2c02693

Ciarleglio, G., Cinti, F., Toto, E., & Santonicola, M. G. (2023). Synthesis and Characterization of Alginate Gel Beads with Embedded Zeolite Structures as Carriers of Hydrophobic Curcumin. *Gels*, *9*(9), 714. https://doi.org/10.3390/gels9090714

Ciesielski, S., Górniak, D., Możejko, J., Świątecki, A., Grzesiak, J., & Zdanowski, M. (2014). The Diversity of Bacteria Isolated from Antarctic Freshwater Reservoirs Possessing the Ability to Produce Polyhydroxyalkanoates. *Current Microbiology*, *69*(5), 594–603. https://doi.org/10.1007/s00284-014-0629-1

Clauss, M. J., & Koch, M. A. (2006). Poorly known relatives of Arabidopsis thaliana. *Trends in Plant Science*, *11*(9), 449–459. https://doi.org/10.1016/j.tplants.2006.07.005

Clementi, F., Moresi, M., & Parente, E. (1999). Alginate from Azotobacter vinelandii. In *Carbohydrate Biotechnology Protocols. Methods in Biotechnology* (Vol. 10, pp. 23–42). https://doi.org/10.1007/978-1-59259-261-6_3

Clementi, F., & Parente, E. (1997). Alginate Production by Azotobacter Vinelandii. *Critical Reviews in Biotechnology*, *17*, 327–361. https://doi.org/10.3109/07388559709146618

Colin, C., Akpo, E., Perrin, A., Cornu, D., & Cambedouzou, J. (2024). Encapsulation in Alginates Hydrogels and Controlled Release: An Overview. *Molecules*, *29*(11), 2515. https://doi.org/10.3390/molecules29112515

Cortés-Patiño, S., Vargas, C., Álvarez-Flórez, F., Bonilla, R., & Estrada-Bonilla, G. (2021). Potential of Herbaspirillum and Azospirillum Consortium to Promote Growth of Perennial Ryegrass under Water Deficit. *Microorganisms*, *9*(1), 91. https://doi.org/10.3390/microorganisms9010091

Costa, O. Y. A., Raaijmakers, J. M., & Kuramae, E. E. (2018). Microbial Extracellular Polymeric Substances: Ecological Function and Impact on Soil Aggregation. *Frontiers in Microbiology*, *9*. https://doi.org/10.3389/fmicb.2018.01636

Cruz-Paredes, C., Wallander, H., Kjøller, R., & Rousk, J. (2017). Using community trait-distributions to assign microbial responses to pH changes and Cd in forest soils treated with wood ash. *Soil Biology and Biochemistry*, *112*, 153–164. https://doi.org/10.1016/J.SOILBIO.2017.05.004

Das, H. K. (2019). *Azotobacters as biofertilizer* (pp. 1–43). https://doi.org/10.1016/bs.aambs.2019.07.001

Data Bridge Market Research. (2025, February). https://www.databridgemarketresearch.com/reports/global-bacterial-inoculants-market

Date, R. A. (2001). Advances in inoculant technology: A brief review. *Australian Journal of Experimental Agriculture*, *41*(3), 321–325. https://doi.org/10.1071/EA00006

Devi, R., Behera, B., Raza, M. B., Mangal, V., Altaf, M. A., Kumar, R., Kumar, A., Tiwari, R. K., Lal, M. K., & Singh, B. (2022). An Insight into Microbes Mediated Heavy Metal Detoxification in Plants: a Review. *Journal of Soil Science and Plant Nutrition*, *22*(1), 914–936. https://doi.org/10.1007/s42729-021-00702-x

Dhanasekar, R., Viruthagiri, T., & Sabarathinam, P. L. (2003). Poly(3-hydroxy butyrate) synthesis from a mutant strain Azotobacter vinelandii utilizing glucose in a batch reactor. *Biochemical Engineering Journal*, *16*(1), 1–8. https://doi.org/10.1016/S1369-703X(02)00176-6

Díaz-Barrera, A., Sanchez-Rosales, F., Padilla-Córdova, C., Andler, R., & Peña, C. (2021). Molecular weight and guluronic/mannuronic ratio of alginate produced by Azotobacter

vinelandii at two bioreactor scales under diazotrophic conditions. *Bioprocess and Biosystems Engineering*, *44*(6), 1275–1287. https://doi.org/10.1007/s00449-021-02532-8

Díaz-Barrera, A., & Soto, E. (2010). Biotechnological uses of Azotobacter vinelandii: Current state, limits and prospects. *African Journal of Biotechnology*, *9*(33), 5240–5250.

Díaz-Rodríguez, A. M., Parra Cota, F. I., Cira Chávez, L. A., García Ortega, L. F., Estrada Alvarado, M. I., Santoyo, G., & de los Santos-Villalobos, S. (2025). Microbial Inoculants in Sustainable Agriculture: Advancements, Challenges, and Future Directions. *Plants*, *14*(2), 191. https://doi.org/10.3390/plants14020191

Dingler, Ch., & Oelze, J. (1985). Reversible and irreversible inactivation of cellular nitrogenase upon oxygen stress in Azotobacter vinelandii growing in oxygen controlled continuous culture. *Archives of Microbiology*, *141*(1), 80–84. https://doi.org/10.1007/BF00446744

Dixon, R., & Kahn, D. (2004). Genetic regulation of biological nitrogen fixation. *Nature Reviews Microbiology*, *2*(8), 621–631. https://doi.org/10.1038/nrmicro954

Donati, I., & Christensen, B. E. (2023). Alginate-metal cation interactions: Macromolecular approach. *Carbohydrate Polymers*, *321*, 1–17. https://doi.org/10.1016/J.CARBPOL.2023.121280

Donati, I., & Paoletti, S. (2009). *Material Properties of Alginates*. https://doi.org/10.1007/978-3-540-92679-5_1

dos Reis, G. A., Martínez-Burgos, W. J., Pozzan, R., Pastrana Puche, Y., Ocán-Torres, D., de Queiroz Fonseca Mota, P., Rodrigues, C., Lima Serra, J., Scapini, T., Karp, S. G., & Soccol, C. R. (2024). Comprehensive Review of Microbial Inoculants: Agricultural Applications, Technology Trends in Patents, and Regulatory Frameworks. *Sustainability*, *16*(19), 8720. https://doi.org/10.3390/su16198720

Draget, K. I., Skjåk-Bræk, G., & Stokke, B. T. (2006). Similarities and differences between alginic acid gels and ionically crosslinked alginate gels. *Food Hydrocolloids*, *20*(2-3 SPEC. ISS.), 170–175. https://doi.org/10.1016/j.foodhyd.2004.03.009

Dudun, A., Akoulina, E., Zhuikov, V., Makhina, T., Voinova, V., Belishev, N., Khaydapova, D., Shaitan, K., Bonartseva, G., & Bonartsev, A. (2021). Competitive Biosynthesis of Bacterial Alginate Using Azotobacter vinelandii 12 for Tissue Engineering Applications. *Polymers*, *14*(1), 131. https://doi.org/10.3390/polym14010131

Dusso, D., & Salomon, C. J. (2023). Solving the delivery of Lactococcus lactis : Improved survival and storage stability through the bioencapsulation with different carriers. *Journal of Food Science*, *88*(4), 1495–1505. https://doi.org/10.1111/1750-3841.16538

Ehinmitan, E., Losenge, T., Mamati, E., Ngumi, V., Juma, P., & Siamalube, B. (2024). BioSolutions for Green Agriculture: Unveiling the Diverse Roles of Plant Growth-Promoting Rhizobacteria. *International Journal of Microbiology*, *2024*(1). https://doi.org/10.1155/2024/6181491

Eltaweil, A. S., Abd El-Monaem, E. M., Elshishini, H. M., El-Aqapa, H. G., Hosny, M., Abdelfatah, A. M., Ahmed, M. S., Hammad, E. N., El-Subruiti, G. M., Fawzy, M., & Omer, A. M. (2022). Recent developments in alginate-based adsorbents for removing phosphate ions from wastewater: a review. *RSC Advances*, *12*(13), 8228–8248. https://doi.org/10.1039/D1RA09193J

Ertesvåg, H. (2015). Alginate-modifying enzymes: Biological roles and biotechnological uses. *Frontiers in Microbiology*, *6*(MAY), 1–10. https://doi.org/10.3389/fmicb.2015.00523

Etesami, H., Alikhani, H., & Akbari, A. (2009). Evaluation of plant growth hormones production (IAA) ability by Iranian soils rhizobial strains and effects of superior strains application on wheat growth. *World Appl Sci J*, *6*(11), 1576–1584. http://scholar.google.com/scholar?hl=en&btnG=Search&q=intitle:Evaluation+of+Plant+Growth+Hormones+Production+(+IAA+)+Ability+by+Iranian+Soils+Rhizobial+Strains+and+Effects+of+Superior+Strains+Application+on+Wheat+Growth+Indexes#0

Fadiji, A. E., Xiong, C., Egidi, E., & Singh, B. K. (2024). Formulation challenges associated with microbial biofertilizers in sustainable agriculture and paths forward. *Journal of Sustainable Agriculture and Environment*, *3*(3). https://doi.org/10.1002/sae2.70006

Fernández Farrés, I., & Norton, I. T. (2014). Formation kinetics and rheology of alginate fluid gels produced by in-situ calcium release. *Food Hydrocolloids*, *40*, 76–84. https://doi.org/10.1016/j.foodhyd.2014.02.005

Ferreira, C. M. H., Soares, H. M. V. M., & Soares, E. V. (2019). Promising bacterial genera for agricultural practices: An insight on plant growth-promoting properties and microbial safety aspects. *Science of the Total Environment*, *682*, 779–799. https://doi.org/10.1016/j.scitotenv.2019.04.225

Ferri, M., Ranucci, E., Romagnoli, P., & Giaccone, V. (2017). Antimicrobial resistance: A global emerging threat to public health systems. *Critical Reviews in Food Science and Nutrition*, *57*(13), 2857–2876. https://doi.org/10.1080/10408398.2015.1077192

Flemming, H.-C., & Wingender, J. (2010). The biofilm matrix. *Nature Reviews Microbiology*, *8*(9), 623–633. https://doi.org/10.1038/nrmicro2415

Follett, P. A., Kawabata, A., Nelson, R., Asmus, G., Burt, J., Goschke, K., Ewing, C., Gaertner, J., Brill, E., & Geib, S. (2016). Predation by flat bark beetles (Coleoptera: Silvanidae and Laemophloeidae) on coffee berry borer (Coleoptera: Curculionidae) in Hawaii coffee. *Biological Control*, *101*, 152–158. https://doi.org/10.1016/j.biocontrol.2016.07.002

Franke, P., Freiberger, S., Zhang, L., & Einsle, O. (2025). Conformational protection of molybdenum nitrogenase by Shethna protein II. *Nature*, *637*(8047), 998–1004. https://doi.org/10.1038/s41586-024-08355-3

Fukami, J., Nogueira, M. A., Araujo, R. S., & Hungria, M. (2016). Accessing inoculation methods of maize and wheat with Azospirillum brasilense. *AMB Express*, *6*(1), 1–13. https://doi.org/10.1186/s13568-015-0171-y

Gaby, J. C., & Buckley, D. H. (2012). A comprehensive evaluation of PCR primers to amplify the nifH gene of nitrogenase. *PLoS ONE*, *7*(7). https://doi.org/10.1371/journal.pone.0042149

Galloway, J. N., Townsend, A. R., Erisman, J. W., Bekunda, M., Cai, Z., Freney, J. R., Martinelli, L. A., Seitzinger, S. P., & Sutton, M. A. (2008). Transformation of the Nitrogen Cycle: Recent Trends, Questions, and Potential Solutions. *Science*, *320*(5878), 889–892. https://doi.org/10.1126/science.1136674

Gao, R., Zhao, D., Zhou, X., Wan, Z., Wang, X., Rao, H., Liu, X., Gao, X., & Hao, J. (2025). Advances in polysaccharide-based biopolymers for probiotic encapsulation: From single polysaccharides to composite systems. *Current Research in Food Science*, *11*, 101186. https://doi.org/10.1016/j.crfs.2025.101186

Garcha, S. (2023). Present Scenario: Status of the Biofertilizer Industry in India. In *Metabolomics, Proteomes and Gene Editing Approaches in Biofertilizer Industry* (pp. 21–36). Springer Nature Singapore. https://doi.org/10.1007/978-981-99-3561-1_2

Ghosh, S., Lahiri, D., Nag, M., Dey, A., Sarkar, T., Pathak, S. K., Edinur, H. A., Pati, S., & Ray, R. R. (2021). Bacterial biopolymer: Its role in pathogenesis to effective biomaterials. *Polymers*, *13*(8), 1–28. https://doi.org/10.3390/polym13081242

Giese, H., Azizan, A., Kümmel, A., Liao, A., Peter, C. P., Fonseca, J. A., Hermann, R., Duarte, T. M., & Büchs, J. (2014). Liquid films on shake flask walls explain increasing maximum oxygen transfer capacities with elevating viscosity. *Biotechnology and Bioengineering*, *111*(2), 295–308. https://doi.org/10.1002/bit.25015

Glick, B. R. (2012). Plant Growth-Promoting Bacteria: Mechanisms and Applications. *Scientifica*, *2012*, 1–15. https://doi.org/10.6064/2012/963401

González Henao, S., & Ghneim-Herrera, T. (2021). Heavy Metals in Soils and the Remediation Potential of Bacteria Associated With the Plant Microbiome. *Frontiers in Environmental Science*, *9*(April), 1–17. https://doi.org/10.3389/fenvs.2021.604216

Gordon, S. A., & Weber, R. P. (1951). Colorimetric estimation of indoleacetic acid. *Plant Physiology*, *26*, 192–195. https://academic.oup.com/plphys/article/26/1/192/6093171

Goyal, R. K., Mattoo, A. K., & Schmidt, M. A. (2021). Rhizobial–Host Interactions and Symbiotic Nitrogen Fixation in Legume Crops Toward Agriculture Sustainability. *Frontiers in Microbiology*, *12*. https://doi.org/10.3389/fmicb.2021.669404

Gross-Urrego, J. A., Pantoja-Benavides, A. D., Moreno-Poveda, G. A., Ramírez-Godoy, A., Chávez-Arias, C. C., & Restrepo-Díaz, H. (2025). Exogenous Azotobacter vinelandii application as a component of integrated plant nutrient management in “Hass” avocado crops. *Trees*, *39*(5), 98. https://doi.org/10.1007/s00468-025-02667-1

Grzesiak, J., Rogala, M. M., Gawor, J., Kouřilová, X., & Obruča, S. (2024). Polyhydroxyalkanoate involvement in stress-survival of two psychrophilic bacterial strains from the High Arctic. *Applied Microbiology and Biotechnology*, *108*(1), 273. https://doi.org/10.1007/s00253-024-13092-8

Gu, W., & Milton, R. D. (2020). Natural and Engineered Electron Transfer of Nitrogenase. *Chemistry*, *2*(2), 322–346. https://doi.org/10.3390/chemistry2020021

Gunzburg, W. H., Aung, M. M., Toa, P., Ng, S., Read, E., Tan, W. J., Brandtner, E. M., Dangerfield, J., & Salmons, B. (2020). Efficient protection of microorganisms for delivery

to the intestinal tract by cellulose sulphate encapsulation. *Microbial Cell Factories*, *19*(1), 216. https://doi.org/10.1186/s12934-020-01465-3

Gurikar, C., Sreenivasa, M. Y., Nanje Gowda, N. A., & Lokesh, A. C. (2022). Azotobacter—A potential symbiotic rhizosphere engineer. In *Rhizosphere Engineering* (pp. 97–112). Elsevier. https://doi.org/10.1016/B978-0-323-89973-4.00010-7

Haas, D., & Défago, G. (2005). Biological control of soil-borne pathogens by fluorescent pseudomonads. *Nature Reviews Microbiology*, *3*(4), 307–319. https://doi.org/10.1038/nrmicro1129

Haferburg, G., & Kothe, E. (2007). Microbes and metals: Interactions in the environment. *Journal of Basic Microbiology*, *47*(6), 453–467. https://doi.org/10.1002/jobm.200700275

Hafez, M., El-Badry, M. A., Elbarbary, T. A., Ibrahim, I. A., & Abdel-Fatah, Y. M. (2016). Azotobacter vinelandii evaluation and optimization of Abu Tartur Egyptian phosphate ore dissolution. *Original Research Article Saudi Journal of Pathology and Microbiology*, *1*, 80–93. https://doi.org/10.21276/sjpm.2016.1.3.2

Hakim, S., Naqqash, T., Nawaz, M. S., Laraib, I., Siddique, M. J., Zia, R., Mirza, M. S., & Imran, A. (2021). Rhizosphere Engineering With Plant Growth-Promoting Microorganisms for Agriculture and Ecological Sustainability. *Frontiers in Sustainable Food Systems*, *5*. https://doi.org/10.3389/fsufs.2021.617157

Hamzi, H. Q., & Skoog, F. (2015). *Botanical Society of America , Inc . AND LEAF FORM IN TOBACCO PLANTLETS ’. 60*(6), 491–495.

Haruta, S., & Kanno, N. (2015). Survivability of microbes in natural environments and their ecological impacts. *Microbes and Environments*, *30*(2), 123–125. https://doi.org/10.1264/jsme2.ME3002rh

Hernandez-Eligio, A., Castellanos, M., Moreno, S., & Espín, G. (2011). Transcriptional activation of the Azotobacter vinelandii polyhydroxybutyrate biosynthetic genes phbBAC by PhbR and RpoS. *Microbiology*, *157*(11), 3014–3023. https://doi.org/10.1099/mic.0.051649-0

Hert, A. P., Marutani, M., Momol, M. T., Roberts, P. D., & Jones, J. B. (2009). Analysis of pathogenicity mutants of a bacteriocin producing Xanthomonas perforans. *Biological Control*, *51*(3), 362–369. https://doi.org/10.1016/j.biocontrol.2009.07.007

Hider, R. C., & Kong, X. (2010). Chemistry and biology of siderophores. *Natural Product Reports*, *27*(5), 637–657. https://doi.org/10.1039/b906679a

Hilbig, J., Hartlieb, K., Gibis, M., Herrmann, K., & Weiss, J. (2020). Rheological and mechanical properties of alginate gels and films containing different chelators. *Food Hydrocolloids*, *101*, 105487. https://doi.org/10.1016/j.foodhyd.2019.105487

Hoare, T. R., & Kohane, D. S. (2008). Hydrogels in drug delivery: Progress and challenges. *Polymer*, *49*(8), 1993–2007. https://doi.org/10.1016/j.polymer.2008.01.027

https://eur-lex.europa.eu/. (2019).

Hungria, M., Franchini, J. C., Campo, R. J., Crispino, C. C., Moraes, J. Z., Sibaldelli, R. N. R., Mendes, I. C., & Arihara, J. (2006). Nitrogen nutrition of soybean in Brazil: Contributions of biological N $_2$ fixation and N fertilizer to grain yield. *Canadian Journal of Plant Science*, *86*(4), 927–939. https://doi.org/10.4141/P05-098

Ilbert, M., & Bonnefoy, V. (2013). Insight into the evolution of the iron oxidation pathways. *Biochimica et Biophysica Acta - Bioenergetics*, *1827*(2), 161–175. https://doi.org/10.1016/j.bbabio.2012.10.001

Iqbal, Mohd. Z., Singh, K., & Chandra, R. (2024). Recent advances of plant growth promoting rhizobacteria (PGPR) for eco-restoration of polluted soil. *Cleaner Engineering and Technology*, *23*, 100845. https://doi.org/10.1016/j.clet.2024.100845

Jaffur, B. N., Kumar, G., Jeetah, P., Ramakrishna, S., & Bhatia, S. K. (2023). Current advances and emerging trends in sustainable polyhydroxyalkanoate modification from organic waste streams for material applications. *International Journal of Biological Macromolecules*, *253*, 126781. https://doi.org/10.1016/j.ijbiomac.2023.126781

Jiao, W., Chen, W., Mei, Y., Yun, Y., Wang, B., Zhong, Q., Chen, H., & Chen, W. (2019). Effects of Molecular Weight and Guluronic Acid/Mannuronic Acid Ratio on the Rheological Behavior and Stabilizing Property of Sodium Alginate. *Molecules (Basel, Switzerland)*, *24*(23). https://doi.org/10.3390/molecules24234374

John, R. P., Tyagi, R. D., Brar, S. K., Surampalli, R. Y., & Prévost, D. (2011). Bio-encapsulation of microbial cells for targeted agricultural delivery. *Critical Reviews in Biotechnology*, *31*, 211–226. https://doi.org/10.3109/07388551.2010.513327

Johnston, E., Okada, S., Gregg, C. M., Warden, A. C., Rolland, V., Gillespie, V., Byrne, K., Colgrave, M. L., Eamens, A. L., Allen, R. S., & Wood, C. C. (2023). The structural components of the Azotobacter vinelandii iron-only nitrogenase, AnfDKG, form a protein complex within the plant mitochondrial matrix. *Plant Molecular Biology*, *112*(4–5), 279–291. https://doi.org/10.1007/s11103-023-01363-3

Junaid, P. M., Dar, A. H., Dash, K. K., Rohilla, S., Islam, R., Shams, R., Pandey, V. K., Srivastava, S., Panesar, P. S., & Zaidi, S. (2024a). Polysaccharide-based hydrogels for microencapsulation of bioactive compounds: A review. *Journal of Agriculture and Food Research*, *15*, 101038. https://doi.org/10.1016/j.jafr.2024.101038

Junaid, P. M., Dar, A. H., Dash, K. K., Rohilla, S., Islam, R., Shams, R., Pandey, V. K., Srivastava, S., Panesar, P. S., & Zaidi, S. (2024b). Polysaccharide-based hydrogels for microencapsulation of bioactive compounds: A review. *Journal of Agriculture and Food Research*, *15*, 101038. https://doi.org/10.1016/j.jafr.2024.101038

Jung, Y. S., & Kwon, Y. M. (2008). Small RNA ArrF regulates the expression of sodB and feSII genes in Azotobacter vinelandii. *Current Microbiology*, *57*(6), 593–597. https://doi.org/10.1007/s00284-008-9248-z

Kalayu, G. (2019). Phosphate Solubilizing Microorganisms: Promising Approach as Biofertilizers. *International Journal of Agronomy*, *2019*, 1–7. https://doi.org/10.1155/2019/4917256

Kapoor, D. U., Pareek, A., Sharma, S., Prajapati, B. G., Thanawuth, K., & Sriamornsak, P. (2025). Alginate gels: Chemistry, gelation mechanisms, and therapeutic applications with a focus on GERD treatment. *International Journal of Pharmaceutics*, *675*, 125570. https://doi.org/10.1016/j.ijpharm.2025.125570

Karoyo, A., & Wilson, L. (2017). Physicochemical Properties and the Gelation Process of Supramolecular Hydrogels: A Review. *Gels*, *3*(1), 1. https://doi.org/10.3390/gels3010001

KB, S., JJA, P., V, V., & K, S. (2017). Analyzing the Efficacy of Phosphate Solubilizing Microorganisms by Enrichment Culture Techniques. *Biochemistry & Molecular Biology Journal*, *03*(01). https://doi.org/10.21767/2471-8084.100029

Kelbessa, B. G., Dubey, M., Catara, V., Ghadamgahi, F., Ortiz, R., & Vetukuri, R. R. (2023). Potential of plant growth-promoting rhizobacteria to improve crop productivity and

adaptation to a changing climate. *CABI Reviews*. https://doi.org/10.1079/cabireviews.2023.0001

Khan, A., Singh, A. V., Gautam, S. S., Agarwal, A., Punetha, A., Upadhayay, V. K., Kukreti, B., Bundela, V., Jugran, A. K., & Goel, R. (2023). Microbial bioformulation: a microbial assisted biostimulating fertilization technique for sustainable agriculture. *Frontiers in Plant Science*, *14*. https://doi.org/10.3389/fpls.2023.1270039

Kivilcimdan Moral, Ç., & Yildiz, M. (2016). Alginate Production from Alternative Carbon Sources and Use of Polymer Based Adsorbent in Heavy Metal Removal. *International Journal of Polymer Science*, *2016*. https://doi.org/10.1155/2016/7109825

Koller, M. (2019). Switching from petro-plastics to microbial polyhydroxyalkanoates (PHA): the biotechnological escape route of choice out of the plastic predicament? *The EuroBiotech Journal*, *3*(1), 32–44. https://doi.org/10.2478/ebtj-2019-0004

Koller, M., Maršálek, L., de Sousa Dias, M. M., & Braunegg, G. (2017). Producing microbial polyhydroxyalkanoate (PHA) biopolyesters in a sustainable manner. *New Biotechnology*, *37*, 24–38. https://doi.org/10.1016/j.nbt.2016.05.001

Koutsougera, D., Zafeiriou, I., Giannakopoulou, F., Ipsilantis, I., Kalderis, D., Gasparatos, D., & Bilias, F. (2023). Biostimulants: an introduction. In *Biostimulants in Alleviation of Metal Toxicity in Plants* (pp. 21–50). Elsevier. https://doi.org/10.1016/B978-0-323-99600-6.00007-4

Kowalska, E., Ziarno, M., Ekielski, A., & Żelaziński, T. (2022). Materials Used for the Microencapsulation of Probiotic Bacteria in the Food Industry. *Molecules*, *27*(10), 3321. https://doi.org/10.3390/molecules27103321

Kumar, S., Diksha, Sindhu, S. S., & Kumar, R. (2022). Biofertilizers: An ecofriendly technology for nutrient recycling and environmental sustainability. *Current Research in Microbial Sciences*, *3*, 100094. https://doi.org/10.1016/j.crmicr.2021.100094

Kunasundari, B., & Sudesh, K. (2011). Isolation and recovery of microbial polyhydroxyalkanoates. *Express Polymer Letters*, *5*(7), 620–634. https://doi.org/10.3144/expresspolymlett.2011.60

Lahlali, R., Serrhini, M. N., Friel, D., & Jijakli, M. H. (2006). In vitro effects of water activity, temperature and solutes on the growth rate of P. italicum Wehmer and P. digitatum Sacc.

Journal of Applied Microbiology, *101*(3), 628–636. https://doi.org/10.1111/j.1365-2672.2006.02953.x

Larson R.G. (1999). *The Structure and Rheology of Complex Fluids (Topics in Chemical Engineering)* (1st ed.).

Lee, J., Park, H. J., Moon, M., Lee, J. S., & Min, K. (2021). Recent progress and challenges in microbial polyhydroxybutyrate (PHB) production from CO2 as a sustainable feedstock: A state-of-the-art review. *Bioresource Technology*, *339*(June), 125616. https://doi.org/10.1016/j.biortech.2021.125616

Lee, M. S., & Salleh, K. M. (2025). An overview on microalgal polyhydroxybutyrate (PHB) production and improvement of mechanical properties. *International Journal of Biological Macromolecules*, *320*, 146056. https://doi.org/10.1016/j.ijbiomac.2025.146056

Lee, S.-K., Lur, H.-S., Lo, K.-J., Cheng, K.-C., Chuang, C.-C., Tang, S.-J., Yang, Z.-W., & Liu, C.-T. (2016). Evaluation of the effects of different liquid inoculant formulations on the survival and plant-growth-promoting efficiency of Rhodopseudomonas palustris strain PS3. *Applied Microbiology and Biotechnology*, *100*(18), 7977–7987. https://doi.org/10.1007/s00253-016-7582-9

Leif Marvin R. Gonzales, Ramonita A. Caralde, & Maita L. Aban. (2015). Response of Pechay (Brassica napus L.) to Different Levels of Compost Fertilizer. *International Journal of Scientific and Research Publications*, *5*(1).

Li, J., Wang, J., Liu, H., Macdonald, C. A., & Singh, B. K. (2023). Microbial inoculants with higher capacity to colonize soils improved wheat drought tolerance. *Microbial Biotechnology*, *16*(11), 2131–2144. https://doi.org/10.1111/1751-7915.14350

Lo Giudice, A., Poli, A., Finore, I., & Rizzo, C. (2020). Peculiarities of extracellular polymeric substances produced by Antarctic bacteria and their possible applications. *Applied Microbiology and Biotechnology*, *104*(7), 2923–2934. https://doi.org/10.1007/s00253-020-10448-8

Lobo, C. B., Juárez Tomás, M. S., Viruel, E., Ferrero, M. A., & Lucca, M. E. (2019). Development of low-cost formulations of plant growth-promoting bacteria to be used as inoculants in beneficial agricultural technologies. *Microbiological Research*, *219*, 12–25. https://doi.org/10.1016/j.micres.2018.10.012

Lucie Svobodova. (2024). *Stanovení viability u rhizobakteriálních kultur.* Vysoké učení technické v Brně.

Ma, J. F. (2005). Plant root responses to three abundant soil minerals: Silicon, aluminum and iron. *Critical Reviews in Plant Sciences*, *24*, 267–281. https://doi.org/10.1080/07352680500196017

Majkowska-Gadomska, J., Dobrowolski, A., Jadwisieńczak, K. K., Kaliniewicz, Z., & Francke, A. (2021). Effect of biostimulants on the growth, yield and nutritional value of Capsicum annuum grown in an unheated plastic tunnel. *Scientific Reports*, *11*(1), 22335. https://doi.org/10.1038/s41598-021-01834-x

Makarova, A. O., Derkach, S. R., Khair, T., Kazantseva, M. A., Zuev, Y. F., & Zueva, O. S. (2023). Ion-Induced Polysaccharide Gelation: Peculiarities of Alginate Egg-Box Association with Different Divalent Cations. *Polymers*, *15*(5), 1243. https://doi.org/10.3390/polym15051243

Makhaye, G., Mofokeng, M. M., Tesfay, S., Aremu, A. O., Van Staden, J., & Amoo, S. O. (2021). Influence of plant biostimulant application on seed germination. In *Biostimulants for Crops from Seed Germination to Plant Development* (pp. 109–135). Elsevier. https://doi.org/10.1016/B978-0-12-823048-0.00014-9

Malheiro, J., & Simões, M. (2017). Antimicrobial resistance of biofilms in medical devices. In *Biofilms and Implantable Medical Devices* (pp. 97–113). Elsevier. https://doi.org/10.1016/B978-0-08-100382-4.00004-6

Malusá, E., Sas-Paszt, L., & Ciesielska, J. (2012). Technologies for Beneficial Microorganisms Inocula Used as Biofertilizers. *The Scientific World Journal*, *2012*, 1–12. https://doi.org/10.1100/2012/491206

Massana Roquero, D., Othman, A., Melman, A., & Katz, E. (2022). Iron(<scp>iii</scp>)-cross-linked alginate hydrogels: a critical review. *Materials Advances*, *3*(4), 1849–1873. https://doi.org/10.1039/D1MA00959A

Matte, W. D., Oliveira Jr., R. S. de, Machado, F. G., Constantin, J., Biffe, D. F., Gutierrez, F. D. S. D., & Silva, J. R. V. da. (2018). Eficácia de [atrazine + mesotrione] para o controle de plantas daninhas na cultura do milho. *Revista Brasileira de Herbicidas*, *17*(2), 587. https://doi.org/10.7824/rbh.v17i2.587

Meena, V. S., Mishra, P. K., Bisht, J. K., & Pattanayak, A. (2017). Agriculturally important microbes for sustainable agriculture. In *Agriculturally Important Microbes for Sustainable Agriculture* (Vol. 2). https://doi.org/10.1007/978-981-10-5343-6

Meisner, A., Jacquiod, S., Snoek, B. L., ten Hooven, F. C., & van der Putten, W. H. (2018). Drought Legacy Effects on the Composition of Soil Fungal and Prokaryote Communities. *Frontiers in Microbiology*, *9*. https://doi.org/10.3389/fmicb.2018.00294

Mejía, M. Á., Segura, D., Espín, G., Galindo, E., & Peña, C. (2010). Two-stage fermentation process for alginate production by Azotobacter vinelandii mutant altered in poly-β-hydroxybutyrate (PHB) synthesis. *Journal of Applied Microbiology*, *108*(1), 55–61. https://doi.org/10.1111/j.1365-2672.2009.04403.x

Miethke, M., & Marahiel, M. A. (2007). Siderophore-Based Iron Acquisition and Pathogen Control. *Microbiology and Molecular Biology Reviews*, *71*(3), 413–451. https://doi.org/10.1128/mmbr.00012-07

Molina-Romero, D., Baez, A., Quintero-Hernández, V., Castañeda-Lucio, M., Fuentes-Ramírez, L. E., Bustillos-Cristales, M. del R., Rodríguez-Andrade, O., Morales-García, Y. E., Munive, A., & Muñoz-Rojas, J. (2017). Compatible bacterial mixture, tolerant to desiccation, improves maize plant growth. *PLOS ONE*, *12*(11), e0187913. https://doi.org/10.1371/journal.pone.0187913

Monica, S., Panneerselvam, S., Rajasekaran, R., Nalliappan, S., Kailappan, A., & Rangasamy, A. (2025). Recent Advances in Bioinoculant Formulations and Their Shelf-Life: A Review. *Current Microbiology*, *82*(11), 506. https://doi.org/10.1007/s00284-025-04497-3

Montesano, F. F., Parente, A., Santamaria, P., Sannino, A., & Serio, F. (2015). Biodegradable Superabsorbent Hydrogel IncreasesWater Retention Properties of Growing Media and Plant Growth. *Agriculture and Agricultural Science Procedia*, *4*, 451–458. https://doi.org/10.1016/j.aaspro.2015.03.052

More, T. T., Yadav, J. S. S., Yan, S., Tyagi, R. D., & Surampalli, R. Y. (2014). Extracellular polymeric substances of bacteria and their potential environmental applications. *Journal of Environmental Management*, *144*, 1–25. https://doi.org/10.1016/j.jenvman.2014.05.010

Muriel-Millán, L. F., Castellanos, M., Hernandez-Eligio, J. A., Moreno, S., & Espín, G. (2014). Posttranscriptional regulation of PhbR, the transcriptional activator of

polyhydroxybutyrate synthesis, by iron and the sRNA ArrF in Azotobacter vinelandii. *Applied Microbiology and Biotechnology*, *98*(5), 2173–2182. https://doi.org/10.1007/s00253-013-5407-7

Naohara, R., Namai, S., Kamiyama, J., & Ikeda-Fukazawa, T. (2022). Structure and Diffusive Properties of Water in Polymer Hydrogels. *The Journal of Physical Chemistry B*, *126*(40), 7992–7998. https://doi.org/10.1021/acs.jpcb.2c03069

Natzke, J., Noar, J., & Bruno-Bárcena, J. M. (2018). Azotobacter vinelandii nitrogenase activity, hydrogen production, and response to oxygen exposure. *Applied and Environmental Microbiology*, *84*, 1–10. https://doi.org/10.1128/aem.01208-18

Nayak, A. K., Raja, R., Rao, K. S., Shukla, A. K., Mohanty, S., Shahid, M., Tripathi, R., Panda, B. B., Bhattacharyya, P., Kumar, A., Lal, B., Sethi, S. K., Puri, C., Nayak, D., & Swain, C. K. (2015). Effect of fly ash application on soil microbial response and heavy metal accumulation in soil and rice plant. *Ecotoxicology and Environmental Safety*, *114*, 257–262. https://doi.org/10.1016/j.ecoenv.2014.03.033

Neilands, B. B. (1987). Universal chemical assay for the detection and determination of siderophores'. *Analytical Biochemistry*, *160*, 47–56. https://doi.org/10.1016/0003-2697(87)90612-9

Netrusov, A. I., Liyaskina, E. V., Kurgaeva, I. V., Liyaskina, A. U., Yang, G., & Revin, V. V. (2023). Exopolysaccharides Producing Bacteria: A Review. *Microorganisms*, *11*(6), 1541. https://doi.org/10.3390/microorganisms11061541

Noar, J. D., & Bruno-Bárcena, J. M. (2018). Azotobacter vinelandii: The source of 100 years of discoveries and many more to come. *Microbiology (United Kingdom)*, *164*, 421–436. https://doi.org/10.1099/mic.0.000643

Novackova, I., Hrabalova, V., Slaninova, E., Sedlacek, P., Samek, O., Koller, M., Krzyzanek, V., Hrubanova, K., Mrazova, K., Nebesarova, J., & Obruca, S. (2022). The role of polyhydroxyalkanoates in adaptation of Cupriavidus necator to osmotic pressure and high concentration of copper ions. *International Journal of Biological Macromolecules*, *206*(December 2021), 977–989. https://doi.org/10.1016/j.ijbiomac.2022.03.102

Oberoi, K., Tolun, A., Altintas, Z., & Sharma, S. (2021). Effect of Alginate-Microencapsulated Hydrogels on the Survival of Lactobacillus rhamnosus under Simulated Gastrointestinal Conditions. *Foods*, *10*(9), 1999. https://doi.org/10.3390/foods10091999

Obruca, S., Sedlacek, P., Koller, M., Kucera, D., & Pernicova, I. (2018). Involvement of polyhydroxyalkanoates in stress resistance of microbial cells: Biotechnological consequences and applications. *Biotechnology Advances*, *36*, 856–870. https://doi.org/10.1016/j.biotechadv.2017.12.006

Obruca, S., Sedlacek, P., Krzyzanek, V., Mravec, F., Hrubanova, K., Samek, O., Kucera, D., Benesova, P., & Marova, I. (2016). Accumulation of poly(3-hydroxybutyrate) helps bacterial cells to survive freezing. *PLoS ONE*, *11*(6), 1–16. https://doi.org/10.1371/journal.pone.0157778

Obruca, S., Sedlacek, P., Mravec, F., Krzyzanek, V., Nebesarova, J., Samek, O., Kucera, D., Benesova, P., Hrubanova, K., Milerova, M., & Marova, I. (2017). The presence of PHB granules in cytoplasm protects non-halophilic bacterial cells against the harmful impact of hypertonic environments. *New Biotechnology*, *39*, 68–80. https://doi.org/10.1016/j.nbt.2017.07.008

Obruca, S., Sedlacek, P., Slaninova, E., Fritz, I., Daffert, C., Meixner, K., Sedrlova, Z., & Koller, M. (2020). Novel unexpected functions of PHA granules. *Applied Microbiology and Biotechnology*, *104*(11), 4795–4810. https://doi.org/10.1007/s00253-020-10568-1

Obulisamy, P. K., & Mehariya, S. (2021). Polyhydroxyalkanoates from extremophiles: A review. *Bioresource Technology*, *325*, 124653. https://doi.org/10.1016/j.biortech.2020.124653

Olanrewaju, O. S., Glick, B. R., & Babalola, O. O. (2017). Mechanisms of action of plant growth promoting bacteria. *World Journal of Microbiology and Biotechnology*, *33*, 1–16. https://doi.org/10.1007/s11274-017-2364-9

Pacheco-Leyva, I., Guevara Pezoa, F., & Díaz-Barrera, A. (2016). Alginate biosynthesis in azotobacter vinelandii: Overview of molecular mechanisms in connection with the oxygen availability. In *International Journal of Polymer Science* (Vol. 2016). Hindawi Limited. https://doi.org/10.1155/2016/2062360

Page, W. J., Tindale, A., Chandra, M., & Kwon, E. (2001). Alginate formation in Azotobacter vinelandii UWD during stationary phase and the turnover of poly-β-hydroxybutyrate. *Microbiology*, *147*(2), 483–490. https://doi.org/10.1099/00221287-147-2-483

Parveen, N., Mishra, R., Singh, D. V., Kumar, P., & Singh, R. P. (2023). Assessment of different carrier materials for the preparation of microbial formulations to enhance the shelf life and its efficacy on the growth of spinach (Spinacia oleracea L.). *World Journal of Microbiology and Biotechnology*, *39*(7), 180. https://doi.org/10.1007/s11274-023-03594-4

Peña, C., Hernández, L., & Galindo, E. (2006). Manipulation of the acetylation degree of Azotobacter vinelandii alginate by supplementing the culture medium with 3-(N-morpholino)-propane-sulfonic acid. *Letters in Applied Microbiology*, *43*(2), 200–204. https://doi.org/10.1111/j.1472-765X.2006.01925.x

Peña, C., Millán, M., & Galindo, E. (2008). Production of alginate by Azotobacter vinelandii in a stirred fermentor simulating the evolution of power input observed in shake flasks. *Process Biochemistry*, *43*(7), 775–778. https://doi.org/10.1016/j.procbio.2008.02.013

Peña, R. J., Trethowan, R., Pfeiffer, W. H., & Ginkel, M. Van. (2002). Quality (End-Use) Improvement in Wheat. *Journal of Crop Production*, *5*(1–2), 1–37. https://doi.org/10.1300/j144v05n01_02

Pérez-Madrigal, M. M., Torras, J., Casanovas, J., Häring, M., Alemán, C., & Díaz, D. D. (2017). Paradigm Shift for Preparing Versatile M2+-Free Gels from Unmodified Sodium Alginate. *Biomacromolecules*, *18*(9), 2967–2979. https://doi.org/10.1021/acs.biomac.7b00934

Pérez-Ramos, A., Nácher-Vázquez, M., Notararigo, S., López, P., & Mohedano, M. L. (2016). Current and Future Applications of Bacterial Extracellular Polysaccharides. In *Probiotics, Prebiotics, and Synbiotics* (pp. 329–344). Elsevier. https://doi.org/10.1016/B978-0-12-802189-7.00022-8

Pezzoni, M., Lemos, M., Pizarro, R. A., & Costa, C. S. (2022). UVA as environmental signal for alginate production in Pseudomonas aeruginosa: role of this polysaccharide in the protection of planktonic cells and biofilms against lethal UVA doses. *Photochemical & Photobiological Sciences*, *21*(8), 1459–1472. https://doi.org/10.1007/s43630-022-00236-w

Phillips, & Williams. (2009). Handbook of hydrocolloids (incl. Alginates). In *Handbook of Hydrocolloids (second Edition)*.

Pieterse, C. M. J., Zamioudis, C., Berendsen, R. L., Weller, D. M., Van Wees, S. C. M., & Bakker, P. A. H. M. (2014). Induced Systemic Resistance by Beneficial Microbes. *Annual Review of Phytopathology*, *52*(1), 347–375. https://doi.org/10.1146/annurev-phyto-082712-102340

Ponce, B., Urtuvia, V., Maturana, N., Peña, C., & Díaz-Barrera, A. (2021). Increases in alginate production and transcription levels of alginate lyase (alyA1) by control of the oxygen transfer rate in Azotobacter vinelandii cultures under diazotrophic conditions. *Electronic Journal of Biotechnology*, *52*, 35–44. https://doi.org/10.1016/j.ejbt.2021.04.007

Ponnuraj, R. K., Rubio, L. M., Grunwald, S. K., & Ludden, P. W. (2005). NAD-, NMN-, and NADP-dependent modification of dinitrogenase reductases from Rhodospirillum rubrum and Azotobacter vinelandii. *FEBS Letters*, *579*(25), 5751–5758. https://doi.org/10.1016/j.febslet.2005.09.057

Pradhan, N., & Sukla, L. B. (2005). Solubilization of Inorganic Phosphate by Fungi Isolated from Agriculture Soil. *African Journal of Biotechnology*.

Prete, R., Alam, M. K., Perpetuini, G., Perla, C., Pittia, P., & Corsetti, A. (2021). Lactic Acid Bacteria Exopolysaccharides Producers: A Sustainable Tool for Functional Foods. *Foods*, *10*(7), 1653. https://doi.org/10.3390/foods10071653

Pyla, R., Kim, T. J., Silva, J. L., & Jung, Y. S. (2009). Overproduction of poly-β-hydroxybutyrate in the Azotobacter vinelandii mutant that does not express small RNA ArrF. *Applied Microbiology and Biotechnology*, *84*(4), 717–724. https://doi.org/10.1007/s00253-009-2002-z

Ramos, P. E., Silva, P., Alario, M. M., Pastrana, L. M., Teixeira, J. A., Cerqueira, M. A., & Vicente, A. A. (2018). Effect of alginate molecular weight and M/G ratio in beads properties foreseeing the protection of probiotics. *Food Hydrocolloids*, *77*, 8–16. https://doi.org/10.1016/j.foodhyd.2017.08.031

Remminghorst, U., & Rehm, B. H. A. (2006). Bacterial alginates: From biosynthesis to applications. *Biotechnology Letters*, *28*(21), 1701–1712. https://doi.org/10.1007/s10529-006-9156-x

Rivier, A. J., Myers, K. S., Garcia, A. K., Sobol, M. S., & Kaçar, B. (2023). Regulatory response to a hybrid ancestral nitrogenase in *Azotobacter vinelandii*. *Microbiology Spectrum*, *11*(5). https://doi.org/10.1128/spectrum.02815-23

Rocha, I., Ma, Y., Souza-Alonso, P., Vosátka, M., Freitas, H., & Oliveira, R. S. (2019). Seed Coating: A Tool for Delivering Beneficial Microbes to Agricultural Crops. *Frontiers in Plant Science*, *10*. https://doi.org/10.3389/fpls.2019.01357

Rousk, J., & Bååth, E. (2007). Fungal biomass production and turnover in soil estimated using the acetate-in-ergosterol technique. *Soil Biology and Biochemistry*, *39*(8), 2173–2177. https://doi.org/10.1016/j.soilbio.2007.03.023

Rubio, L. M., & Ludden, P. W. (2008). Biosynthesis of the iron-molybdenum cofactor of nitrogenase. *Annual Review of Microbiology*, *62*, 93–111. https://doi.org/10.1146/annurev.micro.62.081307.162737

Ryu, C.-M., Farag, M. A., Hu, C.-H., Reddy, M. S., Wei, H.-X., Paré, P. W., & Kloepper, J. W. (2003). Bacterial volatiles promote growth in *Arabidopsis*. *Proceedings of the National Academy of Sciences*, *100*(8), 4927–4932. https://doi.org/10.1073/pnas.0730845100

Sabra, W., Zeng, A.-P., Lünsdorf, H., & Deckwer, W.-D. (2000). Effect of Oxygen on Formation and Structure of *Azotobacter vinelandii* Alginate and Its Role in Protecting Nitrogenase. *Applied and Environmental Microbiology*, *66*(9), 4037–4044. https://doi.org/10.1128/AEM.66.9.4037-4044.2000

Samago, T. Y., Anniye, E. W., & Dakora, F. D. (2018). Grain yield of common bean (Phaseolus vulgaris L.) varieties is markedly increased by rhizobial inoculation and phosphorus application in Ethiopia. *Symbiosis*, *75*(3), 245–255. https://doi.org/10.1007/s13199-017-0529-9

Santos, M. S., Nogueira, M. A., & Hungria, M. (2019). Microbial inoculants: reviewing the past, discussing the present and previewing an outstanding future for the use of beneficial bacteria in agriculture. In *AMB Express* (Vol. 9, Issue 1). Springer. https://doi.org/10.1186/s13568-019-0932-0

Savić Gajić, I. M., Savić, I. M., & Svirčev, Z. (2023). Preparation and Characterization of Alginate Hydrogels with High Water-Retaining Capacity. *Polymers*, *15*(12), 2592. https://doi.org/10.3390/polym15122592

Schalk, I. J. (2025). Bacterial siderophores: diversity, uptake pathways and applications. *Nature Reviews Microbiology*, *23*, 24–40. https://doi.org/10.1038/s41579-024-01090-6

Schalk, I. J., Mislin, G. L. A., & Brillet, K. (2012). Structure, Function and Binding Selectivity and Stereoselectivity of Siderophore-Iron Outer Membrane Transporters. In *Current Topics in Membranes* (Vol. 69). Elsevier. https://doi.org/10.1016/B978-0-12-394390-3.00002-1

Schmidt, F. V., Schulz, L., Zarzycki, J., Prinz, S., Oehlmann, N. N., Erb, T. J., & Rebelein, J. G. (2024). Structural insights into the iron nitrogenase complex. *Nature Structural & Molecular Biology*, *31*(1), 150–158. https://doi.org/10.1038/s41594-023-01124-2

Schmidt, W., Thomine, S., & Buckhout, T. J. (2020). Editorial: Iron Nutrition and Interactions in Plants. *Frontiers in Plant Science*, *10*. https://doi.org/10.3389/fpls.2019.01670

Schoebitz, M., López, M., Roldán, A., & López, M. D. (2013). *Bioencapsulation of microbial inoculants for better soil-plant fertilization. A review Bioencapsulation of microbial inoculants for better soil-plant fertilization. A review. Agronomy for Sustainable Development Bioencapsulation of microbial inoculants for better soil-plant fertilization. A review*. *33*(4), 751–765. https://doi.org/10.1007/s13593-013-0142-0ï

Schoebitz, M., Mengual, C., & Roldán, A. (2014). Combined effects of clay immobilized Azospirillum brasilense and Pantoea dispersa and organic olive residue on plant performance and soil properties in the revegetation of a semiarid area. *Science of The Total Environment*, *466–467*, 67–73. https://doi.org/10.1016/j.scitotenv.2013.07.012

Sedlacek, P., Slaninova, E., Koller, M., Nebesarova, J., Marova, I., Krzyzanek, V., & Obruca, S. (2019). PHA granules help bacterial cells to preserve cell integrity when exposed to sudden osmotic imbalances. *New Biotechnology*, *49*(May 2018), 129–136. https://doi.org/10.1016/j.nbt.2018.10.005

Setubal, J. C., dos Santos, P., Goldman, B. S., Ertesvåg, H., Espin, G., Rubio, L. M., Valla, S., Almeida, N. F., Balasubramanian, D., Cromes, L., Curatti, L., Du, Z., Godsy, E., Goodner, B., Hellner-Burris, K., Hernandez, J. A., Houmiel, K., Imperial, J., Kennedy, C., … Wood, D. (2009). Genome Sequence of *Azotobacter vinelandii* , an Obligate Aerobe Specialized To Support Diverse Anaerobic Metabolic Processes. *Journal of Bacteriology*, *191*(14), 4534–4545. https://doi.org/10.1128/JB.00504-09

Shah, A., Nazari, M., Antar, M., Msimbira, L. A., Naamala, J., Lyu, D., Rabileh, M., Zajonc, J., & Smith, D. L. (2021). PGPR in Agriculture: A Sustainable Approach to Increasing Climate Change Resilience. *Frontiers in Sustainable Food Systems*, *5*. https://doi.org/10.3389/fsufs.2021.667546

Shahid, S., Razzaq, S., Farooq, R., & Nazli, Z. i. H. (2021). Polyhydroxyalkanoates: Next generation natural biomolecules and a solution for the world's future economy. *International Journal of Biological Macromolecules*, *166*, 297–321. https://doi.org/10.1016/j.ijbiomac.2020.10.187

Shailendra Singh, G. G. (2015). Plant growth promoting rhizobacteria (PGPR): Current and future prospects for development of sustainable agriculture. *Journal of Microbial & Biochemical Technology*, *7*, 96–102. https://doi.org/10.4172/1948-5948.1000188

Silva, T. L. da, Vidart, J. M. M., Silva, M. G. C. da, Gimenes, M. L., & Vieira, M. G. A. (2017). Alginate and Sericin: Environmental and Pharmaceutical Applications. *Biological Activities and Application of Marine Polysaccharides*. https://doi.org/10.5772/65257

Skjåk-Bræk, G., Zanetti, F., & Paoletti, S. (1989). Effect of acetylation on some solution and gelling properties of alginates. *Carbohydrate Research*, *185*, 131–138. https://doi.org/10.1016/0008-6215(89)84028-5

Soares, M., & Rousk, J. (2019). Microbial growth and carbon use efficiency in soil: Links to fungal-bacterial dominance, SOC-quality and stoichiometry. *Soil Biology and Biochemistry*, *131*, 195–205. https://doi.org/10.1016/J.SOILBIO.2019.01.010

Sofia Orišková. (2020). *Inkorporace mikrobiálních buněk do hydrogelových nosičů.* Vysoké učení technické v Brne.

Song, X., Liu, M., Wu, D., Griffiths, B. S., Jiao, J., Li, H., & Hu, F. (2015). Interaction matters: Synergy between vermicompost and PGPR agents improves soil quality, crop quality and crop yield in the field. *Applied Soil Ecology*, *89*, 25–34. https://doi.org/10.1016/j.apsoil.2015.01.005

Sosnik, A. (2014). Alginate Particles as Platform for Drug Delivery by the Oral Route: State-of-the-Art. *ISRN Pharmaceutics*, *2014*, 1–17. https://doi.org/10.1155/2014/926157

Spaepen, S., & Vanderleyden, J. (2011). *Auxin and Plant-Microbe Interactions*. 1–14.

Steinbuchel, A., Aerts, K., Babel, W., Follner, C., Kiebergesell, M., Madkour, M. H., Mayer, F., Pieper-Furst, U., Pries, A., Valentin, H. E., & Wieczorek, R. (1995). Considerations on the structure and biochemistry of bacterial polyhydroxyalkanoic acid inclusions. *Canadian Journal of Microbiology*, *41*(SUPPL. 1), 94–105. https://doi.org/10.1139/m95-175

Steinbüchel, A., & Füchtenbusch, B. (1998). Bacterial and other biological systems for polyester production. *Trends in Biotechnology*, *16*(10), 419–427. https://doi.org/10.1016/S0167-7799(98)01194-9

Sumbul, A., Ansari, R. A., Rizvi, R., & Mahmood, I. (2020). Azotobacter: A potential bio-fertilizer for soil and plant health management. *Saudi Journal of Biological Sciences*, *27*(12), 3634–3640. https://doi.org/10.1016/j.sjbs.2020.08.004

Sütekin, S. D. (2024). Green Synthesis of Smart Hydrogels via Radiation Crosslinking of Sodium Alginate and Citric Acid for pH-Sensitive Doxycycline Hyclate Release. *Iğdır Üniversitesi Fen Bilimleri Enstitüsü Dergisi*, *14*(4), 1655–1671. https://doi.org/10.21597/jist.1512940

Svenningsen, N. B., Martínez-García, E., Nicolaisen, M. H., de Lorenzo, V., & Nybroe, O. (2018). The biofilm matrix polysaccharides cellulose and alginate both protect Pseudomonas putida mt-2 against reactive oxygen species generated under matric stress and copper exposure. *Microbiology*, *164*(6), 883–888. https://doi.org/10.1099/mic.0.000667

Takimoto, R., Tatemichi, Y., Aoki, W., Kosaka, Y., Minakuchi, H., Ueda, M., & Kuroda, K. (2022). A critical role of an oxygen-responsive gene for aerobic nitrogenase activity in Azotobacter vinelandii and its application to Escherichia coli. *Scientific Reports*, *12*(1), 4182. https://doi.org/10.1038/s41598-022-08007-4

Tan, G. Y. A., Chen, C. L., Ge, L., Li, L., Wang, L., Zhao, L., Mo, Y., Tan, S. N., & Wang, J. Y. (2014). Enhanced gas chromatography-mass spectrometry method for bacterial polyhydroxyalkanoates analysis. *Journal of Bioscience and Bioengineering*, *117*(3), 379–382. https://doi.org/10.1016/j.jbiosc.2013.08.020

Tanmoy, D. S., & LeFevre, G. H. (2024). Development of composite alginate bead media with encapsulated sorptive materials and microorganisms to bioaugment green stormwater infrastructure. *Environmental Science: Water Research & Technology*, *10*(8), 1890–1907. https://doi.org/10.1039/D4EW00289J

Tec-Campos, D., Zuñiga, C., Passi, A., Del Toro, J., Tibocha-Bonilla, J. D., Zepeda, A., Betenbaugh, M. J., & Zengler, K. (2020). Modeling of nitrogen fixation and polymer production in the heterotrophic diazotroph Azotobacter vinelandii DJ. *Metabolic Engineering Communications*, *11*, e00132. https://doi.org/10.1016/j.mec.2020.e00132

Thorneley, R. N., & Ashby, G. A. (1989). Oxidation of nitrogenase iron protein by dioxygen without inactivation could contribute to high respiration rates of Azotobacter species and facilitate nitrogen fixation in other aerobic environments. *The Biochemical Journal*, *261*(1), 181–187. https://doi.org/10.1042/bj2610181

Threatt, S. D., & Rees, D. C. (2023). Biological nitrogen fixation in theory, practice, and reality: a perspective on the molybdenum nitrogenase system. *FEBS Letters*, *597*(1), 45–58. https://doi.org/10.1002/1873-3468.14534

Tian, J., Ge, F., Zhang, D., Deng, S., & Liu, X. (2021). Roles of Phosphate Solubilizing Microorganisms from Managing Soil Phosphorus Deficiency to Mediating Biogeochemical P Cycle. *Biology*, *10*(2), 158. https://doi.org/10.3390/biology10020158

Tienda, S., Gutiérrez-Barranquero, J. A., Padilla-Roji, I., Arrebola, E., de Vicente, A., & Cazorla, F. M. (2024). Polyhydroxyalkanoate production by the plant beneficial rhizobacterium Pseudomonas chlororaphis PCL1606 influences survival and rhizospheric performance. *Microbiological Research*, *278*, 127527. https://doi.org/10.1016/j.micres.2023.127527

Trujillo-Roldán, M. A., Peña, C., Ramirez, O. T., & Galindo, E. (2001). Effect of oscillating dissolved oxygen tension on the production of alginate by Azotobacter vinelandii. *Biotechnology Progress*, *17*(6), 1042–1048. https://doi.org/10.1021/bp010106d

Tsegaye, Z., Alemu, T., Desta, F. A., & Assefa, F. (2022). Plant growth-promoting rhizobacterial inoculation to improve growth, yield, and grain nutrient uptake of teff varieties. *Frontiers in Microbiology*, *13*. https://doi.org/10.3389/fmicb.2022.896770

Upadhyay, S. K., Singh, J. S., & Singh, D. P. (2011). Exopolysaccharide-Producing Plant Growth-Promoting Rhizobacteria Under Salinity Condition. *Pedosphere*, *21*(2), 214–222. https://doi.org/10.1016/S1002-0160(11)60120-3

Urbanova, M., Pavelkova, M., Czernek, J., Kubova, K., Vyslouzil, J., Pechova, A., Molinkova, D., Vyslouzil, J., Vetchy, D., & Brus, J. (2019). Interaction Pathways and Structure–

Chemical Transformations of Alginate Gels in Physiological Environments. *Biomacromolecules*, *20*(11), 4158–4170. https://doi.org/10.1021/acs.biomac.9b01052

Urtuvia, V., Maturana, N., Acevedo, F., Peña, C., & Díaz-Barrera, A. (2017). Bacterial alginate production: an overview of its biosynthesis and potential industrial production. *World Journal of Microbiology and Biotechnology*, *33*, 1–10. https://doi.org/10.1007/s11274-017-2363-x

Valetti, L., Iriarte, L., & Fabra, A. (2016). Effect of previous cropping of rapeseed (Brassica napus L.) on soybean (Glycine max) root mycorrhization, nodulation, and plant growth. *European Journal of Soil Biology*, *76*, 103–106. https://doi.org/10.1016/j.ejsobi.2016.08.005

van Gijtenbeek, L. A., & Kok, J. (2017). Illuminating Messengers: An Update and Outlook on RNA Visualization in Bacteria. *Frontiers in Microbiology*, *8*. https://doi.org/10.3389/fmicb.2017.01161

Vassilev, N., & de Oliveira Mendes, G. (2018). Solid-State Fermentation and Plant-Beneficial Microorganisms. In *Current Developments in Biotechnology and Bioengineering* (pp. 435–450). Elsevier. https://doi.org/10.1016/B978-0-444-63990-5.00019-0

Vassilev, N., Vassileva, M., Martos, V., Garcia del Moral, L. F., Kowalska, J., Tylkowski, B., & Malusá, E. (2020). Formulation of Microbial Inoculants by Encapsulation in Natural Polysaccharides: Focus on Beneficial Properties of Carrier Additives and Derivatives. *Frontiers in Plant Science*, *11*. https://doi.org/10.3389/fpls.2020.00270

Vejan, P., Khadiran, T., Abdullah, R., Ismail, S., & Dadrasnia, A. (2019). Encapsulation of plant growth promoting Rhizobacteria—prospects and potential in agricultural sector: a review. In *Journal of Plant Nutrition* (Vol. 42, Issue 19, pp. 2600–2623). Taylor and Francis Inc. https://doi.org/10.1080/01904167.2019.1659330

Vergel-Castro, C., & Boom-Cárcamo, E. (2025). Challenges and opportunities in the use of microbial inoculants in hydroponic crops: A literature review. *The Microbe*, *9*, 100556. https://doi.org/10.1016/j.microb.2025.100556

Vessey, J. K. (2003). Plant growth promoting rhizobacteria as biofertilizers. *Plant and Soil*, *255*(2), 571–586. https://doi.org/10.1023/A:1026037216893

Wang, C., Pan, G., Lu, X., & Qi, W. (2023). Phosphorus solubilizing microorganisms: potential promoters of agricultural and environmental engineering. *Frontiers in Bioengineering and Biotechnology*, *11*. https://doi.org/10.3389/fbioe.2023.1181078

Wang, J., Salem, D. R., & Sani, R. K. (2019). Extremophilic exopolysaccharides: A review and new perspectives on engineering strategies and applications. *Carbohydrate Polymers*, *205*, 8–26. https://doi.org/10.1016/j.carbpol.2018.10.011

Wang, S., Wei, Y., Wang, Y., & Cheng, Y. (2023). Cyclodextrin regulated natural polysaccharide hydrogels for biomedical applications-a review. *Carbohydrate Polymers*, *313*, 120760. https://doi.org/10.1016/j.carbpol.2023.120760

Wang, Y., Shen, Z., Wang, H., Song, Z., Yu, D., Li, G., Liu, X., & Liu, W. (2024). Progress in Research on Metal Ion Crosslinking Alginate-Based Gels. *Gels*, *11*(1), 16. https://doi.org/10.3390/gels11010016

Wang, Z., Zhou, X., Sheng, L., Zhang, D., Zheng, X., Pan, Y., Yu, X., Liang, X., Wang, Q., Wang, B., & Li, N. (2023). Effect of ultrasonic degradation on the structural feature, physicochemical property and bioactivity of plant and microbial polysaccharides: A review. *International Journal of Biological Macromolecules*, *236*, 123924. https://doi.org/10.1016/j.ijbiomac.2023.123924

Wei, L., Li, Y., Noguera, D. R., Zhao, N., Song, Y., Ding, J., Zhao, Q., & Cui, F. (2017). Adsorption of Cu2+ and Zn2+ by extracellular polymeric substances (EPS) in different sludges: Effect of EPS fractional polarity on binding mechanism. *Journal of Hazardous Materials*, *321*, 473–483. https://doi.org/10.1016/j.jhazmat.2016.05.016

Wu, L., Jiang, Y., Zhao, F., He, X., Liu, H., & Yu, K. (2020). Increased organic fertilizer application and reduced chemical fertilizer application affect the soil properties and bacterial communities of grape rhizosphere soil. *Scientific Reports*, *10*(1), 9568. https://doi.org/10.1038/s41598-020-66648-9

Yang, C. H., Wang, M. X., Haider, H., Yang, J. H., Sun, J. Y., Chen, Y. M., Zhou, J., & Suo, Z. (2013). Strengthening alginate/polyacrylamide hydrogels using various multivalent cations. *ACS Applied Materials and Interfaces*, *5*(21), 10418–10422. https://doi.org/10.1021/am403966x

Yousefi, S., Kartoolinejad, D., Bahmani, M., & Naghdi, R. (2017). Effect of Azospirillum lipoferum and Azotobacter chroococcum on germination and early growth of hopbush shrub (Dodonaea viscosa L.) under salinity stress. *Journal of Sustainable Forestry*, *36*(2), 107–120. https://doi.org/10.1080/10549811.2016.1256220

Yu, R., Liu, Z., Yu, Z., Wu, X., Shen, L., Liu, Y., Li, J., Qin, W., Qiu, G., & Zeng, W. (2019). Relationship among the secretion of extracellular polymeric substances, heat resistance, and bioleaching ability of Metallosphaera sedula. *International Journal of Minerals, Metallurgy and Materials*, *26*(12), 1504–1511. https://doi.org/10.1007/s12613-019-1851-4

Yuan, Y., Yin, M., Chen, L., Liu, F., Chen, M., & Zhong, F. (2022). Effect of calcium ions on the freeze-drying survival of probiotic encapsulated in sodium alginate. *Food Hydrocolloids*, *130*, 107668. https://doi.org/10.1016/j.foodhyd.2022.107668

Zafar-ul-Hye, M., Ahmad, M., & Shahzad, S. M. (2013). Synergistic effect of rhizobia and plant growth promoting rhizobacteria on the growth and nodulation of lentil seedlings under axenic conditions. *Soil and Environment*, *32*(1), 79–86.

ACC	1-Aminocyclopropane-1-carboxylate
ADP	Adenosine diphosphate
ATP	Adenosine triphosphate
ATPase	Adenosine triphosphatase
CAGR	Compound Annual Growth Rate
CAS	Chrome azurol S (siderophore assay)
cdw	Cell dry weight
CFU	Colony forming unit
CoA	Coenzyme A
DNR	Nitrogenreductase
DNA	Deoxyribonucleic acid
DNS	3,5-Dinitrosalicylic acid
DOT	Dissolved oxygen tension
EPS	Extracellular polymeric substances
EPs	Exopolysaccharides
ETC	Electron transport chain
FAD	Flavin adenine dinucleotide
$FADH_2$	Reduced flavin adenine dinucleotide
FDA	Flourescein diacetate
FTIR	Fourier-transform infrared spectroscopy
G	Guluronic acid
G'	Storage modulus
G"	Loss modulus
G*	Complex modulus
GC	Gas chromatography
GC-FID	Gas chromatography with flame ionization detector
GDP	Guanosine diphosphate
GDL	Glucono-δ-lactone
GRAS	Generally Recognized as Safe
HPLC	High-performance liquid chromatography
IAA	Indole-3-acetic acid
ISR	Induced systemic resistance
LOS	Limiting oscillation strain
LVR	Linear viscoelastic region
lcl-PHA	Long-chain-length polyhydroxyalkanoate
mcl-PHA	Medium-chain-length polyhydroxyalkanoate

M	Mannuronic acid
M/G ratio	Mannuronic to guluronic acid ratio
MOPS	3-(N-morpholino)propanesulfonic acid
mcl-PHA	Medium-chain-length polyhydroxyalkanoate
NAD^+	Nicotinamide adenine dinucleotide
NADH	Nicotinamide adenine dinucleotide
$NADP^+$	Nicotinamide adenine dinucleotide phosphate
NADPH	Nicotinamide adenine dinucleotide phosphate
OD	Optical density
PHB	Polyhydroxybutyrate
PHB^{-4}	mutant deficient in PHB metabolism
PGP	Plant growth-promoting
PGPR	Plant growth-promoting rhizobacteria
PI	Propidium iodide
PSM	Phosphate-solubilizing microorganisms
RNA	Ribonucleic acid
ROS	Reactive oxygen species
scl-PHA	Short-chain-length polyhydroxyalkanoate
SEM	Scanning electron microscopy
SRFs	Slow release fertilizers
TCA	Tricarboxylic acid (cycle)
TEM	Transmission electron microscopy
WC	Water content
WHC	Water-holding capacity

8 CURRICULUM VITAE

Name and Surname: Diana Černayová

Scopus ID: 59740532700

E-mail: xccernayova@vutbr.cz

Education

2020 – present; Doctoral Studies, Biophysical Chemistry, Brno University of Technology (BUT), Brno, Czech Republic

2018 – 2020; Master's Studies, Chemistry for Medical Applications, BUT, Brno, Czech Republic

2015 – 2018; Bachelor's Studied, Chemistry for Medical Applications, BUT, Brno, Czech Republic

Courses

Pedagogical Qualification for Teaching at Secondary Vocational Schools (Pedagogical Minimum), 2023

Internships

June–December 2023; Internship at Microbial Ecology with the supervisions of prof. Johannes Rous; Lund University, Lund, Sweden

February – June 2019; Studies at Faculty of Biotechnology, Ljubljana University, Ljubljana, Slovenia

Work experience

2025 – present; Project Manager, TRL Drones, Brno Czech Republic

2020 – 2025; Laboratory Technician for biotechnology; The Material Research Centre, Faculty of Chemistry, BUT, Czech Republic

2017–2019; Quality Controller; Brenntag Slovakia, Slovakia

9 LIST OF PUBLICATIONS

Articles in Journals with Impact factor

ČERNAYOVÁ, D.; SÚKENÍK, M.; OBRUČA, S.; SMILEK, J.; KALINA, M.; MRÁZOVÁ, K.; HRUBANOVÁ, K.; KRZYŽÁNEK, V.; SEDLÁČEK, P. Self-entrapment of<i> Azotobacterii vinelandii cultures by gelation of their exopolysaccharides: A way towards next-generation bioinoculants. Carbohydrate Polymers, 2025, vol. 360, no. C, p. 1-11. ISSN: 0144-8617.

HRABALOVÁ, V.; ČERNAYOVÁ, D.; NÁBĚLEK, J.; MATĚJKA, F.; POŘÍZKA, J.; DIVIŠ, P.; OBRUČA, S. Biotransformation of ferulic acid into valuable products employing halophilic bacterium Halomonas neptunia. Biocatalysis and Agricultural Biotechnology, 2025, vol. 66, no. 6, p. 1-10. ISSN: 1878-8181.

MRÁZOVÁ, K.; ČERNAYOVÁ, D.; HAVLÍČKOVÁ, A.; HRUBANOVÁ, K.; OBRUČA, S.; SEDLÁČEK, P.; KRZYŽÁNEK, V. Enhanced electron microscopy imaging for a detailed structural study of alginate hydrogel containing the encapsulated cells. Carbohydrate Polymers, 2025, vol. 368, no. november, ISSN: 0144-8617.

Conference Contributions

SLANINOVÁ, E.; SEDLÁČEK, P.; ČERNAYOVÁ, D.; ŠEDRLOVÁ, Z.; OBRUČA, S.; KRZYŽÁNEK, V.; NEBESÁŘOVÁ, J. Production and Characterization of Polyhydroxybutyrate in Cyanobacteria. Tomáškovy dny 2020XXIX. konference mladých mikrobiologů. 1. Brno: Masarykova Univerzita, 2020. p. 51-51. ISBN: 978-80-210-9611-0.

ČERNAYOVÁ, D.; SLANINOVÁ, E.; SEDLÁČEK, P.; OBRUČA, S. Production of polyhydroxyalkanoates and alginate by plant growth promoting rhizobacteria Azotobacter vinelandii. Tomáškovy dny 2021 35. konference mladých mikrobiologů. 1. Vydala Masarykova univerzita, Žerotínovo nám. 617/9, 601 77 Brno1. elektronické vydání, 2021: Tomáškovy dny 2021XXX. konference mladých mikrobiologů, 2021. ISBN: 978-80-210-9882-4.

SLANINOVÁ, E.; ČERNAYOVÁ, D.; ŠEDRLOVÁ, Z.; MRÁZOVÁ, K.; SEDLÁČEK, P.; NEBESÁŘOVÁ, J.; OBRUČA, S. Instrumental characterization of Cyanobacteria as Polyhydroxybutyrate Producer. World Academy of Science, Engineering and Technology. 2021. p. 75-75. ISSN: 1307-6892.

ČERNAYOVÁ, D.; SÚKENÍK, M.; SEDLÁČEK, P.; OBRUČA, S. Self encapsulation of plant growth-promoting bacteria Azotobacter vinelandii for their use as next-generation bioinoculants. CHEMIE JE ŽIVOT 2021. 1. Brno: Vysoké učení technické v Brně, Fakulta chemická, 2021. p. 32-33. ISBN: 978-80-214-6002-7.

SLANINOVÁ, E.; ČERNAYOVÁ, D.; ŠEDRLOVÁ, Z.; MRÁZOVÁ, K.; SEDLÁČEK, P.; NEBESÁŘOVÁ, J.; OBRUČA, S. Characterization of cyanobacteria as polyhydroxybutyrate producer. 2021. p. 100-100.

SLANINOVÁ, E.; RUBANOVÁ, B.; ČERNAYOVÁ, D.; NOVÁČKOVÁ, I.; HAVLÍKOVÁ, M.; MRÁZOVÁ, K.; SEDLÁČEK, P.; OBRUČA, S. Study of aeration and light/dark conditions on production of polyhydroxyalkanoates in bacteria Rhodospirillium rubrum. 2022. p. 1 (1 s.).

ČERNAYOVÁ, D.; SÚKENÍK, M.; SLANINOVÁ, E.; SEDLÁČEK, P.; OBRUČA, S. Generation of New Bio-Inoculants Using Self-encapsulation of Plant-growth Promoting Bacteria Azotobacter vinelandii. The Biomania Student Scientific Meeting. 1st. Brno, Czech Republic; 1st edition 2022: Masaryk University Press, 2022. p. 112-112. ISBN: 978-80-280-0040-0.

ČERNAYOVÁ, D.; SÚKENÍK, M.; SLANINOVÁ, E.; SEDLÁČEK, P.; OBRUČA, S. PRODUKCIA BIOPOLYMÉROV BAKTÉRIOU AZOTOBACTER VINELANDII A JEJ NÁSLEDNÁ ENKAPSULÁCIA. 2022.

ČERNAYOVÁ, D.; SEDLÁČEK, P.; SLANINOVÁ, E.; TRUDIČOVÁ, M.; GAŠPAROVÁ, D.; OBRUČA, S. Preparation of New Generation of Bio-inoculants and their viability for applicational potential in agriculture. Sion, Switzerland: HES-SO Valais-Wallis, 2022.

ČERNAYOVÁ, D.; SEDLÁČEK, P.; SLANINOVÁ, E.; TRUDIČOVÁ, M.; OBRUČA, S. Next Generation of Bio-inoculants, their Preparation and Viability for the Agricultural Applications. 2022.

ČERNAYOVÁ, D.; SÚKENÍK, M.; SLANINOVÁ, E.; OBRUČA, S.; SEDLÁČEK, P. The role of Azotobacter vinelandii as a bioinoculant and its capability if biopolymer production and biological activities. 2023.

ČERNAYOVÁ, D.; SEDLÁČEK, P.; SÚKENÍK, M.; SLANINOVÁ, E.; TRUDIČOVÁ, M.; OBRUČA, S. Self-entrapment of plant growth-promoting bacteria in gel matrix and their use as new generation bioinoculants. Milovy, Devět skal: 2023. p. 163-176.

ČERNAYOVÁ, D.; SÚKENÍK, M.; KALINA, M.; SLANINOVÁ, E.; SEDLÁČEK, P.; OBRUČA, S. The Use of Biopolymers for Development of New Type of Bacterial Bioinoculants. European Symposium on Biopolymers 2023, Brno, Czech Republic: 2023.

SÚKENÍK, M.;ČERNAYOVÁ, D.;SEDLÁČEK, P. Self-entrapment of Plant Growth Promoting Rhizobacteria by gelation of their exopolysaccharides. Chemie je život 2023. 1. Brno: Vysoké učení technické v Brně, Fakulta chemická, 2023. p. 66-67. ISBN: 978-80-214-6204-5.

ČERNAYOVÁ, D.; ROUSK, J.; SEDLÁČEK, P.; OBRUČA, S. The impact of hydrogel bioinoculants in plant resistance to drought conditions. International Conference on Chemical Technology, Mikulov: 2024.

MRÁZOVÁ, K.; HAVLÍČKOVÁ, A.; ČERNAYOVÁ, D.; HRUBANOVÁ, K.; SEDLÁČEK, P.; KRZYŽÁNEK, V. Changes in the hydrogel structure depending on the crosslinking agent seen by electron microscopy. Microscopy 2024. Book of abstracts. 1st. Brno: Czechoslovak Microscopy Society, 2024. p. 121-121. ISBN: 978-80-909216-0-3.

SÚKENÍK, M.;ČERNAYOVÁ, D.;SEDLÁČEK, P.;KALINA, M.;OBRUČA, S. INOVATIVNÍ BAKTERIÁLNÍ BIOINOKULANTY NA BÁZI BIOPOLYMERŮ. ROSTEME S CHEMIÍ II. ročník. 1. Pardubice: Univerzita Pardubice, 2024. s. 41-41. ISBN: 978-80-7560-510-8.

MRÁZOVÁ, K.; HAVLÍČKOVÁ, A.; ČERNAYOVÁ, D.; HRUBANOVÁ, K.; SEDLÁČEK, P.; KRZYŽÁNEK, V. Cryo-EM as a tool for observing alginate-based hydrogels. The 17th European Microscopy Congress. 1st. Copenhagen: EMC, 2024.

ČERNAYOVÁ, D.; ROUSK, J.; SEDLÁČEK, P.; OBRUČA, S. Hydrogel Bioinoculants: Enhancing Plant resistance to Drought Stress. Book of Abstracts "9th Meeting Chemistry & Life for Sustainable Future". 9. Brno: Brno University of Technology, 2024.

SÚKENÍK, M.; ČERNAYOVÁ, D.; KALINA, M.; HLAVÁČKOVÁ, B.; SEDLÁČEK, P.; OBRUČA, S. INNOVATIVE BIOFERTILIZER FORMULATION UTILIZING SELF-GELATING AZOTOBACTER VINELANDII. XIVth INTERDISCIPLINARY MEETING

OF YOUNG LIFE SCIENTISTS. Czech Chemical Society Symposium Series. Czech Chemical Society Symposium Series. Praha: Česká společnost chemická, 2025. p. 62-62. ISBN: 2336-7210. ISSN: 2336-7210.

MRÁZOVÁ, K.; HAVLÍČKOVÁ, A.; ČERNAYOVÁ, D.; SEDLÁČEK, P.; KRZYŽÁNEK, V. Approach to Imaging Bacterial Cells Encapsulated in Alginate Hydrogel Using LV-STEM. Microscopy 2025. Book of abstracts. 1st. Brno: Czechoslovak Microscopy Society, 2025. p. 35-36. ISBN: 978-80-909216-1-0.

MRÁZOVÁ, K.; HAVLÍČKOVÁ, A.; ČERNAYOVÁ, D.; SEDLÁČEK, P.; KRZYŽÁNEK, V. Structural Stabilization of Alginate for Imaging Hydrogel-encapsulated Bacterial Cells Using LV-STEM. 17th Multinational Congress on Microscopy: book of abstract. 1st. Ljubljana: Slovene Society for Microscopy, 2025. p. 277-278. ISBN: 978-961-94264-4-9.

MRÁZOVÁ, K.; HAVLÍČKOVÁ, A.; ČERNAYOVÁ, D.; SEDLÁČEK, P.; KRZYŽÁNEK, V. Imaging of Alginate-encapsulated Azotobacter vinelandii Cells: Insights into Hydrogel–Cell Interactions Using LV-STEM. Imaging Principles of Life 2025 ABSTRACT BOOK. Rozdrojovice: Czech-Bioimaging, 2025. p. 43-43.

10 SUPPLEMENTARY

Table 9 Bacterial growth of A. vinelandii DSM 720 on various carbon substrates in concentration 20 g/L throughout 93 hours. The bacteria grew in 96-hole plate at 30°C while constant shaking 250 rpm and measured on selected times by ELISA Multi mode Reader at 630 nm.

			DSM 720							
Hours	**Fructose**	**Glucose**	**Sucrose**	**Xylose**	**Arabinose**	**Celobiose**	**Maltose**	**Laktose**	**Glycerol**	**Starch**
0	**0.088**	**0.087**	**0.086**	0.095	0.088	0.086	**0.085**	0.092	0.086	0.097
10	**0.161**	**0.180**	**0.333**	0.341	0.345	0.326	**0.290**	0.346	0.165	0.208
25	**0.250**	**0.227**	**0.198**	0.134	0.147	0.153	**0.177**	0.148	0.159	0.168
45	**0.452**	**0.474**	**0.397**	0.182	0.161	0.163	**0.324**	0.168	0.209	0.187
69	**0.500**	**0.552**	**0.483**	0.179	0.201	0.191	**0.392**	0.197	0.240	0.319
74	**0.502**	**0.593**	**0.510**	0.215	0.218	0.284	**0.491**	0.338	0.238	0.357
93	**0.614**	**0.684**	**0.636**	0.211	0.314	0.389	**0.549**	0.326	0.370	0.213

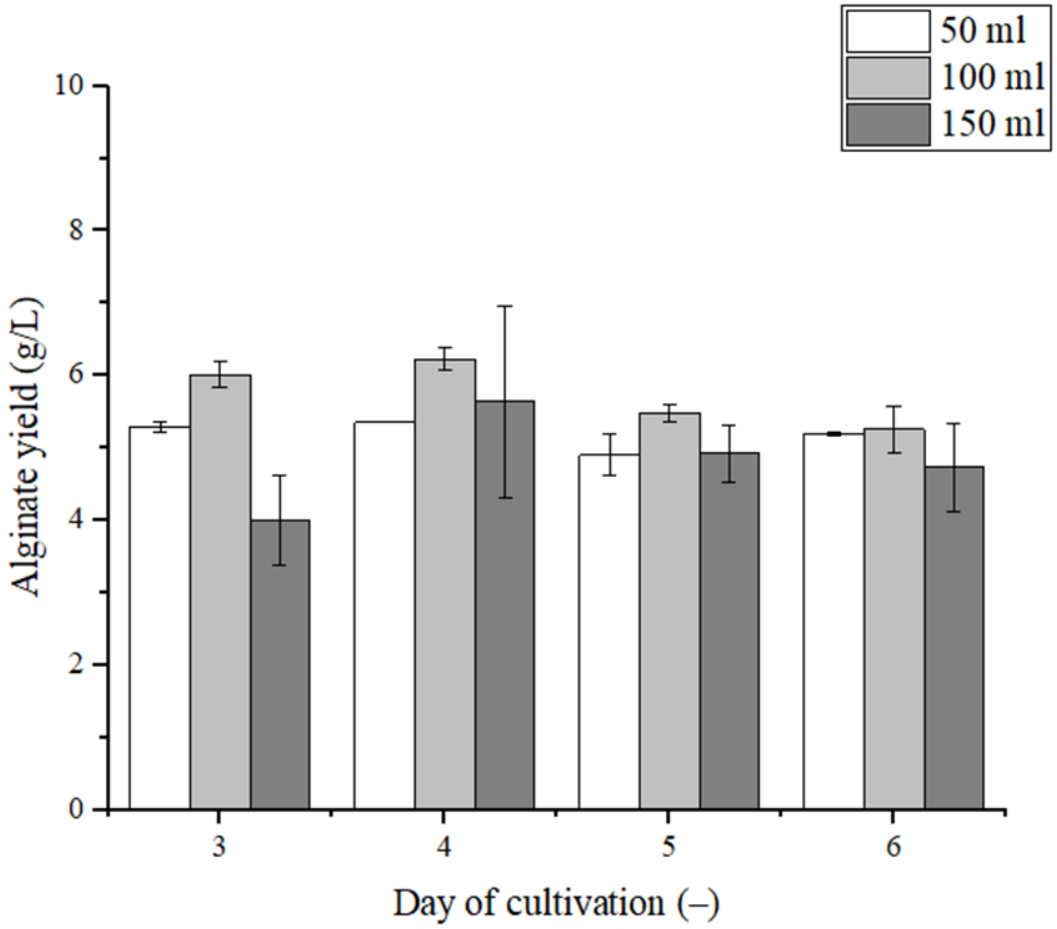

Figure 39 Determination of alginate yield throughout 3 – 6 days of cultivation for strain CCM 289. Different media volumes were tested with the same agitation speed (210 rpm).

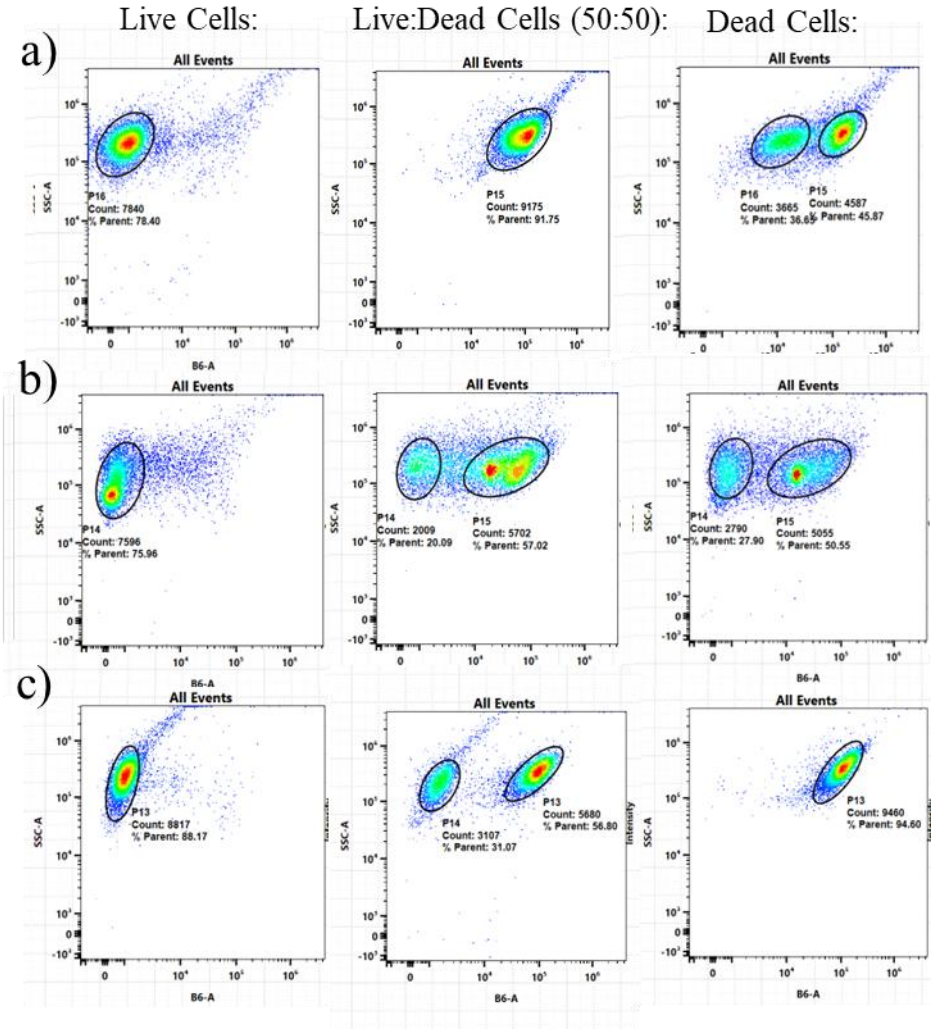

Figure 40 Flow cytometry determination of viability different strain of bacteria Azotobacter vinelandii dyed by Propidium Iodine (*a- DSM 87, b- CCM 289, c-720*) *for three teratments: live cells, died cells* (*exposed 30 mins in boiling water*) *and mix of live and dead cells in ratio 1:1.*

Figure 41 Pot experiment in laboratory conditions to test A. vinelandii cultures as bioinoculants using lettuce as a model plant: three treatments were tested: bacterial gelled cultures, bacterial liquid inoculants and control without any addition of PGPR

10.1 SELF-ENTRAPMENT OF *AZOTOBACTER VINELANDII* CULTURES BY GELATION OF THEIR EXOPOLYSACCHARIDES: A WAY TOWARDS NEXT-GENERATION BIOINOCULANTS

Carbohydrate Polymers 360 (2025) 123607

Contents lists available at ScienceDirect

Carbohydrate Polymers

journal homepage: www.elsevier.com/locate/carbpol

Self–entrapment of *Azotobacter vinelandii* cultures by gelation of their exopolysaccharides: A way towards next–generation bioinoculants

Diana Černayová [a], Martin Súkeník [a], Stanislav Obruča [a], Jiří Smilek [a], Michal Kalina [a], Kateřina Mrázová [a,b], Kamila Hrubanová [b], Vladislav Krzyžánek [b], Petr Sedláček [a,*]

[a] Faculty of Chemistry, Brno University of Technology, Purkyňova 118, 612 00 Brno, Czech Republic
[b] Institute of Scientific Instruments, The Czech Academy of Sciences, Královopolská 147, 61264 Brno, Czech Republic

ARTICLE INFO

Keywords:
Azotobacter vinelandii
Alginate
Polyhydroxyalkanoates
Hydrogels
Bioinoculants

ABSTRACT

Encapsulation of Plant Growth-Promoting Rhizobacteria (PGPR) in hydrogel carriers is a cutting-edge approach in developing agricultural bioinoculants, aiming to improve soil fertility and crop yield. Hydrogels provide protection against environmental stress, though traditional methods using external gel-forming agents limit economic viability. This study presents a novel approach, demonstrating the entrapment of *Azotobacter vinelandii*, a promising PGPR, within a gel matrix formed by Ca^{2+}-induced crosslinking of its own exopolysaccharide, alginate. Among the five strains evaluated, *A. vinelandii* DSM 87, DSM 720, and DSM 13529 showed the highest alginate production, peaking at 4.9 ± 0.6 g/L, 3.5 ± 0.5 g/L, 3.8 ± 0.8 g/L, and enabling stable gel formation by the fourth day of cultivation. These strains also exhibited molecular weights and chemical structures of alginate suitable for effective gelation upon Ca^{2+} addition. Additionally, these strains demonstrated significant plant growth-promoting activities, including indole acetic acid production (up to 10.5 μg/mL), siderophore release, and phosphate solubilization, further validating their potential for sustainable bioinoculant production. Finally, the viability of the *A.vinelandii* cells released from the gels was experimentally verified. Our findings support a feasible, cost-effective method for bioinoculant production that leverages *A. vinelandii*'s intrinsic capabilities, offering a sustainable alternative to conventional agricultural practices.

1. Introduction

Over the centuries, the agricultural industry evolved into an extensive form to meet the demands of billions of people. Hand in hand with high demands, many great challenges have also had to be surpassed to get maximal yields from the arable lands. In general, the use of chemical fertilizers is adopted as a general strategy to improve yields of plants and crops (Duncan et al., 2018). Nevertheless, intensive employment of chemical fertilizers in agriculture brings numerous environmental risks and issues (Ferreira et al., 2019). Therefore, the application of biological fertilizers, also termed bioinoculants, has recently become a subject of global interest (Santos et al., 2019). Such biological agents are based on plant growth-promoting bacteria (PGPR) and they positively stimulate the growth of plants by providing multiple beneficial effects (Song et al., 2015).

However, the main obstacle in bioinoculants is the loss of the viability of the bacterial culture during storage and especially after application when PGPR often struggle to survive in the competitive and unpredictable soil environment. Encapsulating PGPR in alginate gels was reported as an efficient strategy to solve these viability issues (Bashan et al., 2014; Santos et al., 2019). Hydrogels are water-rich, three-dimensional polymer networks widely used as carriers for active compounds or microorganisms in biomedical, biotechnological, and agricultural applications (Qin et al., 2024). Alginate, a carbohydrate polymer primarily derived from brown algae, is among the most common bacterial exopolysaccharides (Salimi & Farrokh, 2023). It readily forms gels upon the addition of Ca^{2+} and other metal ions, creating a network structure described by the so-called egg-box model (Donati & Christensen, 2023; a schematic representation of alginate structure and the egg-box gel model is provided in Fig. S1 in Supplementary Information).

In the gel bioinoculants, alginate provides a protective matrix that ensures the viability and stability of PGPR, facilitating their controlled release and prolonged shelf life (Martínez-Cano et al., 2022;

* Corresponding author.
E-mail address: sedlacek-p@fch.vut.cz (P. Sedláček).

https://doi.org/10.1016/j.carbpol.2025.123607
Received 20 January 2025; Received in revised form 17 March 2025; Accepted 12 April 2025
Available online 13 April 2025

Shcherbakova et al., 2018). This encapsulation method protects the bacteria from environmental stresses, such as drought, UV radiation and soil pathogens, thereby maintaining their efficacy in promoting plants growth and health (Souza-Alonso et al., 2021; Strobel et al., 2018; Vejan et al., 2019). For instance, encapsulated *Enterobacter* sp. SA-10 in alginate and biochar significantly improved chili plant growth by enhancing leaf area, diameter, and dry weight compared to non-encapsulated treatments (Siti Anis Syaziana et al., 2024). Similarly, *Ochrobactrum ciceri* encapsulated in alginate beads demonstrated effective biocontrol against chili collar rot, reducing disease incidence by 70 % and improving plant growth parameters (Riaz et al., 2023). Alginate encapsulation also supports the biocontrol of soil-borne pathogens, as demonstrated by the reduction of *Verticillium* wilt severity in tomatoes, where alginate-encapsulated PGPR stimulated plant defense mechanisms (Oulad Ziane et al., 2024).

Furthermore, alginate encapsulation facilitates the use of PGPR as biofertilizers and biopesticides, offering an eco-friendly alternative to chemical fertilizers and pesticides, thus contributing to sustainable agricultural practices (Balla et al., 2022; Pereira et al., 2023). The slow and controlled release of bacteria from alginate beads enhances rhizospheric colonization and nutrient bioavailability, which is crucial for improving soil fertility and plant nutrition (Dellagnezze & Sierra-Garcia, 2023; Shcherbakova et al., 2018). The use of alginate also allows for the incorporation of other beneficial substances, such as humic acid, which can further enhance the growth-promoting effects of the encapsulated bacteria (Sivakumar et al., 2014). Additionally, alginate encapsulation can be industrially scaled, as demonstrated by the successful microencapsulation of *Methylobacterium radiotolerans*, a plant-beneficial bacterium, using a spray-drying technique that maintains high viability of the bacteria (Strobel et al., 2018). Overall, encapsulation of PGPR in alginate gels represents a promising strategy for enhancing crop yield, managing plant diseases, and promoting sustainable agriculture by leveraging beneficial microorganisms in a controlled and efficient manner.

Despite these promising advantages, the use of alginate for hydrogel-based bioinoculant formation also poses some challenges. First, technoeconomic analysis proved that the costs of raw sodium alginate represent about 19 % of annual operating costs in microencapsulation of bioactives in alginate gels (Strobel et al., 2020). Furthermore, the conventional process requires homogeneous dispersion of the cell culture in a viscous solution of the gel-forming polymer (or vice versa), which further increases technological and economic demands of bioinoculant production (Vejan et al., 2019). This could be the primary explanation for why alginate-based bioinoculants, despite being frequently seen as the next frontier in biofertilizers (Bashan et al., 2014), continue to linger at the experimental stage of technology.

To address these limitations, we propose a novel bioinoculant production method based on the unique capabilities of *Azotobacter vinelandii*, a non-pathogenic, gram-negative PGPR bacterium (Urtuvia et al., 2017) that synthesizes two important biopolymers: intracellular poly (3–hydroxybutyrate) (PHB) and extracellular alginate (Noar & Bruno-Bárcena, 2018). The intracellular accumulation of PHB increases bacterial robustness against environmental stresses (Obruca et al., 2020), which is crucial for successful bioinoculant application. More importantly for our concept, the bacterial synthesis of alginate enables its direct utilization as a gel-forming agent, allowing for the entrapment (hereafter termed self-entrapment or self-encapsulation) of bacterial cells within their own cultivation media, without the need for costly external substances or complex technological procedures.

We hypothesize that self-encapsulation of *Azotobacter vinelandii* within its own exopolysaccharide-derived gel provides a cost-effective and technologically simplified alternative to conventional bioinoculant encapsulation methods. Therefore, this study specifically evaluates the feasibility of this innovative approach by assessing selected *A. vinelandii* strains for their plant growth-promoting activities and capacities for PHB and alginate production. Subsequently, we investigate the effectiveness of their encapsulation in self-produced alginate matrices, along with detailed characterization of the resulting gels in terms of mechanical properties, morphology, and viability of the encapsulated cultures.

2. Material and methods

2.1. Microbial cultures and cultivation

Freeze–dried bacterial cultures of *Azotobacter vinelandii* (DSM 85; DSM 87; DSM 576; DSM 720; DSM 13529) were obtained from the German Collection of Microorganisms and Cell Cultures; Braunschweig, Germany. Freeze-dried culture of *Pantonea ananatis* CCM 2407 was obtained from the Czech Collection of Microorganisms; Brno, Czech Republic. The bacterial cultures were maintained as frozen stock cultures at −80 °C in the presence of glycerol (10 % *v/v*). Cultivations for the inoculum preparation were performed in 100 mL Erlenmeyer flasks containing 35 mL of modified Ashby's medium (glucose 20.0 g/L, yeast extract 6.0 g/L, Na_2HPO_4 2.0 g/L, $MgSO_4.7H_2O$ 0.3 g/L, $(NH_4)_2SO_4$ 0.6 g/L) for 24 h at 30 °C with constant shaking at 180 rpm. After 24 h, the inoculum was transferred (5 % *v/v*) into mineral medium of the same composition as the one described above, only with dispersed $CaCO_3$ 2.0 g/L added. The media were sterilized at 120 °C for 15 min.

Cultivations for alginate production and for gelation tests were performed in 250 mL Erlenmeyer flasks with 150 mL medium under permanent shaking at 220 rpm at 30 °C. All these cultivations were performed in duplicates. After the defined period, the cultivations were terminated, and the cells were either harvested by centrifugation (6000 rpm for 5 min) for further analysis or used directly in the liquid medium for gel preparation as described below.

Cultivation for indole acetic acid (IAA) production assay (described below) was performed in King B media containing glycerol 15 g/L, peptone 20 g/L, K_2HPO_4 1.15 g/L, and $MgSO_4.7H_2O$ 1.50 g/L. Stock bacterial cultures of *A.vinelandii* and *P. ananatis* of the volume of 0.75 mL were pipetted into 3 mL autoclaved tubes containing King B medium supplemented with 2.5 mM tryptophan. The cultivation was performed at 30 °C with constant shaking at 180 rpm for 3 days. King B medium (described above), without the addition of tryptophan, was also used for quantitative siderophore production assay, further explained in 2.4.2.

During cultivation, bacterial growth was monitored indirectly by measuring optical density at 630 nm using a Nanophotometer Implen P300. Samples were diluted with distilled water as necessary, and distilled water was used as a blank. Moreover, 10 mL of bacterial cultures were collected daily and centrifuged at 6000 rpm for 5 min. Supernatant containing alginate was separated from sediment and precipitated with ethanol for further analysis described in 2.2. The sediment containing the biomass was washed with 10 mL of distilled water and dried at 70 °C to constant weight.

2.2. Determination of biopolymers and structural analysis of alginate

The poly(3–hydroxybutyrate) (PHB) content in dry biomass was quantified by directly methanolyzing the dry biomass sample, converting the polymer into hydroxybutyric acid methyl ester without prior extraction. This process followed the method of Brandl et al. (1988). The methyl ester was then detected via gas chromatography on a Trace 1300 GC system (Thermo Scientific), equipped with a ZB–WAXplus column (30 m, 0.50 mm) and a flame-ionization detector (GC–FID). Commercial PHB (Sigma-Aldrich) was used as the standard, with benzoic acid as an internal standard. Each sample was analyzed in triplicate.

The alginate was precipitated from supernatant by using cold ethanol (96 %) (Clementi et al., 1999) and quantified gravimetrically. Generally, 3 mL of supernatant was mixed with 6 mL of cold ethanol (4 °C), and the sample was centrifuged at 4500 rpm for 15 mins at 4 °C. The supernatant was poured out and the precipitated alginate was washed with distilled water and a double volume of ethanol. Afterwards, the centrifugation

was repeated. The supernatant was poured out again and the final precipitated alginate was dried in a thermostat at 70 °C for 24–48 h and weighted. The analysis was performed in duplicates for each bacterial culture.

Dried precipitated alginate samples were analyzed using a Fourier transform infrared (FTIR) spectrometer iS50 (Thermo Scientific, Waltham, MA, USA). Measurements were performed at ambient temperature (in an air-conditioned room) with a built-in single-reflection diamond attenuated total reflectance (ATR) crystal. Each absorption spectrum was obtained as an average of 16 scans with a resolution of 4 cm^{-1} and a data spacing of 0.5 cm^{-1}. For each *A. vinelandii* strain, five independent spectra of isolated alginate were recorded. From each measured spectrum, absorbances at 780, 810, 1600, and 1720 cm^{-1} were used to calculate structural parameters (M/G ratio, acetylation ratio) following the method described by Bonartseva et al. (2017).

Molecular weights of precipitated alginate were analyzed using size exclusion chromatography coupled with multi-angle light scattering (Dawn Heleos II, Wyatt Technology, Santa Barbara, CA, USA) and differential refractometry (Optilab T-rEX, Wyatt Technology, Santa Barbara, CA, USA). 2.0 mg of the dried alginate was dissolved in 1.5 mL of 50 mmol/L sodium citrate solution and subsequently passed through syringe filters with nylon membrane (0.45 μm). A total of 100 μL of each sample was injected into the size exclusion chromatography system (Infinity 1260 system with PL aquagel-OH MIXED-H column, Agilent Technologies, Santa Clara, CA, USA). As a mobile phase, 50 mmol/L of sodium citrate (filtered through 0.1 μm membrane filters) at a flow rate of 0.6 mL/min was used. To determine the weight-average molecular weight (M_w), ASTRA software (version 7.3.2, Wyatt Technology, Santa Barbara, CA, USA) was used.

2.3. Self–entrapment of the microbial culture into the hydrogel matrix

For the basic tests of gelation ability, the as-cultivated bacterial cultures (3 mL) were added dropwise into a double volume (6 mL) of calcium chloride solution (2 % *w*/*w*) via slow pipetting to form macrogels. The process of gelation was done at room temperature without stirring the mixture to avoid disintegration and to preserve the gel's shape. The time of the gelation was set up for 30 min and followed by the filtration of prepared gels carefully through filter paper (category KA 1) or nylon layer to remove the redundant $CaCl_2$ solution.

Furthermore, preparation of the gel beads and particles of a uniform size under controlled conditions was tested as well. For the preparation of macroscopic gel beads, custom-made culture dropping device was assembled using the Razel E-99 syringe pump and a common laboratory syringe (a photograph of the apparatus is shown in Fig. S6, Supplementary information). For the preparation of gel microparticles, commercial encapsulator BUCHI B-395 was used. The bacterial culture was transferred at the flow rate of 30 mL/min through nozzle of the size 450 μm into calcium chloride solution (2 % *w*/*w*) being stirred at 55 rpm in a Petri dish. The encapsulation process frequency was optimized at 3000 Hz and the voltage at 1500 V.

2.4. Screening tests for plant growth-promoting properties

2.4.1. Production of indole acetic acid

The standard VIS spectroscopic analysis was employed (Gordon & Weber, 1951): 0.5 mL supernatant from the centrifuged (5400 ×*g* and 10 mins) bacterial culture (cultivated in King B media) was used and mixed with 0.5 mL Salkowski reagent ($FeCl_3.6H_2O$ 12 g/L, 96 %H_2SO_4 421 mL/L) (Ambrosini & Passaglia, 2017). The samples were incubated for 30 min in the dark, and their visible spectra (350–850 nm) were recorded using a Hitachi U 3900 spectrometer (Hitachi, Japan). Absorbance at 530 nm was used to determine the concentration of IAA. Pure IAA (Sigma-Aldrich) was used as a calibration standard, *Pantonea ananatis* CCM 2407 was used as a positive control.

2.4.2. Production of siderophores

The method for identifying isolates capable of producing siderophores is based on the use of Chromazurol S (CAS), a blue dye (Neilands, 1987). When bacteria produce siderophores, the binding of iron (III) changes the color of Chromazurol S from blue to light red, resulting in visible halo zones around bacterial colonies. Iron CAS agar plates were prepared by mixing CAS reagent with five-fold diluted sterile King B (described above). Agar plates were inoculated with bacterial cultures and positive control (*Pantonea ananatis*) and an uninoculated plate was taken as a negative control. After inoculation, plates were incubated at 30 °C for 3–5 days in the dark and observed for the formation of halo zone around the bacterial colonies (Ambrosini & Passaglia, 2017).

For the quantitative determination of siderophore activity in a liquid medium, a 3-day-old bacterial culture grown in King B medium was centrifuged at 5400 ×*g* for 10 min. The supernatant was then mixed with an equal volume of CAS reagent. After 20 min of incubation in the dark, absorbance was measured at 630 nm to determine the siderophore concentration in the sample. Siderophore activity, expressed in psu, was calculated as the relative decrease in absorbance compared to the correspondingly diluted CAS reagent, following the method described by Arora and Verma (2017).

2.4.3. Phosphate solubilization

The medium used for the phosphate solubilization assay (Pikovskaya medium) contained glucose (10 g/L), tricalcium phosphate (5 g/L), yeast extract (0.5 g/L), calcium chloride (0.1 g/L), magnesium sulphate heptahydrate (0.25 g/L), and agar 15 g/L. The medium was sterilized by autoclaving at 121 °C for 15 min. After inoculation with *A. vinelandii* cultures and positive control (*P. ananatis*), plates were incubated at 30 °C for 3–5 days and observed for the formation of clear halo zones around or beneath the colonies.

2.5. Characterization of the gel formulations

2.5.1. Mechanical properties

The gels prepared by self–entrapping of the bacterial cultures DSM 87, DSM 720, and DSM 13529 were further analyzed to investigate their rheological properties. Macro–gel samples were prepared by mixing 10 mL of the respective culture with 20 mL of crosslinking solution (2 % *w*/*w* $CaCl_2$) and leaving the system to solidify for 30 mins. The viscoelastic properties of the hydrogels were assessed using amplitude (strain) sweep oscillatory measurements conducted on a Discovery HR-2 rheometer (TA Instruments, Inc., USA) equipped with a Peltier temperature control unit. A cross-hatched steel geometry system with a 20 mm diameter was employed as a sensor, chosen specifically for its ability to prevent sensor wall slip—an issue commonly encountered in rheological, particularly oscillatory, tests of hydrogel samples.

All measurements were performed with the gap between the roughened plates set to 1 mm. The hydrogel specimens (20 mm in diameter) were placed on the lower plate, after which the upper plate was lowered to the trim gap (1.1 mm). Any excess sample was carefully removed before the sensor was adjusted to the final measuring gap (1.0 mm) and allowed to equilibrate at 25 °C for 180 s. This temperature was maintained consistently throughout the experiment. The axial force applied during compression to the measuring gap did not exceed 5 N. The oscillation frequency was fixed at 1 Hz, while the deformation amplitude was increased logarithmically from an initial value of 0.01 % to 1000 % (logarithmic sweep, 6 points per decade).

2.5.2. Morphological analysis by electron microscopy

The encapsulated bacterial cultures were processed using cryogenic methods of sample fixation before being imaged in either transmission or scanning mode. For the TEM analysis, a piece of the sample was cut off using a scalpel and placed on 3 mm Au/Cu carriers type A and covered with the flat side of 3 mm Au/Cu carrier type B. The samples

were fixed using high-pressure freezing (EM ICE, Leica Microsystems, Vienna, Austria), followed by freeze substitution (EM AFS2, Leica Microsystems, Vienna, Austria). The substitution solution contained 1 % OsO_4 and 0.1 % uranyl acetate in fresh acetone and the procedure was set to −90 °C for 60 h. Afterwards, the samples were heated up to −54 °C with the speed of 2 °C per hour. This temperature was kept constant for 8 h. Subsequently, the samples were heated up to −24 °C with the speed of 5 °C per hour and kept at that temperature for 15 h. The procedure concluded with the final phase at 4 °C for 18 h. The fixed samples were infiltrated with epoxy resin (Epoxy Embed-ding Medium kit, Sigma Aldrich, Darmstadt, Germany) and cured for 48 h at 62 °C. The embedded samples were cut into ultrathin sections (~80 nm) using a diamond knife (Ultra 45°, DiATOME, Nidau, Switzerland) and ultramicrotome (EM UC7, Leica Microsystems, Vienna, Austria). The sections were placed on PELCO Cu 200 Mesh TEM grids and stained using conventional staining agents: 2 % uranyl acetate solution in water and Reynolds 3 % lead citrate solution. Samples were observed by TEM (Morgagni, FEI) at 80 kV.

For the cryo–SEM imaging, hydrogel samples were cut to fit into side A of 6 mm aluminum carriers for high pressure freezing procedure. The carriers containing the sample were filled with media from the cultivation and fixed using high-pressure freezing (EM ICE, Leica Microsystems, Vienna, Austria). Frozen samples were transferred into a cryogenic vacuum chamber (ACE600, Leica Microsystems), where they were fractured followed by sublimation at −95 °C for 7 min. Hydrogel samples containing bacteria were imaged in a scanning electron microscope (Magellan 400/L, FEI) equipped with a cryo-stage, at −120 °C using a 1–2 keV electron beam.

2.5.3. Verification of A. vinelandii viability after gelation

To obtain a sufficient sample volume for viability and bioactivity analyses, larger quantities of encapsulated *Azotobacter vinelandii* cells were prepared under sterile conditions. Specifically, a 50 mL culture of *A. vinelandii* (DSM 87, DSM 720, and DSM 13529) was mixed with an equal volume (50 mL) of a sterile 2 % (*w*/w) $CaCl_2$ solution. Following a 10-min gel formation period, the residual liquid was removed, and a saline solution (0.9 g/L NaCl) was added to achieve a final volume of 100 mL. Liquid samples from the supernatant above the gel matrix were collected at 1-h and 24-h intervals for further analysis (flow cytometry, inoculation on agar plates).

The viability of *A. vinelandii* cells released from the gel matrix was evaluated using a flow cytometer NL-2000 (Cytek Biosciences, Fremont, CA, USA) with a propidium iodide (PI) fluorescent probe (Johnson et al., 2013). Supernatant samples were subjected to serial decimal dilution up to a thousand-fold, followed by staining with 4 μL of PI (1 mg/mL). The samples were incubated in darkness for 15 min before analysis by flow cytometry.

The cultivability of released *A. vinelandii* cells was confirmed by plating the supernatant samples onto agar plates (15 g/L agar) based on modified Ashby's medium (see 2.1). The inoculated plates were incubated at 30 °C for 3–4 days to assess colony formation.

To evaluate functional bioactivity of the cells released from the gel, the ability to produce indole-3-acetic acid (IAA) was tested following the methodology outlined in 2.4.1. Additionally, siderophore production was assessed using a qualitative assay on agar plates supplemented with iron CAS, according to the procedure described in 2.4.2. Phosphate solubilization activity was determined by cultivating released *A. vinelandii* cells on Pikovskaya's medium (see 2.4.3), with a modified supplementation of tricalcium phosphate (5 g/L) to enhance the clarity of halo zones formed around the colonies.

2.6. Statistical analysis

All cultivations, including those for polymer production, gelation, and bioactivity assays, were performed in parallel as duplicates. For each cultivation, optical density (OD) and poly(3-hydroxybutyrate) (PHB) content were measured in at least three independent replicates. Alginate concentration and molecular weight were determined once per duplicate, along with the rheological properties of the gels (examined only for DSM 87, DSM 720, and DSM 13529). Structural parameters derived from FTIR spectrometry were calculated based on five independent spectra for alginate isolated from each strain. Quantitative bioactivity assays, including indole-3-acetic acid (IAA) production and siderophore activity in liquid medium, were conducted for two samples per cultivation duplicate. Results are presented as mean ± standard deviation (SD) across all tables, figures, and text.

3. Results and discussion

3.1. Screening of Azotobacter vinelandii strains for biopolymers production

We have tested five strains of *A.vinelandii* regarding their potential in development of gel bioinoculants based on the novel self–entrapment concept. We have focused primarily on the production of alginate as the gel forming polymer and on the respective gel–forming abilities of the strains, along with the basic screening of their plant-growth promoting properties. Furthermore, we evaluated the accumulation of polyhydroxyalkanoates in the cultures as it was recently demonstrated that this ability enhances bacterial stress resistance (Obruca et al., 2018).

In order to promote the production of alginate, the selected strains were cultivated in modified Ashby's medium in nitrogen–limited conditions, with glucose serving as a carbon source and the addition of $CaCO_3$ supporting alginate synthesis and maintaining pH of bacterial culture. The cultivation was carried out for 7 days, during which the optical density (OD) of bacterial culture was measured daily. Starting at 72 h, after the bacterial strains had already reached the exponential phase, we tested all the strains for both of the analyzed biopolymers in 24–hour interval. The results of OD values, alginate yields and PHB content are provided Supplementary information (Fig. S2) for each strain.

A.vinelandii belongs among the most efficient bacterial producers of alginate (Serrato, 2022). It is well documented that the alginate production begins in the exponential growth phase, and when the bacterial growth gets into the stationary phase, production of alginate decreases (Ponce et al., 2021). It has also been reported that the production of alginate provides *A.vinelandii* with a desiccation–resistance to maintain hydration of the cell, serving as a barrier against heavy metal toxicity, and forms a diffusion barrier against oxygen to limit its transfer to the nitrogenase enzyme complex (Urtuvia et al., 2017).

Alginate was produced by all the investigated strains, particularly during the late exponential and early stationary phase (4th to 6th day), as demonstrated by peak production values, summarized in Table 1. The highest peak production of alginate was obtained by the strain DSM 87 (4.9 ± 0.6 g/L), followed by the strain DSM 13529 (3.8 ± 0.8 g/L) on the 5th day of cultivation. These production rates of alginate align also with the literature, where obtained 3.5 g/L of alginate employing *A. vinelandii* ATTC 9046 (Trujillo-Roldán et al., 2015).

For preparation of alginate hydrogels, different concentration ranges of alginate and calcium chloride are used. Typically, alginate concentration can vary from 1 to 10 % *w*/*w* (Hu et al., 2021), affecting gel strength and stability. In our study, the peak alginate content in *A. vinelandii* cultures ranged from 2 to almost 5 g/L. Recent study (Hu et al., 2022) focused on gelation behavior with alginate concentrations varying between 1 and 5 g/L, while gel forming tendency was exhibited by alginate with concentration 4 and 5 g/L. Savić Gajić et al. also prepared hydrogels with different concentration of alginate (0.1–2.9 % *w*/*v*) and $CaCl_2$ (0.4–4.6 % *w*/*v*), studying their water-retaining capacity and demonstrating gel forming ability even with small concentration of alginate (0.1 % *w*/*v*) (Savić Gajić et al., 2023).

Nevertheless, the gelation ability of the alginate solution upon Ca^{2+} addition is not solely dependent on the alginate content but is critically

Table 1
Summary of properties of analyzed *A. vinelandii* strains: production yields and structural characteristics of alginate, quantitative bioactivity assay results, and gelation ability with Ca^{2+}.

Strain	alginate production		alginate structure*			bioactivity**		gelation ability***
	max. Alginate production (g/L)	time of max. Alginate production	molecular weight (kDa)	M/G ratio (A_{810}/A_{790})	acetylation ratio (A_{1720}/A_{1600})	IAA production (μg/mL)	siderophore activity (psu#)	
DSM 85	2.14 ± 0.01	day 6	319 ± 1	2.2 ± 0.1	0.06 ± 0.01	8.7 ± 0.8	5 ± 2	no gel formation
DSM 87	4.87 ± 0.57	day 5	493 ± 15	1.7 ± 0.1	0.54 ± 0.01	10.5 ± 1.9	26 ± 11	compact gel
DSM 576	3.09 ± 1.19	day 5	181 ± 0	2.8 ± 0.3	0.17 ± 0.02	8.5 ± 1.6	39 ± 18	weak, easily disintegrating gel
DSM 720	3.52 ± 0.54	day 6	345 ± 3	1.6 ± 0.3	0.08 ± 0.02	9.0 ± 1.1	36 ± 23	compact gel
DSM 13529	3.78 ± 0.78	day 5	308 ± 6	2.0 ± 0.5	0.10 ± 0.03	7.6 ± 0.8	19 ± 10	compact gel

* structural characteristics of alginate isolated from *A. vinelandii* cultures on day 4 of cultivation.
** positive control (*P. anantis*): IAA production: 67 ± 4.2 μg/mL, siderophore production: 42 ± 17 psu.
*** describes the best gelation performance upon addition to a 2 % *w/w* $CaCl_2$ solution throughout the entire monitored period. The time-dependent progression of gelation ability is provided in the Supplementary information (Table S1).
# psu = % of decolorization of CAS reagent.

influenced by its structure. One of the crucial physico-chemical parameters of the produced alginates is their molecular weight (M_w), as it affects the viscosity and gelling capability of their aqueous dispersions as well as material properties of the resulting gels. Molecular weight of alginate is known to be dependent on cellular respiration; thus, the intensity of shaking is an important factor (Díaz-Barrera et al., 2021).

In our study, M_w of bacterial alginate ranged from 181 up to 500 kDa (see Table 1). On the 4th day of cultivation, when bacterial strains were grown with significant alginate amount, the strain DSM 87 reached M_w of almost 500 kDa even though alginate yield was <2 g/L. With the strains DSM 85, DSM 720 and DSM 13529, approximately equivalent M_w was observed. The strain DSM 576 produced alginate of a molecular weight of 181 kDa, similar to what was reported (Clementi & Parente, 1997) after 48 h of cultivation. In bioreactor cultivation performed by Díaz-Barrera et al. (2021), the alginate M_w increased from 200 kDa up to the maximum of 520 kDa. M_w higher than ~240 kDa has a significant influence on the strength of the alginate gels, fostering stronger cross linking, which results in a robust gel structure (Fernández Farrés & Norton, 2014). However, in some cases even alginate with M_w below 100 kDa can form gel (Ramos et al., 2018). Despite the differences in the alginate M_w extracted from *A.vinelandii* in our study, the results indicate a strong possibility for gelation potential, further described in 3.2.

Aside from M_w, the molecular structure of alginate also plays a crucial role in gelation. Primarily, the mannuronic-to-guluronic residues (M/G) ratio is a key determinant of alginate's gelation properties. Alginates with a higher guluronate (G) content tend to form stronger gels due to the greater affinity of G residues for Ca^{2+} ions. This is because G residues can establish more stable egg-box junctions (see the schematic representation in Fig. S1, Supplementary material), leading to a denser cross-linked network (Donati & Christensen, 2023). Furthermore, the presence of acetyl groups in alginate increases viscosity while reducing its affinity for calcium ions, thereby negatively affecting the gelation process (Skjåk-Bræk et al., 1989).

FTIR spectrometry was used to analyze the molecular structure of the produced alginates. The average spectra for alginates synthesized by different *A. vinelandii* strains are provided in the Supplementary information (Fig. S3). Specific IR absorbances at 780 cm^{-1}, 810 cm^{-1}, and 1720 cm^{-1} were used to estimate the content of guluronate, mannuronate, and acetyl groups, respectively, as previously suggested for *Azotobacter*-derived alginates by Bonartseva et al. (2017). The resulting FTIR-based structural parameters are summarized in Table 1. The M/G ratio in the analyzed alginates ranged from 1.6 to 2.2, corresponding to a relative G content of 26 % to 37 %, which aligns well with the monomer composition of *A. vinelandii* alginate reported in the aforementioned study (Bonartseva et al., 2017). Among the analyzed cultures, the highest G content was observed in DSM 87, while DSM 576 exhibited the lowest. Conversely, DSM 87 displayed significantly higher degree of *O*-acetylation compared to other analyzed strains.

In addition to alginate, *A. vinelandii* is also capable of producing polyhydroxyalkanoates (Dujjanutat et al., 2024). As we have already pointed out, the accumulation of polyhydroxyalkanoates (including PHB as their main representative) enhances stress and starvation resistance of the bacterial culture (Sedlacek et al., 2019), which is crucial property with respect to bioinoculant application. Therefore, PHB accumulation was considered when screening the potential for bioinoculant preparation in various strains of *A.vinelandii*. Published values of accumulated PHB in *A.vinelandii* range from 20 up to 50 % of cell dry weight (cdw), depending on carbon sources (Page & Knosp, 1989). In some cases, specifically under nitrogen–limited conditions, the production of PHB can reach up to 74 % of cdw (Yoneyama et al., 2015). In our study, PHB content in the cells peaked after 3–4 days of cultivation before gradually decreasing. The time-dependent progression of PHB accumulation throughout cultivation is provided in the Supplementary information (Fig. S2). The maximum PHB content among the tested strains ranged from 16 ± 7 % cdw (DSM 576) to 47 ± 5 % cdw (DSM 720).

Production of both alginate and PHB constitute energy–demanding processes with the oxygen playing a crucial role, whose biosynthetic mechanisms are not yet fully explored. As expected, our results confirmed the higher PHB accumulation in the beginning of the bacterial cultivation, whereas production of alginate peaks at later phases of bacterial growth. Furthermore, the production of alginate is positively impacted by aeration, thus agitation speed and volume of media is an important factor (Castillo et al., 2020).

Most published reports focused on maximizing either PHB or alginate production. We have employed a different strategy. In general, the synthesis of alginate and PHB competes for carbon resources and maximizing the yield of one typically leads to a substantial decrease in the production of the other (Noar & Bruno-Bárcena, 2018). However, our primary focus was cultivating bacteria for bioinoculant applications, which entails finding an optimal balance of biopolymer's content and quality. The primary goal was to achieve an alginate level sufficient to induce bacterial self–gelation without the need for additional gel forming polymer. In the context of published studies on preparation and mechanical properties of calcium alginate gels, both the peak yields and the structural parameters of produced alginates seem sufficient to provide the bacterial cultures with Ca–induced gelation ability (Rodríguez-Dorado et al., 2019).

Furthermore, we also intended for the bacterial cultures to contain a significant, albeit not maximal, portion of PHB. This feature might be of crucial importance for the survival of bacterial cells during storage and

application to the soil. The importance of PHB accumulation by PGPR for commercial bioinoculants has been already emphasized (Kadouri et al., 2003; Tal & Okon, 1985) and it has been confirmed to increase the stress resistance of PHB–producing *A. brasilense* cultures. In the previous works, the PHB content of 40 % cdw (i.e. comparable with the values observed in this study) was sufficient for providing significantly higher survival rate in the presence of stress factors such as ultraviolet irradiation, desiccation, and osmotic pressure. Additionally, the PHB–rich culture was also found to provide enhanced nitrogen fixation. Furthermore, Alves et al. (2019) have reported the importance of PHB metabolism to the plant growth promoting ability of *Herbaspirillum seropedicae*. The strains producing higher amounts of PHB (above 10 % of cdw) grew better under microaerobic conditions typical for soils, and colonized roots with significantly increased root area and the number of lateral roots compared to those of PHB–negative strains. Altogether, the cultures of *A.vinelandii* strains produced in this study showed auspicious biopolymer production characteristics regarding their potential use in bioinoculant production.

3.2. Gel formation capability of the bacterial cultures

Our novel concept is based on direct gelation of bacterial culture

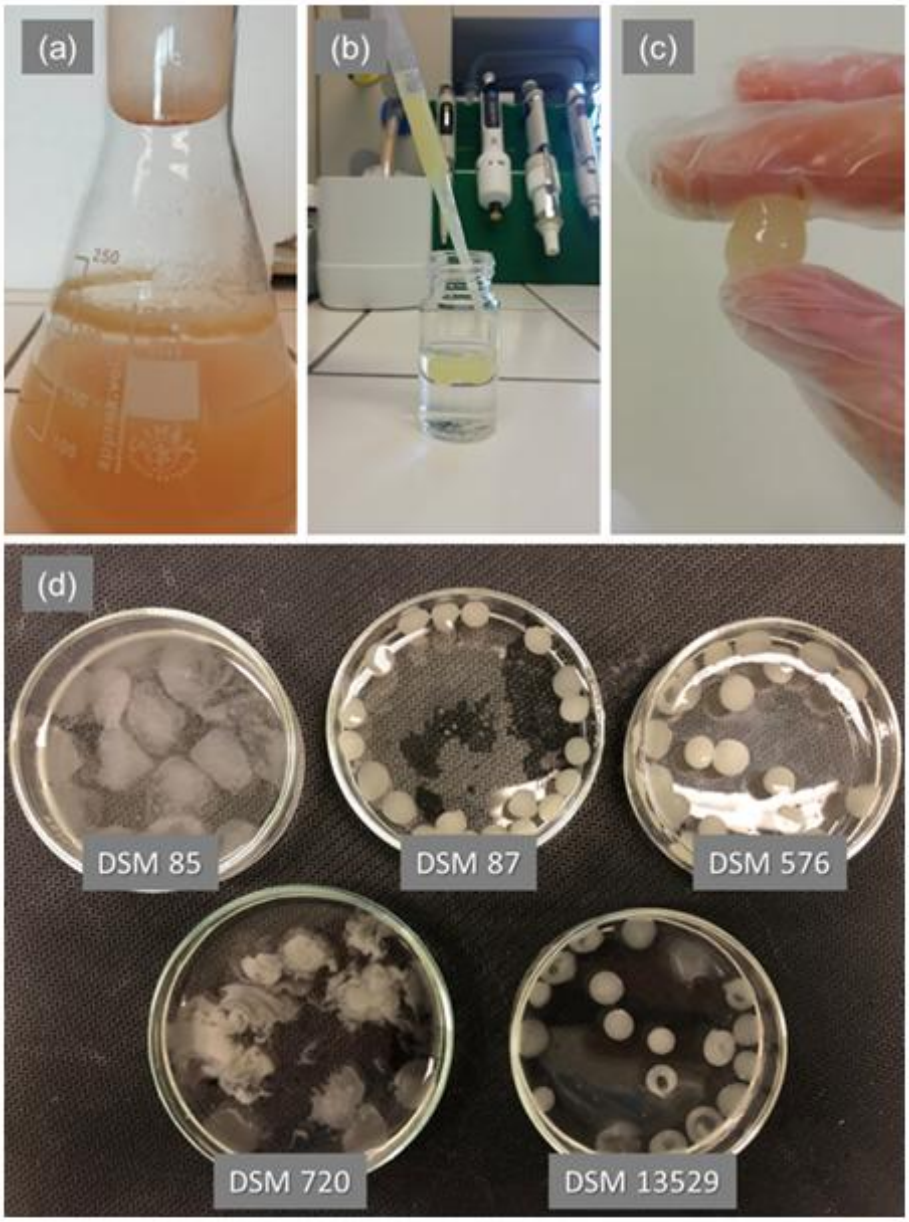

Fig. 1. Schematic representation (a – c) and results for the 4th day of cultivation (d) of the simple test used for screening of gelation ability of various *A.vinelandii* strains. The as-cultivated culture (a) is added dropwise (b) to the crosslinking solution (2 % *w*/*w* $CaCl_2$), where the compact gel beads (c) are formed rapidly, provided the culture has gel-forming properties.

without addition of any external gelation polysaccharide. Therefore, we tested gel formation potential of the bacterial cultures during their cultivation using the simple methodology demonstrated in Fig. 1. The grown bacterial culture rich in self–produced alginate is added dropwise into crosslinking solution containing calcium ions (2 % *w/w*). If successful, this process results in the formation of macro-gels with incorporated viable bacterial cells.

Starting from the 3rd day of cultivation, some of the bacterial cultures began to exhibit gel formation capacity when being pipetted into calcium ion solution (see Table 1, time progression of the gelation ability is supplemented in Table S1, Supplementary information). Only the strain DSM 85 formed just a turbid solution with all its tested cultures. As expected, the delayed production of alginate by the strain DSM 720, resulted in delayed gelation ability of its cultures (stable gels were not formed until the 5th day of the cultivation, see Fig. 1 and Table S1). In contrast, strain DSM 576 provided apparently compact gels since the 3rd day. However, the gels disintegrated easily during manipulation or in contact with water. Even though all the strains showed comparable production of alginate by the fifth day of cultivation (1.9–4.9 g/L), only the strains DSM 87, DSM 720 and DSM 13529 formed stable gels that maintained their shape even when handled. The lack of the gelation ability of the DSM 85 strain may be linked to its overall lower alginate productivity, while the weak mechanical properties of the gels formed by DSM 576 can be attributed to the lower molecular weight and guluronate content of the produced alginate (see Table 1). On the other hand, DSM 87 demonstrated good gelation ability despite having the highest degree of acetylation, as confirmed by FTIR. Since bacterial alginates are exclusively acetylated at mannuronic acid residues (Gacesa, 1998), our results support the dominant role of guluronate residues in *A. vinelandii* alginate gelation with Ca^{2+}. This suggests that optimizing cultivation conditions to increase the G-content could potentially enhance gelation ability in the two remaining *A. vinelandii* strains as well. However, in this study, only the gels formed by DSM 87, DSM 720, and DSM 13529 were subjected to further investigation.

3.3. Screening of plant–growth promoting properties of A. vinelandii strains

As mentioned above, plant growth-promoting bacteria influence plants through various mechanisms, including production of phytohormones, pathogen suppression, and modulation of soil microbiome (Olanrewaju et al., 2017). We have focused on the production of indole acetic acid (model phytohormone), and on the capability to solubilize iron and phosphates to provide a comparative confirmation of PGP activities of the tested *A.vinelandii* strains (Olanrewaju et al., 2017). Results of quantitative bioactivity assays are summarized in Table 1, pictures of agar plates qualitatively illustrating the iron and phosphate utilizations are supplemented in Supplementary information (Fig. S4).

Indole acetic acid (IAA) is one of the best-known auxins, primarily promoting root growth. According to literature (Shailendra Singh, 2015), approximately 80 % of soil bacteria produce IAA which results in an expansion of the root system, increasing branching and providing greater contact area with the soil, leading to enhanced plant's uptake of minerals and nutrients. In our study, production of IAA was confirmed in all the strains, with DSM 87 exhibiting the highest IAA production (10.5 µg/mL) among all of the *Azotobacter* strains (see Table 1). This represents about 15 % of IAA production by *P. ananatis* (67.6 µg/mL) used as a positive control. For remaining *A.vinelandii* strains, IAA production ranges from 11 % to 13 % when compared to *Pantonea ananatis*.

The production of siderophores is another recognized feature of PGPR. Iron is an essential nutrient for all organisms; however, it is sparingly soluble in its predominant form as ferric ions (Fe^{3+}), making it challenging for organisms to assimilate it (Ma, 2005). Siderophores are metal-chelating compounds with high affinity for iron (Schalk, 2025) that facilitate the transport of iron into cells, thereby positively stimulating plant growth. Siderophore production in *Azotobacter* strains was assessed through both quantitative and qualitative tests, using chrom azurol S (CAS) reagent. The bacterial strains capable of producing siderophores generated light orange halo zones around the colonies. All the strains exhibited positive siderophore–producing capabilities both in the qualitative (agar plate) and quantitative (liquid medium) test. In the qualitative siderophore production assay, clearly visible halo zones were observed for all *A.vinelandii* strains (see Fig. S4, Supplementary information). From the quantitative point of view, the highest siderophore activity (in psu representing % of decolorization of CAS reagent) was determined for the DSM 576 (39 psu) and DSM 720 (36 psu) strains (Table 1), which corresponds to 86 % and 93 % of the siderophore activity in *P. ananatis* culture (42 psu) used as a positive control.

Another important role of biofertilizers is enriching soil with phosphorus. However, phosphates in soil are found mainly in insoluble form, making it difficult for plants to absorb them, however, some PGPR are capable of phosphate solubilization (Aasfar et al., 2021). In our study, phosphate solubilization was assessed qualitatively by growth of *A. vinelandii* on Pikovskaya's medium, with addition of tricalcium phosphate creating clear halo zones around or beneath the bacterial colonies due to production of organic acids dissolving inorganic phosphates (Hafez et al., 2016). For all tested *A. vinelandii* strains, the halo zones became visible on the agar plates after careful removal of a colony (see Fig. S4, Supplementary information). Among those, the strains DSM 87 and DSM 720 demonstrate less intense zones, which may indicate lower ability of phosphate solubilization.

Overall, *A.vinelandii* bioactivity has been widely confirmed. Aside of the IAA and siderophore production and the phosphate solubilization as confirmed in this study, *A.vinelandii* has been reported to contain nitrogenase enzyme, resulting in nitrogen availability in the soil, which plays an important role in utilizing bacteria as biofertilizers via enriching soil fertility with organic nitrogen (Natzke et al., 2018). Generally, the members of the genus *Azotobacter* are considered promising candidate bioinoculants and soil biological enhancers (Aasfar et al., 2021). Our results indicate that, with respect to the defined concept of the next generation bioinoculants, the selected strains of *A. vinelandii* are of great promise, since apart from their capacity of biopolymers production, they also possess the crucial PGP abilities.

3.4. Mechanical properties, microstructure and viability of encapsulated a.vinelandii cells in gel formulations

To confirm the fully crosslinked nature and to compare the mechanical (viscoelastic) properties of the three obtained gel formulations, oscillatory rheometry was used. The samples were subjected to strain sweeps to evaluate the presence of properties typical for viscoelastic materials with fully cross–linked structures. The key parameters obtained by the analysis were the storage and loss moduli, characterizing the elastic and viscous, respectively, contributions to the deformation behavior. The measured data were plotted on the increasing amplitude of deformation (see Fig. 2a–c). For fully cross-linked gels, in the linear viscoelastic (LVE) region (i.e. for deformations below the point of irreversible breakdown of the network), the storage modulus values exceed those of the loss modulus and these values remain relatively independent of the strain amplitude. This pattern was confirmed for all the tested gels. The values of complex moduli (calculated from the storage and loss moduli as described in Kavanagh and Ross-Murphy (1998), Fig. 2d) in LVE region do not vary significantly among the three strains and the range of the determined values (1.4 kPa for DSM 720 to 4.2 kPa for DSM 13529) is in good agreement with the published viscoelastic parameters for Ca-alginate gels formed from the alginate solutions with similar concentration (Larsen et al., 2015). Comparable values of the complex moduli in LVE region point to similar crosslinking density in all of the analyzed gels. The solid-like mechanical properties of the materials are further illustrated by the low values of phase angle (Fig. 2d), which represents the rheometric parameter allowing differentiation between predominantly elastic (phase angle $<45°$), and viscous (phase

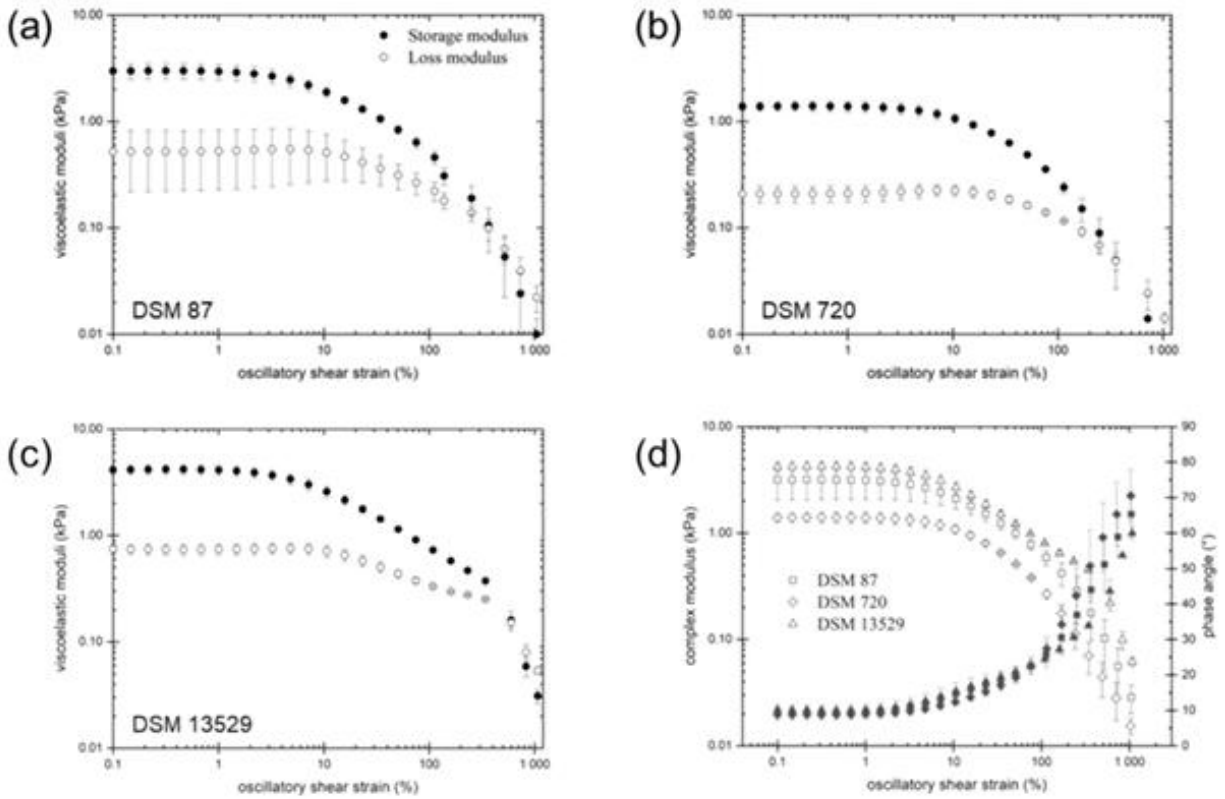

Fig. 2. Rheological characterization of gels formed by three gel-producing *A. vinelandii* strains. (a–c) Dependence of viscoelastic moduli on deformation strain for the as-prepared gels. (d) Dependence of complex modulus (open symbols) and phase angle (filled symbols) on deformation strain for the as-prepared gels.

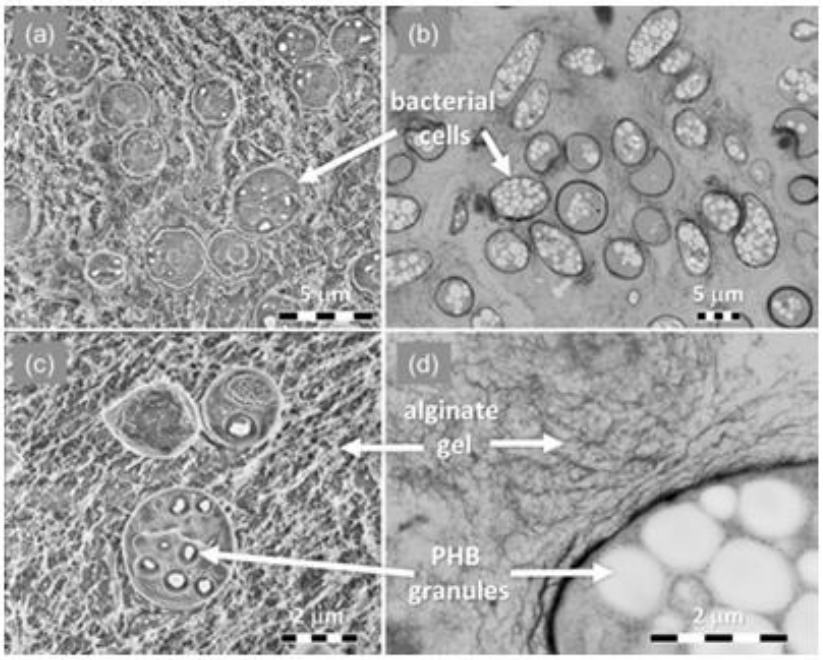

Fig. 3. Morphological analysis of bioinoculant gel formed by crosslinking of the *A.vinelandii* DSM 87 culture. Cryo-SEM images (a, c) and TEM images (b, d) of the bioinoculant gel formed by ionic crosslinking with $CaCl_2$ (2 % *w/w*) of the as-cultivated *A. vinelandii* DSM 87 strain.

angle >45°) deformations typical for solids and liquids, respectively, as described in detail in (Kavanagh & Ross-Murphy, 1998).

The LVE region for bacterial gels typically ends at approximately 2–3 % of the amplitude of shear deformation, signifying that the gel remains stable when subjected to deformation within this range. Once the LVE region is surpassed, the material's bonds begin to break irreversibly, resulting in the formation of small fragments. These fragments introduce internal friction, converting deformation energy into heat. In the final stage, the gel material reaches 'crossover point', at which the storage and loss moduli become equal, and the deformation of the gel is permanent and irreversible. No significant differences were found in parameters that describe this behavior (i.e. deformation strain values that correspond to the end of LVE or crossover) among the three tested gels, which indicates similar type of bonds that form the crosslinks in their networks. Overall, the three gel-forming strains produced materials with similar mechanical properties, indicating the similarity of the internal gel networks both from the qualitative (type of bonding) and quantitative (crosslinking density) point of view.

The detailed internal structure of the hydrogels (prepared in the same way as the gels for the rheological characterization) was analyzed by scanning electron cryo–microscopy (cryo–SEM) and transmission electron microscopy (TEM). The results of the analyses are shown in the Fig. 3. The results of electron microscopy imaging reveal a high density of encapsulated bacteria within the hydrogels, interconnected by a dense alginate network. The encapsulated cells are intact, no apparent signs of loss of membrane integrity or other cell damage were found. Furthermore, the high content of PHB granules in the *A.vinelandii* cells is also clearly observed.

Beyond the visual control of cell integrity in microstructural analysis, the survival of *A. vinelandii* cells during Ca^{2+}-induced gelation was experimentally verified. To assess this, cultures of three compact gel-forming strains (DSM 87, DSM 720, and DSM 13529) were crosslinked with $CaCl_2$ under sterile conditions. The aqueous cell suspensions obtained after 1 and 24 h of release from the gels were subsequently analyzed. Flow cytometry with propidium iodide was used to quantify the fraction of viable cells (the results are provided in the Supplementary information, Fig. S5) according to our previous work (Kroupova et al., 2025). For all three analyzed strains, the fraction of viable cells exceeded 50 % at both time points for gel-released cells. The total number of released cells, as determined by flow cytometry, was consistently on the order of 10^8 cells per milliliter. The highest survival rate, approximately 90 % for both release times, was observed for strain DSM 720. Additionally, for all three strains, the cultivability of the released cells was confirmed by inoculating the suspensions onto agar plates. The retention of bioactivity was further verified. Siderophore activity and phosphate solubilization were confirmed by inoculating the suspension of released cells onto agar plates amended with CAS reagent and Pikovskaya medium, respectively. Lastly, IAA production was tested by cultivating the released cells in King B medium supplemented with tryptophan. The supernatant of the culture was then mixed with Salkowski reagent, and the presence of IAA was confirmed by the development of a red color. An example of the qualitative results from cultivability and bioactivity assays for the suspension of cells released from gels crosslinked with *A. vinelandii* DSM87 culture is provided in the Supplementary information (Fig. S5).

3.5. Automatized encapsulation techniques

As stated previously, encapsulation of cells of PGPR in a gel matrix is known to improve the efficiency of inoculation and consequently the effect on plant growth. Furthermore, maintaining a consistent and uniform size of the gel beads ensures control in the application of bacterial bioinoculants and leads to a standardized process achieving predictable effectiveness and reliability in releasing bacteria from the gel beads.

Therefore, we also confirmed the compatibility of self–encapsulation concept with techniques for automatized preparation of bioinoculant beads of specific sizes ranging from micrometer up to millimeter scale. The bioinoculant beads were prepared using automatic custom–made device, where a uniform bead size in the scale of millimeters can be adjusted by the dimensions of the used syringe needle (the apparatus is shown in Fig. S6a, Supplementary information). Similarly, we have experimentally verified that the proposed self-encapsulation gelation can also be performed using commercial micro-encapsulation facilities while still allowing for the production of gel beads at microscale. An example of gel microbeads prepared with the use of microencapsulator Buchi B–395 combined with the 450 μm nozzle is shown in Supplementary information (Fig. S6c).

Obviously, the variability in the size of the bioinoculant gel particles allows control over the rate of the PGPR cell release from the gel as the specific surface of the particles may be altered. Furthermore, smaller beads can establish closer contact with the seeds. Microbeads, owing to their smaller size, can accurately target seeds and the loss of bacterial cells during the encapsulation is lower when compared to large beads. Additionally, the application of microbeads is versatile, they can be directly coated onto seeds, or sprayed onto soil, making manipulation easier (John et al., 2011).

4. Conclusion

This study introduces a promising and economically viable approach to bioinoculant production through the self-entrapment of *Azotobacter vinelandii* cultures within their own exopolysaccharide-derived gel matrix. By leveraging the natural gelation properties of *A. vinelandii*-produced alginate, our method eliminates the need for costly external gelation agents, streamlining production while maintaining the well-documented benefits of the gel matrix that enhance bioinoculant efficacy.

The present work primarily serves as a proof of concept for this self-encapsulation strategy. Future research will focus on optimizing gelation conditions to improve encapsulation efficiency, mechanical stability, and microbial viability. Additionally, further processing of the resulting formulations will be explored, particularly in terms of controlled water removal to extend shelf life and ensure long-term stability without compromising bacterial activity and viability.

Beyond formulation advancements, upcoming studies will evaluate the plant growth-promoting effects of various bioinoculant formulations using agriculturally relevant crops, such as corn and lettuce, in both controlled pot trials and field experiments. These investigations will provide crucial insights into the practical application and agronomic benefits of this novel encapsulation approach, paving the way for its potential commercialization and widespread use in sustainable agriculture.

CRediT authorship contribution statement

Diana Černayová: Writing – original draft, Investigation. **Martin Súkeník:** Writing – review & editing, Investigation. **Stanislav Obruča:** Writing – review & editing, Writing – original draft, Supervision, Methodology, Conceptualization. **Jiří Smilek:** Writing – review & editing, Investigation. **Michal Kalina:** Writing – review & editing, Investigation. **Kateřina Mrázová:** Writing – review & editing, Investigation, Conceptualization. **Kamila Hrubanová:** Writing – review & editing, Investigation, Funding acquisition. **Vladislav Krzyžánek:** Writing – review & editing, Methodology, Investigation. **Petr Sedláček:** Writing – review & editing, Writing – original draft, Supervision, Methodology, Investigation, Formal analysis, Conceptualization, Funding acquisition.

Author contributions

The manuscript was written through contributions of all authors. All authors have given approval to the final version of the manuscript.

Declaration of competing interest

The authors declare that they have no known competing financial interests or personal relationships that could have appeared to influence the work reported in this paper.

Acknowledgements

This study was funded by the project GA23-06757S of the Czech Science Foundation (GACR). Microscopic analysis was provided by CF ISI EM, Czechia, and by the Electron Microscopy Facility (VBCF), Austria, thanks to the financial support of MSM100652102 and LM2023050 MEYS CR. Martin Sukenik acknowledge financial support from JCMM Brno Ph.D. Talent.

Appendix A. Supplementary data

Supplementary data to this article can be found online at https://doi.org/10.1016/j.carbpol.2025.123607.

Data availability

Data are available from the corresponding author on request.

References

Aasfar, A., Bargaz, A., Yaakoubi, K., Hilali, A., Bennis, I., Zeroual, Y., & Meftah Kadmiri, I. (2021). Nitrogen fixing *Azotobacter* species as potential soil biological enhancers for crop nutrition and yield stability. *Frontiers in Microbiology, 12*, 1–19. https://doi.org/10.3389/fmicb.2021.628379

Alves, L. P. S., do Amaral, F. P., Kim, D., Bom, M. T., Gavídia, M. P., Teixeira, C. S., Holthman, F., Pedrosa, F. de O., de Souza, E. M., Chubatsu, L. S., Müller-Santos, M., & Stacey, G. (2019). Importance of poly- 3-hydroxybutyrate metabolism to the ability of *Herbaspirillum seropedicae* to promote plant growth. Applied and Environmental Microbiology, 85, 1–14. doi:https://doi.org/10.1128/AEM.02586-18.

Ambrosini, A., & Passaglia, L. M. P. (2017). Plant Growth–Promoting Bacteria (PGPB): Isolation and Screening of PGP Activities. Current Protocols in Plant Biology, 2, 190–209. doi:https://doi.org/10.1002/pb.20054.

Arora, N. K., & Verma, M. (2017). Modified microplate method for rapid and efficient estimation of siderophore produced by bacteria. *3. Biotech, 7*, 1–9. https://doi.org/10.1007/s13205-017-1008-y

Balla, A., Silini, A., Cherif-Silini, H., Chenari Bouket, A., Alenezi, F. N., & Belbahri, L. (2022). Recent advances in encapsulation techniques of plant growth-promoting microorganisms and their prospects in the sustainable agriculture. *Applied Sciences (Switzerland), 12*, 1–18. https://doi.org/10.3390/app12189020

Bashan, Y., de-Bashan, L. E., Prabhu, S. R., & Hernandez, J. P. (2014). Advances in plant growth-promoting bacterial inoculant technology: Formulations and practical perspectives (1998-2013). *Plant and Soil, 378*, 1–33. https://doi.org/10.1007/s11104-013-1956-x

Bonartseva, G. A., Akulina, E. A., Myshkina, V. L., Voinova, V. V., Makhina, T. K., & Bonartsev, A. P. (2017). Alginate biosynthesis by *Azotobacter* bacteria. *Applied Biochemistry and Microbiology, 53*, 52–59. https://doi.org/10.1134/S0003683817010070

Brandl, H., Gross, R. A., Lenz, R. W., & Fuller, R. C. (1988). *Pseudomonas oleovorans* as a source of poly (β-hydroxyalkanoates) for potential applications as biodegradable polyesters. *Applied and Environmental Microbiology, 54*, 1977–1982. https://doi.org/10.1128/aem.54.8.1977-1982.1988

Castillo, T., García, A., Padilla-Córdova, C., Díaz-Barrera, A., & Peña, C. (2020). Respiration in *Azotobacter vinelandii* and its relationship with the synthesis of biopolymers. *Electronic Journal of Biotechnology, 48*, 36–45. https://doi.org/10.1016/j.ejbt.2020.08.001

Clementi, F., Moresi, M., & Parente, E. (1999). Alginate from Azotobacter vinelandii. In carbohydrate biotechnology protocols. *Methods in Biotechnology, 10*, 23–42. https://doi.org/10.1007/978-1-59259-261-6_3

Clementi, F., & Parente, E. (1997). Alginate production by *Azotobacter Vinelandii*. *Critical Reviews in Biotechnology, 17*, 327–361. https://doi.org/10.3109/07388559709146618

Dellagnezze, B. M., & Sierra-Garcia, I. N. (2023). Immobilization of microbial inoculants for improving soil nutrient bioavailability. In *Microbial Inoculants: Recent Progress and Applications* (pp. 161–181). https://doi.org/10.1016/B978-0-323-99043-1.00004-9

Díaz-Barrera, A., Sanchez-Rosales, F., Padilla-Córdova, C., Andler, R., & Peña, C. (2021). Molecular weight and guluronic/mannuronic ratio of alginate produced by *Azotobacter vinelandii* at two bioreactor scales under diazotrophic conditions. *Bioprocess and Biosystems Engineering, 44*(6), 1275–1287. https://doi.org/10.1007/s00449-021-02532-8

Donati, I., & Christensen, B. E. (2023). Alginate-metal cation interactions: Macromolecular approach. *Carbohydrate Polymers, 321*, 1–17. https://doi.org/10.1016/J.CARBPOL.2023.121280

Dujjanutat, P., Singhaboot, P., & Kaewkannetra, P. (2024). Repeated fed-batch culture strategy for the synthesis of Polyhydroxybutyrate (PHB) biopolymers from sugar cane juice using *Azotobacter vinelandii*. *Polymers, 16*. https://doi.org/10.3390/polym16223156

Duncan, E. G., O'Sullivan, C. A., Roper, M. M., Biggs, J. S., & Peoples, M. B. (2018). Influence of co-application of nitrogen with phosphorus, potassium and Sulphur on the apparent efficiency of nitrogen fertiliser use, grain yield and protein content of wheat: Review. *Field Crops Research, 226*, 56–65. https://doi.org/10.1016/j.fcr.2018.07.010

Fernández Farrés, I., & Norton, I. T. (2014). Formation kinetics and rheology of alginate fluid gels produced by in-situ calcium release. *Food Hydrocolloids, 40*, 76–84. https://doi.org/10.1016/j.foodhyd.2014.02.005

Ferreira, C. M. H., Soares, H. M. V. M., & Soares, E. V. (2019). Promising bacterial genera for agricultural practices: An insight on plant growth-promoting properties and microbial safety aspects. *Science of the Total Environment, 682*, 779–799. https://doi.org/10.1016/j.scitotenv.2019.04.225

Gacesa, P. (1998). Alginate biosynthesis-recent and future prospects. *Microbiology, 144*, 1133–1143. https://doi.org/10.1099/00221287-144-5-1133

Gordon, S. A., & Weber, R. P. (1951). Colorimetric estimation of indoleacetic acid. *Plant Physiology, 26*, 192–195. https://academic.oup.com/plphys/article/26/1/192/6093171.

Hafez, M., El-Badry, M. A., Elbarbary, T. A., Ibrahim, I. A., & Abdel-Fatah, Y. M. (2016). *Azotobacter vinelandii* evaluation and optimization of Abu Tartur Egyptian phosphate ore dissolution. *Original Research Article Saudi Journal of Pathology and Microbiology, 1*, 80–93. https://doi.org/10.21276/sjpm.2016.1.3.2

Hu, C., Lu, W., Mata, A., Nishinari, K., & Fang, Y. (2021). Ions-induced gelation of alginate: Mechanisms and applications. *International Journal of Biological Macromolecules, 177*, 578–588. https://doi.org/10.1016/j.ijbiomac.2021.02.086

Hu, C., Lu, W., Sun, C., Zhao, Y., Zhang, Y., & Fang, Y. (2022). Gelation behavior and mechanism of alginate with calcium: Dependence on monovalent counterions. *Carbohydrate Polymers, 294*, 1–11. https://doi.org/10.1016/j.carbpol.2022.119788

John, R. P., Tyagi, R. D., Brar, S. K., Surampalli, R. Y., & Prévost, D. (2011). Bio-encapsulation of microbial cells for targeted agricultural delivery. *Critical Reviews in Biotechnology, 31*, 211–226. https://doi.org/10.3109/07388551.2010.513327

Johnson, S., Nguyen, V., & Coder, D. (2013). Assessment of cell viability. *Current Protocols in Cytometry, 64*, 1–26. https://doi.org/10.1002/0471142956.cy0902s64

Kadouri, D., Jurkevitch, E., & Okon, Y. (2003). Involvement of the reserve material poly-β-hydroxybutyrate in *Azospirillum brasilense* stress endurance and root colonization. *Applied and Environmental Microbiology, 69*, 3244–3250. https://doi.org/10.1128/AEM.69.6.3244-3250.2003

Kavanagh, G. M., & Ross-Murphy, S. B. (1998). Rheological characterization of polymer gels. *Progress in Polymer Science, 23*, 533–562. https://doi.org/10.1016/S0079-6700(97)00047-6

Kroupova, Z., Slaninova, E., Mrazova, K., Krzyzanek, V., Hrubanova, K., Fritz, I., & Obruca, S. (2025). Evaluating stress resilience of cyanobacteria through flow cytometry and fluorescent viability assessment. *Folia Microbiologica, 70*, 205–223. https://doi.org/10.1007/s12223-024-01212-w

Larsen, B. E., Bjørnstad, J., Pettersen, E. O., Tønnesen, H. H., & Melvik, J. E. (2015). Rheological characterization of an injectable alginate gel system. *BMC Biotechnology, 15*, 1–12. https://doi.org/10.1186/s12896-015-0147-7

Ma, J. F. (2005). Plant root responses to three abundant soil minerals: Silicon, aluminum and iron. *Critical Reviews in Plant Sciences, 24*, 267–281. https://doi.org/10.1080/07352680500196017

Martínez-Cano, B., Mendoza-Meneses, C. J., García-Trejo, J. F., Macías-Bobadilla, G., Aguirre-Becerra, H., Soto-Zarazúa, G. M., & Feregrino-Pérez, A. A. (2022). Review and perspectives of the use of alginate as a polymer matrix for microorganisms applied in agro-industry. *Molecules, 27*, 1–20. https://doi.org/10.3390/molecules27134248

Natzke, J., Noar, J., & Bruno-Bárcena, J. M. (2018). *Azotobacter vinelandii* nitrogenase activity, hydrogen production, and response to oxygen exposure. *Applied and Environmental Microbiology, 84*, 1–10. https://doi.org/10.1128/aem.01208-18

Neilands, B. B. (1987). Universal chemical assay for the detection and determination of siderophores. *Analytical Biochemistry, 160*, 47–56. https://doi.org/10.1016/0003-2697(87)90612-9

Noar, J. D., & Bruno-Bárcena, J. M. (2018). *Azotobacter vinelandii*: The source of 100 years of discoveries and many more to come. *Microbiology (United Kingdom), 164*, 421–436. https://doi.org/10.1099/mic.0.000643

Obruca, S., Sedlacek, P., Koller, M., Kucera, D., & Pernicova, I. (2018). Involvement of polyhydroxyalkanoates in stress resistance of microbial cells: Biotechnological consequences and applications. *Biotechnology Advances, 36*, 856–870. https://doi.org/10.1016/j.biotechadv.2017.12.006

Obruca, S., Sedlacek, P., Slaninova, E., Fritz, I., Daffert, C., Meixner, K., Sedrlova, Z., & Koller, M. (2020). Novel unexpected functions of PHA granules. *Applied Microbiology and Biotechnology, 104*, 4795–4810. https://doi.org/10.1007/s00253-020-10568-1

Olanrewaju, O. S., Glick, B. R., & Babalola, O. O. (2017). Mechanisms of action of plant growth promoting bacteria. *World Journal of Microbiology and Biotechnology, 33*, 1–16. https://doi.org/10.1007/s11274-017-2364-9

Oulad Ziane, S., Imehli, Z., El Alaoui Talibi, Z., Ibnsouda Koraichi, S., Meddich, A., & El Modafar, C. (2024). Biocontrol of tomato *Verticillium wilt* disease by plant growth-promoting bacteria encapsulated in alginate extracted from brown seaweed. *International Journal of Biological Macromolecules, 276*, 1–9. https://doi.org/10.1016/j.ijbiomac.2024.133800

Page, W. J., & Knosp, O. (1989). Hyperproduction of poly-β-Hydroxybutyrate during exponential growth of *Azotobacter vinelandii* UWD. *Applied and Environmental Microbiology, 55*, 1334–1339. https://doi.org/10.1128/aem.55.6.1334-1339.1989

Pereira, J. F., Oliveira, A. L. M., Sartori, D., Yamashita, F., & Mali, S. (2023). Perspectives on the use of biopolymeric matrices as carriers for plant-growth promoting bacteria in agricultural systems. *Microorganisms, 11*, 1–17. https://doi.org/10.3390/microorganisms11020467

Ponce, B., Urtuvia, V., Maturana, N., Peña, C., & Díaz-Barrera, A. (2021). Increases in alginate production and transcription levels of alginate lyase (alyA1) by control of the oxygen transfer rate in *Azotobacter vinelandii* cultures under diazotrophic conditions. *Electronic Journal of Biotechnology, 52*, 35–44. https://doi.org/10.1016/j.ejbt.2021.04.007

Qin, C., Wang, H., Zhao, Y., Qi, Y., Wu, N., Zhang, S., & Xu, W. (2024). Recent advances of hydrogel in agriculture: Synthesis, mechanism, properties and applications. *European Polymer Journal, 219*, 1–22. https://doi.org/10.1016/J.EURPOLYMJ.2024.113376

Ramos, P. E., Silva, P., Alario, M. M., Pastrana, L. M., Teixeira, J. A., Cerqueira, M. A., & Vicente, A. A. (2018). Effect of alginate molecular weight and M/G ratio in beads properties foreseeing the protection of probiotics. *Food Hydrocolloids, 77*, 8–16. https://doi.org/10.1016/j.foodhyd.2017.08.031

Riaz, G., Shoaib, A., Javed, S., Perveen, S., Ahmed, W., El-Sheikh, M. A., & Kaushik, P. (2023). Formulation of the encapsulated rhizospheric *Ochrobactrum ciceri* supplemented with alginate for potential antifungal activity against the chili collar rot pathogen. *South African Journal of Botany, 161*, 586–598. https://doi.org/10.1016/j.sajb.2023.08.048

Rodríguez-Dorado, R., López-Iglesias, C., García-González, C. A., Auriemma, G., Aquino, R. P., & Del Gaudio, P. (2019). Design of aerogels, cryogels and xerogels of alginate: Effect of molecular weight, gelation conditions and drying method on particles' micromeritics. *Molecules, 24*, 1–12. https://doi.org/10.3390/molecules24061049

Salimi, F., & Farrokh, P. (2023). Recent advances in the biological activities of microbial exopolysaccharides. *World Journal of Microbiology and Biotechnology, 39*, 1–22. https://doi.org/10.1007/s11274-023-03660-x

Santos, M. S., Nogueira, M. A., & Hungria, M. (2019). Microbial inoculants: Reviewing the past, discussing the present and previewing an outstanding future for the use of beneficial bacteria in agriculture. *AMB Express, 9*, 1–22. https://doi.org/10.1186/s13568-019-0932-0

Savić Gajić, I. M., Savić, I. M., & Svirčev, Z. (2023). Preparation and characterization of alginate hydrogels with high water-retaining capacity. *Polymers, 15*, 1–13. https://doi.org/10.3390/polym15122592

Schalk, I. J. (2025). Bacterial siderophores: Diversity, uptake pathways and applications. *Nature Reviews Microbiology, 23*, 24–40. https://doi.org/10.1038/s41579-024-01090-6

Sedlacek, P., Slaninova, E., Koller, M., Nebesarova, J., Marova, I., Krzyzanek, V., & Obruca, S. (2019). PHA granules help bacterial cells to preserve cell integrity when exposed to sudden osmotic imbalances. *New Biotechnology, 49*, 129–136. https://doi.org/10.1016/j.nbt.2018.10.005

Serrato, R. V. (2022). Bacterial alginate biosynthesis and metabolism. In Dr. I. A. A. Severo, Dr. A. B. Mariano, & Dr. J. V. C. Vargas (Eds.), *Alginate - applications and future perspectives* (Vol. 1). IntechOpen. doi:https://doi.org/10.5772/intechopen.109295.

Shailendra Singh, G. G. (2015). Plant growth promoting rhizobacteria (PGPR): Current and future prospects for development of sustainable agriculture. *Journal of Microbial & Biochemical Technology, 7*, 96–102. https://doi.org/10.4172/1948-5948.1000188

Shcherbakova, E. N., Shcherbakov, A. V., Rots, P. Y., Gonchar, L. N., Mulina, S. A., Yahina, L. M., … Chebotar, V. K. (2018). Inoculation technology for legumes based on alginate encapsulation. *Agronomy Research, 16*, 2156–2168. https://doi.org/10.15159/AR.18.186

Siti Anis Syaziana, N., Othman, N. M. I., Aida Soraya, S., Ali, T. K. Z., & Musliyana, M. (2024). Isolation and characterization of encapsulated plant growth-promoting *Enterobacter* sp. SA10 for enhancing chili growth. *Journal of King Saud University, Science, 36*, 1–7. https://doi.org/10.1016/j.jksus.2024.103197

Sivakumar, P., Parthasarthi, R., & Lakshmipriya, V. (2014). Encapsulation of plant growth promoting inoculant in bacterial alginate beads enriched with humic acid. *International Journal of Current Microbiology and Applied Sciences, 3*, 415–422. https://www.semanticscholar.org/paper/b608c7a008fb407504a2f3c386c33d348939b2cd.

Skjåk-Bræk, G., Zanetti, F., & Paoletti, S. (1989). Effect of acetylation on some solution and gelling properties of alginates. *Carbohydrate Research, 185*, 131–138. https://doi.org/10.1016/0008-6215(89)84028-5

Song, X., Liu, M., Wu, D., Griffiths, B. S., Jiao, J., Li, H., & Hu, F. (2015). Interaction matters: Synergy between vermicompost and PGPR agents improves soil quality, crop quality and crop yield in the field. *Applied Soil Ecology, 89*, 25–34. https://doi.org/10.1016/j.apsoil.2015.01.005

Souza-Alonso, P., Rocha, M., Rocha, I., Ma, Y., Freitas, H., & Oliveira, R. S. (2021). *Encapsulation of Pseudomonas libanensis in alginate beads to sustain bacterial viability and inoculation of Vigna unguiculata under drought stress., 3 Biotech, 11*, 1–12. https://doi.org/10.1007/s13205-021-02818-4

Strobel, S. A., Allen, K., Roberts, C., Jimenez, D., Scher, H. B., & Jeoh, T. (2018). Industrially-scalable microencapsulation of plant beneficial bacteria in dry cross-linked alginate matrix. *Industrial Biotechnology, 14*(3), 138–147. https://doi.org/10.1089/ind.2017.0032

Strobel, S. A., Knowles, L., Nitin, N., Scher, H. B., & Jeoh, T. (2020). Comparative technoeconomic process analysis of industrial-scale microencapsulation of bioactivities in cross-linked alginate. *Journal of Food Engineering, 266*, 1–8. https://doi.org/10.1016/j.jfoodeng.2019.109695

Tal, S., & Okon, Y. (1985). Production of the reserve material poly-β-hydroxybutyrate and its function in *Azospirillum brasilense* cd. *Canadian Journal of Microbiology, 31*, 608–613. https://doi.org/10.1139/m85-115

Trujillo-Roldán, M. A., Monsalve-Gil, J. F., Cuesta-Álvarez, A. M., & Valdez-Cruz, N. A. (2015). La producción, el peso molecular y el poder viscosificante del alginate producido por *Azotobacter vinelandii* es afectado por la fuente de carbono en cultivos sumergidos. *DYNA (Colombia), 82*, 21–26. https://doi.org/10.15446/dyna.v82n194.44201

Urtuvia, V., Maturana, N., Acevedo, F., Peña, C., & Díaz-Barrera, A. (2017). Bacterial alginate production: An overview of its biosynthesis and potential industrial production. *World Journal of Microbiology and Biotechnology, 33*, 1–10. https://doi.org/10.1007/s11274-017-2363-x

Vejan, P., Khadiran, T., Abdullah, R., Ismail, S., & Dadrasnia, A. (2019). Encapsulation of plant growth promoting rhizobacteria—Prospects and potential in agricultural sector: A review. *Journal of Plant Nutrition, 42*, 2600–2623. https://doi.org/10.1080/01904167.2019.1659330

Yoneyama, F., Yamamoto, M., Hashimoto, W., & Murata, K. (2015). Production of polyhydroxybutyrate and alginate from glycerol by *Azotobacter vinelandii* under nitrogen-free conditions. *Bioengineered, 6*, 209–217. https://doi.org/10.1080/21655979.2015.1040209

10.2 BIOTRANSFORMATION OF FERULIC ACID INTO VALUABLE PRODUCTS EMPLOYING HALOPHILIC BACTERIUM *HALOMONAS NEPTUNIA*

Biocatalysis and Agricultural Biotechnology 66 (2025) 103586

Contents lists available at ScienceDirect

Biocatalysis and Agricultural Biotechnology

journal homepage: www.elsevier.com/locate/bab

Biotransformation of ferulic acid into valuable products employing halophilic bacterium *Halomonas neptunia*

Vendula Hrabalová, Diana Černayová, Jakub Nábělek, Filip Matějka, Jaromír Pořízka, Pavel Diviš, Stanislav Obruča *

Institute of Food Chemistry and Biotechnology, Faculty of Chemistry, Brno University of Technology, Purkynova 118, 612 00, Brno, Czech Republic

ARTICLE INFO

Keywords:
Halomonas neptunia
Halophiles
Ferulic acid
Biotransformation
Vanillic acid
Encapsulation

ABSTRACT

This study investigates the potential of the halophilic bacterium *Halomonas neptunia* for the biotransformation of ferulic acid (FA) into valuable aromatic compounds, with a focus on vanillic acid (VA). *H. neptunia* demonstrated high efficiency in FA conversion, producing VA as the predominant metabolite alongside minor amounts of vanillin, vanillyl alcohol, and 4-vinylguaiacol. A key advantage of *H. neptunia* is its halotolerance, enabling biotransformation at NaCl concentrations up to 10 wt. %, which significantly reduces contamination risks from common mesophilic microflora and facilitates non-sterile process operation. *H. neptunia* cells were encapsulated in alginate-based hydrogel beads using a semi-automated encapsulation system to enhance the efficiency and reusability of the bacterial culture. Encapsulation markedly improved the transformation efficiency of FA (initial concetration of 500 mg/L), with VA concentrations reaching 370 mg/L and conversion rate 85.5 mol. % after 72 h in the first cycle. In subsequent cycles, the initial FA concentration was increased to 460 mg/L. Nearly complete conversion of FA to VA was observed, suggesting a highly positive effect of adaptation of the bacterial culture to the presence of FA. The process demonstrated stability across multiple cycles, supporting its potential for semi-continuous or continuous operation. Additionally, crude FA extracted from wheat bran was successfully used as a substrate without requiring extensive purification, further enhancing the process's sustainability. These findings highlight *H. neptunia* as a promising candidate for industrial-scale FA biotransformation, offering a robust, low-contamination, and scalable approach to producing high-value aromatic compounds.

1. Introduction

Ferulic acid (FA) is a phenolic substance of natural origin that is a common component of plant biomass. In plants, this substance is found either as a free molecule or predominantly, it is covalently bound to lignin and hemicelluloses, and it contributes significantly to the structure and mechanical properties of the plant cell wall (Mathew, 2008). A relatively simple isolation process can obtain ferulic acid from a wide range of plant sources, including food industry waste materials such as wheat or corn bran (Gopalan and Nampoothiri, 2018), brew spent grains (Al-Shwafy et al., 2023), or pineapple peels (Tang, 2020). Ferulic acid is a very interesting substance, which, due to its anti-oxidative and anti-microbial effects, is considered a very valuable natural food additive that has the potential to significantly increase the stability and shelf life of many foods or replace some synthetic excipients. Furthermore, its

* Corresponding author.
E-mail address: obruca@fch.vut.cz (S. Obruča).

https://doi.org/10.1016/j.bcab.2025.103586
Received 24 February 2025; Accepted 13 April 2025
Available online 14 April 2025

anti-inflammatory, anti-thrombotic, and anti-cancer activities suggest numerous applications in pharmaceutics, healthcare, and cosmetics (Mussatto et al., 2007).

Ferulic acid can also be used as a precursor for the production of other substances with even significantly higher added and market value. A prime example is the microbial biotransformation of ferulic acid to vanillin and its derivates, primarily vanillic acid (VA) and vanillyl alcohol. These are substances that are generally known for their characteristic "vanilla" taste and smell and are therefore used in the food industry as flavoring agents (Martau et al., 2021). Beyond their sensory properties, vanillin derivatives also possesses numerous valuable characteristics. For example, VA is known to inhibit undesirable oxidative and inflammatory processes, stimulate the immune system, and protect the nervous system, liver, and cardiovascular system. These important pharmaceutical activities suggest that vanillic acid may be a valuable active ingredient in the treatment of conditions such as Alzheimer's disease, obesity, and diabetes (Ingole et al., 2021).

Another important metabolite of FA is 4-vinylguaiacol (4VG), which has been shown to possess potent anticancer activities against drug-resistant human colorectal cancer cells (Li et al., 2019) and also acts as an inhibitor of the epidermal growth factor receptor in human breast cancer cells (Sudhagar et al., 2018). Beyond its anticancer properties, 4VG is also valued in the pharmaceutical, cosmetic, and food industries due to its flavor and fragrance properties (Sunao et al., 2016).

At the same time, vanillin and its derivatives are also of great interest from a materials chemistry point of view as components for preparing and modifying the properties of many polymeric materials (Zhang et al., 2015; Rigo et al., 2024).

As indicated above, the metabolic activity of microorganisms can prepare vanillin and its derivatives from ferulic acid. Many microorganisms have been shown to convert FA to vanillin and related compounds. These include yeasts such as *Saccharomyces cerevisiae* (Huang et al., 1993) or *Rhodotorula mucilaginosa* (Bettio et al., 2021), fungi belonging to the genus *Aspergillus* (Tang, 2020), and bacteria such as *Bacillus subtilis* (Chen et al., 2016), *Cupriavidus* sp. B-8 (Chai et al., 2013), *Pseudomonas putida* (Yamada et al., 2007), *Streptomyces sannensis* (Ghosh et al., 2007), *Streptomyces setonii* (Muheim and Lerch, 1999), or *Amycolaptosis* sp. CSW4 (Xiao-kui and Andrew, 2014). Several metabolic pathways are known to convert ferulic acid to vanillin and its derivatives. The specific metabolic process and the range of products formed depend primarily on the microorganism used and partly on the process conditions. Besides microorganisms that transform ferulic acid through homologous metabolic pathways, many studies and processes utilize metabolic engineering tools, with most cases employing strains of *Escherichia coli* as the biological platform (Chen et al., 2017; Yoon et al., 2005; Yoon et al., 2007; Lee et al., 2009).

Traditional microbial biotechnology processes using pure cultures of mesophilic microorganisms often suffer from relatively low-cost competitiveness when there is a chemical-based alternative to produce the same product. A key factor is the susceptibility of these bioprocesses to contamination. Maintaining sterility add significant costs and often prevents the implementation of advantageous continuous or semi-continuous cultivation One of the main reasons for this is the susceptibility of the classical biotechnological process to contamination by common microflora, which entails high costs to ensure the sterility of the process and also usually hinders the possibility of realizing production in the form of advantageous continuous or semi-continuous cultivation. A possible solution to this serious limitation is the concept of Next-Generation Industrial Biotechnology (NGIB), which uses extremophilic microorganisms as production units. These organisms have adapted during evolution to extreme environments such as high osmotic strength of the environment, high/low temperature, or extreme pH values. These extreme conditions typically prevent significant contamination in NGIB processes. This dramatically reduces equipment and energy demands while facillitating continous cultivationn (Chen et al., 2018).

While mesophillic microorganisms have been the primary focus for the ferulic acid biotransformation, the potential of extremophiles has been largely unexplored. There are very few reports on the utilization of thermophilic (Hrabalová et al., 2024) or halophilic microorganisms (Tang et al., 2022; Vyrides et al., 2015) for the biotransformation of ferulic acid. However, the conversion of ferulic acid to vanillin and its derivatives following the concept of next-generation industrial biotechnology may represent both a technologically and an economically significant advantage.

Halomonas species are halophilic bacteria that thrive inhigh–salinity environments, typically preferring 5–25 wt% NaCl. They are gram-negative, heterotrophic, obligately aerobic gamma-proteobacteria with relatively low nutritional requirements and high catabolic and metabolic flexibility. Some *Halomonas* strains have found applications in NGIB due to their properties, particularly as promising producers of biopolymers like polyhydroxyalkanoates (Rizki et al., 2023) and polysaccharides (Llamas et al., 2006). They can produce technologically important enzymes, known as extremozymes (*Halomonas* strain WDG195), as well as various low-molecular-weight compounds, including ectoins (Fatollahi et al., 2021), 3-hydroxybutyrate and oxaloacetate, and tetrahydropyrimidine. They have also shown promise as plant growth-promoting bacteria (A novel halophilic *Halomonas* sp), and in the degradation of anthropogenic pollutants like polyaromatic hydrocarbons (Halomonas capable of degrading polyaromatic) and phenol (Haddadi and Shavandi, 2013). The original scientific literature includes references describing some members of the genus *Halomonas* for biotransformation of ferulic acid (Tang et al., 2022; Vyrides et al., 2015; Abdelkafi et al., 2006; Abdelkafi et al., 2008).

Bearing in mind NGIB concept with halophilic bacteria, we screened several *Halomonas* species for their ability to biotransform ferulic acid. These include *H. halophila* CCM 3662, *H. organivorans* CCM 7142T, *H. elongata* CCM 3756, *H. neptunia* CCM 7107 and *H. hydrothermalis* CCM 7104. Among all the tested strains, *Halomonas neptunia* CCM 7107 demonstrated the highest potential. Consequently, we decided to investigate its biotransformation capabilities, optimize key cultivation parameters to enhance process efficiency, and test the feasibility of encapsulating the bacterial cells in a gel-based matrix. This approach represents a promising step toward developing a sustainable continuous process for ferulic acid biotransformation.

2. Materials and Methods

2.1. Microorganisms and cultivations

Halophilic bacterial strains *H. halophila* CCM 3662, *H. organivorans* CCM 7142T, *H. elongata* CCM 3756, *H. neptunia* CCM 7107 and *H. hydrothermalis* CCM 7104 were purchased from the Czech Collection of Microorganisms, Brno, Masaryk University.

H. halophila was cultivated aerobically in 100 mL Erlenmeyer flasks at 30 °C with constant agitation (180 rpm) for 24 h in a complex medium (50 mL) consisting of 15 g/L peptone, 3 g/L yeast extract, 66 g/L NaCl, and 1 g/L glucose. *H. elongata* was cultivated in a complex medium consisting of 5 g/L nutrient broth, 30 g/L NaCl and 1 g/L $MgCl_2 \bullet 6\ H_2O$ with the same cultivation conditions as *H. halophila*. The halophilic bacterial strains *H. organivorans*, *H. neptunia* and *H. hydrothermalis* were cultivated in a complex medium consisting of 10 g/L yeast extract, 5 g/L peptone, 1 g/L glucose, 81 g/L NaCl, 9.6 g/L $MgSO_4 \bullet 7\ H_2O$, 7 g/L $MgCl_2 \bullet 6\ H_2O$, 0.36 g/L $CaCl_2 \bullet 2\ H_2O$, 2 g/L KCl, 0.06 g/L $NaHCO_3$, 0.026 g/L NaBr, again under the same cultivation conditions as previous strains.

The mineral medium used for the experiment consisted of 3 g/L $(NH_4)_2SO_4$, 11.1 g/L $Na_2HPO_4 \bullet 12\ H_2O$, 1.05 g/L KH_2PO_4, 0.2 g/L $MgSO_4 \bullet 7\ H_2O$ and the appropriate amount of NaCl for each bacterial strain (as for the complex medium). After sterilization, 20 g/L glucose and 1 mL/L MES trace element solution were added to the media.

The complex medium was inoculated with 1 mL of cryo-culture, which was stored at −80 °C in 10 % glycerol. After being cultivated for 24 h, the bacterial culture was centrifuged at 3460×*g* for 5 min and then resuspended in a new medium of the same composition, with the addition of commercial ferulic acid (purchased from Merck).

During the cultivation of individual bacterial strains, screening was performed to select suitable bacteria for further biotransformation experiments. Key parameters such as optical density and, in particular, the concentration of compounds formed by ferulic acid biotransformation were regularly sampled and evaluated. For analyses, 10 mL of cell suspension was collected and subsequently centrifuged (5 min at 3460×*g*). The supernatants obtained were measured using HPLC-UV-Vis to quantify FA and its biotransformation metabolites.

2.2. Encapsulation of microbial culture into alginate-gel microbeads

The grown bacterial culture of *H. neptunia* (50 mL) was centrifuged (5 min, 3460×*g*), and the supernatant was removed. The bacterial pellet was then resuspended in phosphate buffer containing 2 wt% alginate. From this mixture, alginate beads were prepared using an encapsulator (BUCHI B-395) with set parameters of 1200 V and 370 Hz, under constant airflow. To form microbeads of uniform size, a nozzle with a diameter of 750 μm was used, while calcium chloride (2 wt%) served as the gelation agent. The solution with encapsulated bacteria was constantly stirred to prevent microbead agglomeration. After 20 min of gelation time, microbeads were filtered out of $CaCl_2$ using filtration paper (KA 1, Verkon). This was followed by standard cultivation on tempered shakers with sampling at 0, 24, 48, 72, and 144 h to assess the ability of the encapsulated microbial culture to biotransform FA into value-added substances. After the last sampling, the encapsulated particles were again filtered from the media and transferred to fresh media of 50 mL volume with NaCl (50 g/L). Even in the second step of incubation, samples were collected at 0, 24, 48, 72, and 144 h during the culture to assess the activity of the encapsulated microbial culture.

2.3. Ferulic acid isolation from wheat bran

Ferulic acid was extracted from wheat bran obtained from Mlýny J. Voženílek, s.r.o. Wheat bran (25 g/L) was treated with 0.5 M sodium hydroxide, heated to 50 °C, and stirred for 4 h. The pH was then adjusted to 3 using HCl, and the mixture was centrifuged (5190×*g*, 10 min) to collect the supernatant. XAD-16 adsorbent (1 g per 150 ml) was added to the supernatant and stirred for 50 min at room temperature. After adsorption, the adsorbent was removed, washed, and desorbed using 0.5 wt. % NaOH. The resulting solution was stirred for 50 min and then neutralized with HCl. Neutralization with HCl generates NaCl, which is beneficial as the employed bacterium requires it for growth. The process of isolating ferulic acid had a yield of 30.3 ± 3.8 %. The low yield was likely due to the co-adsorption of other components from the wheat bran, primarily proteins.

2.4. Analytical methods

During the cultivation process, samples were collected, and the concentration of potential metabolites of FA biotransformation was measured. For the analyses, 10 mL of cell suspension was collected and centrifuged (5 min; 3460×*g*). High-Performance Liquid Chromatography with Ultraviolet/Visible Spectroscopy (HPLC-UV-Vis) using a LC-10AD system (Shimadzu, Kyoto, Japan) was employed to quantify FA and its biotransformation metabolites in the resulting supernatants. HPLC separation was performed using gradient elution on a Kinetex® 2.6 μm EVO C18 100 Å 150 × 4.6 mm column at 35 °C and 250 bar. The mobile phase consisted of acetonitrile and 0.1 % acetic acid. The gradient program was as 0.6 mL/min, and the injection volume was 10 μL. Ferulic acid (FA), vanillic acid (VA), vanillyl alcohol (VOH), vanillin (VAN), and 4-vinyl guaiacol (4VG) (all purchased from Merck) were used as external standards. Detection was performed with a PDA detector using the following wavelength: FA – 330 nm; VOH and 4VG – 230 nm; VA and VAN – 280 nm. The media's optical density at 630 nm (distilled water was used as blank) was also measured spectrophotometrically for each culture.

3. Results and discussion

3.1. Screening of biotransformation potential in selected halophilic bacteria

The genus *Halomonas* is well known for its ability to thrive in high-salt environments, making it a strong candidate for industrial biotechnology applications. These bacteria can synthesize various industrially relevant biomolecules under non-sterile conditions, significantly reducing process costs and complexity (Biswas et al., 2023). In the first step of our study, we conducted an experimental screening of different *Halomonas* strains. The primary objective was to evaluate their capacity to metabolically degrade FA and convert it into valuable metabolites, specifically focusing on the formation of VA and 4VG (See Table 1).

Biotransformation using halophilic bacteria was effectively demonstrated with the strains *Halomonas organivorans* and *Halomonas neptunia*, which converted FA into vanillic acid via their metabolic pathways. Both bacterial strains exhibited very high efficiency of FA elimination (98–100 %), indicating their extraordinary efficiency respect to FA degradation. The conversion efficiency of FA to VA for *H. organivorans* reached 15 wt%, whereas *H. neptunia* achieved a notably higher value of 59 wt%. *H. neptunia* is an intriguing bacterium that has already been identified as a promising producer of bioprotectants ectoines from waste cheese whey (Orhan and Ceyran, 2024). Additionally, it has been reported as a potential candidate for the biotechnological production of polyhydroxyalkanoates—microbial bioplastics—using waste frying oils as a substrate (Pernicova et al., 2019), and industrially relevant enzymes (Orhan and Akincioglu, 2020). It was also reported that the bacterium reveals desirable metabolic features with respect to the transformation of aromatic compounds; in particular, it was capable of bioconversion of tyrosol into hydroxytyrosol and 3,4-dihydroxyphenylacetic acid (Liebgott

Table 1
Screening of selected bacterial strains.

Bacterial strain	Decrease of FA [%]	VA*	4VG*
H. halophila (CCM 3662)	2		
H. organivorans (CCM 7142T)	98		
H. elongata (CCM 3756)	58		
H. neptunia (CCM 7107)	100		
H. hydrothermalis (CCM 7104)	60		

* green color indicates those strains that were able to biotransform FA with an initial concentration of 500 mg/L into value-added substances with a concentration >50 mg/L (10%)

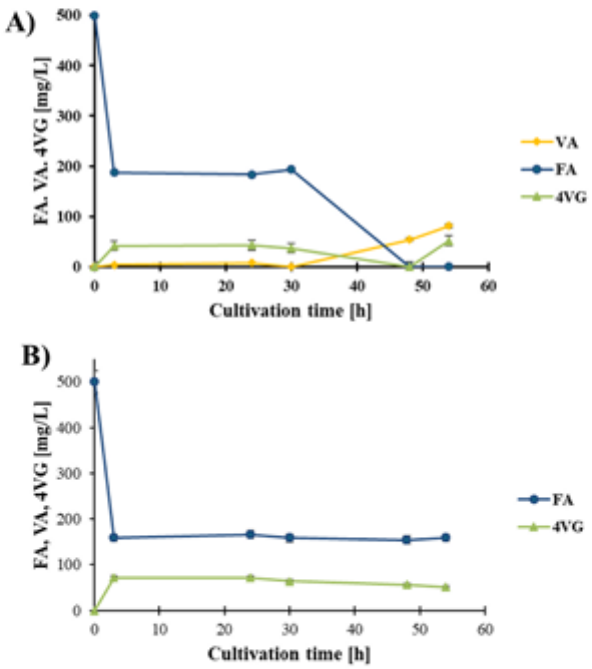

Fig. 1. Biotransformation of FA in A) complex cultivation medium and B) mineral medium by employing *H. neptunia*, cultivation conditions: 30 °C, 180 rpm, inotial concentration of NaCl was 500 mg/L.

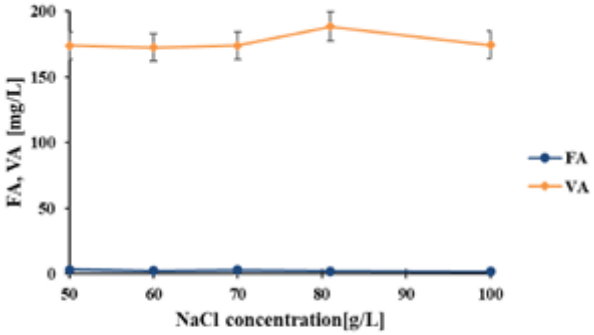

Fig. 2. Influence of initial NaCl concentration in the mineral medium on FA biotransformation by empyloing *H. neptunia*, results measured after 72 h of cultivation using an initial FA concentration was set at 500 mg/L.

Table 2
Identification of the optimal initial concentration of FA for its biotransformation by *H. neptunia* (after 72 h).

Residual concentration of FA and its metabolites	*Initial concentration of ferulic acid* [mg/L]				
	300	500	600	800	1000
Ferulic acid [mg/L]	6.3 ± 0.4	2.8 ± 0.2	167.4 ± 11.2	194.5 ± 13.2	246.3 ± 15.4
Vanillic acid [mg/L]	85.0 ± 5.0	120.1 ± 4.2	26.9 ± 0.8	48.3 ± 2.1	2.8 ± 0.1
4-vinylguaiacol [mg/L]	n. d.	n. d.	n. d.	n. d.	208.2 ± 21.7

et al., 2007). These findings clearly demonstrate the biotechnological significance, metabolic versatility, and robustness of this bacterium. Our results indicate that this halophilic bacterium could also be considered a promising chassis for the biotransformation of FA.

3.2. Identification of crucial parameters of FA biotransformation while employing H. neptunia

In further experiments, we aimed to identify and investigate the key parameters that could influence the biotransformation of FA into high-value metabolites. First, we examined the effect of the cultivation medium. To this end, we cultivated *H. neptunia* in the presence of 500 mg/L of FA using either a complex or a mineral medium. The results are presented in Fig. 1.

Based on the results, the complex medium was selected for further biotransformation experiments. This decision was driven by the observation that, over time, *H. neptunia* was able to completely metabolize FA in the complex medium, actively excreting VA and 4VG into the cultivation medium. The molar yield of VA and 4VG reached 18.8 mol. % and 13.4 mol. % for VA and 4VG, respectively, after 54 h of cultivation in a complex medium. In contrast, when the mineral medium was used, the FA concentration decreased only during the initial 3 h of cultivation and remained nearly unchanged throughout the experiment. A possible explanation is that some enzymes involved in FA metabolism may require specific co-factors (e.g., metal ions, vitamins) that are readily available in complex media but absent or limited in mineral media, which could account for incomplete FA metabolism in the mineral medium. Furthermore, since FA metabolism is typically a redox-driven process (Xu et al., 2024), another contributing factor could be differences in the redox balance between the two cultivation media. Certain metabolic pathways require electron donors or acceptors (e.g., NADH, $FADH_2$), which are more readily available in complex media, potentially enhancing FA transformation. Nevertheless, all subsequent experiments were conducted using the complex medium.

Another key cultivation parameter investigated concerning FA transformation was the NaCl concentration in the cultivation medium. NaCl is essential for the halophilic bacterial strain's survival and helps prevent contamination by common mesophilic microorganisms from the surrounding environment (Dutta and Bandopadhyay, 2022). Fig. 2 shows that salinity between 50 and 100 g/L does not substantially affect *H. neptunia*'s biotransformation of FA since FA was almost completely eliminated and converted to VA with 43.5 mol% efficiency. From a biotechnological and industrial perspective, this is advantageous, as the salt concentration can be adjusted according to external conditions without disrupting the biotransformation process. Economically, the process is more cost-effective due to lower salt requirements, while maintaining high yields and enhanced robustness against contamination. For further experiments, NaCl concentration of 81 g/L, identified as optimal for our strain (Orhan and Ceyran, 2024), was selected.

Furthermore, we investigated the impact of the initial FA concentration on the biotransformation efficiency of *H. neptunia*. The results are presented in Table 2. The initial FA concentration was tested in the range of 300–1000 mg/L. The highest transformation efficiency was achieved at an FA concentration of 500 mg/L, which resulted in the highest conversion rate to VA (27.7 mol. %).

A further increase in FA concentration led to incomplete metabolization of FA, as indicated by a high residual FA concentration in the cultivation medium after incubation, and a decrease in VA yields. At the highest initial FA concentration tested, bacterial metabolism shifted, with 4VG becoming the predominant product (26.9 mol.% conversion). A similar effect was recently described in *C. thermodepolymerans*, where high FA concentrations primarily resulted in vanillyl alcohol production, while lower FA doses favored VA formation (Hrabalová et al., 2024). Thus, in the case of *H. neptunia*, excessive FA loading may shift the biotransformation pathway

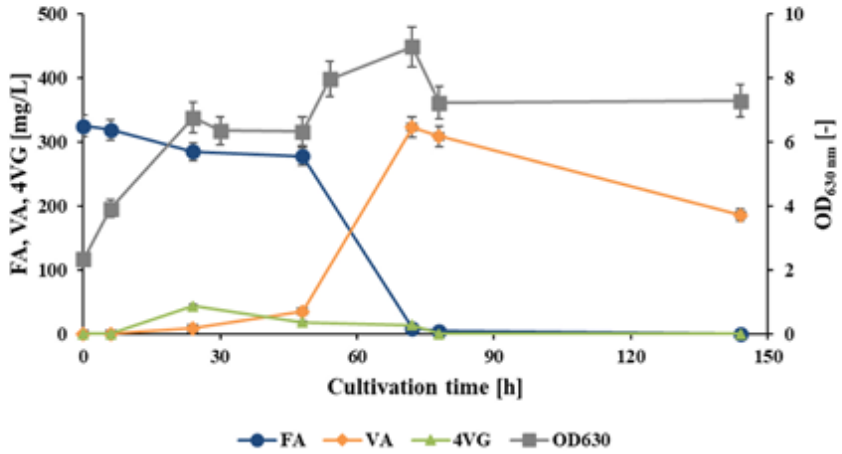

Fig. 3. Growth curve of *H. neptunia* in complex medium with 500 mg/L FA, and biotransformation curve of FA conversion to VA as a function of time, 30 °C, 180 rpm, 81 g/L NaCl.

Table 3
Concentration of the resulting sensory active compounds from cultivation solely on crude FA isolated from wheat bran and on crude FA obtained from what bran supplemented with complex medium components.

	crude FA				Crude FA + complex medium			
c [mg/L]	0 h	48 h	72 h	144 h	0 h	48 h	72 h	144 h
FA	640.4 ± 20.1	9.7 ± 0.2	9.5 ± 0.5	6.9 ± 0.2	640 ± 20	200 ± 16	n. d.	4 ± 1
VA	n. d.	2.8 ± 0.2	3.4 ± 0.4	2.8 ± 0.1	n. d.	n. d.	92 ± 1	n. d.
VAN	n. d.	4.9 ± 0.1	4.4 ± 0.8	5.5 ± 0.5	n. d.	n. d.	n. d.	n. d.
4VG	n. d.	n. d.	160.2 ± 20.6	n. d.	n. d.	160 ± 20	170 ± 30	150 ± 10

from VA towards 4VG, which could be exploited for technological applications to selectively obtain the desired product.

In the next phase of the experiment, we decided to follow the time course of biotransformation of the FA process under optimized conditions by analysis of FA and respective metabolites as well as the optical density of the bacterial culture (OD630 nm) during the cultivation; the results are shown in Fig. 3. During the growth of the bacterial culture in the presence of FA, a rapid increase in biomass was observed from the beginning of cultivation, without a detectable lag phase. Subsequently, the growth curve entered a stationary phase until the 48th hour. From this point onward, a renewed growth phase accompanied by slight fluctuations in optical density was observed. The maximum optical density was recorded at the 72 nd h of cultivation, aligning with optimization experiments that identified this time point as critical for biotransformation. The data indicate that the bacterium effectively transformed FA, partially metabolizing it while primarily converting it into high-value-added substances. The period between 48 and 72 h can be considered the key phase for biotransformation, as the major conversion of FA to VA (~320 mg/L) occurred during this time. The conversion efficiency of FA to vanillic acid at 72 h reached nearly 79 wt%, highlighting *H. neptunia* as a highly promising candidate for this biotransformation process. Further prolongation of cultivation resulted in a decrease in VA, indicating that, in the late stationary phase, the bacterial culture could further metabolize VA, likely due to the exhaustion of other external carbon sources present in the complex medium.

3.3. Employment of H. neptunia for biotransformation of crude FA isolated from wheat bran

FA is a key component of lignin in lignocellulosic materials, where it is bound to polysaccharides via ester linkages (Oliveira et al., 2015). FA can be easily isolated from various low-cost lignocellulosic sources, including wheat bran, a major byproduct of cereal processing (Pazo-Cepeda et al., 2020). In this study, FA was extracted via alkaline hydrolysis, followed by sorption onto a specialized resin. The crude FA obtained through this simple and robust approach cannot be considered a pure compound, as it contains various impurities, including proteins and carbohydrates. Nevertheless, we propose that such contaminants do not act as significant inhibitors of bacterial metabolism. Therefore, even crude FA derived from wheat bran can serve as a viable substrate for the biotransformation into VA or 4-vinylguaiacol 4VG by *H. neptunia*, without requiring costly and technologically complex purification steps. Furthermore, since alkaline hydrolysis is carried out using NaOH, followed by neutralization with HCl, the resulting crude FA contains a high concentration of NaCl. Therefore, the use of a halophilic bacterium is highly advantageous, as it can thrive in such saline conditions, making the biotransformation process more efficient and robust.

We employed two different approaches for cultivating *H. neptunia* on crude FA isolated from wheat bran. At first, only crude FA was used as a cultivation medium, providing that impurities present in crude FA may serve as nutrient sources for bacterial culture. It should be pointed out that the FA concentration of the crude FA solution reached 640 mg/L, which is very close to the optimal FA

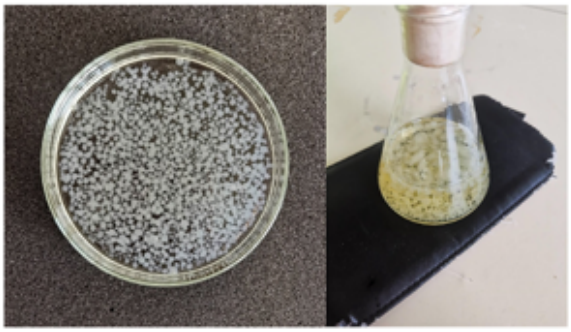

Fig. 4. *H. neptunia* encapsulated in alginate and transferred to a complex medium in an Erlenmeyer flask containing ferulic acid.

concentration for VA production. The results are shown in Table 3.

On crude FA, 4VG was the major product of FA metabolism, with the highest titer (160 ± 20 mg/L; 32.3 mol. %) obtained after 72 h of cultivation. Other phenolic compounds resulting from the biotransformation of ferulic acid, such as VA and vanillin, were detected in lower concentrations. In this case, the conversion efficiency of ferulic acid to 4VG reached approximately 33 wt%. By 48 h, nearly all FA had been consumed, suggesting that the bacteria utilized it as a primary carbon source for metabolic and energy processes, particularly under conditions where rich nutrient sources were limited.

In addition to cultivating *H. neptunia* solely on crude FA derived from wheat bran, we also conducted an experiment supplementing the crude FA with nutrients from a complex medium (Table 3). Results from cultivation on hydrolysate supplemented with complex medium components were even more promising. In addition to 4VG, which was again detected at the dominant metabolite with highest concentration at 72 h of incubation (170 ± 30 mg/L), a high concentration of VA was also measured at hour 72 (92 ± 1 mg/L). When cultivated on hydrolysate supplemented with a complex medium, the bacteria likely utilized the complex medium components as the primary carbon sources, with FA playing only a minor role, as indicated by its high concentration after 48 h. Successful conversion to vanillic acid was observed after 72 h, with a conversion yield of nearly 15 wt%, confirming the optimal biotransformation timeframe. Simultaneously, 4VG was successfully produced (170 mg/L, 34.3 mol.% conversion). Notably, metabolization of the crude FA resulted primarily in 4VG.

As demonstrated, 4VG is the main product of FA transformation by *H. neptunia* when the culture is overloaded with FA. It is highly likely that, in the case of crude FA, the bacterial culture was exposed not only to moderate concentrations of FA but also to other phenolic compounds, which contributed to metabolic overload and shifted the transformation pathway toward 4VG as the dominant product—whereas in the case of pure FA, this metabolic shift was observed only at significantly higher FA concentrations (see Table 2).

Based on the obtained results, the probable metabolic pathway of FA conversion in *H. neptunia* can be deduced. At the beginning of the biotransformation, a significant amount of 4-vinylguaiacol 4VG is formed (see Fig. 3). Notably, 4VG is also the primary metabolite of FA transformation by *H. neptunia* when the bacterial culture is overloaded with FA. This suggests that the initial step in FA metabolism in *H. neptunia* is the non-oxidative decarboxylation of FA into 4VG. It is highly likely that 4VG is subsequently converted into vanillin. However, vanillin was rarely detected in our experiments, and its concentration was typically very low. The most probable reason for this is that vanillin undergoes quick further intracellular conversion, specifically oxidation to VA, which is excreted by the cells as the major transformation product of FA metabolism in *H. neptunia*. A similar metabolic pathway for FA transformation—i.e., the decarboxylation of FA to 4VG, conversion of 4VG to vanilin and oxidation of vanillin to VA—has already been described in several bacterial strains, such as *Streptomyces setonii* (Max et al., 2012) and *Enterobacter* spp. (Hunter et al., 2012).

The ability to selectively control the major products (4VG or VA) by adjusting simple cultivation parameters like time or initial FA concentration is a significant technological advantage. Furthermore, a deeper understanding of FA metabolism in *H. neptunia* and the identification of key enzymes and their corresponding genes would be highly beneficial. This would serve as the initial step toward leveraging metabolic engineering tools to further enhance the process—both in terms of yield and efficiency—and to direct it toward the production of specific desired metabolites.

3.4. Encapsulation of H. neptunia culture for biotranfotrmation of FA

Encapsulation of microbial cultures in biotechnology offers several significant advantages. Firstly, it enables the reuse of microbial cells without the need for repeated propagation and cultivation, which positively impacts process economics. Another key benefit of culture encapsulation is its ability to facilitate the transformation reaction in a continuous flow system. When cells are entrapped within a gel matrix, the risk of leaching from the reactor is eliminated.

Consequently, several research groups have explored the use of immobilized microbial cultures for FA biotransformation. For instance, Yan et al. successfully immobilized *Bacillus subtilis* for semi-continuous vanillin production from FA (Yan et al., 2016). However, in practical applications, microbial contamination remains a major challenge in continuous cultures, even when using immobilized cells. A promising solution to this issue is the utilization of halophilic bacteria such as *H. neptunia*, which thrive in high-salinity environments. The elevated salinity of the cultivation medium significantly reduces the risk of contamination, making

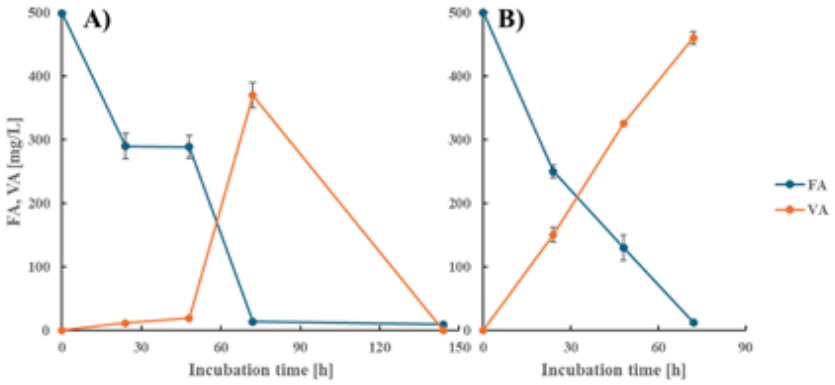

Fig. 5. FA biotransformation into VA by encapsulated culture of *H. neptunia* during the first A) and second B) incubation cycle; mineral medium, 81 g/L NaCl, 30 °C, 180 rpm.

these systems more robust for long-term operation.

We therefore investigated the potential of encapsulating *H. neptunia* in an alginate gel matrix for FA biotransformation. The entrapment of microbial cells within a suitable hydrogel is considered a promising approach, as it is gentle on the cells while providing desirable properties and efficiency. Alginate is widely recognized as an effective material for microbial cell encapsulation, offering numerous advantages across various applications. For instance, the encapsulation of *Bifidobacterium animalis* in alginate composites demonstrates the material's ability to form stable, well-organized microparticle structures that protect the bacteria and facilitate their controlled release via Fickian diffusion, making it suitable for applications in dairy fermentation and oral delivery (Vincekovic et al., 2024). Similarly, in agricultural applications, alginate-based formulations have been shown to enhance the shelf stability of microbial inoculants and protect them from environmental stressors (Kucharzyk et al., 2023).

Hence, we developed a protocol for the encapsulation of *H. neptunia* into alginate-based beads using a semi-automatic encapsulator. The detailed protocol for bead preparation is provided in the Materials and Methods section of this article, and the encapsulated beads are visualized in Fig. 4. The encapsulated culture was subsequently incubated in a complex medium supplemented with 500 mg/L FA in the presence of 50 g/L NaCl. Samples were taken at specific time points during cultivation, and after 144 h, the encapsulated bacteria were filtered from the medium and transferred into fresh complex medium, again supplemented with ferulic acid under identical conditions as in the first cycle. The media were sampled at selected time intervals, and all samples were subsequently analyzed by HPLC-UV-Vis, enabling the identification and quantification of FA elimination and VA produced by the *H. neptunia* bacterial culture. The results are shown in Fig. 5.

Cultivation experiments with encapsulated *H. neptunia* show promising results, indicating that encapsulation in alginate hydrogel significantly enhances FA transformation to VA. After 72 h of incubation in the first cycle, the concentration of VA in the medium containing alginate-encapsulated *H. neptunia* reached 370 mg/L, corresponding to a conversion rate of 85.5 mol. %, the highest value observed so far in this study. Moreover, the system demonstrated even greater efficiency in the second cultivation cycle, where the VA concentration reached 460 mg/L after 72 h, corresponding to a complete conversion of FA into VA. This substantial improvement in culture performance between the first and second cycles can be attributed to the adaptation of *H. neptunia* to the presence of FA and the activation of relevant metabolic pathways.

Our findings clearly demonstrate that encapsulating *H. neptunia* in alginate beads significantly enhances FA biotransformation. Furthermore, this process can be operated in a semi-continuous cyclic mode and, potentially, in a fully continuous flow system with high efficiency. The halophillic nature of the culture and the high NaCl concentration also protect the process from contamination by mesophillic microflora.

4. Conclusion

This study represents a pioneering exploration of the biotechnological potential of *Halomonas neptunia* in the biotransformation of FA. Our findings demonstrate that *H. neptunia* is a unique halophilic bacterium capable of efficiently converting FA into valuable aromatic compounds, primarily VA, under high-salinity conditions. Its remarkable halotolerance not only enhances process robustness by minimizing contamination risks but also opens avenues for cost-effective, non-sterile bioprocessing. Additionally, the encapsulation of *H. neptunia* in alginate-based hydrogel beads further improved the transformation efficiency and reusability of the bacterial culture, highlighting the feasibility of a semi-continuous or even fully continuous process.

Given these promising results, further research should focus on several key areas to maximize the industrial applicability of *H. neptunia* in FA biotransformation. First, a comprehensive metabolic and genomic analysis of this bacterium is needed to elucidate the enzymatic pathways involved in FA conversion. Such insights will provide the foundation for targeted metabolic engineering strategies to enhance product specificity and yield. Second, further optimization of microbial encapsulation techniques, including modifications in hydrogel composition and bead stability, could enhance the longevity and efficiency of the biocatalyst. Finally, the most critical step in advancing this process toward industrial application is the verification of a fully continuous flow

biotransformation system. This would allow for uninterrupted FA conversion, further increasing productivity and economic viability.

Overall, this pilot study underscores the enormous potential of *H. neptunia* in sustainable biotransformation processes, paving the way for next-generation industrial biotechnology applications that leverage halophilic microorganisms for high-value biochemical production.

CRediT authorship contribution statement

Vendula Hrabalová: Investigation, Visualization, Writing – original draft. **Diana Černayová:** Investigation, Writing – review & editing. **Jakub Nábělek:** Investigation, Writing – review & editing. **Filip Matějka:** Investigation. **Jaromír Pořízka:** Investigation, Writing – review & editing. **Pavel Divis:** Funding acquisition, Writing – review & editing. **Stanislav Obruča:** Conceptualization, Supervision, Writing – original draft.

Declaration of competing interest

The authors declare the following financial interests/personal relationships which may be considered as potential competing interests: Pavel Divis reports a relationship Czech Technological Agency that includes: funding grants. Stanislav Obruca has patent # PV 2023–330 pending to none. Other authors declare that they have no known competing financial interests or personal relationships that could have appeared to influence the work reported in this paper.

Acknowledgments

This study was supported by grant project of Czech Technological Agency (TAČR) FW02020135 and project of Czech Science Agency (GAČR) GA23-06757S.

Data availability

Data will be made available on request.

References

Abdelkafi, Slim, Sayadi, Sami, Zouhaier, Ben ALI.GAM., Casalot, Laurence, Labat, Marc, 2006. Bioconversion of ferulic acid to vanillic acid by Halomonas elongata isolated from table-olive fermentation. FEMS (Fed. Eur. Microbiol. Soc.) Microbiol. Lett. 262 (1), 115–120. https://doi.org/10.1111/j.1574-6968.2006.00381.x. ISSN 03781097. Dostupné z.

Abdelkafi, Slim, Labat, Marc, Zouhaier Ben Ali, G.A.M., Lorquin, Jean, Casalot, Laurence, Sayadi, Sami, 2008. Optimized conditions for the synthesis of vanillic acid under hypersaline conditions by Halomonas elongata DSM 2581T resting cells. World J. Microbiol. Biotechnol. 24 (5), 675–680. https://doi.org/10.1007/s11274-007-9523-3. ISSN 0959-3993. Dostupné z.

Shwafy, Al, Khaled, W.A., Chadni, Morad, Hariz, Abg zamari, Haziq, Muhd, Ioannou, Irina, 2023. Enzymatic extraction of ferulic acid from brewer's spent grain: effect of physical pretreatments and optimization using design of experiments. Online. Biocatal. Agric. Biotechnol. 51. https://doi.org/10.1016/j.bcab.2023.102779. ISSN 18788181.

Bettio, Giulia, Caroline Zardo, Luíza, Rosa, Carlos Augusto, Záchia Ayub, Marco Antônio, 2021. Bioconversion of ferulic acid into aroma compounds by newly isolated yeast strains of the Latin American biodiversity. Biotechnol. Prog. 37 (1). https://doi.org/10.1002/btpr.3067. ISSN 8756-7938. Dostupné z.

Biswas, Jhuma, Jana, Santosh Kumar, Mandal, Sukhendu, 2023. Biotechnological impacts of halomonas: a promising cell factory for industrially relevant biomolecules. Online Biotechnol. Genet. Eng. Rev. 39 (2), 348–377. https://doi.org/10.1080/02648725.2022.2131961. ISSN 0264-8725.

Chai, Li-yuan, Zhang, Huan, Yang, Wei-chun, Zhu, Yong-hua, Yang, Zhi-hui, Zheng a Yue, Yu, Chen, hui, 2013. Biodegradation of ferulic acid by a newly isolated strain of cupriavidus sp. B-8. J. Cent. S. Univ. 20 (7), 1964–1970. https://doi.org/10.1007/s11771-013-1696-3. ISSN 2095-2899. Dostupné z.

Chen, Peng, Yan, Lei, Wu, Zhengrong, et al., 2016. A microbial transformation using Bacillus subtilis B7-S to produce natural vanillin from ferulic acid. Sci. Rep. 6 (1). https://doi.org/10.1038/srep20400. ISSN 2045-2322. Dostupné z.

Chen, Zhenya, Shen, Xiaolin, Wang, Jian, Wang, Jia, Zhang, Ruihua, Rey, Justin Forrest, Yuan, Qipeng, Yan, Yajun, 2017. Establishing an Artificial Pathway for De Novo Biosynthesis of Vanillyl Alcohol in Escherichia coli. ACS Synth. Biol. 6 (9), 1784–1792. https://doi.org/10.1021/acssynbio.7b00129. ISSN 2161-5063. Dostupné z.

Chen, Guo-Qiang, Jiang, Xiao-Ran, 2018. Next generation industrial biotechnology based on extremophilic bacteria. Curr. Opin. Biotechnol. 50, 94–100. https://doi.org/10.1016/j.copbio.2017.11.016. ISSN 09581669. Dostupné z.

Dutta, Bhramar, Bandopadhyay, Rajib, 2022. Biotechnological potentials of halophilic microorganisms and their impact on mankind. Online Beni-Suef University Journal of Basic and Applied Sciences 11 (1). https://doi.org/10.1186/s43088-022-00252-w. ISSN 2314-8543.

Fatollahi, Parvaneh, Ghasemi, Mina, Sadeghi, Fatemeh YAZDIAN a Akram, 2021. Ectoine production in bioreactor by Halomonas elongata DSM2581: using MWCNT and Fe-nanoparticle. Biotechnol. Prog. 37 (1). https://doi.org/10.1002/btpr.3073. ISSN 8756-7938. Dostupné z.

Ghosh, Shashwati, Sachan, Ashish, Sukanta Kumar SEN a Adinpunya MITRA, 2007. Microbial transformation of ferulic acid to vanillic acid by Streptomyces sannanensis MTCC 6637, 34 (2), 131–138. https://doi.org/10.1007/s10295-006-0177-1.

Gopalan, Nishant, Nampoothiri, K. Madhavan, 2018. Biorefining of wheat bran for the purification of ferulic acid. Online Biocatal. Agric. Biotechnol. 15, 304–310. https://doi.org/10.1016/j.bcab.2018.07.004. ISSN 18788181.

Haddadi, Azam, Shavandi, Mahmoud, 2013. Biodegradation of phenol in hypersaline conditions by halomonas sp. strain PH2-2 isolated from saline soil, 85, 29–34. https://doi.org/10.1016/j.ibiod.2013.06.005.

Hrabalová, Vendula, Opial, Tomáš, Musilová, Jana, Sedlář, Karel, Obruča, Stanislav, 2024. Biotransformation of ferulic acid into vanillyl alcohol and vanillic acid employing thermophilic bacterium Caldimonas thermodepolymerans. Online. Enzyme and Microbial Technology 179. https://doi.org/10.1016/j.enzmictec.2024.110475. ISSN 01410229.

Huang, Z., Rosazza, L.Dostal a J.P., 1993. Microbial transformations of ferulic acid by Saccharomyces cerevisiae and Pseudomonas fluorescens. Appl. Environ. Microbiol. 59 (7), 2244–2250. https://doi.org/10.1128/aem.59.7.2244-2250.1993. ISSN 0099-2240. Dostupné z.

Hunter, William J., Manter, Daniel K., Van Der La, Daniel, 2012. Biotransformation of ferulic acid to 4-Vinylguaiacol by Enterobacter soli and E. aerogenes. Online Curr. Microbiol. 65 (6), 752–757. https://doi.org/10.1007/s00284-012-0222-4. ISSN 0343-8651.

Ingole, Ashwini, Megha, P.K.A.D.A.M., Dalu, Aishwarya P., et al., 2021. A review of the pharmacological characteristics of vanillic acid. J. Drug Deliv. Therapeut. 11 (2-), 200–204. https://doi.org/10.22270/jddt.v11i2-S.4823. ISSN 2250-1177. Dostupné z.
Kucharzyk, Katarzyna H., Fulwider, Veronica M., Duong, Anthony, Duffy, Mark, Cafmeyer, Jeff, et al., 2023. Assessment of long-term stability of encapsulated agricultural biologicals in lipid-coated alginate beads. https://doi.org/10.1021/acsagscitech.2c00273.
Lee, Eun-Gyeong, Yoon, Sang-Hwal, Das, Amitabha, et al., 2009. Directing vanillin production from ferulic acid by increased acetyl-CoA consumption in recombinant Escherichia coli. Biotechnol. Bioeng. 102 (1), 200–208. https://doi.org/10.1002/bit.22040. ISSN 00063592. Dostupné z.
Li, Lulu, Long, Liangkun, Ding, Shaojun, 2019. Bioproduction of high-concentration 4-Vinylguaiacol using whole-cell catalysis harboring an organic solvent-tolerant phenolic acid decarboxylase from bacillus atrophaeus. Online. Front. Microbiol. 2019–8–6. https://doi.org/10.3389/fmicb.2019.01798 roč. 10. ISSN 1664-302X.
Liebgott, Pierre-Pol, Labat, Marc, Casalot, Laurence, Amouric, Agnès, Lorquin, Jean, 2007. Bioconversion of tyrosol into hydroxytyrosol and 3,4-dihydroxyphenyl-acetic acid under hypersaline conditions by the new halomonas sp. strain HTB24. Online. FEMS (Fed. Eur. Microbiol. Soc.) Microbiol. Lett. 276 (1), 26–33. https://doi.org/10.1111/j.1574-6968.2007.00896.x. ISSN 03781097.
Llamas, Inmaculada, del Moral, Ana, Martínez-Checa, Fernando, Arco, Yolanda, Quesada, Soledad ARIAS a Emilia, 2006. Halomonas maura is a physiologically versatile bacterium of both ecological and biotechnological interest. Antonie Leeuwenhoek 89 (3–4), 395–403. https://doi.org/10.1007/s10482-005-9043-9. ISSN 0003-6072. Dostupné z.
Xiao-kui, Ma, Andrew, J., 2014. DAUGULIS. Effect of bioconversion conditions on vanillin production by amycolatopsis sp. ATCC 39116 through an analysis of competing by-product formation. Bioproc. Biosyst. Eng. 37 (5), 891–899. https://doi.org/10.1007/s00449-013-1060-x. ISSN 1615-7591. Dostupné z.
MartăU, Gheorghe Adrian, CăLINOIU, Lavinia-Florina, Vodnar, Dan Cristian, 2021. Bio-vanillin: towards a sustainable industrial production, 109, 579–592. https://doi.org/10.1016/j.tifs.2021.01.059.
Mathew, Sindhu a T., 2008. Emilia ABRAHAM. Bioconversions of ferulic acid, an hydroxycinnamic acid. Crit. Rev. Microbiol. 32 (3), 115–125. https://doi.org/10.1080/10408410600709628. ISSN 1040-841X. Dostupné z.
Max, Belén, Carballo, Julia, Cortés, Sandra, Domínguez, Jose M., 2012. Decarboxylation of ferulic acid to 4-Vinyl guaiacol by Streptomyces setonii. Online Appl. Biochem. Biotechnol. 166 (2), 289–299. https://doi.org/10.1007/s12010-011-9424-7. ISSN 0273-2289.
Muheim, Lerch, A. a K., 1999. Towards a high-yield bioconversion of ferulic acid to vanillin. Appl. Microbiol. Biotechnol. 51 (4), 456–461. https://doi.org/10.1007/s002530051416. ISSN 0175-7598. Dostupné z.
Mussatto, S.I., Roberto, G. Dragone a I.C., 2007. Ferulic and p-coumaric acids extraction by alkaline hydrolysis of brewer's spent grain. Ind. Crop. Prod. 25 (2), 231–237. https://doi.org/10.1016/j.indcrop.2006.11.001. ISSN 09266690. Dostupné z.
Oliveira, D.E., Matias, Dyoni, Finger-Teixeira, Aline, Mota, Thatiane Rodrigues, et al., 2015. Ferulic acid: a key component in grass lignocellulose recalcitrance to hydrolysis. Plant Biotechnol. J. 13 (9), 1224–1232. https://doi.org/10.1111/pbi.12292. ISSN 14677644. Dostupné z.
Orhan, Furkan, Akincioglu, Hülya, 2020. Determination of carbonic anhydrase enzyme activity in halophilic/halotolerant bacteria. Online Appl. Soil Ecol. 155. https://doi.org/10.1016/j.apsoil.2020.103650. ISSN 09291393.
Orhan, Furkan, Ceyran, Ertuğrul, 2024. Valorisation of cheese whey for ectoine production by halomonas neptunia. Online Int. J. Dairy Technol. 77 (1), 146–155. https://doi.org/10.1111/1471-0307.13008. ISSN 1364-727X.
Pazo-Cepeda, Victoria, Benito-Román, Óscar, Navarrete, Alexander, Alonso, Esther, 2020. Valorization of wheat bran: ferulic acid recovery using pressurized aqueous ethanol solutions. Online Waste and Biomass Valorization 11 (9), 4701–4710. https://doi.org/10.1007/s12649-019-00787-7. ISSN 1877-2641.
Pernicova, Iva, Kucera, Dan, Nebesarova, Jana, Kalina, Michal, Novackova, Ivana, et al., 2019. Production of polyhydroxyalkanoates on waste frying oil employing selected halomonas strains. Online Bioresour. Technol. 292. https://doi.org/10.1016/j.biortech.2019.122028. ISSN 09608524.
Rigo, Elena, Totée, Cédric, Ladmiral, Vincent, Caillol, Sylvain, Lacroix-Desmazes, Patrick, 2024. 4-Vinyl guaiacol: a key intermediate for biobased polymers. Online Molecules 29 (11). https://doi.org/10.3390/molecules29112507. ISSN 1420-3049.
Rizki, Wa Ode Sri, Ratnaningsih, Enny, Hertadi, Rukman, 2023. Production of poly-(R)-3-hydroxybutyrate from halophilic bacterium salinivibrio sp. utilizing palm oil mill effluent as a carbon source. Online Biocatal. Agric. Biotechnol. 47. https://doi.org/10.1016/j.bcab.2022.102558. ISSN 18788181.
Sudhagar, S., Sathya, S., Anuradha, R., Gokulapriya, G., Geetharani, Y., et al., 2018. Inhibition of epidermal growth factor receptor by ferulic acid and 4-vinylguaiacol in human breast cancer cells. Online. Biotechnology Letters 40 (2), 257–262. https://doi.org/10.1007/s10529-017-2475-2. ISSN 0141-5492.
Sunao, M., Ito, T., Hiroshima, K., Sato, M., Uehara, T., Ohno, T., Watanabe, S., Takahashi, H., Hashizume, K., 2016. Analysis of volatile phenolic compounds responsible for 4-vinylguaiacol-like odor characteristics of sake. Food Sci. Technol. Res. 22 (1), 111–116.
Tang, Pei Ling a Osman HASSAN., 2020. Bioconversion of ferulic acid attained from pineapple peels and pineapple crown leaves into vanillic acid and vanillin by Aspergillus Niger I-1472. BMC Chemistry 14 (1). https://doi.org/10.1186/s13065-020-0663-y. ISSN 2661-801X. Dostupné z.
Tang, Hao, Wang, Ming-Jun, Gan, Xiao-Feng, Li, Yuan-Qiu, 2022. Funneling lignin-derived compounds into polyhydroxyalkanoate by Halomonas sp. Y3. Online. Bioresour. Technol. 362. https://doi.org/10.1016/j.biortech.2022.127837. ISSN 09608524.
Vinceković, Marko, Živković, Lana, Turkeyeva, Elmira, Mutaliyeva, Botagoz, Madybekova, Galiya, et al., 2024. Development of alginate composite microparticles for encapsulation of Bifidobacterium animalis subsp. lactis. Online Gels 10 (11). https://doi.org/10.3390/gels10110752. ISSN 2310-2861.
Vyrides, Ioannis, Agathangelou, Maria, Dimitriou, Rodothea, Souroullas, Konstantinos, Salamex, Anastasia, et al., 2015. Halomonas sp. B15 isolated from Larnaca Salt Lake in Cyprus that generates vanillin and vanillic acid from ferulic acid. Online. World Journal of Microbiology and Biotechnology 31 (8), 1291–1296. https://doi.org/10.1007/s11274-015-1876-4. ISSN 0959-3993.
Xu, Lingxia, Liaqat, Fakhra, Sun, Jianzhong, Khazi, Mahammed Ilyas, Xie, Rongrong, et al., 2024. Advances in the vanillin synthesis and biotransformation: a review. Online. Renew. Sustain. Energy Rev. 189. https://doi.org/10.1016/j.rser.2023.113905. ISSN 13640321.
Yamada, Mamoru, Okada, Yukiyoshi, Nagasawa, Toyokazu Yoshida a Toru, 2007. Biotransformation of isoeugenol to vanillin by Pseudomonas putida IE27 cells. Appl. Microbiol. Biotechnol. 73 (5), 1025–1030. https://doi.org/10.1007/s00253-006-0569-1. ISSN 0175-7598. Dostupné z.
Yan, Lei, Chen, Peng, Zhang, Shuang, Li, Suyue, Yan, Xiaojuan, et al., 2016. Biotransformation of ferulic acid to vanillin in the packed bed-stirred fermentors. Online Sci. Rep.. https://doi.org/10.1038/srep34644, 2016-12-16, roč. 6, č. 1. ISSN 2045-2322.
Yoon, Sang-Hwal, Cui, L.I., Ju-Eun, K.I.M., et al., 2005. Production of vanillin by metabolically engineered Escherichia coli. Biotechnol. Lett. 27 (22), 1829–1832. https://doi.org/10.1007/s10529-005-3561-4. ISSN 0141-5492. Dostupné z.
Yoon, S.-H., Lee, E.-G., Das, A., et al., 2007. Enhanced vanillin production from recombinant E. coli using NTG mutagenesis and adsorbent resin. Biotechnol. Prog. 0 (0). https://doi.org/10.1021/bp070153r, 0-0. ISSN 8756-7938. Dostupné z.
Zhang, Chaoqun, Samy, A., Kessler, Madbouly a Michael R., 2015. Renewable polymers prepared from vanillin and its derivatives. Macromol. Chem. Phys. 216 (17), 1816–1822. https://doi.org/10.1002/macp.201500194. ISSN 10221352. Dostupné z.

10.3 ENHANCED ELECTRON MICROSCOPY IMAGING FOR A DETAILED STRUCTURAL STUDY OF ALGINATE HYDROGEL CONTAINING THE ENCAPSULATED CELLS

Carbohydrate Polymers 368 (2025) 124239

Contents lists available at ScienceDirect

Carbohydrate Polymers

journal homepage: www.elsevier.com/locate/carbpol

Enhanced electron microscopy imaging for a detailed structural study of alginate hydrogel containing the encapsulated cells

Kateřina Mrázová [a,b], Diana Černayová [b], Anna Havlíčková [a,b], Kamila Hrubanová [a], Stanislav Obruča [b], Petr Sedláček [b], Vladislav Krzyžánek [a,*]

[a] Institute of Scientific Instruments of the Czech Academy of Sciences, v. v. i., Královopolská 147, 612 00 Brno, Czech Republic
[b] Faculty of Chemistry, Brno University of Technology, Purkynova 118, 612 00 Brno, Czech Republic

ARTICLE INFO

Keywords:
Alginate
Azotobacter vinelandii
electron microscopy
Encapsulation

ABSTRACT

Hydrogels are widely applicable in medicine, biotechnology, etc. A specific example is bacterial alginate produced by plant growth-promoting rhizobacterium *Azotobacter vinelandii*, which encapsulates the cells within its hydrogel network, offering promising applications in agriculture. To better understand the properties and behaviour of hydrogel, it is important to study its architecture. However, due to high-water content and fine structure of hydrogel samples, their preparation for electron microscopy is challenging. In this study, we developed an optimised protocol for preparing complex samples of *A. vinelandii* cells encapsulated in alginate hydrogel for imaging by low-voltage scanning transmission electron microscopy. Our approach addresses structural instability and artefact formation typically encountered during sample dehydration and staining. We demonstrated that careful timing of $CaCl_2$ addition, after initial fixation, is essential. Equally important is the careful selection of its concentration to maintain hydrogel integrity while preserving cellular morphology. The inclusion of lead citrate staining step enhanced the contrast within hydrogel matrix, allowing for improved visualisation of fine details. This refined protocol enables high-resolution imaging of alginate-based hydrogels containing embedded cells while preserving the key structural features. It is compatible with various transmission electron microscopy techniques and may be adapted for use with other soft biomaterials.

1. Introduction

Hydrogels are cross-linked polymeric networks with the capacity to absorb and retain substantial amounts of water, which renders them highly versatile materials with broad applications in medicine, the food industry, or even biotechnology (Correa et al., 2021). Understanding the relationship between their internal structure and application-relevant properties requires a reliable method for visualising their internal morphology and architecture. However, the imaging of hydrogels still poses a major challenge in electron microscopy because of the high-water content and delicate structure of the polymer network. Many studies rely on various scanning electron microscopy (SEM) techniques. One of the most commonly used combinations of the sample preparation methods and imaging techniques is freeze-drying or lyophilisation, followed by the room temperature SEM (Dodero et al., 2019; Nita et al., 2021). This approach provides not only a detailed view of the gel structure, but has also been used to image objects such as cells frequently encapsulated in alginate-based hydrogels (Paci et al., 2022; Zheng et al., 2012). The combination of these techniques provides an easy and affordable means of observation of such complex samples for most laboratories.

Nevertheless, it should be noted that depending on the freezing temperatures and drying rate, the pore size and thus the overall structure of the studied sample might be affected (Aston et al., 2016; Kaberova et al., 2020; Park et al., 2002; Zhong et al., 2011). A possible alternative to avoid such artefacts is using the environmental SEM (ESEM), which allows the imaging of the hydrated samples without the need for complete dehydration (Kaberova et al., 2020). The pressure in the chamber of this specific type of microscope is substantially higher than that of a conventional SEM, which, on one hand, may decrease the resolution of the microscope but, on the other, enables the observation of hydrated samples and thus avoids significant shrinkage (Michler & Lebek, 2016; Stabentheiner et al., 2010).

Another approach enabling the observation of the highly hydrated

* Corresponding author.
E-mail address: krzyzanek@isibrno.cz (V. Krzyžánek).

https://doi.org/10.1016/j.carbpol.2025.124239
Received 1 July 2025; Received in revised form 11 August 2025; Accepted 13 August 2025
Available online 14 August 2025

samples with minimal drying artefacts is the cryogenic SEM (cryo-SEM). Several studies have implemented different vitrification techniques in combination with the freeze-fracture method to investigate various types of hydrogels (Aston et al., 2016; Jayawardena et al., 2023; Koch & Wlodarczyk-Biegun, 2020; Merryweather et al., 2023; Trudicova et al., 2020). The freezing rate, as previously noted for lyophilisation and conventional SEM, is the key factor to be considered. Depending on the selected method of the sample fixation (plunge freezing into liquid ethane, high-pressure freezing, etc.), the observed structure of the hydrogel might be altered (Aston et al., 2016; Park et al., 2002). Even though the cryo-SEM provides valuable information about the surface of hydrogels, or even some internal structures in case of combination with the freeze-fracture method, its resolution in imaging a fine hydrogel network remains limited. To observe a more detailed view of such fine structures, transmission electron microscopy (TEM) has also been explored as a method of choice in various studies, both at room temperature (Ganachaud et al., 2013; Kiyama et al., 2023; Leal-Egaña et al., 2011; Wright et al., 2009) and cryogenic conditions (Hule et al., 2008; Londono-Calderon et al., 2019). While freezing temperature and drying rate are the key factors for proper sample preparation protocols for the SEM methods, the dehydration step in the TEM protocols is critical. The suitable conditions for the dehydration of such samples depend on the type of hydrogel since some hydrogels exhibit substantial morphological stability when replacing water with, for example, ethanol as a dehydration agent (Roux et al., 2023; Ye et al., 2024). In contrast, other hydrogel materials show significant shrinkage and other types of alterations to their native state if exposed to such a protocol (Hermansson et al., 2016; Tkalec et al., 2016).

Hydrogels are gaining increasing attention in sustainable agriculture, particularly as the carriers for the plant growth-promoting rhizobacteria (PGPR) in the development of biological fertilisers (Bashan et al., 2014; Qin et al., 2024). In such systems, the hydrogel matrix enhances the bacterial viability and enables a gradual release under field conditions. One such PGPR is *Azotobacter vinelandii*, which is known for nitrogen fixation, secretion of auxin precursors, phosphate solubilisation, and siderophore production, all of which promote plant development (Ferreira et al., 2019; Gurikar et al., 2016; Nosrati et al., 2014; Sahoo & Pradhan, 2023). Additionally, *A. vinelandii* produces an extracellular alginate, which serves as a protective barrier against environmental stress and supports the activity of the nitrogenase, an oxygen-sensitive enzyme essential for nitrogen fixation (Çam & Bicek, 2023; Moradali & Rehm, 2019; Núñez et al., 2022; Sabra et al., 2000). Building on these natural properties, we recently introduced a self-gelling strategy in which *A. vinelandii* becomes immobilised within its own alginate, cross-linked by calcium ions added directly to the culture medium (Černayová et al., 2025). This eliminates the need for the external gelling agents while preserving the structural and functional advantages of alginate matrices. Alginate is a linear copolymer composed of two types of monomeric units: β-D-mannuronic acid (M) and α-L-guluronic acid (G), arranged in homopolymeric (MM, GG) or heteropolymeric (MG) blocks. These blocks determine the physicochemical properties of the polymer, such as gel strength, elasticity, and water retention. In particular, G-blocks interact with divalent calcium ions to form the so-called egg-box structures, which stabilise the three-dimensional network of the gel (Aarstad et al., 2019; Guo et al., 2020; Hu et al., 2022; Ren et al., 2024). The efficiency of the gelation and the final material properties thus depend not only on the monomer ratio, but also on the concentration of alginate and calcium ions utilised during the crosslinking.

The ultrastructure of *A. vinelandii* has been studied previously (Cagle et al., 1972; Sadoff, 1975; Vela et al., 1970; Wyss et al., 1961), but to the best of our knowledge, encapsulated *A. vinelandii* in alginate hydrogel has not yet been observed except for the first attempts presented in our recent pioneer study involving cryogenic electron microscopy techniques (Černayová et al., 2025). Most of the previously published studies employing transmission electron microscopy (TEM) relied on conventional chemical sample preparation techniques. Such protocols mostly rely on the fixation by glutaraldehyde and/or formaldehyde, the postfixation by osmium tetroxide, followed by dehydration by, e.g., ethanol and embedding in epoxy resin. The ultrathin sections are then stained using conventional reagents such as uranyl acetate or lead salts (Hashimoto et al., 2013; Hitchins & Sadoff, 1970; Lin et al., 1978; Moreno et al., 2019; Yoneyama et al., 2015; Zhang et al., 2018). Other studies also explored alternative fixatives or contrast-enhancing agents such as $KMnO_4$, ruthenium red, or lyophilisation before the fixation (Cagle et al., 1972; Lin & Sadoff, 1968; Parker & Socolofsky, 1966; Vela et al., 1970). However, none of these approaches are tailored to the highly hydrated hydrogel samples, nor address the encapsulation context relevant for the bioinoculant applications.

This study presents a novel sample preparation protocol designed for ultrastructural analysis of the bio-hydrogel samples using *Azotobacter vinelandii* encapsulated in an alginate hydrogel as a model system. The protocol aims to preserve the cellular ultrastructure as well as the fine hydrogel network for imaging by electron microscopy. Although optimised for the low-voltage scanning transmission electron microscopy (LV-STEM), it may be applied across a wide range of transmission electron microscopy techniques. We hypothesise that a combination of carefully optimised $CaCl_2$ concentrations and tailored contrasting steps would effectively overcome the limitations of the conventional sample preparation methods for hydrogels, which often fail to preserve both biological and polymeric structures simultaneously. By maintaining an appropriate and stable Ca^{2+} concentration throughout the workflow, the hydrogel matrix remains preserved while minimising the osmotic stress to the cells. Besides alginate-*A. vinelandii* systems, this protocol offers a versatile and adaptable strategy for the high-resolution visualisation of various bio-hydrogel complexes, allowing detailed insight into cell-matrix interactions at the nanoscale.

2. Materials and methods

2.1. Cultivation of Azotobacter vinelandii

Freeze-dried bacterial culture *Azotobacter vinelandii* CCM 289 was obtained from the Czech Collection of Microorganisms (Brno, Czech Republic). The bacterial cultures were maintained as frozen stock cultures at −80 °C in the presence of glycerol (10 % *v*/v). The bacterial media, containing modified Ashby's medium (glucose 20.0 g/L, yeast extract 6.0 g/L, Na_2HPO_4 2.0 g/L, $MgSO_4.7H_2O$ 0.3 g/L, $(NH_4)_2SO_4$ 0.6 g/L and $CaCO_3$ 1.0 g/L) were prepared for the inoculum medium (35 mL of medium into 100 mL Erlenmeyer flask) and the mineral medium (100 mL of medium into 250 mL Erlenmeyer flask), following sterilisation at 120 °C for 15 min. After the sterilisation, the media were cooled down, inoculated with stock cultures and cultivated for 24 h at 30 °C with constant shaking at 180 rpm. After 24 h, the grown inoculum was transferred (5 % v/v) into the mineral medium and cultivated for four days at 30 °C with constant shaking at 220 rpm. The cultivations in the inoculum and mineral media were performed in parallel.

2.2. Alginate hydrogel preparation and characterisation

The cultivated fully-grown culture, in the volume of 10 mL, was gently dropped by pipette into 10 mL of calcium ion solution (2 % *w*/w), immediately forming the hydrogels. To strengthen and stabilise the gel structure, the gelation time was set at 20 min at room temperature. Following the gelation, the remaining non-gelatinised solution with the excess calcium chloride was carefully poured off.

Bacterially produced alginate was subjected to structural analysis in a manner similar to our previous work (Černayová et al., 2025). Briefly, the molecular weight was determined by the exclusion chromatography (Infinity 1260 system with PL aquagel-OH MIXED-H column, Agilent Technologies, Santa Clara, CA, USA) with the multi-angle light scattering (Dawn Heleos II, Wyatt Technology, Santa Barbara, CA, USA) and

differential refractometry (Optilab T-rEX, Wyatt Technology, Santa Barbara, CA, USA). The solution of 50 mmol/L sodium citrate was used as the mobile phase at a rate of 0.6 mL/min. The average molecular weight (M_w) was determined by using the ASTRA software (version 7.3.2, Wyatt Technology, Santa Barbara, CA, USA). Fourier transform infrared (FTIR) spectroscopy (spectrometer iS50 Thermo Scientific, Waltham, MA, USA) was utilised to determine the M/G unit ratio and acetylation. The absorbances at 780, 810, 1600, and 1720 cm^{-1} were used to calculate the studied structural parameters. For the analysis of Mw, 58 values were used from a total of 18 experiments, which were performed in 3 to 6 replicates; 9 different spectra were used to determine the M/G ratio and acetylation ratio. Employing the analyses described above, the molecular weight (M_w) was determined to be 738.808 ± 48.276 kDa, the M/G ratio (A_{810}/A_{780}) to be 2.36 ± 0.27, and the acetylation ratio to be (A_{1720}/A_{1600}) 0.20 ± 0.06.

2.3. Electron microscopy

The samples of the alginate-encapsulated *Azotobacter vinelandii* cells were cut by a sharp razor blade into small cubes of approximately 1 mm^3 size. A crosslinking agent, $CaCl_2$, was added to almost all steps of the preparation protocol to prevent Ca^{2+} from leaching out of the hydrogel network and thus to preserve the structure of the alginate hydrogel during the chemical preparation procedure. To test the stability of the hydrogel as well as the osmotic stability of the cells, three types of protocols varying in the concentration of the crosslinking agent were tested: the fixation without $CaCl_2$ followed by 1 % $CaCl_2$ in the next steps, the fixation without $CaCl_2$ followed by 0.5 % $CaCl_2$ in the next steps, and 0.5 % $CaCl_2$ already in the fixation step. The detailed protocols may be found in the Appendix A. Supplementary data. Generally, the samples were fixed overnight in 2.5 % glutaraldehyde and 2 % formaldehyde solution in 0.1 mol/L HEPES buffer. The postfixation step involved 1 % OsO_4 with 1 % $K_3[Fe(CN)_6]$ in 0.1 mol/L HEPES buffer. For the en-bloc staining, an alternative contrasting agent based on the lanthanoid compounds (Moscardini et al., 2020) was employed. Samples were then dehydrated using methanol in a rising concentration series. The samples were embedded in Spurr's epoxy resin and left for polymerisation for 48 h at 62 °C. To compare the cellular ultrastructure as well as to confirm the changes of the alginate structure in the intercellular areas of the sample, a control sample of pure, unencapsulated *A. vinelandii* cells was also prepared. The cell suspension was subjected to the same protocol as the encapsulated samples; however, the cell suspension sample was not exposed to $CaCl_2$ in any step of the procedure.

The cured blocks of the samples were cut into ultrathin sections by a diamond knife (Ultra 45°, DiATOME, Nidau, Switzerland) and an ultramicrotome (EM UC7, Leica Microsystems, Vienna, Austria). In our previous work, we demonstrated that LV-STEM sufficiently increases the contrast of the biological samples without conventional staining (Mrazova et al., 2023). The samples in this study were therefore analysed in the scanning electron microscope (Magellan 400/L, FEI, Hillsboro, OR, USA) equipped with a STEM3+ detector, using a 20 keV electron beam. Nevertheless, to assess whether the conventional staining agents would either further reveal fine ultrastructural details in our complex samples or mask them instead, half of the samples were also contrasted on the grids using Reynolds' lead citrate.

3. Results

3.1. The effect of the crosslinking agent concentration on the cellular ultrastructure

To evaluate the impact of the crosslinking agent concentration, present in various steps of the sample preparation protocol, three distinct protocols were compared, along with a control sample consisting of the non-encapsulated cells. We aimed to preserve not only the cellular ultrastructure, but also the integrity of the alginate hydrogel network. For a better understanding of the cellular ultrastructure and the influence of each protocol on the cell, Fig. 1a) provides the representation of an average *A. vinelandii* cell with typical components marked and explained in the caption, while Fig. 1b) illustrates the different areas of the specimen from which the sample was taken and which will be further compared to each other in this chapter.

Fig. 2 illustrates the influence of $CaCl_2$ concentration on cells of *A. vinelandii*. The ultrathin sections of the samples were taken from the edge of the sample – the region where the bulk of the samples had been in contact with all the reagents for the longest time, and therefore, its fixation, resin infiltration, etc., should be the most thorough. If we compare the control sample of the non-gelled culture with the samples that have been encapsulated, we may notice a significant difference in the respective types of sample preparation protocol used. While both types of samples, fixed without the presence of $CaCl_2$ in culture media (Fig. 2a, b), show a properly fixed ultrastructure, the cells of the sample with 0.5 % $CaCl_2$, that were already present in the fixative solution, suffered from osmotic damage.

The comparison of the images taken from the edge of the sample (Fig. 2) with those from the centre (Fig. 3) reveals a similar trend in the ultrastructure of the samples. Inside the cells, as is more apparent in the images shown in Fig. 3, the individual reagents and resin had more difficulty in permeating the entire sample volume. Hence, we may notice a slightly worse fixation for all the sample types as well as more frequent washing out of the polyhydroxyalkanoates (PHA) granules due to the worse embedding state. Since the control sample of the pure cultures was prepared as a suspension at all instances, no such embedding artefacts are apparent in the control sample ultrastructure shown in Fig. 3d.

3.2. The effect of the crosslinking agent concentration on the structure of the alginate hydrogel network

If we look closely back at the images presented in Chapter 3.1, it is apparent that even at low magnifications, fine structures are visible around the cells. These structures are consistent with a hydrogel network and were also present in the areas more distant from the cells. In contrast, samples from cultures without crosslinking agent exhibited similar structures only immediately adjacent to the cells. A more detailed view of the hydrogel (Fig. 4) suggests that the concentration of a crosslinking agent, present in the sample preparation reagents, also affects the network. A distinct polymer network was observed in the sample treated with 1 % $CaCl_2$, not only surrounding the immediate vicinity of the cells, but also extending into the more distant areas of the sample. However, if we compare this structure to the samples treated with 0.5 % $CaCl_2$ during/after the fixation, the polymer network displays significant differences. A sample without a crosslinking agent present in the fixation step shows that the polymer network was highly diluted. As such, only a small presence of fibres might have been observed, both in the cells and in the open areas of the sample. Interestingly, samples with 0.5 % $CaCl_2$ added during fixation displayed a network structure more comparable to that in the 1 % $CaCl_2$ sample, indicating that the timing of crosslinker addition also affects the preservation of the hydrogel. If we compare all the cross-linked samples with a pure culture control, we discover that the fibres of the cross-linked hydrogel are clearly defined in the images and form a network that is more or less entangled, depending on the method of preparation, and is found even outside the immediate vicinity of the cells. The pure culture sample, on the other hand, contains the alginate only in the form of fine filaments distributed just in the immediate vicinity of the cells without any significant organisation.

By examining the images taken from the edge (Fig. 4) and centre of the sample (Fig. 5), we discover that the pattern closely resembles the previously described trends observed in the previous Chapter focusing on bacterial cells. While the overall effect of crosslinker concentration remains similar, the hydrogel network in the central regions appears

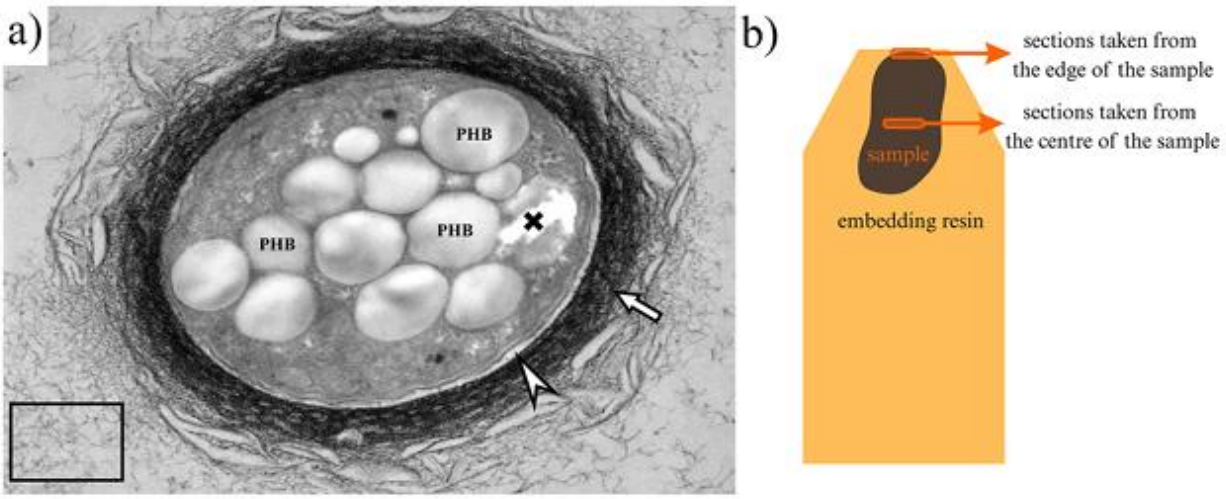

Fig. 1. a) Cellular ultrastructure of *Azotobacter vinelandii* encapsulated in Ca^{2+} alginate hydrogel. Granules containing polyhydroxybutyrate are marked "PHB", the intine layer of the capsule "arrowhead", the exine layer of the capsule "arrow", the hydrogel network "frame", and the poorer embedding artefact "cross". Scale bar: 500 nm. b) Illustration of the different areas from which the ultrathin sections were taken to compare the capacity of the preparation protocol to infiltrate the entire sample volume.

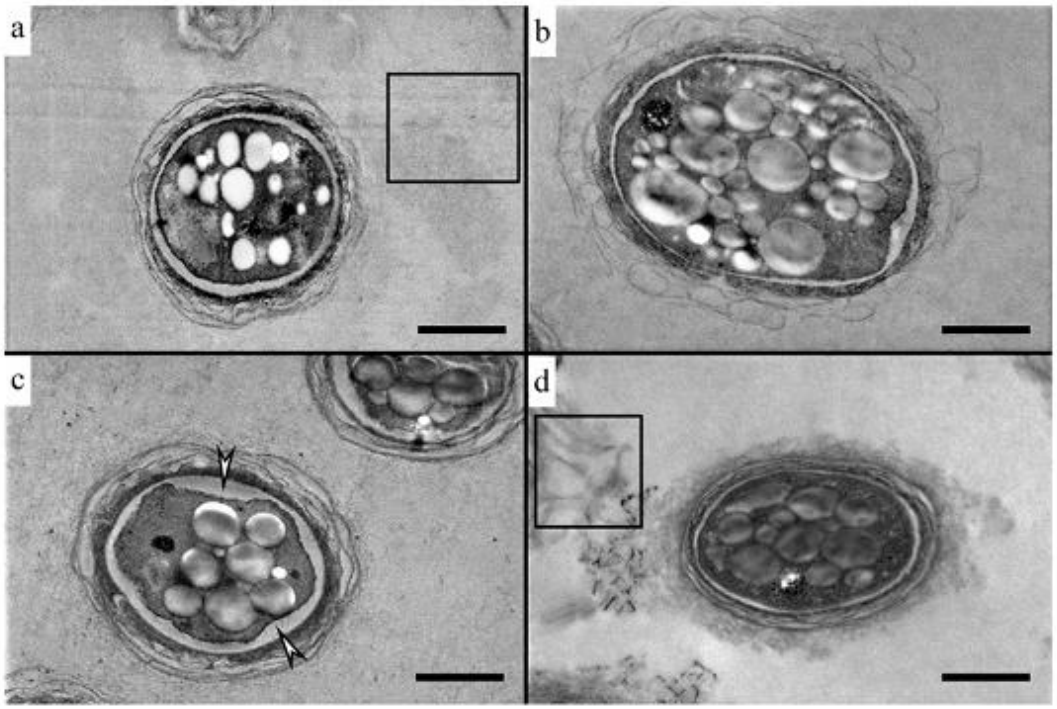

Fig. 2. Comparison of the influence of the sample preparation protocol on the structure of A. vinelandii: a) 1 % $CaCl_2$ after the fixation step, b) 0.5 % $CaCl_2$ after the fixation step, c) 0.5 % $CaCl_2$ during the whole sample preparation, and d) control unencapsulated cultures. The ultrathin sections were taken from the edge of the sample. An arrowhead indicates osmotic damage to the cells, a frame indicates examples of fine structures representing alginate fibres. Scale bar: 1 μm.

consistently less dense across all preparation types. It is also important to mention that in case of all the samples, an inhomogeneous distribution of net density has been observed throughout the volume. The densest regions were located in the closest proximity to the cells.

3.3. Influence of the on-grid staining on the overall structure of the sample

Brief staining using Reynold's lead citrate directly on the grids was applied to evaluate the effect of the conventional staining protocol on our specific samples, considering our previous study on low-voltage electron microscopy in microbial research. It was suggested that by

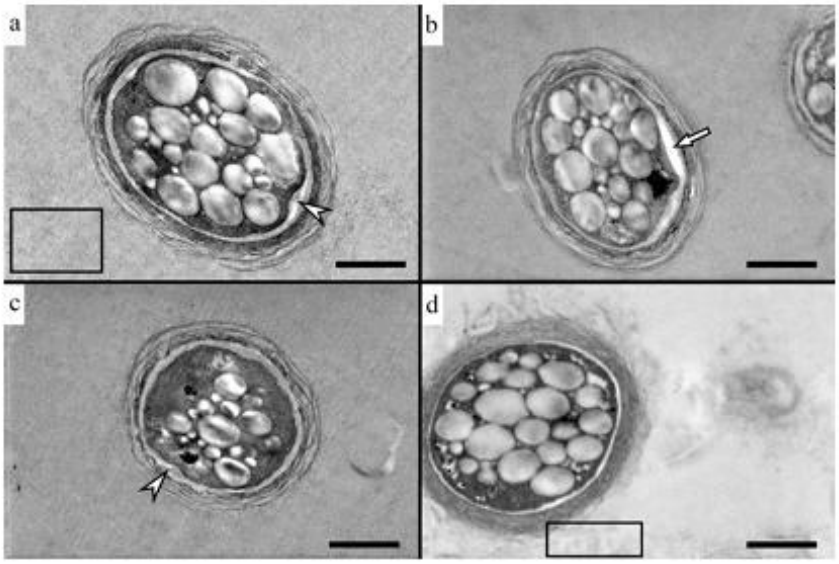

Fig. 3. Comparison of the influence of the sample preparation protocol on the structure of *A. vinelandii*: a) 1 % $CaCl_2$ after the fixation step, b) 0.5 % $CaCl_2$ after the fixation step, c) 0.5 % $CaCl_2$ during the whole sample preparation, and d) control unencapsulated cultures. The ultrathin sections were taken from the centre of the sample. An arrowhead indicates poor fixation/osmotic damage to the cells, while the poor infiltration of the embedding resin is marked with an arrow, and a frame indicates examples of fine structures representing alginate fibres. Scale bar: 1 μm.

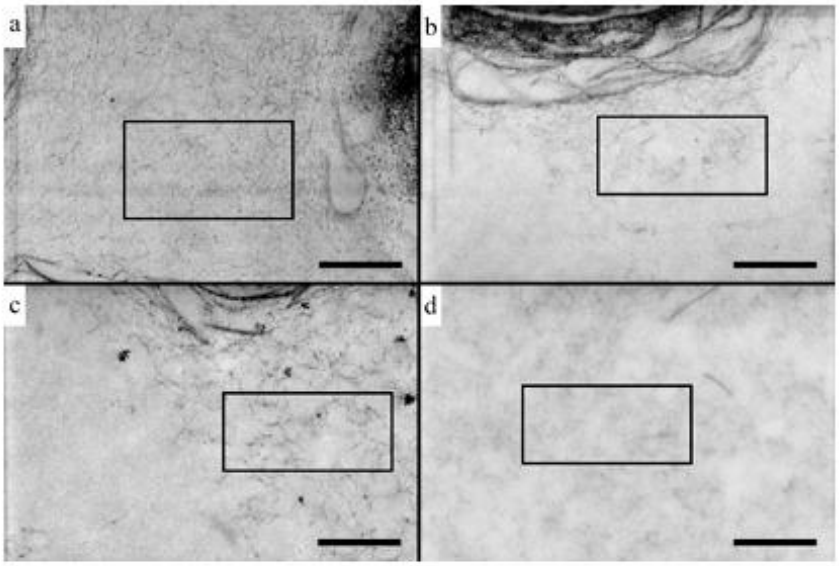

Fig. 4. Comparison of the influence of the sample preparation protocol on the structure of alginate hydrogel: a) 1 % $CaCl_2$ after the fixation step, b) 0.5 % $CaCl_2$ after the fixation step, c) 0.5 % $CaCl_2$ during the whole sample preparation, and d) control unencapsulated cultures. A frame indicates examples of fine structures representing alginate fibres. The ultrathin sections were taken from the edge of the sample. Scale bar: 400 nm.

using low-voltage microscopy, it is possible to avoid the staining of the sections with heavy metal salts to obtain similar, and in some ways even more detailed, views of the cellular ultrastructure (Mrazova et al., 2023). Since the structures within the cells were already sufficiently contrasted by using our basic protocol, we were particularly interested in whether the structures of the alginate net would be enhanced and would reveal finer details.

In Fig. 6, it is possible to notice that there is indeed an enhanced contrast of the individual polymer fibres, and the structures further confirm the initial observations from Chapter 3.2. Namely, the best-preserved hydrogel net is visible in the sample treated with 1 % $CaCl_2$, followed by the sample treated with 0.5 % $CaCl_2$, even in the fixation step, while the sample with 0.5 % $CaCl_2$ after the fixation step shows that the polymer net was partially dissolved and washed out during the sample preparation. In addition to the polymer net, other structures were also highlighted, such as vesicles (Fig. 7), which were found not only in the intine layer of the cell capsule but also in the exine and intercellular space.

However, this approach proved to be less suitable for imaging the overall cellular ultrastructure, as shown in Fig. 8. Further addition of a staining agent to the preparation protocol resulted in too much contrast of the cells in the section, hence covering some structures. This effect is

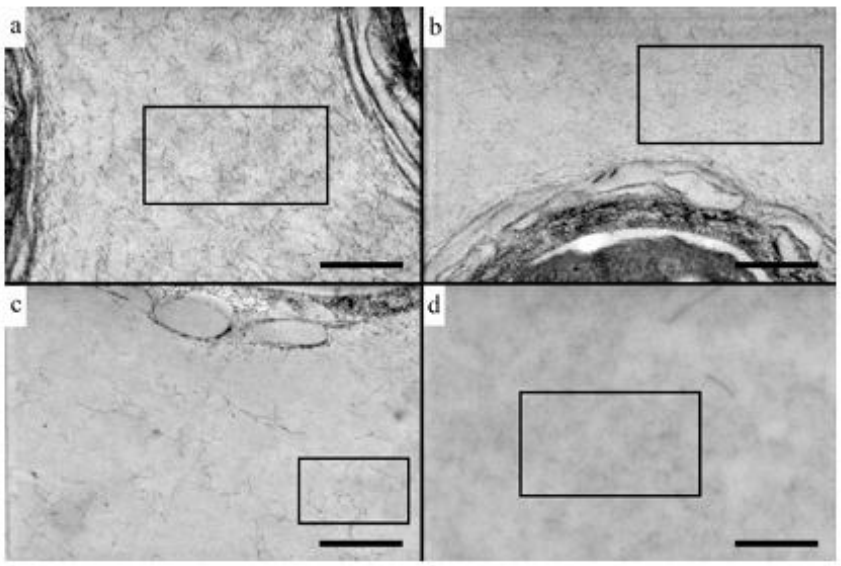

Fig. 5. Comparison of the influence of the sample preparation protocol on the structure of alginate hydrogel: a) 1 % $CaCl_2$ after the fixation step, b) 0.5 % $CaCl_2$ after the fixation step, c) 0.5 % $CaCl_2$ during the whole sample preparation, and d) control unencapsulated cultures. A frame indicates examples of fine structures representing alginate fibres. The ultrathin sections were taken from the centre of the sample. Scale bar: 400 nm.

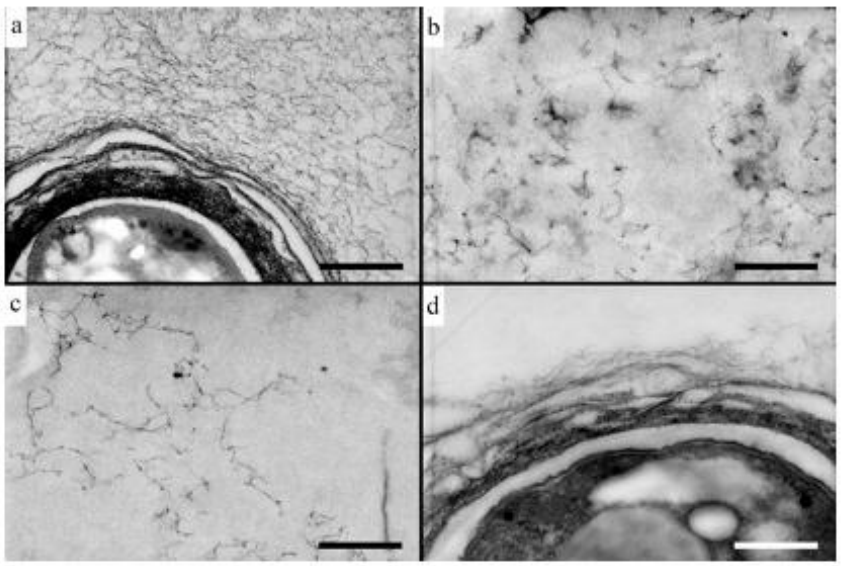

Fig. 6. Influence of lead citrate staining on the alginate hydrogel ultrastructure: a) 1 % $CaCl_2$ after the fixation step, b) 0.5 % $CaCl_2$ after the fixation step, c) 0.5 % $CaCl_2$ during the whole sample preparation, and d) control unencapsulated cultures. Scale bar: 400 nm.

most evident in the exine part of the cell capsule, where it is difficult to distinguish the fibrous pattern in the densest part surrounding the cells.

4. Discussion

Our experiments on the effect of the addition of a crosslinking agent during the preparation of the encapsulated cell samples for observation by STEM indicate that for both *A. vinelandii* cells and the structure of the alginate hydrogel, the addition of 1 % $CaCl_2$ to the reagent solutions is the best approach. However, it is important that the initial fixation step of the ultrastructure is carried out without a crosslinking agent. Due to the addition of 0.5 % already during the fixation, it was discovered that osmotic damage to the bacterial cells occurs. It is important to mention the limited long-term stability of ionically cross-linked alginate hydrogel in physiological conditions. The three-dimensional structure of these hydrogels may dissolve when divalent Ca^{2+} ions are released from the network due to the exchange reaction with monovalent ions from the surrounding liquid phase (Lee & Mooney, 2012).

Therefore, maintaining a stable concentration of Ca^{2+} in the environment surrounding the samples to help prevent the leaching of Ca^{2+} ions from the polymer net is crucial. It has been previously described that when alginate hydrogel is placed in a new aqueous environment with a different ion concentration, bivalent ions may be replaced by the monovalent ones (e.g., H^+ or Na^+), and the hydrogel changes its properties (Malektaj et al., 2023; Urbanova et al., 2019). However, the addition of Ca^{2+} was omitted from the UA-zero contrasting step to avoid

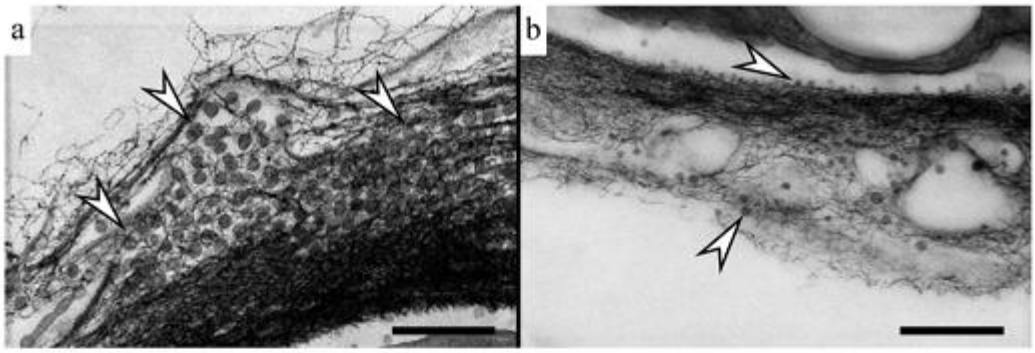

Fig. 7. Details of the *A. vinelandii* polymer capsule containing the vesicles: a) 1 % $CaCl_2$ after the fixation step, scale bar: 300 nm; b) control unencapsulated cultures. An arrowhead indicates the vesicles. Scale bar: 200 nm.

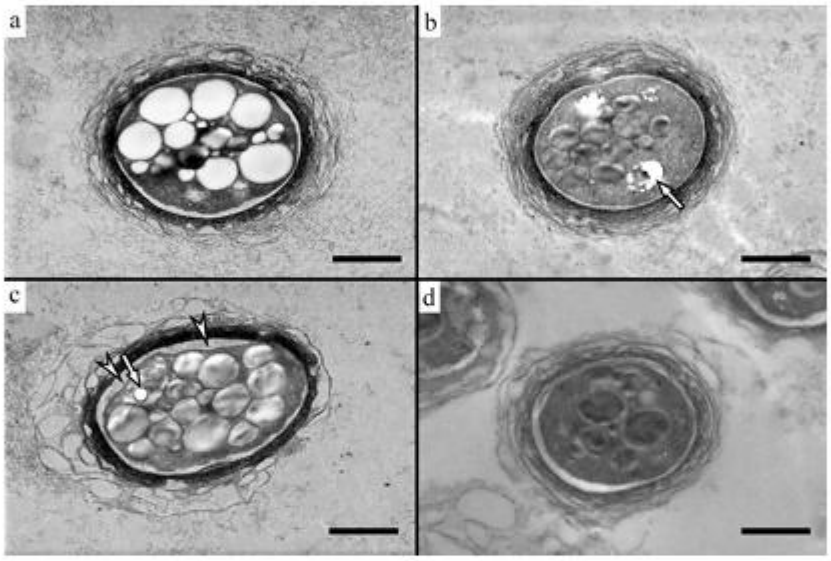

Fig. 8. Influence of lead citrate staining on the *A. vinelandii* ultrastructure: a) 1 % $CaCl_2$ after the fixation step, b) 0.5 % $CaCl_2$ after the fixation step, c) 0.5 % $CaCl_2$ during the whole sample preparation, and d) control unencapsulated cultures. An arrowhead indicates osmotic damage to the cells, while the poor infiltration of the embedding resin is marked with an arrow. Scale bar: 1 μm.

an unwanted reaction with the contrasting agent and a possible formation of precipitates and to prevent the disturbance of the subsequent polymerisation process during the resin saturation as well. Moreover, we believe that the samples were already sufficiently stabilised at the time of the resin embedding since no macroscopic changes in their structure or volume were observed when compared to, e.g., dehydration without Ca^{2+} stabilisation, where significant shrinkage occurred.

Another important factor in the preparation of such complex samples for electron microscopy is the diffusion limitation of the individual reagents. As already mentioned in Chapter 3.2, an inhomogeneous gel structure was observed throughout the sample volume. Since the gel was formed from bacteria-produced alginate and not from a standardised commercial polymer, a certain degree of heterogeneity is to be expected. Nevertheless, it did not interfere with the observation of the experimental progress with different Ca^{2+} concentrations. However, slight differences were also perceived in terms of the cell ultrastructure and quality of the fixation or resin permeation. One might anticipate that due to the nanoporous structure of the alginate hydrogels, diffusion limitations will occur. The reagents might not have thus reached the centre of the sample on an equal level when compared to the peripheral parts that were in direct contact with the reagents (Caccavo et al., 2018; Growney Kalaf et al., 2016). On the other hand, the more impeded diffusion into the centre of the sample may also explain the poorer resin embedding. We tried to minimise this artefact by using Spurr's low-viscosity resin and by changing the dehydrating agent from the commonly used ethanol to methanol. If we compare the boiling points of the commonly used dehydrating agents, ethanol and acetone, we will find that the more volatile acetone evaporates significantly more quickly in the sample. Hence, it is more likely that ethanol might have remained in the sample, which we had also observed in our preliminary experiments with reduced sample embedding quality. On the other hand, acetone is not a suitable solvent for $CaCl_2$ to achieve the desired concentration. Therefore, methanol was chosen because of its boiling point closer to that of acetone and, at the same time, its $CaCl_2$ solubility closer to that of ethanol.

Staining of the ultrathin sections in combination with low-voltage electron microscopy proved to be an efficient step for highlighting the fine structures of the alginate net. However, the polymeric capsule surrounding the cells was over-contrasted and, in some cells, even some of the patterns of exine structures were hidden. Although lead citrate is a non-specific contrast agent, it is expected to bind more strongly to negatively charged components such as hydroxyl groups, regions with

which osmium tetroxide reacts, or to phosphate groups (Ellis, 2007; Reynolds, 1963). To achieve specific enhancement of the polysaccharide structures, the involvement of the ruthenium red dye, which had been used previously in some protocols to study *A. vinelandii* (Cagle et al., 1972; Cagle & Vela, 1971), was considered. Nevertheless, our combination of low-voltage imaging of the samples without additional staining and after on-section staining provided us with rather comprehensive information about the full range of the structures of these complex samples.

5. Conclusion

The conventional electron microscopy analysis of hydrogels, particularly those based on carbohydrates, remains technically challenging. In this study, we addressed the limitations by developing an optimised preparation protocol for imaging alginate-based hydrogels encapsulating the living cells. The entrapped culture of *Azotobacter vinelandii*, a gram-negative bacterium with agronomic relevance as a biofertiliser, was utilised as a model system.

Our findings emphasise the critical role of $CaCl_2$, the alginate crosslinking agent, in stabilising the hydrogel's ultrastructure during the electron microscopy sample preparation. To prevent osmotic damage to the bacterial cells, $CaCl_2$ was added only after the initial fixation step. A concentration of 1 % $CaCl_2$ was sufficient to maintain the hydrogel integrity throughout all the reagent exchanges. Furthermore, the inclusion of a lead citrate staining step enhanced the visibility of fine structural details within the hydrogel matrix. The final protocol combines low-voltage transmission electron microscopy with minimal staining, enabling a detailed visualisation of delicate, hydrated biological materials without excessive artefacts.

Our results provide a practical and adaptable approach to the ultrastructural analysis of the alginate and other carbohydrate-based hydrogels, particularly in combination with the encapsulated cells or similarly morphologically complex elements. This methodology may serve as a foundation for future investigations into hydrogel-based delivery systems and other biologically relevant soft materials.

Supplementary data to this article can be found online at https://doi.org/10.1016/j.carbpol.2025.124239.

CRediT authorship contribution statement

Kateřina Mrázová: Writing – original draft, Visualization, Validation, Methodology, Investigation, Data curation, Conceptualization. **Diana Černayová:** Writing – original draft, Investigation. **Anna Havlíčková:** Writing – review & editing, Validation, Methodology, Data curation. **Kamila Hrubanová:** Writing – review & editing, Funding acquisition. **Stanislav Obruča:** Writing – review & editing, Supervision. **Petr Sedláček:** Writing – review & editing, Supervision, Funding acquisition. **Vladislav Krzyžánek:** Writing – review & editing, Supervision, Project administration, Funding acquisition.

Funding

This study was funded by the project GA23-06757S of the Czech Science Foundation (GACR). We also acknowledge the Core Facility Electron Microscopy and Raman Spectroscopy, supported by the Czech-BioImaging large RI project (LM2023050 funded by MEYS CR), for providing access to the instrumentation and technical support.

Declaration of competing interest

The authors declare that they have no known competing financial interests or personal relationships that could have appeared to influence the work reported in this paper.

Data availability

Data will be made available on request.

References

Aarstad, O. A., Stanisci, A., Sætrom, G. I., Tøndervik, A., Sletta, H., Aachmann, F. L., & Skjåk-Bræk, G. (2019). Biosynthesis and function of long Guluronic acid-blocks in alginate produced by Azotobacter vinelandii. *Biomacromolecules, 20*(4), 1613–1622. https://doi.org/10.1021/acs.biomac.8b01796

Aston, R., Sewell, K., Klein, T., Lawrie, G., & Grøndahl, L. (2016). Evaluation of the impact of freezing preparation techniques on the characterisation of alginate hydrogels by cryo-SEM. *European Polymer Journal, 82*, 1–15. https://doi.org/10.1016/j.eurpolymj.2016.06.025

Bashan, Y., de-Bashan, L. E., Prabhu, S. R., & Hernandez, J.-P. (2014). Advances in plant growth-promoting bacterial inoculant technology: Formulations and practical perspectives (1998–2013). *Plant and Soil, 378*, 1–33. https://doi.org/10.1007/s11104-013-1956-x

Caccavo, D., Cascone, S., Lamberti, G., & Barba, A. A. (2018). Hydrogels: Experimental characterization and mathematical modelling of their mechanical and diffusive behaviour. *Chemical Society Reviews, 47*(7), 2357–2373. https://doi.org/10.1039/C7CS00638A

Cagle, G. D., & Vela, G. R. (1971). Giant cysts and cysts with multiple central bodies in Azotobacter vinelandii. *Journal of Bacteriology, 107*(1), 315–319. https://doi.org/10.1128/jb.107.1.315-319.1971

Cagle, G. D., Vela, G. R., & Pfister, R. M. (1972). Freeze-etching of Azotobacter vinelandii: Examination of wall, exine, and vesicles. *Journal of Bacteriology, 109*(3), 1191–1197. https://doi.org/10.1128/jb.109.3.1191-1197.1972

Çam, S., & Bicek, S. (2023). The effects of temperature, salt, and phosphate on biofilm and exopolysaccharide production by *Azotobacter* spp. *Archives of Microbiology, 205*(3), 87. https://doi.org/10.1007/s00203-023-03428-9

Černayová, D., Súkeník, M., Obruča, S., Smilek, J., Kalina, M., Mrázová, K., Hrubanová, K., Krzyžánek, V., & Sedláček, P. (2025). Self-entrapment of Azotobacter vinelandii cultures by gelation of their exopolysaccharides: A way towards next-generation bioinoculants. *Carbohydrate Polymers, 360*, Article 123607. https://doi.org/10.1016/j.carbpol.2025.123607

Correa, S., Grosskopf, A. K., Lopez Hernandez, H., Chan, D., Yu, A. C., Stapleton, L. M., & Appel, E. A. (2021). Translational applications of hydrogels. *Chemical Reviews, 121*(18), 11385–11457. https://doi.org/10.1021/acs.chemrev.0c01177

Dodero, A., Pianella, L., Vicini, S., Alloisio, M., Ottonelli, M., & Castellano, M. (2019). Alginate-based hydrogels prepared via ionic gelation: An experimental design approach to predict the crosslinking degree. *European Polymer Journal, 118*, 586–594. https://doi.org/10.1016/j.eurpolymj.2019.06.028

Ellis, E. A. (2007). Poststaining grids for transmission Electron microscopy. In *Electron microscopy methods and protocols* (pp. 97–106). https://doi.org/10.1007/978-1-59745-294-6_6

Ferreira, C. M. H., Vilas-Boas, Â., Sousa, C. A., Soares, H. M. V. M., & Soares, E. V. (2019). Comparison of five bacterial strains producing siderophores with ability to chelate iron under alkaline conditions. *AMB Express, 9*(1), 78. https://doi.org/10.1186/s13568-019-0796-3

Ganachaud, C., Bernin, D., Isaksson, D., & Holmberg, K. (2013). An anomalous behavior of trypsin immobilized in alginate network. *Applied Microbiology and Biotechnology, 97*(10), 4403–4414. https://doi.org/10.1007/s00253-012-4333-4

Growney Kalaf, E. A., Flores, R., Bledsoe, J. G., & Sell, S. A. (2016). Characterization of slow-gelling alginate hydrogels for intervertebral disc tissue-engineering applications. *Materials Science and Engineering, 63*, 198–210. https://doi.org/10.1016/j.msec.2016.02.067

Guo, X., Wang, Y., Qin, Y., Shen, P., & Peng, Q. (2020). Structures, properties and application of alginic acid: A review. *International Journal of Biological Macromolecules, 162*, 618–628. https://doi.org/10.1016/j.ijbiomac.2020.06.180

Gurikar, C., Naik, M. K., & Sreenivasa, M. Y. (2016). Azotobacter: PGPR activities with special reference to effect of pesticides and biodegradation. In *Microbial inoculants in sustainable agricultural productivity* (pp. 229–244). Springer India. https://doi.org/10.1007/978-81-322-2647-5_13

Hashimoto, W., Miyamoto, Y., Yamamoto, M., Yoneyama, F., & Murata, K. (2013). A novel bleb-dependent polysaccharide export system in nitrogen-fixing *Azotobacter vinelandii* subjected to low nitrogen gas levels. *International Microbiology: The Official Journal Of The Spanish Society For Microbiology, 16*(1), 35–44. https://doi.org/10.2436/20.1501.01.178

Hermansson, E., Schuster, E., Lindgren, L., Altskär, A., & Ström, A. (2016). Impact of solvent quality on the network strength and structure of alginate gels. *Carbohydrate Polymers, 144*, 289–296. https://doi.org/10.1016/j.carbpol.2016.02.069

Hitchins, V. M., & Sadoff, H. L. (1970). Morphogenesis of cysts in Azotobacter vinelandii. *Journal of Bacteriology, 104*(1), 492–498. https://doi.org/10.1128/jb.104.1.492-498.1970

Hu, C., Lu, W., Sun, C., Zhao, Y., Zhang, Y., & Fang, Y. (2022). Gelation behavior and mechanism of alginate with calcium: Dependence on monovalent counterions. *Carbohydrate Polymers, 294*, Article 119788. https://doi.org/10.1016/j.carbpol.2022.119788

Hule, R. A., Nagarkar, R. P., Altunbas, A., Ramay, H. R., Branco, M. C., Schneider, J. P., & Pochan, D. J. (2008). Correlations between structure, material properties and bioproperties in self-assembled β-hairpin peptide hydrogels. *Faraday Discussions, 139*, 251. https://doi.org/10.1039/b717616c

Jayawardena, L., Turunen, P., Garms, B. C., Rowan, A., Corrie, S., & Grøndahl, L. (2023). Evaluation of techniques used for visualisation of hydrogel morphology and determination of pore size distributions. *Materials Advances, 4*(2), 669–682. https://doi.org/10.1039/D2MA00932C

Kaberova, Z., Karpushkin, E., Nevoralová, M., Vetrík, M., Šlouf, M., & Dušková-Smrčková, M. (2020). Microscopic structure of swollen hydrogels by scanning Electron and light microscopies: Artifacts and reality. *Polymers, 12*(3), 578. https://doi.org/10.3390/polym12030578

Kiyama, R., Yoshida, M., Nonoyama, T., Sedlačík, T., Jinnai, H., Kurokawa, T., … Gong, J. P. (2023). Nanoscale TEM imaging of hydrogel network architecture. *Advanced Materials, 35*(1). https://doi.org/10.1002/adma.202208902

Koch, M., & Włodarczyk-Biegun, M. K. (2020). Faithful scanning electron microscopic (SEM) visualization of 3D printed alginate-based scaffolds. *Bioprinting, 20*, Article e00098. https://doi.org/10.1016/j.bprint.2020.e00098

Leal-Egaña, A., Braumann, U.-D., Díaz-Cuenca, A., Nowicki, M., & Bader, A. (2011). Determination of pore size distribution at the cell-hydrogel interface. *Journal of Nanobiotechnology, 9*(1), 24. https://doi.org/10.1186/1477-3155-9-24

Lee, K. Y., & Mooney, D. J. (2012). Alginate: Properties and biomedical applications. *Progress in Polymer Science, 37*(1), 106–126. https://doi.org/10.1016/j.progpolymsci.2011.06.003

Lin, L. P., Pankratz, S., & Sadoff, H. L. (1978). Ultrastructural and physiological changes occurring upon germination and outgrowth of Azotobacter vinelandii cysts. *Journal of Bacteriology, 135*(2), 641–646. https://doi.org/10.1128/jb.135.2.641-646.1978

Lin, L. P., & Sadoff, H. L. (1968). Encystment and polymer production by Azotobacter vinelandii in the presence of β-Hydroxybutyrate. *Journal of Bacteriology, 95*(6), 2336–2343. https://doi.org/10.1128/jb.95.6.2336-2343.1968

Londono-Calderon, A., Nayak, S., Mosher, C. L., Mallapragada, S. K., & Prozorov, T. (2019). New approach to electron microscopy imaging of gel nanocomposites in situ. *Micron, 120*, 104–112. https://doi.org/10.1016/j.micron.2019.02.010

Malektaj, H., Drozdov, A. D., & deClaville Christiansen, J. (2023). Mechanical properties of alginate hydrogels cross-linked with multivalent cations. *Polymers, 15*(14), Article 3012. https://doi.org/10.3390/polym15143012

Merryweather, D. J., Weston, N., Roe, J., Parmenter, C., Lewis, M. P., & Roach, P. (2023). Exploring the microstructure of hydrated collagen hydrogels under scanning electron microscopy. *Journal of Microscopy, 290*(1), 40–52. https://doi.org/10.1111/jmi.13174

Michler, G. H., & Lebek, W. (2016). Electron microscopy of polymers. In *Polymer morphology* (pp. 37–53). Wiley. https://doi.org/10.1002/9781118892756.ch3.

Moradali, M. F., & Rehm, B. H. A. (2019). The role of alginate in bacterial biofilm formation. In , *12. extracellular sugar-based biopolymers matrices* (pp. 517–537). https://doi.org/10.1007/978-3-030-12919-4_13

Moreno, S., Castellanos, M., Bedoya-Pérez, L. P., Canales-Herrerías, P., Espín, G., & Muriel-Millán, L. F. (2019). Outer membrane protein i is associated with poly-β-hydroxybutyrate granules and is necessary for optimal polymer accumulation in azotobacter vinelandii on solid medium. *Microbiology (United Kingdom), 165*(10), 1107–1116. https://doi.org/10.1099/mic.0.000837

Moscardini, A., Di Pietro, S., Signore, G., Parlanti, P., Santi, M., Gemmi, M., & Cappello, V. (2020). Uranium-free X solution: A new generation contrast agent for biological samples ultrastructure. *Scientific Reports, 10*(1), 11540. https://doi.org/10.1038/s41598-020-68405-4

Mrazova, K., Bacovsky, J., Sedrlova, Z., Slaninova, E., Obruca, S., Fritz, I., & Krzyzanek, V. (2023). Urany-less low voltage transmission electron microscopy: A powerful tool for ultrastructural studying of cyanobacterial cells. *Microorganisms, 11*(4), Article 888. https://doi.org/10.3390/microorganisms11040888

Nita, L. E., Chiriac, A. P., Ghilan, A., Rusu, A. G., Tudorachi, N., & Timpu, D. (2021). Alginate enriched with phytic acid for hydrogels preparation. *International Journal of Biological Macromolecules, 181*, 561–571. https://doi.org/10.1016/j.ijbiomac.2021.03.164

Nosrati, R., Owlia, P., Saderi, H., Rasooli, I., & Ali Malboobi, M. (2014). Phosphate solubilization characteristics of efficient nitrogen fixing soil Azotobacter strains. *Iranian Journal of Microbiology, 6*(4), 285–295. http://www.ncbi.nlm.nih.gov/pubmed/25802714.

Núñez, C., López-Pliego, L., Ahumada-Manuel, C. L., & Castañeda, M. (2022). Genetic regulation of alginate production in *Azotobacter vinelandii* a bacterium of biotechnological interest: A mini-review. *Frontiers in Microbiology*. https://doi.org/10.3389/fmicb.2022.845473

Paci, C., Iberite, F., Arrico, L., Vannozzi, L., Parlanti, P., Gemmi, M., & Ricotti, L. (2022). Piezoelectric nanocomposite bioink and ultrasound stimulation modulate early skeletal myogenesis. *Biomaterials Science, 10*(18), 5265–5283. https://doi.org/10.1039/D1BM01853A

Park, S.-N., Park, J.-C., Kim, H. O., Song, M. J., & Suh, H. (2002). Characterization of porous collagen/hyaluronic acid scaffold modified by 1-ethyl-3-(3-dimethylaminopropyl)carbodiimide cross-linking. *Biomaterials, 23*(4), 1205–1212. https://doi.org/10.1016/S0142-9612(01)00235-6

Parker, L. T., & Socolofsky, M. D. (1966). Central body of the Azotobacter cyst. *Journal of Bacteriology, 91*(1), 297–303. https://doi.org/10.1128/jb.91.1.297-303.1966

Qin, C., Wang, H., Zhao, Y., Qi, Y., Wu, N., Zhang, S., & Xu, W. (2024). Recent advances of hydrogel in agriculture: Synthesis, mechanism, properties and applications. *European Polymer Journal, 219*, Article 113376. https://doi.org/10.1016/j.eurpolymj.2024.113376

Ren, Y., Wang, Q., Xu, W., Yang, M., Guo, W., He, S., & Liu, W. (2024). Alginate-based hydrogels mediated biomedical applications: A review. *International Journal of Biological Macromolecules, 279*, Article 135019. https://doi.org/10.1016/j.ijbiomac.2024.135019

Reynolds, E. S. (1963). The use of lead citrate at high pH as an electron-opaque stain in electron microscopy. *The Journal of Cell Biology, 17*(1), 208–212. https://doi.org/10.1083/jcb.17.1.208

Roux, D. C. D., Jeacomine, I., Maltrejean, G., Caton, F., & Rinaudo, M. (2023). Characterization of agarose gels in solvent and non-solvent media. *Polymers, 15*(9), Article 2162. https://doi.org/10.3390/polym15092162

Sabra, W., Zeng, A.-P., Lünsdorf, H., & Deckwer, W.-D. (2000). Effect of oxygen on formation and structure of *Azotobacter vinelandii* alginate and its role in protecting Nitrogenase. *Applied and Environmental Microbiology, 66*(9), 4037–4044. https://doi.org/10.1128/AEM.66.9.4037-4044.2000

Sadoff, H. L. (1975). Encystment and germination in Azotobacter vinelandii. *Bacteriological Reviews, 39*(4), 516–539. https://doi.org/10.1128/br.39.4.516-539.1975

Sahoo, R. K., & Pradhan, M. (2023). *Azotobacter vinellandii* SINAz1 increases growth and productivity in rice under salinity stress. *Legume Research, 46*(2), 196–203. https://doi.org/10.18805/LR-4335

Stabentheiner, E., Zankel, A., & Pölt, P. (2010). Environmental scanning electron microscopy (ESEM)—A versatile tool in studying plants. *Protoplasma, 246*(1–4), 89–99. https://doi.org/10.1007/s00709-010-0155-3

Tkalec, G., Kranvogl, R., Perva Uzunalić, A., Knez, Ž., & Novak, Z. (2016). Optimisation of critical parameters during alginate aerogels' production. *Journal of Non-Crystalline Solids, 443*, 112–117. https://doi.org/10.1016/j.jnoncrysol.2016.04.014

Trudicova, M., Smilek, J., Kalina, M., Smilkova, M., Adamkova, K., Hrubanova, K., Krzyzanek, V., & Sedlacek, P. (2020). Multiscale experimental evaluation of agarose-based semi-interpenetrating polymer network hydrogels as materials with tunable rheological and transport performance. *Polymers, 12*(11), Article 2561. https://doi.org/10.3390/polym12112561

Urbanova, M., Pavelkova, M., Czernek, J., Kubova, K., Vyslouzil, J., Pechova, A., Molinkova, D., Vyslouzil, J., Vetchy, D., & Brus, J. (2019). Interaction Pathways and Structure–Chemical Transformations of Alginate Gels in Physiological Environments. *Biomacromolecules, 20*(11), 4158–4170. https://doi.org/10.1021/acs.biomac.9b01052

Vela, G. R., Cagle, G. D., & Holmgren, P. R. (1970). Ultrastructure of Azotobacter vinelandii. *Journal of Bacteriology, 104*(2), 933–939. https://doi.org/10.1128/jb.104.2.933-939.1970

Wright, P. J., Ciampi, E., Hoad, C. L., Weaver, A. C., van Ginkel, M., Marciani, L., … Rayment, P. (2009). Investigation of alginate gel inhomogeneity in simulated gastro-intestinal conditions using magnetic resonance imaging and transmission electron microscopy. *Carbohydrate Polymers, 77*(2), 306–315. https://doi.org/10.1016/j.carbpol.2008.12.025

Wyss, O., Neumann, M. G., & Socolofsky, M. D. (1961). Development and germination of the Azotobacter cyst. *The Journal of Biophysical and Biochemical Cytology, 10*(4), 555–565. https://doi.org/10.1083/jcb.10.4.555

Ye, Y., Wan, Z., Gunawardane, P. D. S. H., Hua, Q., Wang, S., Zhu, J., … Jiang, F. (2024). Ultra-stretchable and environmentally resilient hydrogels via sugaring-out strategy for soft robotics sensing. *Advanced Functional Materials, 34*(26). https://doi.org/10.1002/adfm.202315184

Yoneyama, F., Yamamoto, M., Hashimoto, W., & Murata, K. (2015). Production of polyhydroxybutyrate and alginate from glycerol by Azotobacter vinelandii under nitrogen-free conditions. *Bioengineered, 6*(4), 209–217. https://doi.org/10.1080/21655979.2015.1040209

Zhang, L., Wu, L., Si, Y., & Shu, K. (2018). Size-dependent cytotoxicity of silver nanoparticles to Azotobacter vinelandii: Growth inhibition, cell injury, oxidative stress and internalization. *PLoS One, 13*(12), Article e0209020. https://doi.org/10.1371/journal.pone.0209020

Zheng, H., Tian, W., Yan, H., Yue, L., Zhang, Y., Han, F., Chen, X., & Li, Y. (2012). Rotary culture promotes the proliferation of MCF-7 cells encapsulated in three-dimensional collagen–alginate hydrogels via activation of the ERK1/2-MAPK pathway. *Biomedical Materials, 7*(1), Article 015003. https://doi.org/10.1088/1748-6041/7/1/015003

Zhong, X., Ji, C., Chan, A. K. L., Kazarian, S. G., Ruys, A., & Dehghani, F. (2011). Fabrication of chitosan/poly(ε-caprolactone) composite hydrogels for tissue engineering applications. *Journal of Materials Science: Materials in Medicine, 22*(2), 279–288. https://doi.org/10.1007/s10856-010-4194-2